A MASS SPECTROMETRIC STUDY OF ORGANIC IONS AND NEUTRALS USING (MULTIPLE) COLLISION EXPERIMENTS

By

GRAHAM ANDREW McGIBBON, B.Sc.

A Thesis

Submitted to the School of Graduate Studies

in Partial Fulfilment of the Requirements

for the Degree

Doctor of Philosophy

McMaster University

© Copyright by Graham Andrew McGibbon, September 1994

A MASS SPECTROMETRIC STUDY OF ORGANIC IONS AND NEUTRALS

for Bärbel,
for my parents,
for Ulli

DOCTOR OF PHILOSOPHY (1994) McMASTER UNIVERSITY
(Chemistry) Hamilton, Ontario

TITLE: A Mass Spectrometric Study of Organic Ions and Neutrals Using (Multiple) Collision Experiments

AUTHOR: Graham Andrew McGibbon

SUPERVISOR: Professor Johan K. Terlouw

NUMBER OF PAGES: xix, 254

ABSTRACT

The unimolecular chemistry of selected organic (radical) cations has been studied by mass spectrometry based experiments (metastable ion (MI), collisional activation (CA), collision-induced dissociative ionization (CIDI) and neutralization-reionization (NR) mass spectrometry as well as multiple collision experiments (e.g. CA/CA and NR/CA) and appearance energy (AE) measurements) and ^{2}H, ^{13}C, ^{15}N and ^{18}O isotope labelling experiments in conjunction with ab initio molecular orbital computations.

Hydrogen-bridged (radical) cations, ion-molecule complexes and distonic ions are interesting species, partly because their neutral counterparts are usually unknown but, mostly because of their significance as key intermediates in the unimolecular dissociation reactions of gas phase ions. These types of species were found to play vital roles in the unimolecular chemistry of carbamate radical cations, $RN(H)COOCH_3^{+\bullet}$ {R = H, CH_3}. When R=H, the metastable molecular ions dissociate to two sets of products, $H_2N\text{-}CH\text{-}OH + HCO^{\bullet}$ and $[H_2C{=}O\cdots H\cdots NH_2]^{+\bullet} + CO$, with the first steps of both reactions being: $H_2NCOOCH_3^{+\bullet} \rightarrow H_2N\text{-}C(OH)OCH_2^{+\bullet}$ (distonic ion) $\rightarrow [H_2N\text{-}C{=}O\cdots H\cdots C{=}CH_2]^{+\bullet}$ (hydrogen-bridged ion). Although it does not participate in this chemistry, the imidic acid (iminol) ion, $H\text{-}N{=}C(OH)\text{-}OCH_3^{+\bullet}$, is also stable. However, attempts to generate it led instead to the more stable, but difficult to characterize, distonic ion.

The surprising loss of a methyl radical from metastable N-methyl-O-methyl carbamate radical cations $CH_3N(H)COOCH_3^{+\bullet}$, is proposed to involve equilibration with two distonic isomers, $CH_3N(H)\text{-}^{+}C(OH)OCH_2^{\bullet}$ and $CH_2{=}^{+}N(H)\text{-}^{\bullet}C(OH)OCH_3$, the latter serving as the immediate precursor to the products: $^{\bullet}CH_3$ and the N-carboxyiminium ion, $CH_2{=}N(H)\text{-}COOH^{+}$.

The heats of formation of the molecular ion and the product ion were estimated by additivity methods. A CA/CA experiment ($CH_3N(H)COOCH_3^{\bullet+} \rightarrow CH_3NHCOH^{\bullet+} \rightarrow HNCOH^+$) was used to generate and characterize the elusive isoformylaminylium ion.

The thermodynamic and kinetic stabilities of $CH_5N_2^+$ isomers have been re-evaluated in light of the results obtained from high level ab initio MO calculations and (metastable) AE measurements. NR experiments showed that the neutral $CH_2=NH-NH_2^\bullet$ is a stable species but the majority of neutralized $CH_2=NH-NH_2^+$ ions dissociate into $CH_2=NH$ and $NH_2^\bullet$, a finding that is rationalized in light of the different computed geometries of the ion and radical. Mechanisms are proposed for the metastable dissociation reactions of $CH_5N_2^+$ ions to $HCNH^+ + NH_3$ and to $HC{\equiv}N + NH_4^+$, the latter rationalized in terms of a dissociating $[HC{\equiv}N\cdots NH_4]^+$ ion-dipole complex.

A mechanism for the spontaneous deacetylation of N-acetylmethyliminium ions $CH_3C(=O)-N(H)=CH_2^+$ to $CH_2NH_2^+ + CH_2=C=O$ was proposed. The role of the hydrogen-bridged complex $[O=C=CH_2\cdots H\cdots N(H)=CH_2]^+$ is discussed with emphasis placed on the observation of large isotope effects and exceedingly small translational energy releases as indications of the intermediacy of such ion-molecule complexes. Several other isomeric $C_3H_6NO^+$ ions, which were briefly examined and characterized, are also discussed.

The second part of the thesis focusses on the generation and identification of elusive radicals and molecules by neutralization-reionization mass spectrometry and multiple collision experiments. It begins with a study of three isomeric $[C_2NO]$ cations that were characterized by (multiple) collision experiments. NR and CIDI experiments were used to demonstrate the existence of the corresponding radicals $NCCO^\bullet$, $CNCO^\bullet$ and $CCNO^\bullet$ as stable species in the gas phase.

Appropriate dissociative ionizations were used to produce diamino- and dihydroxy-carbene radical cations. Reduction of the ionized carbenes by single-electron transfer in NR experiments yielded "survivor" signals but collision experiments on the reionized neutrals (NR/CA) were required to unambiguously establish that the prototype carbenes, $H_2N\text{-}\ddot{C}\text{-}NH_2$ and $HO\text{-}\ddot{C}\text{-}OH$, were generated as stable gaseous species, distinct from their isomers formamidine, $H\text{-}N{=}C(H)NH_2$ and formic acid, $O{=}C(H)OH$.

Similarly, a combination of NR mass spectrometry and (multiple) collision experiments on D and ^{15}N labelled isotopomers made it possible to assign structures to the prototype imidic acid, formimidic acid, $H\text{-}N{=}C(H)\text{-}OH$, and aminohydroxycarbene, $H_2N\text{-}\ddot{C}\text{-}OH$, both isomeric with formamide. The ionic precursors $H\text{-}N{=}C(H)\text{-}OH^{\bullet+}$ and $H_2N\text{-}C\text{-}OH^{\bullet+}$ were produced by appropriate dissociative ionizations and direct ionization of formamide yielded $H_2N\text{-}CHO^{\bullet+}$. NR experiments produced intense "survivor" signals. By combining information contained in CA mass spectra of the "survivor" ions with that from labelling experiments, the existence of formimidic acid and aminohydroxycarbene as stable molecules in the gas phase was established. Using the same experimental methodology, the existence of the imidic acid $CH_3\text{-}N{=}C(H)\text{-}OH$ and the carbene $CH_3\text{-}N(H)\text{-}\ddot{C}\text{-}OH$ was also established.

PREFACE

The larger part of this thesis describes results obtained by the author during five years of experimental research in gas phase ion chemistry. This field is ideally suited to investigation by both experimental and theoretical methodologies. Indeed, the common set of conditions involved in mass spectrometric experiments and computational chemistry, i.e. the study of isolated particles, makes the two approaches complementary. For dissociations of ions where unambiguous mechanistic pathways cannot be determined from experimental data alone, computations on a restricted set of possibilties may determine the feasibility of particular proposals. Sometimes energetic data from calculations anchored to experimental values may serve to substantiate or eliminate potential intermediates or products. Permission to use the integral collaborative contributions of the computational chemists, Prof. Dr. Paul J.A. Ruttink (Chapters 2 and 5), Dr. Carol A. Kingsmill (Chapters 3 and 6-8), Dr. Gijs Schaftenaar (Chapter 2), Dr. Ron Postma (Chapter 2) and Dr. Harald F. van Garderen (Chapter 5), herein is greatly appreciated. Finally, one other individual deserves special mention in the context of collaboration: Dr. Peter C. Burgers. His insights, suggestions and critical evaluations have significantly shaped the way that these results have been presented and it was therefore a great pleasure to finally meet face-to-face with him in August of this year at his home prior to the 13th IMSC.

The permission of *Elsevier* and *John Wiley & Sons* to present, in this thesis, data and text which have already been published in ten individual manuscripts is greatly appreciated. Some results and conclusions from a published study of dimethylsulfoxide are given in the INTRODUCTION in order to illustrate the mass spectrometric techniques essential to the experimental work described in this thesis

LIST OF PUBLICATIONS

1. The imidic acids HN=C(H)-OH and CH_3N=C(H)-OH and their tautomeric carbenes H_2N-$\ddot{C}$-OH and CH_3N(H)-$\ddot{C}$-OH; Stable species in the gas-phase by one-electron reduction of their radical cations; G.A. McGibbon, P.C. Burgers and J.K. Terlouw; Int. J. Mass Spectrom. Ion Processes 136 (1994) 191-208.

2. Dihydroxycarbene HO-$\ddot{C}$-OH: Its formation by electron transfer to its cation; P.C. Burgers, G.A. McGibbon and J.K. Terlouw; Chem. Phys. Letters 224 (1994) 539-543.

3. Experimental evidence for gaseous diaminocarbene H_2N-$\ddot{C}$-NH_2 and its radical cation; G.A. McGibbon and J.K. Terlouw; Chem. Phys. Letters 222 (1994) 129-134.

4. O-protonated sulfine H_2C=S=OH^+: Its generation from ionized dimethylsulfoxide by delayed dissociation; G.A. McGibbon, P.C. Burgers and J.K. Terlouw; Chem. Phys. Letters 218 (1994) 499-503.

5. The elusive HN=C-OH^+ ion characterized by a double collision experiment in the mass spectrometer; G.A. McGibbon, J.K. Terlouw and P.C. Burgers; Rapid Commun. Mass Spectrom. 7 (1993) 138-141.

6. Aspects of the CH_5N_2 potential energy surface: Ions CH_3NHNH^+, $CH_3NNH_2^+$ and $CH_2NHNH_2^+$ and $CH_2NHNH_2^{\bullet}$ radicals studied by theory and experiment; H.F. van Garderen, P.J.A. Ruttink, P.C. Burgers, G.A. McGibbon and J.K. Terlouw; Int. J. Mass Spectrom. Ion Processes 121 (1992) 159-182.

7. The isomeric C_2NO^+ ions $NCCO^+$, $CNCO^+$, $CCNO^+$ and their neutral counterparts are stable species in the gas-phase; G.A. McGibbon, C.A. Kingsmill, J.K. Terlouw and P.C. Burgers; Int. J. Mass Spectrom. Ion Processes 121 (1992) R11-R18.

8. Deacetylation of gaseous amidoalkylating reagents (N-acyliminium ions) via iminium/ketene complexes; An unprecedented isotope effect; P.C. Burgers, C.A. Kingsmill, G.A. McGibbon and J.K. Terlouw; Org. Mass Spectrom. 27 (1992) 398-405.

9. The gas phase chemistry of the methyl carbamate radical cation. II . A test case for ion structure assignment; G.A. McGibbon, C.A. Kingsmill, J.K. Terlouw and P.C. Burgers; Org.Mass Spectrom. 27 (1992) 126-134.

10. The gas phase determination of the stabilization energy for α- and β-silyl substituents on vinyl cations by mass spectrometry; G.A. McGibbon, M.A.Brook and J.K. Terlouw; J. Chem. Soc. Chem. Commun. 4 (1992) 360-362.

11. Ion permeability through bilayer lipid membranes for biosensor development: control by chemical modification of interfacial regions between phase domains; D.P. Nikolelis, J.D. Brennan, R.S. Brown, G. McGibbon and U.J. Krull; Analyst 116 (1991) 1221-1226.

12. The gas phase chemistry of the methyl carbamate radical cation $H_2NCOOCH_3^{+\bullet}$: Isomerization into distonic ions, hydrogen-bridged radical cations and ion dipole complexes; G. Schaftenaar, R. Postma, P.J.A. Ruttink, P.C. Burgers, G.A. McGibbon and J.K. Terlouw; Int. J. Mass Spectrom. 100 (1990) 521-544.

13. Fluorescence wavelength, intensity and lifetime for multidimensional transduction of selective interactions of acetylcholine receptor for lipid membranes; U.J. Krull, R.S. Brown, B.D. Hougham, G. McGibbon and E.K. Vandenberg; Talanta 37 (1990) 561-567.

14. Chemical sensors from fluorometric transduction of selective perturbations of domain structures within lipid monolayers; U.J. Krull, J.D. Brennan, R.S. Brown, G. McGibbon and K. Stewart; Int. J. Optoelectronics 4 (1989) 133-146.

ACKNOWLEDGEMENTS

I would like to thank Dr F.P. Lossing for performing appearance energy measurements and Professor J.L. Holmes for providing access to the KRATOS MS 902S instrument (see Chapter 2).

I appreciate the excellent guidance provided by my supervisor Professor J.K. Terlouw and the other members of my PhD committee, Professor M.A. Brook (co-supervisor for two years) and Professor N.H. Werstiuk. I am greatly indebted to Prof. Terlouw, my advisor and mentor, for his continual support, patience, guidance and friendship as he carefully nurtured me from neophyte to ion chemist. I am also extremely grateful to Prof. Michael A. Brook for his co-supervision of my work during my first two years at McMaster (wherein I dabbled in some silicon chemistry which is not represented here) and for always having an open door, a sympathetic ear and time to spare despite his hectic schedule in the subsequent years.

Thanks are also extended to: Dr. Richard W. Smith and Mr. Fajan "Faj" A. Ramelan of the McMaster Regional Center for Mass Spectrometry for their assistance and instruction in the use and maintenance of the mass spectrometers; Dr. A.A. "Saunder" Mommers for his technical assistance and wonderful computer programming skills which have made the ZAB-R so easy to use; Mr. Thomas (Y.C.) "Tom" Wong for his aid with the ZAB-R and for keeping me active in basketball; Dr. Carol Dallaire for valuable discussions, T-shirts and helpful advice about organic synthesis; Mr. Dennis Suh for his assistance with some syntheses and the ZAB-R; Messrs. Ian D. Ireland (C_2NO), Ron Chong (CH_3NO), Hesham Ghobarah and Christopher Roos who helped with mass spectrometric experiments as part of their CHM 4G6 senior undergraduate project

work; Mr. George Timmins for his aid with glassblowing; the other members of Dr. Brook's lab group, especially Mike Roth, Courtney Henry, Grant Crowe and Tom Stefanac; and last but not least, Bärbel for her love, support and help with the final Figures.

The financial support of this work by McMaster University and, in the form of an equipment grant for the ZAB-R, from the Natural Sciences and Engineering Research Council of Canada (NSERC) is greatly appreciated.

TABLE OF CONTENTS

Page

ABSTRACT iii

PREFACE vi

LIST OF PUBLICATIONS vii

ACKNOWLEDGMENTS ix

TABLE OF CONTENTS xi

LIST OF FIGURES xiii

LIST OF ABBREVIATIONS xix

CHAPTER 1 INTRODUCTION 1

1.1 Ion structures and reactions by tandem mass spectrometric methods 2

1.2 Mass spectrometry of neutrals (NRMS and CIDI) 15

1.3 Ion and neutral thermochemistry 27

1.4 Ion structures: Ion-molecule complexes and distonic ions 31

PART I: STRUCTURES AND REACTIONS OF ORGANIC IONS

CHAPTER 2 The gas phase chemistry of methyl carbamate radical cations $H_2NCOOCH_3^{+\bullet}$: Isomerization into distonic ions, hydrogen-bridged radical cations and ion-dipole complexes 47

CHAPTER 3 The gas phase chemistry of the methyl carbamate radical cation $H_2NCOOCH_3^{+\bullet}$. II. A test case for ion structure assignment 77

CHAPTER 4 The gas phase chemistry of N-methyl-O-methyl carbamate radical cations $CH_3N(H)COOCH_3^{+\bullet}$ 100

4.1 How does ionized N-methyl-O-methyl carbamate lose a methyl group? Unimolecular equilibration with two distonic isomers 101

4.2 The elusive $HN{=}C{-}OH^+$ ion characterized by a double collision experiment in the mass spectrometer 117

CHAPTER 5 Aspects of the CH_5N_2 potential energy surface: ions CH_3NHNH^+, $CH_3NNH_2^+$ and CH_2=$NHNH_2^+$ and radicals CH_2=$NHNH_2^\bullet$ studied by theory and experiment..... 127

CHAPTER 6 Deacetylation of gaseous amidoalkylating reagents (N-acyliminium ions) via iminium/ketene complexes; an unprecedented isotope effect..... 157

PART II: ELUSIVE NEUTRALS FROM NRMS EXPERIMENTS

CHAPTER 7 The isomeric C_2NO^+ ions $NCCO^+$, $CNCO^+$, $CCNO^+$ and their neutral counterparts are stable species in the gas phase..... 178

CHAPTER 8 Elusive carbenes by neutralization-reionization mass spectrometry..... 188

8.1 Experimental evidence for gaseous diaminocarbene H_2N-$\ddot{C}$-NH_2 and its radical cation..... 189

8.2 Dihydroxycarbene HO-$\ddot{C}$-OH: its formation in the gas phase by electron transfer to its radical cation..... 199

CHAPTER 9 The imidic acids HN=C(H)-OH and CH_3-N=C(H)-OH and their tautomeric carbenes H_2N-$\ddot{C}$-OH and CH_3-N(H)-$\ddot{C}$-OH: stable species in the gas phase formed by one-electron reduction of their cations..... 210

EXPERIMENTAL..... 242

SUMMARY..... 249

LIST OF FIGURES

Page		
5	**Fig. 1.1**	Schematic of the VG Analytical ZAB-R mass spectrometer.
10	**Fig. 1.2**	(a) MI spectrum of DMSO; (b) MI spectrum of aci-DMSO.
14	**Fig. 1.3**	(a) CID mass spectrum of the m/z 63 $(CH_3SO)^+$ ions generated from DMSO ions decomposing in the ion source; (b) MI/CID spectrum of the m/z 63 ions generated by the loss of $^{\bullet}CH_3$ from metastable $DMSO^{\bullet+}$ ions in the 1FFR.
21	**Fig. 1.4**	(a) [NDMA, O_2] NR mass spectrum of the m/z 63 $(CH_3SO)^+$ ions generated from DMSO ions decomposing in the ion source; (b) [NDMA, O_2] NR mass spectrum of the m/z 63 ions generated by the loss of $^{\bullet}CH_3$ from metastable $DMSO^{\bullet+}$ ions in the 1FFR.
23	**Fig. 1.5**	Schematic depiction of an NR/CID experiment
24	**Fig. 1.6**	(a) MI/CID spectrum obtained in the 3FFR of the m/z 63 ions generated by the loss of $^{\bullet}CH_3$ from metastable $DMSO^{\bullet+}$ ions in the 1FFR; (b) MI/NR/CID spectrum obtained in the 3FFR of the metastable ions generated in the 1FFR.
26	**Fig. 1.7**	CIDI mass spectrum of CH_3-S=O$^{\bullet}$ from $CH_3S(=O)CH_2SCH_3^{\bullet+}$.
52	**Fig. 2.1**	CA mass spectrum of the CH_4NO^+ ions generated by loss of HCO$^{\bullet}$ from ionized methyl carbamate, $H_2NCOOCH_3^{\bullet+}$.
54	**Fig. 2.2**	(A) [Xe, O_2] NR mass spectrum of the CH_4NO^+ ions generated by loss of HCO$^{\bullet}$ from ionized methyl carbamate, $H_2NCOOCH_3^{\bullet+}$; (B) NR mass spectrum of the $CH_2D_2NO^+$ ions generated by loss of DCO$^{\bullet}$ from the labelled ester, $H_2NCOOCD_3^{\bullet+}$.
57	**Fig. 2.3**	[Xe, O_2] NR mass spectrum of the CH_2DNO^+ ions generated by loss of CD_2O from the labelled ester, $H_2NCOOCD_3^{\bullet+}$.

59 **Fig. 2.4** Geometries of $C_2H_5NO_2^{+\bullet}$ isomeric ions and some Transition States optimized at SCF/4-31G** level of theory.

67 **Fig. 2.5** Schematic Representation of the SCF potential energy surface for the isomerization 2 → 5.

69 **Fig. 2.6** Theoretically derived energy diagram for the dissociation reactions of ionized methyl carbamate, $H_2NCOOCH_3^{+\bullet}$.

82 **Fig. 3.1** Geometries of $C_2H_5NO_2^{+\bullet}$ isomeric ions and some Transition Statesoptimized at the 4-31G level of theory.

85 **Fig. 3.2** Calculated energy diagram for the dissociation reactions of ionized methyl carbamate, 1. Not included are isomers 3 and 4, which have been discussed before [2]. The UHF/MP3/6-31G*//4-31G energy levels are designated by the thick solid lines. The RHF/SDCI/6-31G**//4-31G levels designated by the thick dashed lines are taken from Ref.2.

88 **Fig. 3.3** CA mass spectra of the $C_2H_5NO_2^{+\bullet}$ ions generated by CH_3CN loss from CH_3-CH=NN(H)$COOCH_3$ (a) and by direct ionization of methyl carbamate (b).

89 **Fig. 3.4** NR mass spectra of the $C_2H_5NO_2^{+\bullet}$ ions generated by CH_3CN loss from CH_3-CH=NN(H)$COOCH_3$ (a) and by direct ionization of methyl carbamate (b).

91 **Fig. 3.5** MS/MS/MS spectra of $CH_3NO^{+\bullet}$ product ions from $H_2NCOOCH_3^{+\bullet}$ (a) and of the $CH_2DNO^{+\bullet}$ product ions generated from CH_3-CD=NN(H)$COOCH_3$ (b).

95 **Fig. 3.6** Partial CA mass spectra of ionized methyl carbamate (a) and of the $C_2H_4DNO_2^{+\bullet}$ ions generated from CH_3CH=NN(D)$COOCH_3$ (b) and from CH_3CD=NN(H)$COOCH_3$ (c).

106 **Fig. 4.1** Metastable Ion mass spectra of (a) $CH_3N(H)COOCH_3^{+\bullet}$ and (b) $CH_3N(H)COOCH_3^{+\bullet}$.

107 **Fig. 4.2** [2FFR,O_2] CA mass spectrum of the [M - $^\bullet CH_3$]$^+$ ions generated from

Fig. 4.2 continued... $CH_3N(H)COOCH_3^{\bullet+}$ (a) and $CD_3N(H)COOCH_3^{\bullet+}$ (b); NR mass spectrum of the $[M - {}^{\bullet}CH_3]^+$ ions generated from $CH_3N(H)COOCH_3^{\bullet+}$(c).

109 Fig. 4.3 (a) CA mass spectrum of the $HOCO^+$ ions generated from collisionally activated $CH_2=N(H)COOH^+$, (b) CA mass spectrum of the $[C,H,O,{}^{18}O]^+$ ions generated from collisionally activated ^{18}O labelled $CH_2=N(H)COOH^+$ ions.

112 Fig. 4.4 [2FFR,O_2] CA mass spectra of (a) the $[M - {}^{\bullet}CD_2H]^+$ ions generated from $CH_3N(H)COOCD_3^{\bullet+}$ and (b) the $[M - {}^{\bullet}CD_2H]^+$ ions generated from $CH_3N(H)COOCD_2H^{\bullet+}$

114 Fig. 4.5 Collisional activation (a) and neutralization-reionization (b) mass spectra of $CH_3N(H)COOCH_3^{\bullet+}$.

120 Fig. 4.6 Partial [3FFR,He] CA mass spectra of (a) ions 2, $HN=C-OH^+$, generated by the collision induced dissociation of $CH_3N(H)COH^{\bullet+}$ [2FFR,O_2] , (b) ions 1, $H_2N-C=O^+$, generated by the [2FFR,O_2] collision-induced dissociation of $H_2NCOCH_3^{\bullet+}$ and (c) the $[H_2,C,N,O]^+$ ions generated by the [2FFR,O_2] collision induced dissociation of $CH_3(H)N-C(H)=O^{\bullet+}$.

121 Fig. 4.7 Partial [3FFR,He] CA mass spectra of (a) ions $HDN-C=O^+$, generated by the [2FFR,O_2] collision induced dissociation of $HDNCOCH_3^{\bullet}$, (b) ions $DNCOH^+$, generated by the [2FFR,O_2] collision induced dissociation of $CH_3N(D)COH^{\bullet+}$ and (c) ions $HNCOD^+$, generated by the [2FFR,O_2] collision induced dissociation of $CH_3N(H)COD^{\bullet+}$.

131 Fig. 5.1 Geometries of $CH_5N_2^+$ isomeric ions and transition states optimized at the SCF/6-31G** level of theory.

136 Fig. 5.2 Calculated energy diagram for the $CH_5N_2^+$ ions.

141 Fig. 5.3 (a) CA mass spectrum of $CH_5N_2^+$ ions generated in the ion source from $CH_3NHNH_2^{\bullet+}$ ions, (b) CA mass spectrum of $CH_5N_2^+$ ions generated from

Fig. 5.3 Continued... metastable $CH_3NHNH_2^{\bullet+}$ ions. The lower intensity level of the charge stripping peak at m/z 22.5 in the latter spectrum is due to the lower resolving power of the second electric sector compared to the first.

146 Fig. 5.4 (a) NR spectrum of CH_2=ND-ND_2^+. Neutralization agent Xe and oxidation agent O_2. (b) as (a), but neutralization agent N,N-dimethylaniline, see text. (c) CA spectrum of CH_2=ND-ND_2^+, collision gas O_2. (d) CA-NR spectrum of CH_2=ND-ND_2^+; triple collision experiment (see text). Neutralization agent N,N-dimethylaniline, oxidation agent O_2 and collision gas O_2.

149 Fig. 5.5 Calculated energy diagram for the generation and dissociation of $^{\bullet}CH_2$-NH-NH_2, 3$^{\bullet}$, in a Neutralization-Reionization experiment.

160 Fig. 6.1 Metastable peak for CH_3-C(=O)N(H)=CH_2^+ → $CH_2NH_2^+$ + CH_2=C=O.
Inset: main beam with energy scale as indicated.

160 Fig. 6.2 Partial CA mass spectra of CH_3-C(=O)N(H)=CH_2^+ , A, CH_3-C(=O)N(D)=CH_2^+ , B, and CD_3-C(=O)N(D)=CH_2^+, C.

165 Fig. 6.3 Geometries of $C_3H_6NO^+$ isomeric ions and some Transition States at the MP3 /6-31G $^{\bullet}$//4-31G level of theory.

167 Fig. 6.4 The calculated $C_3H_6NO^+$ potential energy surface.

180 Fig. 7.1 Calculated 6-31G$^{\bullet}$ geometries (bond lengths in ångströms) and E_{rel} values (kcal mol^{-1}, UMP3/6-31G$^{\bullet}$//6-31G$^{\bullet}$ + (0.9) ZPVE) for the C_2NO cations 1$^+$ and 2$^+$ and the neutrals 2$^{\bullet}$ and 3$^{\bullet}$. Numbers in brackets refer to the charge distribution, in $e^{\bullet}$, derived from a Mulliken population analysis of the UMP3/6-31G$^{\bullet}$//6-31G$^{\bullet}$ results.

184 Fig. 7.2 (DMA,O_2) NR spectrum of product ions 3$^+$ from the collision induced dissociation 84$^{\bullet+}$ [O←N=C-C≡N→$O^{\bullet+}$] → 54$^{\bullet+}$ [CCNO$^+$] + NO; (b) (O_2) CIDI spectrum of neutrals 3 generated by the collision induced dissociation 84$^{\bullet+}$ [O←N=C-C≡N→$O^{\bullet+}$] → 54$^{\bullet}$ [CCNO$^{\bullet}$] + NO^+; (c) and (d) (DMA,O_2) NR spectra of the C_2NO^+ ions 2$^+$ and 1$^+$, generated from methylisocyanate and pyruvonitrile respectively.

193 **Fig. 8.1** [O_2] Collisional Activation (CA) and [NDMA/O_2] Neutralization-Reionization (NR) mass spectra (2FFR) of m/z 44 formamidine ions $1^{\bullet+}$, items a and b respectively, and m/z 44 diaminocarbene ions $2^{\bullet+}$, items c and d respectively. The m/z 12-17 region in spectra c and d has been amplified by 3x.

197 **Fig. 8.2** Collisional Activation (CA) mass spectra of m/z 48 $D_2N\text{-}C\text{-}ND_2^{\bullet+}$ ions [3FFR He] generated from the *survivor* ions in the [NDMA/O_2] NR spectrum, item a, and from source generated ions, item b. The m/z 12-20 region in both spectra has been amplified by 3x.

202 **Fig. 8.3** Partial CA mass spectra [3FFR, He] of source generated ions $HC(=O)OH^{\bullet+}$ and $HO\text{-}C\text{-}OH^{\bullet+}$, items a and b, and of the *survivor* ions $HC(=O)OH^{\bullet+}$ and $HO\text{-}C\text{-}OH^{\bullet+}$ from the [NDMA/O_2] NR spectra, items c and d.

204 **Fig. 8.4** [NDMA/O_2] NR mass spectra of $HC(=O)OH^{\bullet+}$ (item a) and $HO\text{-}C\text{-}OH^{\bullet+}$ (item b). In the corresponding CA mass spectra [2FFR, O_2] the m/z 28/29 ratios are 5.7 and 2.5.

213 **Fig. 9.1** Calculated energy diagram for formamide (1), formimidic acid (2) and aminohydroxy carbene (3) and their radical cations $1^{\bullet+}$ - $3^{\bullet+}$. Energies in kcal/mol are relative to ΔH_f (exp.) 1 (- 44 kcal/mol [8a]). The ordering of the levels for the ions was taken from the MR-CI (Pople) ab initio calculations in ref. 9, those for the neutral species are from ab initio calculations reported in ref. 7, 9 and this work. The energies of the ions and neutrals are connected via the adiabatic IE of 1, 10.1 eV [8a]; the levels for the dissociation products all refer to experimental values taken from ref. 8a.

220 **Fig. 9.2** Partial CID mass spectra (He,3FFR) of m/z 28 generated from collisionally activated (O_2,2FFR) ions $H_2N\text{-}CH(=O)^{\bullet+}$ or $H_2N\text{-}C\text{-}OH^{\bullet+}$ (item A) and $H\text{-}N{=}C(H)OH^{\bullet+}$ ions (item B).

223 **Fig. 9.3** Partial (He, 3FFR) CID mass spectra of source generated ions $D_2{}^{15}N\text{-}CD(=O)^{\bullet+}$ (item A) and $D_2{}^{15}N\text{-}C\text{-}OD^{\bullet+}$ (item C) and the (He, 3FFR) CID spectra of their NR "survivor" ions , (items B and D) respectively.

224 **Fig. 9.4** Partial CID mass spectra (He, 3FFR) of m/z 30 and m/z 31 generated from collisionally activated (O_2, 2FFR) ions $D_2{}^{15}N\text{-}C\text{-}OD^{\bullet+}$, items A and B respectively, and ions $D_2{}^{15}N\text{-}CD(=O)^{\bullet+}$, items C and D respectively.

226 **Fig. 9.5** Neutralization-Reionization mass spectra (NDMA/O_2, 2FFR) of $H_2N\text{-}CH(=O)^{\bullet+}$, $\mathbf{1}^{\bullet+}$, (item A), $H\text{-}N{=}C(H)OH^{\bullet+}$, $\mathbf{2}^{\bullet+}$, (item B) and $H_2N\text{-}C\text{-}OH^{\bullet+}$, $\mathbf{3}^{\bullet+}$ (item C); inset item C: neutralization with cyclopropane. Product ion yields were $\Sigma[I^+]/[M^{\bullet+}]$ = 0.0010, 0.0002 and 0.0004 for $\mathbf{1}^{\bullet+}$, $\mathbf{2}^{\bullet+}$ and $\mathbf{3}^{\bullet+}$ respectively.

228 **Fig. 9.6** Partial CID mass spectra (He, 3FFR) of NR "survivor" ions (top spectra) and CID spectra [He, 3FFR) of source generated ions (bottom spectra) of $H_2N\text{-}CH(=O)^{\bullet+}$, $\mathbf{1}^{\bullet+}$, $H\text{-}N{=}C(H)OH^{\bullet+}$, $\mathbf{2}^{\bullet+}$, and $H_2N\text{-}C\text{-}OH^{\bullet+}$, $\mathbf{3}^{\bullet+}$.

235 **Fig. 9.7** CID mass spectra [He, 3FFR] of source generated ions $CH_3N(H)\text{-}C\text{-}OH^{\bullet+}$, $\mathbf{3a}^{\bullet+}$, (item A) $CH_3\text{-}N{=}C(H)OH^{\bullet+}$, $\mathbf{2a}^{\bullet+}$, (item C) and $CH_3N(H)\text{-}CH(=O)^{\bullet+}$,$\mathbf{1a}^{\bullet+}$, (item E) and CID spectra [He, 3FFR] of NR "survivor" ions, items B, D and F respectively.

236 **Fig. 9.8** Neutralization-Reionization mass spectra [NDMA/O_2, 2FFR] of $CH_3N(H)\text{-}C\text{-}OH^{\bullet+}$, $\mathbf{3a}^{\bullet+}$, (item A) $CH_3\text{-}N{=}C(H)OH^{\bullet+}$, $\mathbf{2a}^{\bullet+}$, (item B) $CH_3N(H)\text{-}CH(=O)^{\bullet+}$, $\mathbf{1a}^{\bullet+}$ (item C) and $[CH_2\text{-}N(H)\text{-}C(H)OH]^{\bullet+}$, $\mathbf{1d}^{\bullet+}$, (item D).

LIST OF ABBREVIATIONS

acc.	=	acceleration
AE	=	appearance energy
B	=	magnetic sector
CA	=	collisional activation (see also CID)
CASSCF	=	complete active space self-consistent field
CE	=	charge exchange
CI	=	configuration interaction (theoretical)
CI	=	chemical ionization (experimental)
CID	=	collision-induced dissociation (see also CA)
CIDI	=	collision-induced dissociative ionization
CP	=	cyclopropane
CR	=	charge-reversal
CS	=	charge-stripping
DMSO	=	dimethylsulfoxide, $(CH_3)_2S=O$
E_h	=	hartree (1 hartree = 627.52 kJ)
ΔE_h	=	energy width of peak at height h
EI	=	electron ionization
ESA	=	electrostatic analyser
eV	=	electron Volt (1 eV = 96.48 kJ/mol)
FFR	=	field free region
ΔH_f	=	enthalpy of formation
HF	=	Hartree-Fock
IE	=	ionization energy
k	=	rate constant
kcal/mol	=	kilocalories per mole (1kcal/mol = 4.184 kJ/mol)
KER	=	kinetic energy release
kJ/mol	=	kiloJoules per mole
MC	=	multi-configuration
MI	=	metastable ion
MO	=	molecular orbital
MP	=	Møller-Plesset (perturbation theory)
MS	=	mass spectrometry
NDMA	=	N,N-dimethylaniline
m/z	=	mass to charge ratio
NR(MS)	=	neutralization-reionization (mass spectrometry)
PA	=	proton affinity
q	=	charge
r,R	=	radius
SCF	=	self-consistent field
T	=	kinetic energy release (value)
TPEPICO	=	threshold photo electron photo ion coincidence
TS	=	transition state
ZAB-R	=	three sector mass spectrometer
ZPVE	=	zero-point vibrational energy

CHAPTER 1

INTRODUCTION

Ionization of a molecule is a fundamental physical process; one which may dramatically affect its intrinsic reactivity, including its unimolecular isomerization and dissociation behaviour. Since the turn of the century, it has become apparent that mass spectrometric methodology is ideally suited for the generation of charged species in the gas phase and the study of their reactivity. Rapid technological development has led to increasingly sophisticated instrumentation and this, coupled with experimental innovations, has made mass spectrometry an invaluable tool in research ranging from astrochemistry to environmental chemistry and bio-chemistry [1]. Still, the technique is most widely used to analyze and identify molecular structures from the fragmentation patterns exhibited by their ionized forms. Empirical rationalizations of mass spectra have been postulated for many classes of organic compounds [2]. However, the following comment from a well-known textbook [2a]: *"The interpretation of mass spectra is based on the chemistry of gaseous ions..."* may serve as a reminder that a sound knowledge of gas phase ion chemistry [3] is a prerequisite for the confident assignment of molecular structures.

Essentially, ion chemistry research is concerned with the aspects of ion structure (conventionally this refers to atom connectivity), thermochemistry and reactivity, including rearrangement and dissociation processes. An outline of the basic principles of the common techniques used to probe structures and reaction mechanisms of ions in the gas phase is given in section 1.1. Neutralization-reionization mass spectrometry (NRMS) [4] is one of the more recent techniques introduced for this purpose. More noteworthy though, is its capacity for the tailor-made synthesis and characterization of

elusive neutral species. This topic has rapidly developed during the past decade and its principles, accomplishments and limitations have already been the subject of several review articles. Section 1.2 comprises a synopsis of this new technique and its applications.

Theoretical chemistry or rather computational chemistry, is being increasingly used as a complementary or even alternative method of studying gas phase ions [5]. In ab initio molecular orbital calculations, energetics and structure go hand-in-hand and they are well suited to treat isolated gaseous species. The present day calculations provide reliable molecular structure information (3-dimensional geometries, not just atom connectivities). They can also reliably predict stable isomeric forms and their relative energies and be used to elucidate key aspects of reaction mechanisms. Introductory paragraphs on these methods are given in Section 1.3.

In recent years, experimental and theoretical studies of the reaction mechanisms of ionized molecules have led to the postulation of the existence of several types of remarkably stable intermediates [6] for which the corresponding neutral species are unknown, unstable or highly reactive. Among the most interesting of these ions are ion-molecule complexes, which include hydrogen-bridged ions and ion-dipole complexes. Hydrogen-bridged radical cations in particular have been invoked with increasing frequency in the past decade as stable intermediates in the isomerization/dissociation pathways of a wide range of oxygen-containing molecular ions. Nevertheless, there remains a scarcity of unambiguous experimental evidence for their existence. These types of ions are differentiated and described in Section 1.4.

1.1 Ion structures and reactions by tandem mass spectrometric methods

The classic critical review of Holmes [7] on the standard tandem mass spectrometric (MS/MS) [8] techniques in use for "Assigning structures to ions in the gas phase" and its predecessors [9] form the basis for the following outline. The methods

described rely heavily on comparisons with reference data and are most powerful when used collectively and in conjunction with isotopic labelling experiments.

Following a brief discussion of the origin and properties of metastable ions and the energetics of dissociation reactions, this section will focus on the use of various types of collision experiments. How (multiple) collision techniques can be used to probe ion structures and dissociation pathways will be illustrated using selected results from a recent study of ionized dimethylsulfoxide (DMSO).

Introduction to the gas phase chemistry of ionized DMSO

DMSO, $CH_3S(=O)CH_3$, is an important organic compound [10]. It is a powerful dipolar non-hydroxylic solvent as well as a highly effective reagent for the oxidation of primary and secondary alcohols to carbonyl compounds and, not surprisingly, it and its less illustrious isomers, *aci*-DMSO, $CH_2=S(OH)CH_3$, and methyl methanesulfenate, CH_3SOCH_3, have also been the subject of previous experimental and theoretical studies as ions and neutrals in the gas phase [11].

In the context of ionic dissociations it has generally been assumed, quite reasonably, that loss of $^{\bullet}CH_3$ from ionized DMSO produces $CH_3S=O^+$, **1**, by direct bond cleavage. Turecek et al. [11c] characterized the isomeric ions $CH_3S=O^+$, **1** and $CH_2=S=OH^+$, **2**, by collision experiments and showed that the above assumption does hold for the (high energy) DMSO ions dissociating in the **ion source** of the mass spectrometer. However, recent state-of-the-art ab initio calculations [11a] predict that $CH_2=S=OH^+$, **2** lies 84 kJ/mol lower in energy than **1**, with the global minimum on the $(C,H_3,S,O)^+$ potential energy surface being the isomer $HSC(H)OH^+$, lying another 92 kJ/mol lower. Turecek et al. [11c] also observed that ionized methanesulfenic acid, $CH_3SOH^{\bullet+}$, preferentially loses the H atom bonded to C, which, barring a reverse term for O-H cleavage, supports the theoretical prediction that **2** has a lower heat of formation than **1**.

If the barrier for isomerization, via a 1,3-hydrogen shift, of the DMSO ion into its *aci*-tautomer, $CH_2=S(OH)CH_3^{\bullet+}$ lies below the dissociation limit for loss of $^{\bullet}CH_3$ from **1** (the reaction of second lowest energy requirement, see section 1.3), it is feasible that at **low internal energies**, ion **2** is produced instead :

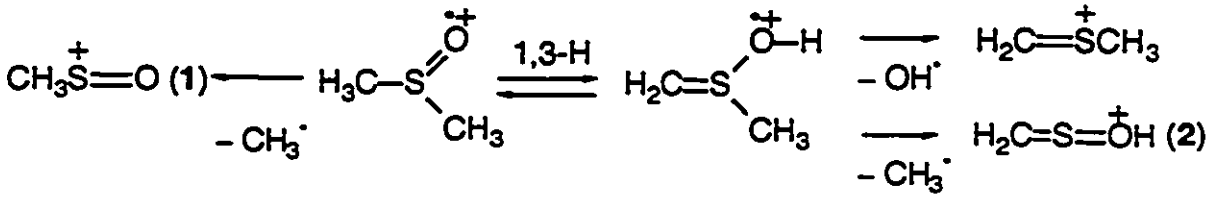

This question was answered in a recent study [12]. Using multiple collision experiments, it could be shown that loss of a methyl radical from ionized DMSO does indeed produce the O-protonated sulfine ion $CH_2=S=OH^+$, **2**. As mentioned above, selected results from this study, which *inter alia* led to a substantial revision of the ΔH_f of CH_3-S=O$^+$, are interspersed throughout this chapter to facilitate explanation of the experimental methodology.

The Mass Spectrometer and its principles

Electron ionization of a molecule, $M_1 + e^- \rightarrow M_1^{\bullet+} + 2e^-$, a *vertical* process in the Franck-Condon sense, is accompanied by the deposition of excess (potential or internal) energy if, as is normally the case, the kinetic energy of the impinging electron exceeds the ionization energy of the molecule, $IE(M_1)$. The excess energy is generally rapidly dispersed among the rotational and vibrational modes of the nascent molecular ions. Those molecular ions that have acquired sufficient internal energy will subsequently undergo successive rearrangement/dissociation reactions prior to detection, which in a sector mass spectrometer takes place within approximately 10 μs.

Theoretical treatments (QET/RRKM [13]) of unimolecular ion fragmentations [14] have been developed. They can in principle be used to predict the appearance of mass

spectra but in actual practice, their use is hampered by the fact that the relative abundances of the molecular and fragment ions in a mass spectrum are reflective of ions produced in the source of the mass spectrometer. Such ions comprise a broad and ill-defined range of internal energies and they may dissociate via a great many competitive and consecutive processes. Fortunately, it is also possible to study the fragmentation characteristics of ions possessing a narrow range of internal energies. Although this can be realized using a variety of instruments [8c,15], it proves advantageous to use a sector mass spectrometer of reversed geometry, where the magnet (B) precedes the electrostatic analyser (E). The VG Analytical ZAB-R [16] instrument used in our studies has such a configuration, see the simplified diagram of the instrument in Figure 1.1. The ZAB-R is in fact a unique three sector mass spectrometer of $B(\perp Q)E_1E_2$ geometry ($\perp Q$ indicates a perpendicularly mounted quadrupole mass analyser [17]) suited to perform experiments on (mass) selected ions [8]. In order to discuss the basics of these types of experiments, the operating principles of the instrument will first be briefly described.

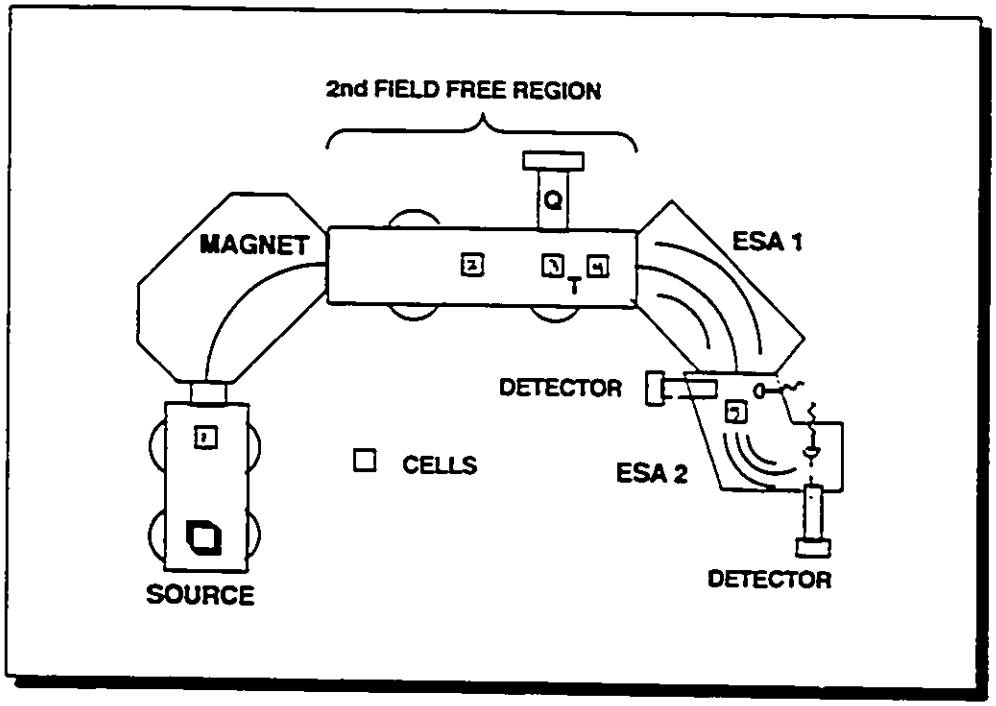

Fig. 1.1 Schematic of the VG Analytical ZAB-R mass spectrometer.

Molecular and fragment ions of charge z (or more properly ze, where z is an integer and $e = 1.6 \cdot 10^{-19}$ C) formed inside the source of the instrument are extracted therefrom, within microseconds, by a small potential gradient and then are accelerated through a voltage drop (V_{acc}), typically 8 - 10 kV, each obtaining translational energy:

$$zeV_{acc} = (mv^2) / 2 \qquad \text{Eq. (1.1)}$$

where m is the ion's mass (in atomic mass units) and v its velocity. Thus all ions having a given charge have the same translational energy.

The radial trajectory of ions in a magnetic field (B) is governed by the force relation:

$$Bzev = mv^2 / r \qquad \text{Eq. (1.2)}$$

and from these equations the following relationship obtains for source generated ions:

$$m/z = B^2er^2 / 2V_{acc} \qquad \text{Eq. (1.3)}$$

or equivalently (when r is in cm, V_{acc} in volts and B in teslas, 1 Tesla = 10^4 gauss):

$$m/z = 4.83 \cdot 10^3 (B^2r^2 / V_{acc}) \qquad \text{Eq. (1.3a)}$$

The selective transmission of ions through the magnetic sector according to their mass-to-charge ratio (m/z) can thus be accomplished, at a fixed accelerating voltage, by adjusting the flow of the current through the coils of the electromagnet.

Following the magnet, the ZAB-R has one large curved parallel-plate electric-sector analyser (ESA1) and then one with a smaller radius (ESA2). Transmission through an ESA in a circular path of radius R takes place when the centrifugal force on the ion is balanced by the force from the electric field (E_{ESA}) :

$$zeE_{ESA} = mv^2 / R \qquad \text{Eq. (1.4)}$$

The transmission of ions from the source through ESA1 is realized under the condition:

$$E_{ESA1} = 2V_{acc} / R_{ESA1} \qquad \text{Eq. (1.5)}$$

Transmission of source generated mass selected ions occurs when E_{ESA1} is set equivalent to the above value.

Until now, the possibility that some ions may dissociate outside of the ion source has not been entertained. A small percentage of ions do so spontaneously in their flight

to the detector and they are called *metastable* ions [18a,eb]. The instrument parameters constrain our observations to metastable dissociations having rates in the microsecond time-frame, i.e. for rate constants, k, predominantly in the range, 10^4 to 10^6 s^{-1}. Since rate constants are known to be rapidly increasing (to a maximum of ~10^{12} for a rearrangement reaction) functions of internal energy, the internal energies of metastable ions lie within narrow bounds. The term "first field free region (1FFR) metastable" refers to ions which dissociate in the ZAB-R between the ion source and the magnetic sector. The 2FFR describes the zone following the magnet up to ESA1 and the 3FFR lies between ESA1 and ESA2. In the general metastable dissociation of a parent ion to a daughter ion and a neutral, $M_p^+ \rightarrow M_d^+ + M_n$, the translational energy of M_p^+ ($m/z = (M_p)$) is partitioned between the products M_d^+ and M_n, such that M_d^+ will pass through the ESA when $E_{ESA}\{M_d^+\} = (M_d) / (M_p) \cdot E_{ESA}\{M_p^+\}$. The fragment ion M_d^+ also has reduced momentum, $(M_d) \cdot v = (M_d) \cdot (2\, zV_{acc} / (M_p))^{1/2}$, found using Eq. 1.1 and so for a dissociation that occurs in the 1FFR one finds, by substituting the reduced momentum into Eq. 1.2, that M_d^+ will be transmitted through the magnet an apparent m/z value of $(M_d)^2/(M_p)$. For example, in the experiments of Figure 1.2b, m/z 63 $[C,H_3,O,S]^+$ daughter ions generated from $DMSO^{\bullet+}$ (m/z 78) in the 1FFR were mass selected by setting the magnet to pass ions of mass- to-charge $(63)^2 / 78$ (i.e., m/z 50.9) and since V_{acc} was 8000 eV, these ions had (63/78) · 8000 = 6462 eV of translational energy.

With reversed geometry BE instruments, it is most common to obtain metastable ion (MI) mass spectra in the 2FFR. This is accomplished by setting the magnet to pass M_p^+ and then scanning ESA1. Having a second ESA, the ZAB-R also offers the possibility to obtain 3FFR MI mass spectra. This is done by setting the voltage difference of ESA1 = $2V_{acc} / R_{ESA1}$ thereby transmitting the "main beam" of stable, that is non-dissociating, ions through ESA1 to the 3FFR, and then scanning ESA2.

The abundance of the peaks in an MI mass spectrum are typically less than 1% of

the main ion beam intensity but they are relatively much broader. This broadening is a natural consequence of the conversion of internal energy of M_p^+ into kinetic energy of the separating fragments M_d^+ and M_n. The kinetic energy release, T, involved in this conversion is an intrinsic property of a particular dissociation process and its value may range from less than 1 meV to more than 1 eV. T values can readily be obtained by measuring the width of a metastable peak at height h, (ΔE_h), and using [18]:

$$T_h = (M_p)^2 \cdot V_{acc} \cdot (\Delta E_h)^2 / 16 \cdot (M_d) \cdot (M_n) \cdot (E_{ESA})^2 \qquad \text{(Eq. 1.6)}$$

with E_{ESA} = the electric sector voltage for transmission of the main beam and ΔE_h = the energy width of the metastable peak at height h. Kinetic energy release values are invariably obtained under conditions of high energy resolution, i.e. a main ion beam energy width of a few volts. This contribution to the overall energy width of the metastable peak may be ignored if it is relatively small. However, if the contribution is not negligible the following correction (although it is exact strictly for Gaussian-shaped peaks) can usually be applied: $\Delta E_h\,[\text{corrected}] = (\Delta E_h^2\{M_d^+\} - \Delta E_h^2\{M_p^+\})^{1/2}$. While most experiments on mass selected ions are performed under conditions of maximum sensitivity, that is with all beam defining slits open, increased mass and energy resolution can be realized at the expense of sensitivity by reducing the slit widths.

Metastable peak shapes and abundances are known to have important implications with regard to structures, isomerization energy barriers and the partitioning of energy upon dissociation of mass-selected ions [9a,18,19]. Isomeric ions which do not interconvert prior to dissociation will inevitably exhibit MI mass spectra having different peak shapes and abundances. A peak of simple Gaussian shape suggests that only one fragmentation is responsible for producing the corresponding ion, whereas a composite Gaussian peak shape indicates: (i) that an ion loses two isobaric fragments or, (ii) that an ion fragments to yield a pair of isomeric daughter ions or, (iii) that two isomeric ions dissociate, either via different reacting configurations to yield the same daughter ion or by loss of a particular neutral. Fragmentations that are linked to

relatively large energy releases lead to flat- or dish-topped peaks. Such peaks indicate the presence of energy barriers to the reverse reaction.

The Appearance Energy (AE) of the daughter ion M_d^+ is another important energetic quantity. The AE represents the minimum experimentally accessible energy required for the observation of M_d^+ generated from M_p^+ in either the ion source or a field free region. Measurement of the (metastable) ion signal for M_d^+ as a function of the ionizing (preferably monochromatic) electron energy yields a vanishing point which represents the (metastable) ion appearance energy. If the amount of extra energy needed to produce an observable signal on the time-scale of the experiment, that is the kinetic shift, and the reverse activation energy, ε^{rev}, are negligibly small, then from the relationship :

$$AE(M_d^+) = \Delta H_f(M_d^+) + \Delta H_f(M_n) - \Delta H_f(M_p) + \varepsilon^{rev} \qquad \text{(Eq. 1.7)}$$

the enthalpy of M_d^+ is obtained, provided $\Delta H_f(M_n)$ and $\Delta H_f(M_p)$ are known or can be accurately estimated. It is important to note that the following condition must also apply: $\Delta H_f^\circ(M_1^+) < \Delta H_f^\circ(M_2^+) + \Delta H_f^\circ(M_3)$.

MI mass spectra of DMSO and aci-DMSO

The MI mass spectrum of DMSO radical cations (Figure 1.2a) shows that DMSO ions undergo predominantly two dissociations in the microsecond time-frame, namely, loss of $^\bullet OH$ and $^\bullet CH_3$. The kinetic energy releases measured at half height ($T_{0.5}$) for these reactions were 23 and 18 meV (~ 3 kJ/mol) [12], in excellent agreement with those previously reported [11e,f]. These relatively small energy releases indicate negligible reverse terms, ε^{rev}, but they do not preclude rearrangement, as loss of $^\bullet OH$ from $DMSO^{\bullet+}$ obviously requires. For *aci*-DMSO ions the two MI peak intensities are no longer similar (Figure 1.2b); a m/z 61 : 63 ratio of approximately 4 : 1 is instead observed. The $T_{0.5}$ value for loss of $^\bullet OH$, 6 meV, has become much smaller while that for loss of $CH_3^\bullet$ has remained about the same. Perhaps more striking is the difference

in the shape and intensity of m/z 48 in the two mass spectra: in DMSO's MI mass spectrum the weak peak is clearly composite, the broad component having been ascribed to the formation of the more stable products $CH_4S^{\bullet+} + CH_2O$ and the narrow one to $SO^{\bullet+} + C_2H_6S$ [11f]. The intense m/z 48 MI peak from *aci*-DMSO ions has a simple Gaussian shape indicating the formation of only one ionic product, $CH_4S^{\bullet+}$. Comparison of these MI spectra does not give reason to exclude the possibility that some of the DMSO ions isomerize prior to their dissociation but clearly the two ions do not isomerize freely, i.e. to the extent that they become indistinguishable.

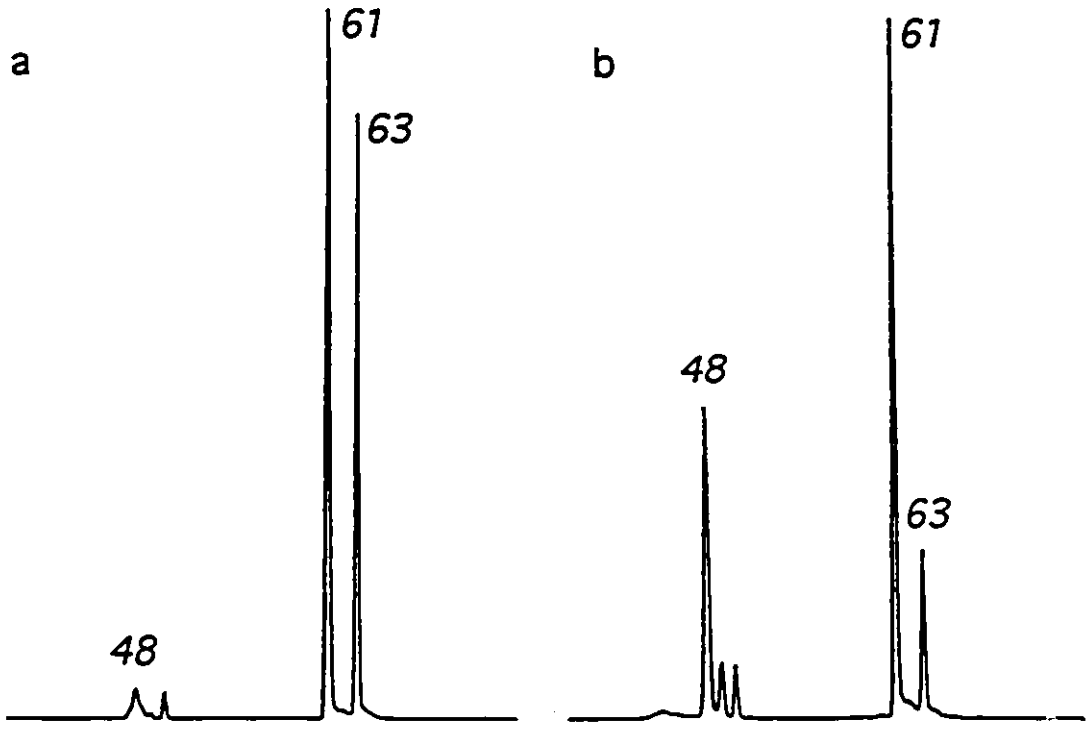

Fig. 1.2 (a) MI mass spectrum of DMSO; (b) MI mass spectrum of aci-DMSO.

Collision-Induced Processes

It has been known since the early days of mass spectrometry that the presence of gaseous atoms or molecules in the FFR's can lead to the *collision-induced dissociation* (CID) [8,20] of the fast moving ions. It can also lead, albeit generally to a smaller extent, to other reactions, namely charge stripping (CS), charge reversal (CR) and the charge-exchange neutralization discussed in Section 1.3 [8a,20a]. For singly charged ions, the interaction between the collision gas and an ion with keV translational energy is rapid and causes Franck-Condon-like excitation of the ion. This activation (from whence comes CID's other moniker: collisional activation, CA) step, leads to ions having a range of internal energies, not unlike that produced by electron ionization. A fraction of these ions will be able to access high energy direct bond fission reactions characteristic of the structure of the ion. This valuable capability of the technique was realized and exploited extensively by McLafferty, soon after he [21a] and Jennings [21b] introduced it.

In practice CID or CA mass spectra are obtained in the same way as MI mass spectra, except that a collision gas is deliberately introduced into a small collision cell in the appropriate FFR. Hence, an ion of a particular mass may be selected from the ion source and its CID mass spectrum can be considered a mass spectrum of a mass selected ion (MS/MS). Several factors affect the appearance of CID mass spectra: primarily the nature and pressure of the target gas, but also the internal and kinetic energy of the ion. Typically helium or oxygen are used as collision gases. Helium is quite efficient: being light and having a high IE, losses from scattering and neutralization processes are minimized. Oxygen provides a "softer" and heavier target. It induces charge stripping more readily and since it is the most common reionization agent for neutralization-reionization experiments, its use facilitates comparisons between the two types of spectra. The pressure of the gas is not normally measured directly. Instead, it is monitored by a gauge located outside the collision cell and a

pressure giving a 10-30% attenuation of the main beam, which corresponds to the single collision regime [7], is utilized.

It has been argued that differences in the internal energy of ions sampled in a CID experiment can lead to changes in the observed fragmentation patterns [7,20]. More important though is the translational energy of the ion, since it directly influences the amount of energy deposited by the collision event [22]. In general, the intensities of the peaks corresponding to low energy dissociations will be affected to a greater extent than structurally diagnostic ones of higher energy requirement. However, there are instances where the differentiation of isomers is more easily made on the basis of CID peak intensity ratios as the velocity of the ions diminishes [23]. This is not an insignificant observation, since one question which arises in CID experiments is how to assess the extent to which isomeric or isobaric species contribute to the population of the source generated ion beam.

One of the collision-induced charge permutation reactions, charge stripping (CS), $M_p^+ + G \rightarrow M_p^{2+} + G + e^-$, [8a,20a], may help in this regard since CS mass spectra of isomers can be substantially different even when the corresponding CID spectra are not. The greatest proportion of doubly charged positive ions is usually formed when using O_2 for collisional reduction, presumably because of its higher tendency to allow quasi adiabatic transitions and its capability for electron attachment. Although CS peaks are rarely of comparable intensity to the CID peaks, they may be overlapped by them. The study of doubly charged ions is at the stage of becoming an established aspect of gas phase ion chemistry [24a], thereby providing a complement to condensed phase studies [24b].

Charge-reversal (CR) [8a,20a,25] or charge-inversion of a fast moving positive ion is a two-electron transfer reaction which usually has a low cross-section. However, CR reactions of negative ions i.e., $M_p^- + G \rightarrow M_p^+ + G + 2e^-$ are more efficient and they lead, at least transiently, to positive ions of the same connectivity. This provides a route

to positive ions which may be impossible to generate any other way. Comparisons of this type of CR spectra with CID and $^{-}NR^{+}$ spectra (see below) have been used to establish the correspondence of connectivities for anion/neutral/cation sets [26].

MS/MS/MS: double collision experiments

Multi-sector mass spectrometers equiped with multiple collision cells make it possible to perform a variety of experiments in which sequential collision and/or dissociation steps occur [8a,28]. Some experiments on neutrals which fall into this category will be described in the following section. Many combinations of the processes listed above are possible but the MI/CID and CID/CID combinations are particularly valuable because they can be used to probe the structure of daughter ions directly in cases where isomeric ions could yield isobaric daughter ions having different structures. Isobaric ions have the same nominal mass but different elemental compositions. Knowledge of the daughter ion structure may then answer the question: "what was the structure of the parent it originated from?". This is clearly shown below for ionized DMSO: if the molecular ions dissociate by direct bond fission, then the product ion should be CH_3-S=O^{+}, whereas observation of CH_2=S=OH^{+} would indicate that rearrangement into the *aci*-DMSO radical cation has taken place prior to dissociation.

Collision experiments on $(C,H_3,S,O)^{+}$ ions from ionized DMSO and aci-DMSO ions

In Figure 1.3a our CID mass spectrum of the m/z 63 $(CH_3SO)^{+}$ ions generated from DMSO ions decomposing in the **ion source** is presented. The spectrum is consistent with that reported and discussed by Turecek et al. [11c] and it was readily rationalized on the basis of CH_3-S=O^{+}, **1**. Ion **1** is characterized by $^{\bullet}CH_3$ loss (m/z 48) and CH_3^{+} formation (m/z 15). That it also abundantly loses H_2O (to yield m/z 45, also present in the MI spectrum) is not to say [27], that it should not be represented as CH_2S=O^{+}.

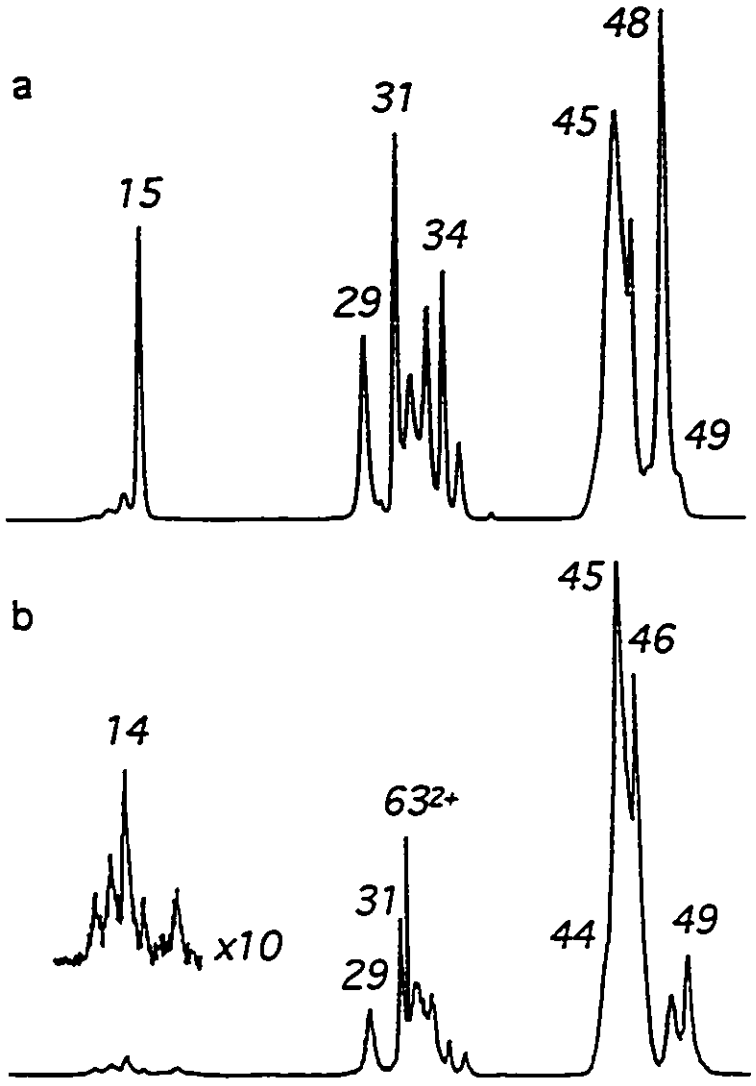

Fig. 1.3 (a) CID mass spectrum of the m/z 63 $(CH_3SO)^+$ ions generated from DMSO ions decomposing in the ion source; (b) MI/CID mass spectrum of the m/z 63 ions generated by the loss of $^{\bullet}CH_3$ from metastable $DMSO^{\bullet+}$ ions in the 1FFR.

The MI/CID mass spectrum of the m/z 63 ions generated by loss of $^{\bullet}CH_3$ from **metastable** $DMSO^{\bullet+}$ ions in the 1FFR is shown in Figure 1.3b. This spectrum is completely different from that shown in Figure 1.3a. In fact, it is entirely compatible with that reported by Turecek [11c] for source generated ions $CH_2{=}S{=}OH^+$, **2**, made from ionized di-n-butylsulfoxide. Ion **2** eliminates CH_2 (m/z 49) and forms $CH_2^{\bullet+}$ ions (m/z 14). Moreover, **2** has a high susceptibility to charge stripping, as evidenced by the presence of a narrow and prominent peak at m/z 31.5, corresponding to the doubly charged ion, $CH_2{=}S{=}OH^{2+}$. Confirmation that metastable *aci*-DMSO ions also dissociate to produce **2**, came from the fact that the MI/CID mass spectrum of those m/z 63 ions was virtually identical with that of metastable DMSO ions [12].

Thus, these single collision experiments indicated that the majority of the low energy DMSO ions disociate to **2**, not **1**. Whether or not this holds true for **all** of the metastable DMSO ions, cannot be inferred from these experiments: note that the spectra of ions of putative structures **1** and **2** do show minor peaks which may be indicative of the presence of the other isomer. One explanation for the presence of such peaks is the occurrence of a **post** collisional isomerization. Alternatively, a mixture of ions has been generated in which one of the isomers dominates. These two possibilities can often be distinguished by performing multiple collision experiments, in particular by performing NR/CID experiments which are described at the end of the next section and more explicitly in Part II of this thesis.

1.2 Mass spectrometry of neutrals (NRMS and CIDI)

The discovery that beams of fast moving **ions** undergo charge exchange with a neutral target gas to form beams of fast moving **neutrals**, gave Lavertu et al. [29], Devienne [30] and McMaster University's Gray and Tomlinson the means to investigate small hypervalent neutrals like He_2, HeH and H_3 [31]. After a period of dormancy, Porter and co-workers utilized the phenomenon in neutralized ion beam spectroscopic

studies of small hypervalent radicals [32]. Trailblazing work by the groups of McLafferty, Holmes, Terlouw and later Schwarz and Harrison developed Neutralization-Reionization mass spectrometry (NRMS) [4] into a powerful technique for generating and identifying elusive organic molecules in the gas phase. Among the many interesting entities characterized by NRMS are some molecules which have been presumed to be incapable of independent existence, e.g. H_2CO_3 (carbonic acid) and H_2SO_3 (sulfurous acid), plus a variety of other acids, enols, (hypervalent) radicals, carbenes, cumulenes, ylids and diradicals, which can be expected to have extremely short lifetimes in solution, as well as many other species of interstellar, atmospheric and organometallic importance [4]. One reason why NRMS has been so successfully applied in the generation of the elusive isomers of many well known molecules (i.e. isomers with elevated enthalpies and enhanced reactivities) is the fact that for many ionic systems, in contrast to the corresponding neutral systems, the "rare" isomer can be as stable, or even more stable, thermodynamically than the "common" isomer and thus the ionized form of the "rare" isomer may often be obtainable by simple dissociative ionization of an appropriate precursor molecule (see Chapters 8 and 9).

The structure of the neutral species produced by dissociation of an ion, be it spontaneous or collision-induced, can be investigated by a related complementary technique dubbed collision-induced dissociative ionization (CIDI) [4f], although some [4a] refer to it under the designation of NRMS.

The standard procedure in an NR experiment is to first generate the (radical) cation AB^+ in the mass spectrometer and to establish its structure and (isomeric or isobaric) purity. Next the NR experiment is performed: neutralization by electron transfer and deflection of the unreacted ionic species is followed (after about 1 μs) by collisional reionization of the fast moving neutralized species (Neutralization (oxidation) of and reionization to negative ions has also been demonstrated, giving rise to the nomenclature $^-NR^-$, $^-NR^+$, $^+NR^-$ and $^+NR^+$ [4h], but the latter is generally

assumed when just NR is used). Ideally, the collisional reionization step leads to the identification of the stable neutral species which correspond to the recovered ion signal and indeed the resulting NR mass spectrum is often recognizably similar to the CID (or even EI) mass spectrum of reference ions. NR mass spectra can readily be obtained from any ion present in the conventional mass spectrum of the compound under investigation. However, the combined neutralization-reionization efficiency is fairly low, typically 0.1 - 0.001 % of the main beam intensity, and thus a high sensitivity is often required.

A closer inspection of the events that may occur in an NR experiment, which are reiterated [4b,f,g] in Scheme 1.1 and below, indicates why neutral structure assignment may not always be a matter of straightforward spectral comparison.

Cell 4 (neutralization)

G_1 +	ABC^+	→	G_1^+ +	ABC				(Eq. 1.8)
G_1 +	ABC^+	→	G_1^+ +	$ABC^{\bullet}$	→	$AB^{\bullet}$ + $C^{\bullet}$		(Eq. 1.9)
					→	**BAC•**		**(Eq. 1.10)**
G_1 +	ABC^+	→	G_1^+ +	$ABC^{+\bullet}$	→	AB^+ + $C^{\bullet}$		(Eq. 1.11)
						$AB^{\bullet}$ + C^+		
				ABC^+	→	AB^+ + $C^{\bullet}$		(Eq. 1.12)
						$AB^{\bullet}$ + C^+		

Cell 5 (reionization)

G_2 +	ABC	→	G_2	+ e^- +	ABC^+	→	AB^+ + $C^{\bullet}$	(Eq. 1.13)
							$AB^{\bullet}$ + C^+	
G_2 +	$AB^{\bullet}$ + $C^{\bullet}$	→	G_2	+ e^- +	AB^+, C^+			(Eq. 1.14)

Scheme 1.1. The principal reactions of the generic ion ABC^+ in a NRMS experiment

Neutralization: After acceleration, typically to 4-10 keV, and mass-selection, the ions ABC^+ enter the first collision gas chamber (Cell 4) where electron-capture from a target gas, G_1, results in the reduction to the neutral species ABC (Eq. 1.8) in a vertical

Franck-Condon transition. All ions ABC^+ which have not been neutralized and also (the relatively minor fraction of) their ionic dissociation products (Eq. 1.11 and 1.12) are effectively removed from the beam by using a charged deflector electrode. The only species which journey on to the second collision gas chamber (Cell 5) are therefore the neutral molecules ABC (having the momentum ABC^+) and their uncharged dissociation products, e.g. AB and C (having the momentum of AB^+ and C^+ respectively).

Reionization: The fast moving neutrals ABC are reionized by collision with a target gas G_2 in the second collision chamber (Eq. 1.13 and 1.14). This oxidation step should be performed such that molecular (survivor) ions and also charged fragment ions are produced. The latter are recorded by scanning ESA2 and they serve to characterize the structure of ABC^+. Because it takes about a microsecond for the neutral generated in Cell 3 to travel to Cell 4, the presence of an ABC^+ signal in the NR mass spectrum indicates that the neutral is stable (has a lifetime > 10^{-6} seconds). However, the mere presence of a recovery ("survivor") signal does not prove that the neutral counterpart of ABC^+ is a stable entity. As shown by Eq. 1.10, it is also possible that all or part of the incipient neutral species ABC isomerize to a (more stable) isomer, BAC, prior to reionization. Therefore, a detailed analysis of the NR and CID mass spectra of isomeric ions is required, particularly in those systems where there is computational or experimental evidence for facile isomerization reactions of the neutral species. When the NR mass spectrum of a given ion is very close to its CID mass spectrum, the conclusion is often warranted that no isomerization has taken place, but only if it has been established (computationally) that there are high barriers towards isomerization. On the other hand, discrepancies between the CID and NR mass spectra of a given species may also find their origin in that NR mass spectra may contain, beside the reionized neutrals ABC and their fragment ions, interfering contributions from reionized neutrals $AB^•$ and $C^•$ produced in the following processes: (i) dissociation of "hot" neutrals $ABC^•$ (Eq. 1.9), (ii) collision-induced dissociation of ABC^+ (Eq. 1.11) and,

(iii) spontaneous dissociation of (metastable) ABC^+ ions (Eq. 1.12). Contributions from (iii) can easily be identified by putting a small voltage (>100 V) on Cell 4, because most of these neutrals are generated outside of the cell, but those resulting from the other two processes are often more difficult to verify.

If the neutralized ion beam is not isomerically pure, the presence of even minor amounts of isomeric (or isobaric) species which have a relatively high NR efficiency may cause additional problems with the interpretation of the NR spectrum. Fortunately, the possibility of obtaining NR/CID mass spectra often resolves these uncertainties (see the example at the end of this section and the studies described in Chapters 8 and 9).

Apart from a high NR efficiency, a balanced distribution of intact ions ABC^+ and structurally characteristic fragment ions, see reaction 1.13a, is desired in any NR experiment. As will be briefly discussed below, this and the degree of interference from the processes mentioned above, can be influenced to some extent by a judicious choice of the neutralization and ionization target gases.

The nature of the neutralization target gas is a crucial factor in a NRMS experiment since it affects the energy defect, Q, of the neutralization reaction [4c]. Since reaction 1.8 represents a Franck-Condon process, the energy deficit for the reaction can be defined as : $Q(G_1) = IE_v(G_1) - NE_v(AB^+)$ (Eq. 1.15)

where the subscript v indicates a vertical (Franck-Condon like) transition and NE is the neutralization (or recombination) energy for the ion going to the neutral. Three situations can occur: (i) $Q \sim 0$: resonant electron transfer, an efficient process; (ii) $Q < 0$: endothermic electron transfer, the energy deficit is provided from a slight diminution of the translational energy of the fast moving ions; and (iii) $Q > 0$: exothermic electron transfer, leading to the generation of species in (electronically) excited states and/or extensive dissociation thereof. Since charge transfer is a vertical process, the extent of overlap between the neutral and ionic states of the target gas will affect the charge exchange efficiency. Lindholm and co-workers have explored this phenomenon using

perpendicularly oriented MS/MS instrumentation [33]. Analogous neutralization target (NT) experiments can be realized on the ZAB-R using the quadrupole mass analyser ($\perp$Q) to detect the ionized target G_1^+ and, in the case of polyatomic targets, any fragment ions derived therefrom; the extent of fragmentation may offer more insight into the energetics of the exchange reaction.

The vertical nature of the neutralization and also the reionization step has another important consequence: if there are large differences in geometry for the ion under investigation and its neutral counterpart, the "survivor" signal in the NR mass spectrum may become vanishingly small. Thus, the absence of a measurable survivor signal does not necessarily imply that a given neutral species is not a stable entity. A case in point is the NR mass spectrum of the long-sought-after molecule ethylenedione, O=C=C=O [34] which is stable in its lowest triplet, but not singlet, state. In other cases, for example the carbenes of Chapter 8, it may also be desirable to determine in which electronic state the neutrals are produced.

In NR experiments, metal vapours are usually very efficient targets and in particular Hg (IE = 10 eV) has been used extensively. However, its use can have deleterious effects on instrument performance, unless it is contained properly [35]. This prompted the use of Xe [4b] which is a permanent gas and is quite efficient even though it has a high IE, 12.13 eV. More recently, vapours from polyatomic organics with lower IE's such as cyclopropane, trimethylamine, N,N-dimethylaniline and CH_3SSCH_3 have also found favour. They have a relatively high neutralization efficiency but are poor targets for collision-induced dissociation. This makes them particularly useful in studies of ions of low recombination energy [16a,36]. Many other targets have been studied [37] and even surface-induced neutralization has been attempted [38].

For collisional reionization, He and O_2 (at a pressure corresponding to single collisions) are the target gases of choice. Helium is usually very efficient but, unlike oxygen, it often induces extensive dissociation. Routine NR mass spectra are therefore

obtained with oxygen.

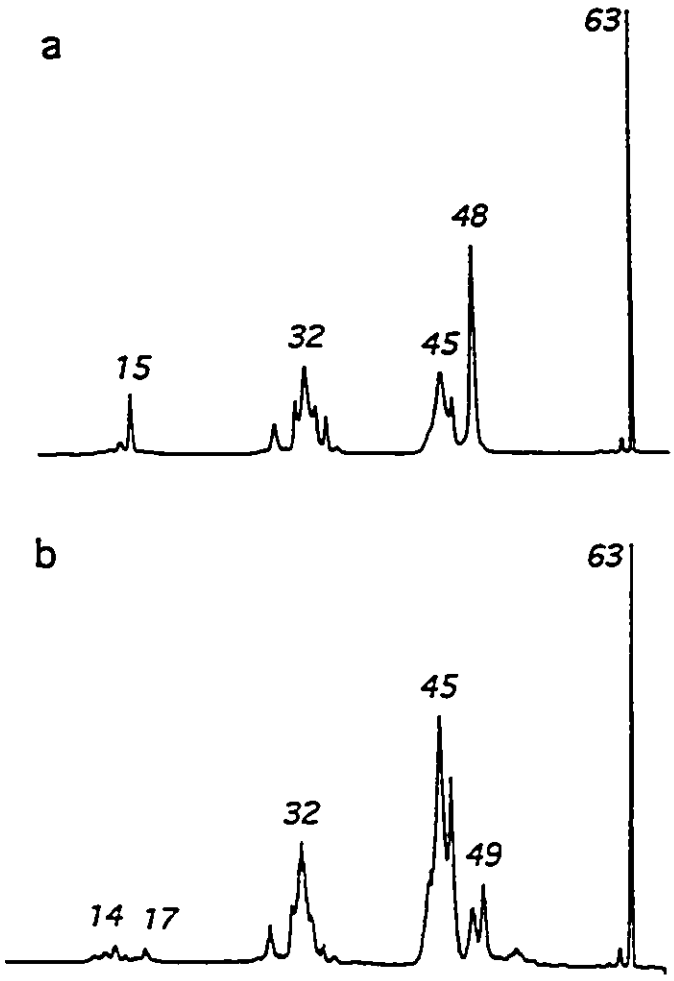

Fig. 1.4 (a) [NDMA, O_2] NR mass spectrum of the m/z 63 $(CH_3SO)^+$ ions generated from DMSO ions decomposing in the ion source; (b) [NDMA, O_2] NR mass spectrum of the m/z 63 ions generated by the loss of $^{\bullet}CH_3$ from metastable $DMSO^{\bullet+}$ ions in the 1FFR.

Neutralization-Reionization (NR) mass spectra of $CH_3S{=}O^+$ and $CH_2{=}S{-}OH^+$

The NR mass spectra of ions of putative structures **1** and **2** generated in our DMSO experiments are shown in Figure 1.4. They are in good agreement with those previously imparted in tabular form by Turecek et al. [11c]. Intense survivor (m/z 63) signals attest to the stability of the neutral counterparts of **1** and **2**. It is further seen that

the NR mass spectra of both are similar to their respective CID mass spectra and so once again there are characteristic differences between the two species. Reionized **1** (Figure 1.4a) shows the direct cleavage products $SO^{\bullet+}$ (m/z 48) and CH_3^+ (m/z 15) whereas **2** (Figure 1.4b) produces SOH^+ (m/z 49) and $CH_2^{\bullet+}$ ions (m/z 14). The enhanced intensity of m/z 48 in the NR mass spectrum of **1** (Figure 1.4a) compared to its CID mass spectrum (Figure 1.3a) probably results from reionized SO molecules produced by the dissociation of excited $CH_3SO^{\bullet}$ radicals.

The experimental results presented so far leave little doubt that the neutral counterparts of **1** and **2** are stable entities. However, they have not provided an unambiguous answer to the question raised earlier: "are the ions **2** generated from **metastable** DMSO ions isomerically pure?". This question will be addressed in the next section.

Collision-induced dissociation after Neutralization-Reionization (NR/CID)

When the identity of the reionized species in an NR experiment and/or the purity of the ions being neutralized is in doubt, the ability to perform MS/MS/MS experiments, especially CID of the NR *survivor* ion may prove invaluable [4c,e,g]. Such experiments, which are depicted schematically in Figure 1.5, are capable of revealing whether the main beam of ions originally consisted entirely of a single isomer species or if the neutrals isomerize to a significant extent (Eq. 1.10). In this context, NR/CID mass spectra may be compared directly with CID mass spectra obtained under the same conditions. If the spectra are the same, this virtually guarantees that the ion flux is pure and that structural integrity is maintained in the NR process. This is because isomeric (or isobaric) species will not normally have identical neutralization and also reionization efficiencies. Unfortunately, when the NR mass spectrum is weak, these revealing experiments may be precluded by a lack of sensitivity.

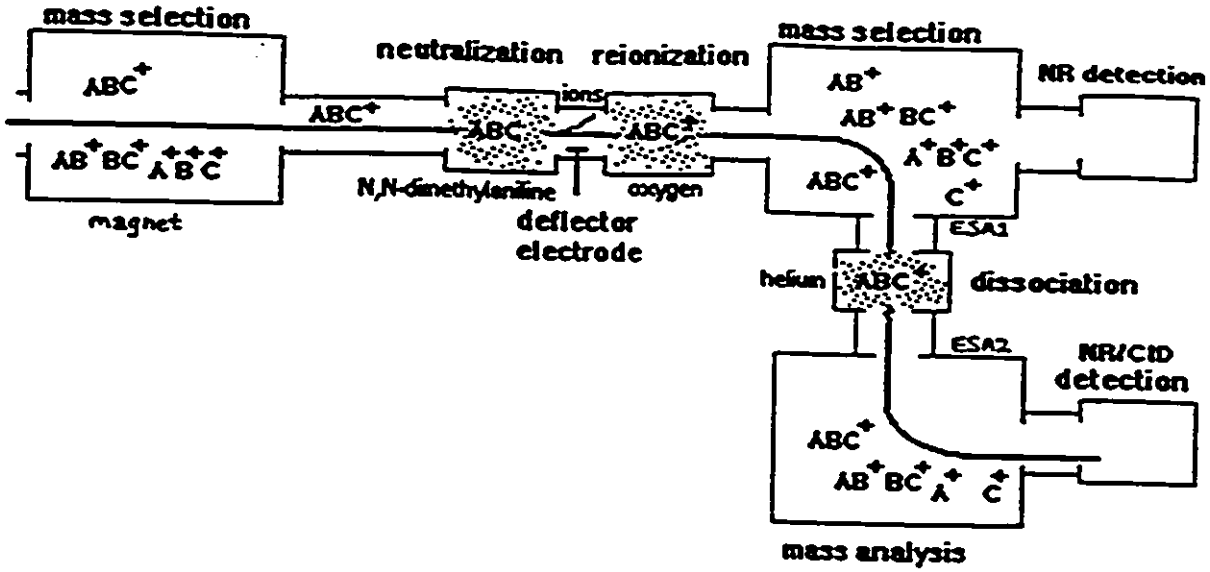

Fig: 1.5 Schematic depiction of an NR/CID experiment.

NR/CID mass spectra of $(C,H_3,S,O)^+$ ions from ionized DMSO

To settle the question raised earlier regarding the isomeric purity of the $(C,H_3,S,O)^+$ ions generated in the DMSO experiments, NR/CID mass spectra were obtained of the **survivor** ions in the NR mass spectra shown in Figure 1.4.

For the low energy DMSO product ions of putative structure **2**, this encompassed a four-stage experiment (MS/MS/MS/MS). First, the daughter ions resulting from the loss of $CH_3^\bullet$ from metastable DMSO ions in the 1FFR of the instrument are selected by B and an NR experiment takes place in the 2FFR. The resulting m/z 63 ions are selected by ESA1 and these ions are collisionally induced to decompose in the 3FFR; the resulting product ions are selected by ESA2 and detected. The resulting MI/NR/CID mass spectrum is shown in Figure 1.6b. It is seen that this spectrum is very close to the MI/CID mass spectrum obtained in the 3FFR of the metastable ions generated in the 1FFR, see Fig. 1.6a. Note that the spectra given in Figures 1.3b and 1.6a are not identical. This is because: (i) the resolution of 2FFR CID mass spectra is higher than that of 3FFR spectra and, (ii) different collision gases were used, O_2 and He,

respectively.

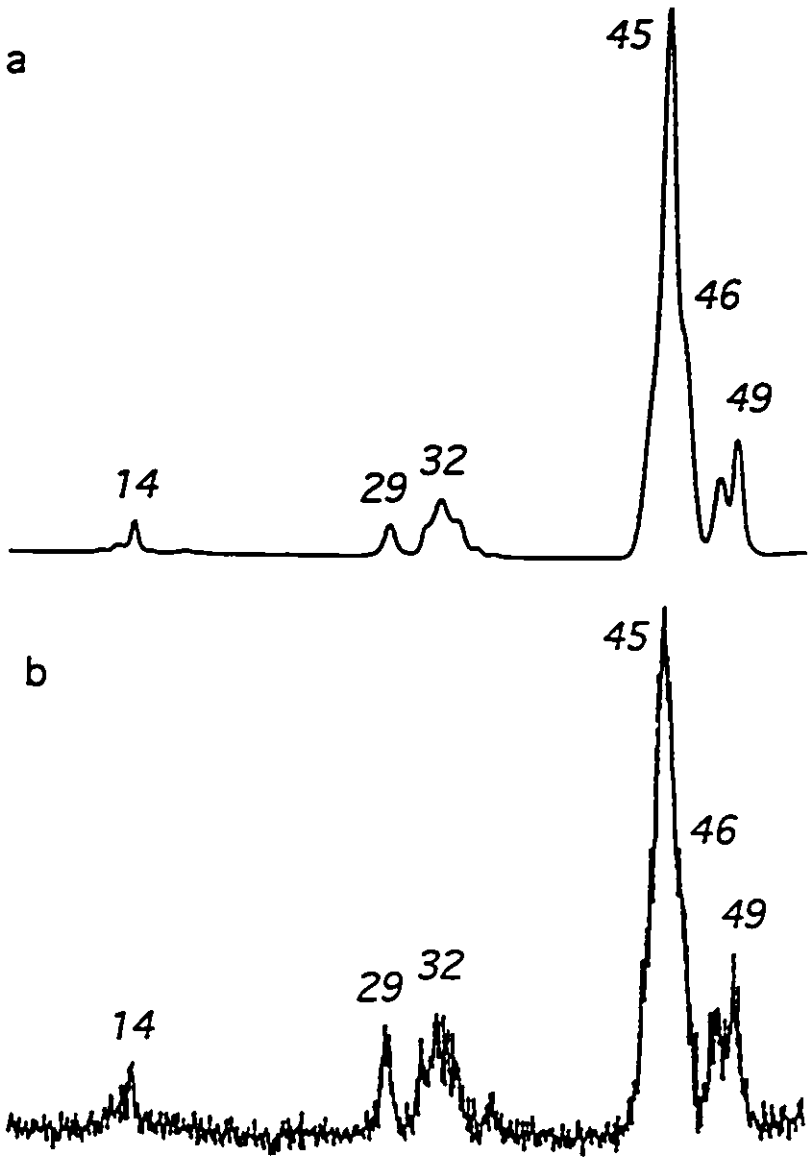

Fig. 1.6 (a) MI/CID mass spectrum obtained in the 3FFR of the m/z 63 ions generated by the loss of $^{\bullet}CH_3$ from metastable $DMSO^{\bullet+}$ ions in the 1FFR; (b) MI/NR/CID mass spectrum obtained in the 3FFR of the metastable ions generated in the 1FFR.

This experiment [12] not only provided convincing evidence that the neutral species **2** does not interconvert with **1**, it also showed that **metastable** DMSO ions produce **2**, virtually free from the isomer **1**. Similar experiments were performed with **source** generated ions [12] and here too the 3FFR NR/CID survivor mass spectrum was close to the 3FFR CID mass spectrum of the ions, thus providing further evidence that the source generated ions are $CH_3S{=}O^+$, **1**.

Collision-induced dissociative ionization (CIDI)

Scrutiny of the neutral species M_n generated in the unimolecular dissociations of ions, $M_p^+ \rightarrow M_d^+ + M_n$, was shunned initially because of a dearth of appropriate methods. The situation changed drastically when the CIDI technique [39], an easily performed variant of NRMS, was introduced. Being an ideal complement to ion characterization methods, it has given invaluable insights into reaction mechanisms. A case in point is the unexpected finding that metastable methyl acetate radical cations $CH_3C(=O)OCH_3^{\bullet+}$ not only lose $CH_3O^\bullet$ radicals but also $CH_2OH^\bullet$ [4b]. Moreover, the virtue of this technique as an auxiliary means to identify neutrals like $CH_3\text{-}C{=}O^\bullet$ [40a,b] and $CH_3O\text{-}C{=}O^\bullet$ [40c,d], which are at best marginally stable in NR experiments, should not be underestimated.

In a CIDI experiment the beam of neutrals, formed by spontaneous dissociation of the mass selected ion in the 2FFR, is isolated by deflecting all the ions out of the flight path prior to entering the collisional ionization chamber (cell 4). Neutrals M_n generated in in this way retain only a fraction, $(M_n) / (M_p) \cdot eV_{acc}$, of the parent ion's translational energy and, unless a large reverse energy is associated with their production, their internal energy content will be low. Studies have shown that the ionization efficiency improves as translational energy increases, declines as internal energy increases and depends on the IE of the target gas [41]. The energy necessary for ionization of M_n (a few eV) is taken from its translational energy (a few keV) and this

causes a (potentially measureable) displacement of the M_n^+ peak by the amount $IE(M_n)$.

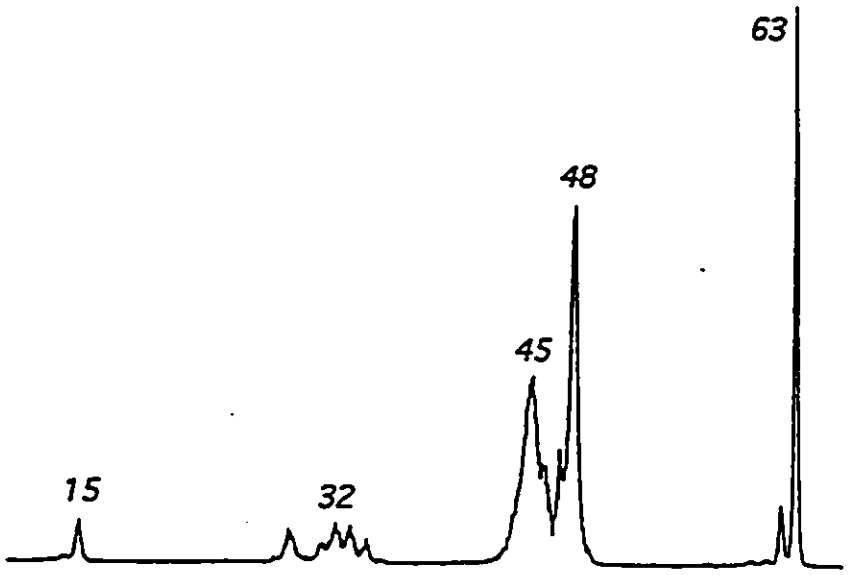

Fig. 1.7 CIDI mass spectrum of CH_3-S=O$^+$ from $CH_3S(=O)CH_2SCH_3^{\bullet+}$.

The CIDI mass spectrum of CH_3-S=O$^+$

The following experiment indicated that the source generated ions may also contain a (minor) contribution from **2**. Ions **1** were independently generated by collisional ionization of the CH_3S=O$^+$ neutrals produced by the spontaneous dissociation reaction: $CH_3S(=O)CH_2SCH_3^{\bullet+} \rightarrow CH_3S$=O$^+$ + $^+CH_2SCH_3$. In the resulting CIDI mass spectrum (Figure 1.7), which closely resembles the CR mass spectrum of CH_3S=O$^-$ [27c], m/z 48 ($SO^{\bullet+}$) is again very intense whereas the high energy CH_2 loss characteristic of ions **2** (m/z 49) is not discernable. It is interesting to note that m/z 15, which corresponds to the reciprocal products ($^+CH_3$ + S=O) of the former reaction, is considerably less intense than m/z 48 since simple energetic considerations favor formation of the methyl cation (by ~12 kcal/mol [42a]).

1.3 Ion and neutral thermochemistry

Empirical sources

Recently Lias et al., published a new compendium of thermochemical data for organic ions and their neutral counterparts [42]. In addition to heat of formation (ΔH_f) values, it provides up-to-date experimental ionization energies (IE) and proton affinities (PA). However, some of the values listed in the compendium were estimated and should thus be used with caution. For ionic or neutral species whose enthalpy of formation has not (yet) been established or is inaccesible, one of several estimation methods may suffice.

Benson's [43] simple additivity schemes are one method which can be used to predict reasonably (± 15 kJ/mol) accurate ΔH_f values for a great many neutral species. Alternatively, isodesmic equations may be used. These rely on the assumption that the difference in enthalpy from a functional group substitution which interconverts two molecules of known ΔH_f will be unchanged when the same substitution is applied to another molecule of known ΔH_f, thereby yielding ΔH_f of the desired species. This method has limitations when extended to ions because the assumption does not necessarily hold for a substitution made in proximity to a charge bearing site [44]. In some of these cases, the empirical relationships proposed by Holmes and Lossing [45] for a variety of odd electron ions or by Benoit and Harrison [46] for even electron ions may prove useful. The status of ion thermochemistry was reviewed not long ago by Holmes [47].

Theoretical approaches

Physico-chemical properties are also increasingly becoming available from ab initio computations [48]. The G2 method recently developed by Pople and Curtiss [49] is able to predict chemically accurate (±10 kJ/mol) heats of formation, ionization energies and proton affinities, but only for small molecules and ions [5a]. This very high

level of theory is achieved by combining results from ab initio calculations at several slightly lower levels of theory. However, these calculations are currently impracticable for larger systems and it is typical in these cases to assess only relative energies of isomers at the lower levels of theory with at least one value anchored to an experimentally established heat of formation. Radom's review [5a] summarizes clearly the thermodynamic parameters accessible for solitary ions and neutrals from ab initio methods. They are the following: geometries and energies of equilibrium structures, dissociation products and transition structures which represent saddle points separating the minimum energy structures. These allow assessment of dissociation energies, reaction barriers, ε^{rev}, and, when both ionic and neutrals forms are studied, IE's and NE's (both adiabatic and vertical) and also PA's.

The standard ab initio approach is to use a variational method, usually the Hartree-Fock (HF) molecular orbital method, to optimize the molecular structure as a function of the total energy of the system using molecular orbitals (MO's) which are derived from a linear combination of atomic orbital (LCAO) basis functions [50]. The number of basis functions utilized (the size of the basis set), affects the reliabilty of the results but the time/cost increases rapidly with size. A number of Pople's basis sets [48] have proved quite popular and the split valence ones (3-21G, 4-31G and 6-31G) generally produce reasonable ΔH_f information. Split valence basis sets with higher numbers use more functions to describe the one-electron orbitals. The quality of the basis set can be improved upon by adding polarization and diffuse functions to heavy atoms, which are denoted by the symbols * and + respectively, e.g. 6-31G*. If such functions are added to hydrogen atoms the symbols are repeated, e.g. 6-31G++. Since geometry optimization is computationally demanding, it is quite common to determine the energy in two steps, first optimizing using a smaller basis set and then, with the nuclei fixed, performing a single point calculation using a larger basis set.

Size consistency is a feature of the HF method. It means that the properties of

molecules of different sizes may be compared. However, there is a major drawback of HF theory: it does not adequately account for the electron-electron interactions. The missing electron correlation can be treated by a variety of methods including (Moller-Plesset [51]) perturbation theory or Configuration Interaction [52]. Most often this is done only at the single point calculation stage and it is indicated in Pople's nomenclature [48] as e.g. MP2/6-31G**//4-31G for perturbation to second order included on a system which was first optimized with the smaller 4-31G basis set.

Semi-empirical methods [53] are less computationally intensive and they have proven useful for investigations of systems beyond the reach of the ab initio methods. However, energetic predictions from these methods should be used cautiously since these methods are limited by their parameterization and the predictions sometimes fall wide of the mark.

DMSO: The structure and enthalpy of formation of the $[M-{}^{\bullet}CH_3]^+$ ions

Recently, using the sophisticated technique of threshcld photoelectron photoion coincidence spectrometry (TPEPICO), Zha et al. [11d] measured the AE for loss of $^{\bullet}CH_3$ from DMSO ions; AE = 10.64 ± 0.07 eV from which ΔH_f (m/z 63) = 736 kJ/mol obtains. This ΔH_f was assumed to be that of $CH_3S{=}O^+$, **1**. However, we have shown [12] that this is not the case and that DMSO ions dissociating near (see below) threshold produce **2**, most likely via rearrangement of DMSO to the *aci*-tautomer. If the rearrangement barrier is also below or close to the dissociation limit for **2** + $^{\bullet}CH_3$ the reported AE corresponds to the formation of ions **2**.

How close to threshold do the metastable ions dissociate? An estimate was obtained from an examination of the metastable ion data (Figure 1.2a) and the precise energetic data of Zha et al. [11d]. According to Zha et al., AE(m/z 63) = 10.64 ± 0.07 eV, whereas the AE(m/z 61) = 10.55 ± 0.07 eV. These represent the two major processes in the μs time-frame. The next higher AE is for m/z 45 and m/z 47, 10.69 ± 0.13 eV, but

these processes are not observed in the MI mass spectrum (weak peaks at m/z 48 and 50 are observed in the MI mass spectrum but these processes were not investigated in the photoionization study [11d]). Given these AE differences and their uncertainties, the upper limit for the internal energy content <E> of the DMSO ions above the dissociation threshold is 0.25 eV (~ 25 kJ/mol). It is appropriate to note that, even close to threshold, m/z 63 is much larger than m/z 61 in the breakdown graph of DMSO [11d] but that the intensity of m/z 63 decreases rapidly at low energies. The metastable peaks for these processes are of roughly equal intensity (Figure 1.2a) which is only compatible with the breakdown graph, if it is assumed that these processes take place very close to threshold, i.e. within 0.05 eV. Note that this is not in contradiction with average kinetic energy releases, <T>, which are not exceedingly small: experiments [53] have indicated that at threshold the fraction <T>/<E> increases rapidly as <E> decreases, as predicted by Klots' equation [55].

The above experimental findings led to the conclusion [12] that low energy DMSO ions produce $[C,H_3,S,O]^+$ ions of structure **2** rather than **1** and that the measured AE of m/z 63 corresponds to **2**, hence $\Delta H_f(\mathbf{2}) = 736$ kJ/mol. In addition, considering the ab initio results of Gozzo and Eberlin [11a], revision of $\Delta H_f(\mathbf{1})$ to 807 - 820 kJ/mol was simultaneously recommended [12].

An independent confirmation of $\Delta H_f(\mathbf{2})$ could come from a determination of the proton affinity of sulfine. Considering the short lifetime, $t_{1/2} \approx 30$ min [56] of gaseous sulfine, ab initio calculations may be the most expedient method of evaluating its proton affinity. Alternatively, $\Delta H_f(\mathbf{1})$ may be realized by a computational evaluation of the energy required for dissociation into $SO^{\bullet+} + {}^{\bullet}CH_3$ or $CH_3^+ + SO$. The validity of this approach was recently demonstrated by Ruttink et al. [11g] whose quantum chemical calculations predicted $\Delta H_f(\mathbf{1}) = 838$ kJ/mol and, gratifyingly, $\Delta H_f(\mathbf{2}) = 739$ kJ/mol.

1.4 Ion structures : Ion-molecule complexes and distonic ions

Bonding and molecular structure are quintessential aspects of chemistry [57,58,59]. The dominant theme in organic chemistry is covalent bonding: the sharing of two electrons between two atomic centres. However hydrogen bonds [60] and other novel patterns where electrons are shared between several atoms exist, and the species which exhibit them continually attract attention [59,61,62]. Interesting too are reactive intermediates, many of which are charged species that are relevant in solution and the gas phase [63]. Among the latter are loosely-bound ion-molecule complexes [A•••B$^+$], whose structures defy conventional covalent bond descriptions [64] . These species owe their stabilization towards dissociation largely to favourable electrostatic interactions, typically 40-125 kJ/mol. One of the objects of this thesis is to obtain more insight into the properties of these species and the roles that they play in the dissociation chemistry of ionized molecules (see Chapters 2, 3, 5 and 6).

From a historical point of view, acceptance of ion-molecule complexes grew out of discussions about possible transient intermediates involved in bimolecular encounters. While the earliest suggestion of complex mediated ion dissociation may date back to 1956 [65], only following the seminal examples of Bowen, Stapleton and Williams [66], Morton [67] and Longevialle and Botter [68] did it became apparent that their involvement in unimolecular ion reactions is a widespread phenomenon. Several comprehensive reviews [64] have been published, which summarize a great deal of the information that has since accrued on these species.

Most of the support for these ion-molecule complexes comes from ab initio MO calculations rather than direct experimental observations; a fact which prompted McAdoo [64e] to advance a set of six experimental criteria for such ions. Morton [69] has pointed out that a type of ion-neutral "complex" not associated with a local minimum on the relevant potential energy hypersurface should be capable of existence if it is restricted by entropic bottlenecks in what he terms a "locked rotor critical

configuration". The majority of ion-molecule complexes considered to date do correspond to energy minima and an introductory description of them is facilitated by their categorization first into two classes: hydrogen-bridged ions and ion-dipole complexes. Ions in both of these classes can be further distinguished as possessing an even or odd number of electrons.

Even-electron proton-bound cations $[A\cdots H\cdots B]^+$ are a well known type of hydrogen-bridged ion; a great variety of such species has been generated via ion-molecule reactions under conditions of chemical ionization or high pressure mass spectrometry. The hydrogen bond energies of symmetric (A=B) type species with bridges of the kind -O···H···O- and -N···H···N- have been shown to be nearly constant, at ~120 and 100 kJ/mol, respectively [70,71]. For unsymmetric species, a reduction in the dissociation energy of the hydrogen bond was found to correlate with increasing difference in the proton affinities (PA's) of A and B and it was further predicted that for an -N···H···O- species having PA(A) = PA(B), a bond energy of ~120 kJ/mol would obtain [71]. Longevialle's review [64c] covers most of the recent experimental and theoretical studies. Among these are reports of more -C···H···O- type [72,73] intermediates involving ketene proton-bound to acetaldehyde [74], acetone [75] or formaldehyde [76] and of the ion $[H_2C{=}CH_2\cdots H\cdots OH_2]^+$ [77]. Ab initio calculations on CH_6NO^+ isomers [78] predict the existence of the -N···H···O- species $[H_3N\cdots H\cdots O{=}C{:}_2]^+$ and $[H_2C{=}N(H)\cdots H\cdots OH_2]^+$ and the stable -C···H···N- bonded ion $[HOC(H)\cdots H\cdots NH_3]^+$ and in Chapter 6 of this thesis $[O{=}C{=}CH_2\cdots H\cdots (H)N{=}CH_2]^+$ is implicated in the dissociation chemistry of the N-acyl- iminium ion [79].

Odd-electron hydrogen-bridged radical cations $[A\cdots H\cdots B]^{\bullet+}$ are rapidly proliferating in the mechanistic proposals of gas phase ions. Leading references may be found in the reviews by Burgers & Terlouw and Heinrich & Schwarz [80b,c]. The generation of hydrogen-bridged radical cations may represent an experimental challenge since they are not easily formed in ion/molecule reactions, but even so there

remains a more difficult inherent problem; that is, how to unambiguously identify them. As Burgers and Terlouw point out [80b]: *"it is often not possible to assign a unique structure to an ion on the basis of reactivity, MI or CID experiments when its isomeric forms are reasonably expected to give closely similar characteristics"*. The poignancy of this predicament is extreme when the hydrogen-bridged ion is expected to fragment in the same manner as a distonic isomer (see below) e.g., $[CH_2=C(H)-O\cdots H\cdots OH_2]^{\bullet+}$ vis-à-vis $H_2O^+-CH_2-{}^{\bullet}CH-OH$ and ${}^{\bullet}CH_2-CH(OH)-{}^+OH_2$ [81], or like an ion-dipole complex (see below) as in the case of the ketene-water complex $[CH_2=C=O/H_2O]^{\bullet+}$ [80d,82]. In such cases, computations of relative energies and isomerization barriers may be the only recourse for assigning structures to experimentally observed species. Reliable information about hydrogen-bridged cations can usually [83] be obtained from ab initio computational methods employing split-valence basis sets in geometry optimizations and polarization functions, electron correlation and zero point vibrational energy (ZPVE) corrections in single point calculations [80d,e]. Structurally, these unconventional ions may have the aspect of a complex between a molecule and a radical cation, i.e., $[A\cdots H-B^{\bullet+}]$, a species wherein a molecule is bound by a proton to a radical i.e., $[A\cdots H^+\cdots B^{\bullet}]$, or perhaps most interestingly an even-electron ion and radical pair i.e., $[A-H^+\cdots B^{\bullet}]$, where the charge and the unpaired electron reside in disparate fragments. The lack of sufficiently reliable data may explain why no empirical thermodynamic relationship has yet been developed for these odd-electron ions [46]. Nevertheless, the energies of known -O···H···O- and -O···H···N- species [4e,84] have been found to adhere reasonably well to the formulae proposed for hydrogen-bridged even-electron ions [70,70b].

The $C_2H_6O_2^{\bullet+}$ [80e,81-83,85] and $C_3H_6O_2^{\bullet+}$ [86,87] systems have proved a veritable cornucopia of hydrogen-bridged radical cations with a total of at least eleven different species, including the preeminent ions $[CH_2=C(H)-O\cdots H\cdots OH_2]^{\bullet+}$ and $[CH_3C=O\cdots H\cdots O=CH_2]^{\bullet+}$, corresponding to potential energy minima. The -C···H···O-

bonded isomers of these two are less stable and lie in relatively shallow wells, as does the $C_2H_6O^{\bullet+}$ ion $[CH_2{=}C(H)\cdots H\cdots OH_2]^{\bullet+}$ [80d,88]. Nonetheless, other ions of this type like $CH_2{=}C(H)\cdots H\cdots O{-}C(H){=}CH_2^{\bullet+}$ [89] or $[CH_2O(H)\cdot H\cdot CO]^{\bullet+}$ (from glycolaldehyde [90]) as well as -C···H···N- and -C···H···C- bridged species akin to these, are gaining further consideration in the dissociation chemistry of ionized glycol [83], acetol [87c], acetic acid [80c,d], acetamide [80c,d,91] and acetone [80c,80d,92]. Recent work in this laboratory indicates that they also play an important role in the chemistry of methyl glycolate and 1,2-propanediol and that previously reported mechanistic proposals [85a, 93] need to be revised. Two -N···H···O- bridged ions feature in a recent study of $CH_5NO^{\bullet+}$ ions by Burgers et al. [94] and others are invoked as key intermediates in the gas phase chemistry of ionized methyl carbamate desrcribed in Chapter 2 of this thesis.

Ion-dipole complexes and *ion-induced dipole complexes*, as their designation implies, derive their stability from favourable electrostatic interactions. For the former the simple formula [64d,e]: $E_{stab} = 288 \cdot q\mu \cos\theta / r^2$ Eq. (1.15) (for an ion having q charges, where μ is the permanent dipole moment of the neutral (in Debye), θ is the angle between the dipole vector and the point charge to dipole axis and r (in Å) is the distance between the dipole and the point charge), provides a reasonable estimate of the complexation (stabilization) energy (in units of kJ/mol).

Ruttink [95] has been able to provide a theoretical formulation supporting the expectation of very small kinetic energy release values (< 1 meV) for metastable dissociations of ion-dipole complexes. Holmes [46] has noted that small energy releases may be the best single observable criterion for inferring the presence of such complexes (see Chapter 6) but it should be noted that the same phenomenon can have other origins [96].

The observation of atom exchange reactions from remote sites in appropriately labelled isotopomers provides strong experimental evidence for the reorientation

capacity of the components of an ion-molecule complex, as is the case in the dissociation reactions of 3-amido steriods bearing an amino substituent on the D-ring [64c]. Computational studies [80c-e] of ion-molecule structures and their related potential energy surfaces indicate a significant freedom of motion and relatively large intercomponent separations which provides support for this capability. Calculations often also predict relatively facile interconversions between isomeric hydrogen-bridged ions and ion-dipole complexes at internal energies below the dissociation threshold.

Examples of ion-molecule systems abound in the reviews [64] and only two new ones are mentioned here: the $C_3H_5O_2^+$ acylium ion-formaldehyde dipole complex [76] and the iminium ion-water dipole complex, $[H_2C{=}NH/H_2O]^{\bullet+}$ [97], both of which have been investigated by experiment and theory.

One final type of complexes that receive only a mention here are π complexes. While these familiar intermediates from solution chemistry [59] are being pondered over in the gas phase dissociations of arenium ions [64b,98], they are not integral to the work described in this thesis.

Distonic and ylid ions have initially also been referred to as ion-dipole complexes [99] but it is now well established that these species are more tightly bound and that they form a well defined class of stable radical cations [100]. The term distonic [101,102] is used to describe radical cations in which the charge and radical sites are formally located at separate heavy atoms e.g. $^{\bullet}CH_2\text{-}CH_2\text{-}^{+}OH_2$, the β-distonic isomer of ionized ethanol and $^{\bullet}CH_2\text{-}NH_3^+$, the ylid isomer of methylamine. It has been observed that distonic ions are more susceptible to charge stripping than their isomers of conventional structure. There is a considerable volume of literature on these species (for leading references see [64a,99,103]) and the work described in Part I (Chapters 2-6) of this thesis attests to the important role these ions play in rearrangement reactions of ions of more conventional structure.

Chapters 2 and 3 discuss the unimolecular chemistry of the methyl carbamate

radical cation, $H_2NCOOCH_3^{\bullet+}$. Its isomerization and dissociation reactions, which involve distonic and hydrogen-bridged radical cations, are studied by MI, CID and NR mass spectrometry, isotopic labelling experiments and ab initio molecular orbital computations.

Chapter 4 discusses the participation of isomeric distonic ions in the unimolecular chemistry of the N-methyl-O-methyl carbamate radical cation, $CH_3N(H)COOCH_3^{\bullet+}$. While thermochemistry and MI, CID and NR mass spectrometry form the core of this study, the value of "double collision" MS/MS/MS-type experiments is also demonstrated by the generation and characterization of the elusive (O-protonated ioscyanic acid) ion $H\text{-}N{=}C\text{-}OH^+$.

Chapter 5 discusses a combined mass spectrometric and (extensive) ab initio computational study of the CH_5N_2 system. The thermodynamic and kinetic stabilities of CH_3NHNH^+, $CH_3NNH_2^+$, $CH_2{=}NH\text{-}NH_2^+$, the ring-closed form of the latter and the hydrogen-bridged species $CH_2{=}N{\cdot}\underline{H}{\cdot}NH_2^+$ are (re)evaluated. Theory is also used in conjunction with NR and multiple collision (NR/CID) experiments to evaluate the stability of the $CH_2{=}NH\text{-}NH_2^{\bullet}$ radical.

In Chapter 6 a mechanism for the gas phase deacetylation reaction of the prototype amidoalkylating reagent, the N-acyliminium ion $CH_2{=}N(H)\text{-}COCH_3^+$, is proposed. The experimental evidence for the intermediate even-electron hydrogen-bridged complex $[CH_2{=}N(H)\cdots H\cdots CH_2{=}C{=}O]^+$ is discussed. Metastable ion and collisional activation mass spectrometry, isotopic labelling experiments and ab initio calculations were also used to study and characterize several other $C_2H_6NO^+$ isomers.

Part II of the thesis focusses on the generation and identification of elusive neutral species by means of collision-induced dissociative ionization (CIDI) and neutralization-reionization (NR) mass spectrometry as well as the valuable multiple collision technique: collision-induced dissociation of NR survivor ions (NR/CID or NR/CA).

Chapter 7 describes the identification, by CIDI, NR and CID/CID (MS/MS/MS) experiments, of three isomeric C_2NO cations and neutrals.

Chapter 8 discusses the generation and characterization of two fundamental, but previously unobserved, carbenes: diaminocarbene (H_2N-C-NH_2) and dihydroxycarbene (HO-C-OH). They are excellent examples of molecules which require NR/CA experiments to enable their unambiguous identification.

Chapter 9 presents experimental evidence for the existence of the imidic acids H-N=C(H)-OH_2 and CH_3-N=C(H)-OH_2 as well as their tautomeric carbenes H_2N-C-OH and CH_3N(H)-C-OH. Characterization of the ionic precursors, which were generated by dissociative ionizations of appropriate precursor molecules, relied on a detailed analysis of CID and CID/CID mass spectra from ^2H and ^{15}N labelled isotopomers. Information from NR/CID mass spectra and labelling experiments was essential for assigning structures to the neutral species produced by electron transfer in NR experiments.

References

1 (a) Adv. Mass Spectrom. Vol. 1, J.D. Waldron (ed.) Pergamon Press: London (1959); (b) ibid. Vol.2, R.M. Elliot (ed.), Pergamon Press: London (1963); (c) ibid. Vol. 3, W.L. Mead (ed.), Elsevier: London (1966); ibid. Vol. 4, E. Kendrick (ed.), Elsevier: London (1971); ibid. Vol. 5, A. Quale (ed.), Elsevier: London (1971); ibid. Vol. 6, A.R. West (ed.), Applied Science: Essex (1974); ibid. Vol. 7, N.R. Daly (ed.), Heyden & Son: London (1978); ibid. Vol. 8, A. Quale (ed.), Heyden & Son: London (1980).

2 (a) F.W. McLafferty and F. Turecek, Interpretation of Mass Spectra (4th Ed.), Univ. Sci. Books, California (1993); (b) H. Budzikiewicz, C. Djerassi and D.H. Williams, Interpretation of Mass Spectra of Organic Compounds, Holden-Day: San Francisco (1964); (c) Mass Spectrometry of Organic Ions, F.W. McLafferty (ed.), Academic Press: New York (1963); (d) J.H. Beynon, Mass Spectrometry and Its Applications to Organic Chemistry, Elsevier: Amsterdam (1960).

3 Gas Phase Ion Chemistry, M.T. Bowers (ed.), Academic Press: New York (1979).

4 (a) C. Wesdemiotis and F. W. Chem. Rev. 87 (1987) 485; (b) J.K. Terlouw and H. Schwarz, Angew. Chem., Int. Ed. Engl. 26 (1987) 805; (c) J.L. Holmes, Mass Spectrom. Rev. 8 (1989) 513; (d) H. Schwarz, Pure Appl. Chem. 61 (1989) 685; (e) J.L. Holmes, Adv. Mass Spectrom. 11 (1989) 53; (f) J.K. Terlouw, Adv. Mass Spectrom. 11 (1989) 984; (g) F.W. McLafferty, Science 247 (1990) 925; (h) F.W. McLafferty, Int. J. Mass Spectrom. Ion Processes 118/119 (1992) 221; (i) F. Turecek, Org. Mass Spectrom. 27 (1992) 1087; (j) N. Goldberg and H. Schwarz, Acc. Chem. Res. (1994) submitted.

5 (a) L. Radom Org. Mass Spectrom. 26 (1991) 359; (b) L. Radom, Int. J. Mass Spectrom. Ion Processes 118/119 (1992) 339 and references therein.

6 H.-F. Grützmacher, Int. J. Mass Spectrom. Ion Processes 118/119 (1992) 825.

7 J.L. Holmes, Org. Mass Spectrom. 20 (1985) 169.

8 (a) K.L. Busch, G.L. Glish and S.A. McLuckey, Mass Spectrometry/Mass Spectrometry, VCH: New York (1988); (b) F.W. McLafferty, Org. Mass Spectrom. 28 (1993) 1403; (c) Tandem Mass Spectrometry, F.W. McLafferty (ed.), Wiley: New York (1983).

9 (a) K. Levsen, Fundamental Aspects of Organic Mass Spectrometry, Verlag Chemie: Weinheim (1978) p.209; (b) J.H. Beynon and R.G. Cooks, Adv. Mass Spectrom. 6 (1974) 835; (c) J.H. Beynon and Gilbert, in ref 3: Vol. 2 (1979), Chapter 13; (d) I. Howe, D.H. Williams and R.D. Bowen, Mass Spectrometry, Principles and Applications (2nd Ed.), McGraw-Hill: New York (1981).

10 (a) Dimethylsulphoxide, Vol. 1, S.W. Jacob, E.E. Rosenbaum and D.C. Wood (eds.), Marcel Dekker: New York (1971); (b) F.G. Bordwell, Acc. Chem. Res. 21 (1988) 456; (c) Synthesis (1981) 165.

11 (a) F.C. Gozzo and M.N. Eberlin, Presented at the 41st ASMS Conference on Mass Spectrometry, San Francisco (1993) Abstract # 974a; (b) S. Wolfe and H.B. Schlegel, Gazz. Chim. Ital. 120 (1990) 285; (c) F. Turecek, D.E. Drinkwater, F.W. McLafferty, J. Am. Chem. Soc. 111 (1989) 7696; (d) Q. Zha, T. Nishimura and G.G. Meissels, Int. J. Mass Spectrom. Ion Processes 83 (1988) 1; (e) L. Carlsen and H. Egsgaard, J. Am. Chem. Soc. 110 (1988) 6701; (f) I.W. Griffiths, I. Howe, R.E. March and J.H. Beynon, Int. J. Mass Spectrom. Ion Processes 54 (1983) 323; (g) P.J.A. Ruttink, P.C. Burgers and J.K. Terlouw, Chem. Phys. Letters (1994) submitted.

12 G.A. McGibbon, P.C. Burgers and J.K. Terlouw, Chem. Phys. Letters 218 (1994) 499.

13 QET is the acronym for "Quasi-equilibrium Theory" see (a) H.M. Rosenstock, M.B. Wallenstein, A.L. Wahrhaftig and H. Eyring, Proc. Nat. Acad. Sci. U.S. 38 (1952) 667 and, RRKM indicates the authors Rice, Ramsberger, Kessel and Marcus who presented an analogous quantum theory (see ref. 14a).

14 (a) P.J. Robinson and K.A. Holbrook, Unimolecular Reactions, Wiley-Interscience: New York (1971); (b) C. Lifshitz, Adv. Mass Spectrom. 11 (1989) 713.

15 (a) T. Matsuo, Org. Mass Spectrom. 26 (1991) 374; (b) A. Fraefel and J. Seibl, Mass Spectrom. Rev. 4 (1985) 151; (c) J.H. Beynon, F.M. Harris, B.N. Green and R.H. Bateman, Org. Mass Spectrom. 17 (1982) 55.

16 (a) T. Wong, J.K. Terlouw, T. Weiske and H. Schwarz, Int. J. Mass Spectrom. Ion Processes 113 (1992) R23; (b) H.F. van Garderen, P.J.A. Ruttink, P.C. Burgers, G.A. McGibbon and J.K. Terlouw, Int. J. Mass Spectrom. Ion Processes 121 (1992) 159.

17 Quadrupole Mass Spectrometry and its Applications, P. Dawson (ed.), Elsevier: Amsterdam (1973)

18 (a) R.G. Cooks, J.H. Beynon, R.M. Caprioli and G.R. Lester, Metastable Ions, Elsevier: New York 1973; (b) J.L. Holmes and J.K. Terlouw, Org. Mass Spectrom. 15 (1980) 383.

19 D.H. Williams, Acc. Chem. Res. 10 (1977) 280.

20 (a) K. Levsen and H. Schwarz, Mass Spectrom. Rev. 2 (1982) 77 ; (b) K. Levsen and H. Schwarz, Angew. Chem. Int. Ed. Engl. 15 (1976) 509.

21 (a) W.F. Haddon and F.W. McLafferty, J. Am. Chem. Soc. 90 (1968) 4745; (b) K.R. Jennings, Int. J. Mass Spectrom. Ion Processes 1 (1968) 227.

22 H.S.W. Massey, Rep. Prog. Phys. 12 (1949) 248.

23 P.C. Burgers, J.L. Holmes, A.A. Mommers and J.E. Szulejko, Org. Mass Spectrom. 18 (1983) 596.

24 (a) K. Lammertsma, P.v.R. Schleyer and H. Schwarz, Angew. Chem. Int. Ed. Engl. 28 (1989) 1321; (b) G.K.S. Prakash, T.N. Rawdah and G.A. Olah, Angew. Chem. Int. Ed. Engl. 22 (1983) 390.

25 M.M. Bursey, Mass Spectrom. Rev. 9 (1990) 555.

26 (a) C.A. Muedas, D. Sülzle and H. Schwarz, Chem. Ber. 125 (1992) 1517; (b) R. Srinivas, D.K. Böhme, D. Sülzle and H. Schwarz, J. Phys. Chem. 95 (1991) 9836; (c) R. Srinivas, D. Sülzle and H. Schwarz, Rapid Commun. Mass Spectrom. 5 (1991) 70; (d) R. Srinivas, D. Sülzle, W. Koch, C.H. DePuy and H.

Schwarz, J. Am. Chem. Soc. 113 (1991) 5970.

27 (a) J.H. Bowie, D.H. Williams, S.-O. Lawesson, J.Ø. Madsen, C. Nolde and G. Schroll, Tetrahedron 22 (1966) 3515; (b) R. Smakman and Th. J. de Boer, Org. Mass Spectrom. 3 (1970) 1561; (c) K.M. Downard, J.H. Bowie, R.A.J. O'Hair, M. Krempp and C.H. DePuy, Int. J. Mass Spectrom. Ion Processes 120 (1992) 217.

28 S. Villeneuve and P.C. Burgers, Org. Mass Spectrom. 21 (1986) 733.

29 R. Lavertu, M. Catté, A. Pentenero and P. Le Goff, C.R. Acad. Sc. Paris, Sér. C 263 (1966) 1099.

30 F.M. Devienne, Entropie 24 (1968) 35.

31 (a) J. Gray and R.H. Tomlinson, Chem. Phys. Letters 3 (1969) 523; (b) J. Gray and R.H. Tomlinson, Chem. Phys. Letters 4 (1969) 251; (c) J. Gray and R.H. Tomlinson, Int. J. Mass Spectrom. Ion Processes 15 (1974) 121.

32 G.I. Gellene and R.F. Porter, Acc. Chem. Res. 16 (1983) 200

33 (a) E. Lindholm, in Ion-Molecule Reactions, Vol. 2, J.L. Franklin (ed.), Plenum: New York (1972) Chapter 10, p. 457; (b) E. Lindholm, in Ion-Molecule Reactions in the Gas Phase, Adv. Chem. Ser. No. 58, P.J. Ausloos (ed.), American Chemical Society: Washington (1966) p. 1; (c) J.M. Tedder and P.H. Vidaud, J. Phys. D: Appl. Phys. 13 (1980) 1949.

34 (a) D. Sülzle and H. Schwarz, Int. J. Mass Spectrom. Ion Processes 120 (1993) 1; (b) H. Chen and J.L. Holmes, Int. J. Mass Spectrom. Ion Processes (1994) in press.

35 (a) D.E. Drinkwater, A. Fura, M.-Y. Zhang and F.W. McLafferty, Org. Mass Spectrom. 26 (1991) 1032; (b) P.C. Burgers, W. Kulik, C. Versluis and J.K. Terlouw, Int. J. Mass Spectrom. Ion Processes 98 (1990) 247.

36 (a) C.E.C.A. Hop, J.L. Holmes, Org. Mass Spectrom. 26 (1991) 476; (b) M.-Y. Zhang and F.W. McLafferty, J. Am. Soc. Mass Spectrom. 3 (1992) 108; (c) S.A. Shaffer, F. Turecek and R.L. Cerny, J. Am. Chem. Soc. 115 (1993) 12117.

37 (a) G.C. Shields, Wennberg, J.B. Wilcox, T.F. Moran, Org. Mass Spectrom 21 (1986) 137; (b) G.C. Shields, P.A. Steiner IV, P.R. Nelson, M.C. Trauner and T.F. Moran, Org. Mass Spectrom 22 (1987) 64; (c) J.B Sedgewick, B.P. Paulson, G.C. Shields and T.F. Moran, Int. J. Mass Spectrom. Ion

Processes 79 (1987) 127.

38 (a) I. Vidavski, R.A. Chorush and F.W. McLafferty, 41st ASMS Conference, San Fransisco, 31 May - 4 June 1994, abst. #492; (b) R.A. Chorush, I. Vidavsky and F.W. McLafferty, Org. Mass Spectrom. 28 (1994) 1016.

39 P.C. Burgers, J.L. Holmes, A.A. Mommers, J.E. Szulejko and J.K. Terlouw, Org. Mass Spectrom. 19 (1984) 442.

40 (a) R. Clair, J.L. Holmes, A.A. Mommers and P.C. Burgers, Org. Mass Spectrom. 20 (1985) 207; (b) J.L. Holmes, A.A. Mommers, J.K. Terlouw and C.E.C.A. Hop, Int. J. Mass Spectrom. Ion Processes 68 (1986) 249; (c) G.A. McGibbon and J.K. Terlouw, unpublished results; (d) T. Wong, J. Warkentin and J.K. Terlouw, Int. J. Mass Spectrom. Ion Processes 115 (1992) 33.

41 (a) D. Harnish and J.L. Holmes, Org. Mass Spectrom 29 (1994) 213; (b) C.E.C.A. Hop, PhD Thesis, Utrecht (1989); (c) P.O. Danis, R. Feng and F.W. McLafferty, Anal. Chem. 58 (1986) 355; (d) G.I. Gellene and R.F. Porter, Int. J. Mass Spectrom. Ion Processes 64 (1985) 55.

42 (a) S.G. Lias, J.E. Bartmess, J.F. Liebman, J.L. Holmes, R.D. Levine and W.G. Mallard, J. Phys. Chem. Ref. Data 17 (Suppl. 1) (1988); see also: (b) J.B. Pedley, R.D. Taylor and S.P. Kirby, Thermochemical Data of Organic Compounds (2nd Ed.), Chapman and Hall: London (1986); and for PA's (c) J.E. Szulejko and T.B. McMahon, University of Waterloo Chem. Phys. Res. Rep. CP-460 (1993).

43 S.W. Benson, Thermochemical Kinetics (2nd Ed.), Wiley: New York (1976).

44 V.V. Takhistov and D.A. Ponomarev, Org. Mass Spectrom. 29 (1994) 395

45 (a) J.L. Holmes and F.P. Lossing, Can. J. Chem. 60 (1982) 2365; (b) J.L. Holmes and F.P. Lossing, Org. Mass Spectrom. 26 (1991) 537.

46 F.M. Benoit and A.G. Harrison, J. Am. Chem. Soc. 99 (1977) 3980.

47 J.L. Holmes, Int. J. Mass Spectrom. Ion Processes 118/119 (1992) 381.

48 W.J. Hehre, L. Radom, P.v.R. Schleyer and J.A. Pople, Ab Initio Molecular Orbital Theory, Wiley: New York (1986).

49 J.A. Pople and L.A. Curtiss, J. Phys. Chem. 91 (1987) 155, 3637.

50 C.C.J. Roothaan, Rev. Mod. Phys. 23 (1951) 69.

51 C. Møller and M.S. Plesset, Phys. Rev. 46 (1934) 818.

52 J.A. Pople, J.S. Binkley and R. Seeger, Int. J. Quantum Chem. Symp. 10 (1976) 1.

53 M.J.S. Dewar, Org. Mass Spectrom. 28 (1993) 305.

54 (a) P.C. Burgers and J.L. Holmes, Rapid Commun. Mass Spectrom. 3 (1989) 279; (b) P.C. Burgers and J.L. Holmes, Adv. Mass Spectrom. 10 (1989) 279.

55 C.E. Klots, J. Chem. Phys. 58 (1973) 5364.

56 E. Block, R.E. Penn, R.J. Olsen and P.F. Sherwin, J. Am. Chem. Soc. 98 (1976) 1264.

57 L. Pauling, The Nature of the Chemical Bond (3rd Ed.), Cornell University Press: Ithica, NY, 1960.

58 (a) R.F.W. Bader, Atoms in Molecules - A Quantum Theory, Oxford University Press: Oxford 1990; (b) R.F.W. Bader, P.L.A. Popelier and T.A. Keith, Angew. Chem. Int. Ed. Engl. 33 (1994) 620.

59 J. March, Advanced Organic Chemistry: reactions, mechanisms, and structure (4th Ed.), Wiley-Interscience: New York (1992) Chapters 1-3.

60 Joesten and Schaad, Hydrogen Bonding, Marcel Dekker: New York (1974).

61 (a) C.A. Ramsden, Chem. Soc. Rev. 23 (1994) 111; (b) J.E. McMurry and T. Lectka, Acc. Chem. Res. 25, (1992) 47.

62 (a) M.J.S. Dewar, Hyperconjugation, Ronald Press : New York (1962); (b) Wheland, Resonance in Organic Chemistry, Wiley: New York (1955).

63 M. Speranza, Int. J. Mass Spectrom. Ion Processes 118/119 (1992) 395.

64 (a) J.S. Splitter, in Applications of Mass Spectrometry to Organic Stereochemistry, J.S. Splitter and F. Turecek (eds.), VCH: New York (1994) Chapter 3; (b) T.H. Morton, Org. Mass Spectrom. 27 (1992) 353; (c) P. Longevialle, Mass Spectrom. Rev. 11 (1992) 157; (d) R.D. Bowen, Acc. Chem. Res. 24 (1991) 364; (e) D.J. McAdoo, Mass Spectrom. Rev. 7 (1988) 363; (f) T.H. Morton, Tetrahedron 38 (1982) 3195.

65 P.N. Rylander and S. Meyerson J. Am. Chem. Soc. 78 (1956) 5799.

66 (a) R.D. Bowen, B.J. Stapleton and D.H. Williams, J. Chem. Soc., Chem. Commun. (1978) 24; (b) R.D. Bowen and D.H. Williams, J. Am. Chem. Soc. 100 (1978) 7454; (c) R.D. Bowen and D.H. Williams, 102 (1980) 2752.

67 T.H. Morton, J. Am. Chem. Soc. 102 (1980) 1596.

68 P. Longevialle and R. Botter J. Chem. Soc., Chem. Commun. (1980) 823.

69 T.H. Morton, Org. Mass Spectrom. 27 (1992) 353.

70 J.W. Larson and T.B. McMahon, J. Am. Chem. Soc. 104 (1982) 6255.

71 M. Meot-Ner, J. Am. Chem. Soc. 106 (1984) 1257.

72 M. Meot-Ner, M.M. Ross, J.E. Campana, J. Am. Chem. Soc. 107 (1985) 4839.

73 (a) J.K. Terlouw, T. Weiske, H. Schwarz, J.L. Holmes, Org. Mass Spectrom. 21 (1986) 665; (b) M.C. Blanchette, J.L. Holmes C.E.C.A. Hop, F.P. Lossing, R. Postma, P.J.A. Ruttink and J.K. Terlouw J. Am. Chem. Soc. 108 (1986) 7589.

74 (a) E. Kluft, N.N.M. Nibbering, M.B. Stringer, P.C.H. Eichinger, J.H. Bowie, Int. J. Mass Spectrom. Ion Processes 85 (1988) 215 ; (b) P.C. Burgers, K.J. van den Berg, H. Visser and J.K. Terlouw, Int. J. Mass Spectrom. Ion Processes 101 (1990) 83.

75 B.L.M. van Baar, J.K. Terlouw, S. Akkök, W. Zummack, T. Weiske and H. Schwarz, Chimia 42 (1988) 226.

76 D. Suh, C.A. Kingsmill, P.J.A. Ruttink, J.K. Terlouw and P.C. Burgers, Org. Mass Spectrom. 28 (1993) 1270 .

77 (a) G. Bouchoux and Y. Hopilliard, J. Am. Chem. Soc. 112 (1990) 9110; (b) D.J. Swanton, D.C.J. Marsden and L. Radom, Org. Mass Spectrom. 26 (1991) 227.

78 G. Bouchoux and Y. Hopilliard, Int. J. Mass Spectrom. Ion Processes 75 (1987) 1.

79 P.C. Burgers, C.A. Kingsmill, G.A. McGibbon and J.K. Terlouw, Org. Mass Spectrom. 27 (1992) 398.

80 (a) E.L. Coitino, A. Lledos, R. Serra, J. Bertran and O.N. Ventura, J. Am. Chem. Soc. 115 (1993) 9121; (b) P.C Burgers and J.K. Terlouw, in Specialist Periodical Reports: Mass Spectrometry, M.E. Rose (ed.), The Royal Society of Chemistry: London, 1989, Vol. 10 Chapter 2; (c) N. Heinrich and H. Schwarz, in Ion and Cluster Ion Spectroscopy and Structure, J.P. Maier (ed.), Elsevier: Amsterdam (1989), p329; (d) N. Heinrich, in Structure/Reactivity and Thermochemistry of Ions, P. Ausloos and S.G. Lias (eds.), D. Reidel: Dordrecht, NL (1987), p271; (e) R. Postma, PhD Thesis, Utrecht (1987).

81 R. Postma, S.P. van Helden, J.H. van Lenthe, P.J.A. Ruttink, J.K. Terlouw and J.L. Holmes Org. Mass

Spectrom. 23 (1988) 503.

82 R. Postma, P.J.A. Ruttink, F.B. van Duijneveldt, J.K. Terlouw and J.L. Holmes Can. J. Chem. 63 (1985) 2798.

83 for an instance where higher levels of theory are needed see: P.J.A. Ruttink and P.C. Burgers Org. Mass Spectrom. 28 (1993) 1087 or chapter 2.

84 J.K. Terlouw, 7th Asilomar Conference on Mass Spectrometry, Pacific Grove, U.S.A., 24-28 Sept. 1989.

85 (a) P.C. Burgers, J.L. Holmes, C.E.C.A. Hop, R. Postma, P.J.A. Ruttink and J.K. Terlouw, J. Am. Chem. Soc. 109 (1987)7315 ; (b) J.R. Cao, M. George, J.L. Holmes, M. Sirois, J.K. Terlouw and P.C. Burgers, J. Am. Chem. Soc. 114 (1992) 2017.

86 (a) J.H. Vadja, A.G. Harrison, A. Hirota and F.W. McLafferty, J. Am. Chem. Soc. 103 (1981) 36; (b) J.K. Terlouw, J.L. Holmes and P.C. Burgers, Int. J. Mass Spectrom. Ion Processes 66 (1985) 239; (c) N. Heinrich, J. Schmidt, H. Schwarz and Y. Apeloig, J. Am. Chem. Soc. 109 (1987) 1317.

87 (a) Wesdemiotis, R. Censcits and F.W. McLafferty, Org. Mass Spectrom. 20 (1985) 98; (b) J.M.H. Pakarinen, P. Vainiotalo, T.A. Pakkanen and H.I. Kenttämaa; (c) M. George, C.A. Kingsmill, D. Suh, J.K. Terlouw and J.L. Holmes, J. Am. Chem. Soc. 116 (1994) 7807.

88 R. Postma, P.J.A. Ruttink, B. Van Baar, J.K. Terlouw, J.L. Holmes and P.C. Burgers, Chem. Phys. Letters 123 (1986) 409.

89 G. Bouchoux, Y. Hopilliard and J. Tortajada, Int. J. Mass Spectrom. Ion Processes 90 (1989) 197 .

90 (a) R. Postma, P.J.A. Ruttink, J.H. van Lenthe and J.K. Terlouw, CPL 156 (1989) 245; (b) P.J.A. Ruttink, in The Structure of Small Molecules and Ions, R. Naaman and Z. Vager (eds.), Plenum Press: New York (1988) 243.

91 (a) T. Drewello, N. Heinrich, W.P.M. Maas, N.M.M. Nibbering, T. Weiske and H. Schwarz, J. Am. Chem. Soc. 109 (1987) 4810; (b) T.H. Morton, Org. Mass Spectrom. 26 (1991) 18.

92 N. Heinrich, F. Louage, C. Lifshitz and H. Schwarz, J. Am. Chem. Soc. 110 (1988) 8183.

93 (a) B.L.M. van Baar, P.C. Burgers, J.L. Holmes and J.K. Terlouw, Org. Mass Spectrom. 23 (1988) 355; (b) J.K. Terlouw, in ref. 90b, p.269.

94 P.C. Burgers, C. Lifshitz, P.J.A. Ruttink, G. Schaftenaar and J.K. Terlouw, Org. Mass Spectrom. 24 (1989) 579.

95 P.J.A. Ruttink, J. Phys. Chem. 91 (1987) 703.

96 (a) R. Stockbauer, Int. J. Mass Spectrom. Ion Processes 25 (1977) 401; (b) N.H. Hijazi, J.L. Holmes and J.K. Terlouw, Org. Mass Spectrom. 14 (1979) 119; (c) A.L. Harkness, Int. J. Mass Spectrom. Ion Processes 10 (1972) 267.

97 W. Heerma, W. Kulik, P.C. Burgers and J.K. Terlouw, Int. J. Mass Spectrom. Ion Proc. 84 (1988) R1.

98 (a) H.-F. Grützmacher, Int. J. Mass Spectrom. Ion Processes 118/119 (1992) 825; (b) U. Filges and H.-F. Grützmacher, Org. Mass Spectrom. 21 (1986) 673.

999 (a) J.K. Terlouw, W. Heerma, G. Dijkstra, J.L. Holmes and P.C. Burgers, Int. J. Mass Spectrom. Ion Processes 47 (1983) 147; (b) G. Frenking and W. Koch, J. Mol. Struct. (Theochem) 110 (1984) 49; (c) H. Schwarz, Mass Spectrosc. (Tokyo) 32 (1984) 3.

100 S. Hammerum, Mass Spectrom. Rev. 7 (1988) 123.

101 L. Radom, W.J. Bouma, R.H. Nobes and B.F. Yates, Pure Appl. Chem. 56 (1984) 1831.

102 B.F. Yates, W.J. Bouma and L. Radom, Tetrahedron 22 (1986) 6225.

103 K.M. Stirk, L.K. M. Kiminkinen and H.I. Kenttämaa, Chem. Rev. 92 (1992) 1649 .

PART I

STRUCTURES AND REACTIONS OF ORGANIC IONS

CHAPTER 2

The gas phase chemistry of methyl carbamate radical cations, $H_2NCOOCH_3^{+\bullet}$: Isomerization into distonic ions, hydrogen-bridged radical cations and ion-dipole complexes.

Introduction

In this chapter the unimolecular dissociations of the methyl carbamate radical cation ion $H_2NCOOCH_3^{+\bullet}$, **1**, are studied using the mass spectrometric techniques of metastable ion (MI), collisional activation (CA), and neutralization-reionization (NR) mass spectrometry as well as appearance energy (AE) measurements and isotope labelling experiments. *Ab initio* molecular orbital computations were used to find equilibrium structures and to locate minimum energy requirement reaction paths for the multistep rearrangement/dissociation reactions.

The experiments and calculations implicate the distonic ion $H_2N\text{-}^{+}C(OH)OCH_2^{\bullet}$, **2**, and hydrogen-bridged radical cations as important intermediates in the spontaneous dissociations of **1**.

The work described here has been published before in an article of the same title: G. Schaftenaar, P.J.A. Ruttink, P.C. Burgers, R. Postma, G.A. McGibbon and J.K. Terlouw *Int. J. Mass Spectrom. Ion Processes*, 100 (1990) 521.

From the inception of organic mass spectrometry it has been realized that many a molecular ion may undergo more or less complex rearrangement reactions. This is especially true for reactions taking place in the microsecond time frame, for the metastable ions. However, rearrangement reactions may also dominate in the sub-microsecond time frame and the resulting ionic products may lead to intense (and even to base) peaks in the conventional mass spectra [1]: 25 years ago it was stated [2] that "the occurrence of such rearrangements is one of the problems which complicate exceedingly the simple interpretation of ionisation and fragmentation processes and is moreover a serious obstacle to the determination of the constitution of the original compound from the mass spectrum". However, even before the above statement was made Biemann [3] wrote, "The formation of rearrangement peaks of high intensity thus requires a certain arrangement of atoms in the molecule, which makes such peaks very useful for the interpretation of mass spectra". Biemann goes on to write, "A deeper knowledge of the mechanism of these rearrangements is extremely important for this purpose". Indeed, it has been repeatedly shown over the past decade that a good understanding of ionic processes, such as rearrangement reactions, can lead to a more confident interpretation of mass spectra of unknowns. In this respect it is worthy to note that in 1983 the name of the International Journal of Mass Spectrometry and Ion Physics was changed to include the word Processes instead of Physics.

Often metastable ions [4] are chosen for mechanistic studies because: (i) their internal energy, although not well defined, lies in a narrow range; (ii) the nominal mass of the neutral expelled can be measured; (iii) when in doubt the structure of the neutral can be assessed by Collision-Induced Dissociative Ionization (CIDI), a variant of Neutralization-Reionization Mass Spectrometry (NRMS) [5] and (iv) the kinetic energy release, even when in the sub-millielectronvolt range, can be accurately measured.

Even within a homologous series of small metastable ions, strikingly different dissociation reactions can be encountered. Consider the following: methylformate ions,

$H\text{-}C(=O)\text{-}OCH_3^{+\bullet}$, produce CO [6], methylacetate ions, $CH_3\text{-}C(=O)\text{-}OCH_3^{+\bullet}$ form $CH_2OH^{\bullet}$ in admixture with $CH_3O^{\bullet}$ [7], ionized methylpropanoate, $CH_3CH_2\text{-}C(=O)\text{-}OCH_3^{+\bullet}$, generates $CH_3O^{\bullet}$ but not $CH_2OH^{\bullet}$ [8] and methylbutyrate ions, $CH_3CH_2CH_2\text{-}C(=O)\text{-}OCH_3^{+\bullet}$, produce $CH_3^{\bullet}$ and C_2H_4 (by the McLafferty rearrangement [9]) . Ethylacetate, $CH_3\text{-}C(=O)\text{-}OCH_2CH_3^{+\bullet}$, amazingly, produces water molecules [10].

From recent work, it has become clear that much can be learned about reaction mechanisms and ion structures by integration of results obtained from state-of-the-art ab initio calculations and from mass spectrometry based experiments [7,11,12]. Previous results [11,12] have shown that ab initio calculations can lead to a proper description of the isomerization/dissociation pathways provided that a split-valence basis set is employed for geometry optimizations and that the final relative energies include the effects of polarization functions and of correlation energy. Using this approach it has become clear that many radical cations exist for which the neutral counterpart is unknown and that such ions are key intermediates in the rearrangement/dissociation pathways of many organic radical cations [7]. Of particular interest are the so called distonic ions [13], hydrogen-bridged radical cations [14] and ion-dipole complexes [11,15]. Distonic ions are those radical cations which have the charge and radical sites at separate heavy atoms, e.g. $^{\bullet}CH_2\text{-}^{+}OH_2$ as opposed to $CH_3OH^{+\bullet}$. In larger distonic ions, e.g. $[^{+}A\text{-}B\text{-}C^{\bullet}\text{-}D]$ often the charged moiety can migrate to the radical centre, thereby generating another distonic ion $[B\text{-}C(\text{-}A^{+})\text{-}D^{\bullet}]$ which in turn can shift its ionized part to the radical site $[B\text{-}^{\bullet}C\text{-}D\text{-}A^{+}]$ [7,13]. Such a sequence can rationalize otherwise mechanistically problematic reactions. In such a rationalization it is assumed that the rearrangements occur stepwise as in the Whitmore mechanism in solution carbenium ion chemistry [16]. Another class of ions which are increasingly being invoked to rationalize fragmentations are hydrogen-bridged radical cations, formally proton-bound molecule radical pairs $A\cdots H^{+}\cdots BH^{\bullet}$ which, unlike their even electron counterparts $A\cdots H^{+}\cdots B$, have only been scantly studied. In such radical ions a hydrogen shift can lead to another hydrogen

bridged cation $^{\bullet}HA{\cdots}H^{+}{\cdots}B$ which in turn can undergo a similar reaction.

Such a sequence has been invoked to explain the seemingly complex unimolecular chemistry of ionized 1,2-ethanediol [14a] and 1,2-propanediol [14b]. With respect to the above it is of interest to note that high level ab-initio calculations have convincingly shown that formation of $^{\bullet}CH_2OH$ from ionized methylacetate proceeds via both distonic ions and hydrogen-bridged radical cations as shown below [12a]:

$$H_3C\text{-}C(=O)\text{-}O\text{-}CH_3^{+\bullet} \rightarrow H_3C\text{-}\dot{C}(\text{-}OH)\text{-}O\text{-}CH_2^{\bullet} \text{ (distonic)} \rightarrow CH_3C{=}O{\cdots}H{\cdots}O{=}CH_2^{+\bullet} \text{ (H-bridged)}$$

$$\downarrow$$

$$CH_3C{=}O^{+} + CH_2OH^{\bullet}$$

A recent computational and experimental study [12b] on the CH_5NO potential energy surface provided evidence that loss of CO from ionized methyl carbamate $H_2NCOOCH_3^{+\bullet}$, **1**, leads to the hydrogen-bridged radical cation $[CH_2{=}O{\cdots}H{\cdots}NH_2]^{+\bullet}$, formally the ionized formaldehyde-ammonia associated molecule and not the conventional species $CH_3ONH_2^{+\bullet}$ (by CO extrusion).

Based on a variety of mass spectrometric experiments it was proposed that the reaction proceeds as follows:

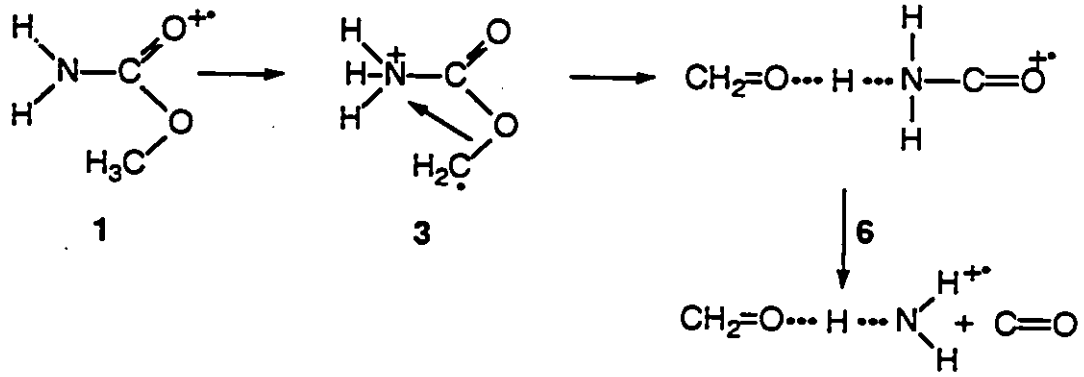

1 **3** **6**

and we note here that this sequence too includes a distonic → hydrogen-bridged transformation by intramolecular hydrogen bonding (chelation). However, it was stressed that without computational support the proposal was only speculative. Thus we embarked upon a computational study of the methyl carbamate rearrangement /dissociation reactions and some further experiments which we report here. Our ab initio

calculations show that loss of CO occurs via a completely different pathway than that shown above. A rationale is also given for the dominant reaction in the microsecond time frame, *viz.* loss of HCO•.

Before presenting the evidence which now leads us to reject the above mechanism it may be useful to briefly summarize the grounds upon which it was based:

(i) the daughter ions are $[CH_2{=}O{\cdots}H{\cdots}NH_2]^{+\bullet}$ and not $CH_3ONH_2^{+\bullet}$ or $^{\bullet}CH_2ONH_3^{+}$.

(ii) $H_2N\text{-}C(=O)\text{-}^{18}O\text{-}^{13}CH_3^{+\bullet}$ specifically loses $^{12}C^{16}O$.

(iii) electron capture by the (rearranged) molecular ions leads to complete breakdown indicating that the neutralized species lie(s) in a shallow well only, as expected for structures akin to **3** and **6**. Major neutral products are $CH_2{=}O$ and $^{\bullet}CH_2OH$, *not* $CH_3O^{\bullet}$ consistent with structures **3** and **6**.

(iv) the CH_5NO daughter ions also fall apart upon neutralization to, among other products, $^{\bullet}CH_2OH$, *not* $CH_3O^{\bullet}$; the CH_2D_3NO daughter ions generated from the OCD_3 labelled carbamate form $^{\bullet}CD_2OH$ and $^{\bullet}CD_2OD$ radicals in a ratio of 2 : 1.

All the above observations lend strong support for the above mechanism.

Results and Discussion

The instrumental and synthetic details [12b,17-19] relevant to the results can be found in the EXPERIMENTAL chapter of this thesis.

Loss of CO is, among metastable ions, a minor reaction path only and most of the metastable ions dissociate by loss of $HC{=}O^{\bullet}$ (95%). Loss of $HC{=}O^{\bullet}$ was not investigated in the previous study [12b] so we consider it here. First of all, what is the structure of the daughter ions? A 1,5-hydrogen shift in **6** followed by loss of $HC{=}O^{\bullet}$ would lead to $H_3N\text{-}CH{=}O^{+}$, **a**. However, formation of the isomeric carbenium ion $H_2N\text{-}CH\text{-}OH^{+}$, **b**, may be energetically more attractive since ion **b** has two powerful electron donating groups attached to the carbenium centre. The proton affinity of formamide $H\text{-}C(=O)\text{-}NH_2$ has been measured [20a], yielding an enthalpy of formation of 123 kcal/mol for the protonated

molecule but its structure, **a** or **b**, has not been determined. However, our theoretical calculations show that ion **b** is considerably more stable than ion **a** (by 14.6 kcal/mol) and thus the protonation of formamide likely yields CH_4NO^+ ion **b**.

The CA mass spectrum of the CH_4NO^+ ions generated by loss of $HC{=}O^{\bullet}$ is shown in Figure 2.1. Spontaneous reactions lead to m/z 18, NH_4^+, which , see Table 2.1, is by far the least energy demanding reaction.

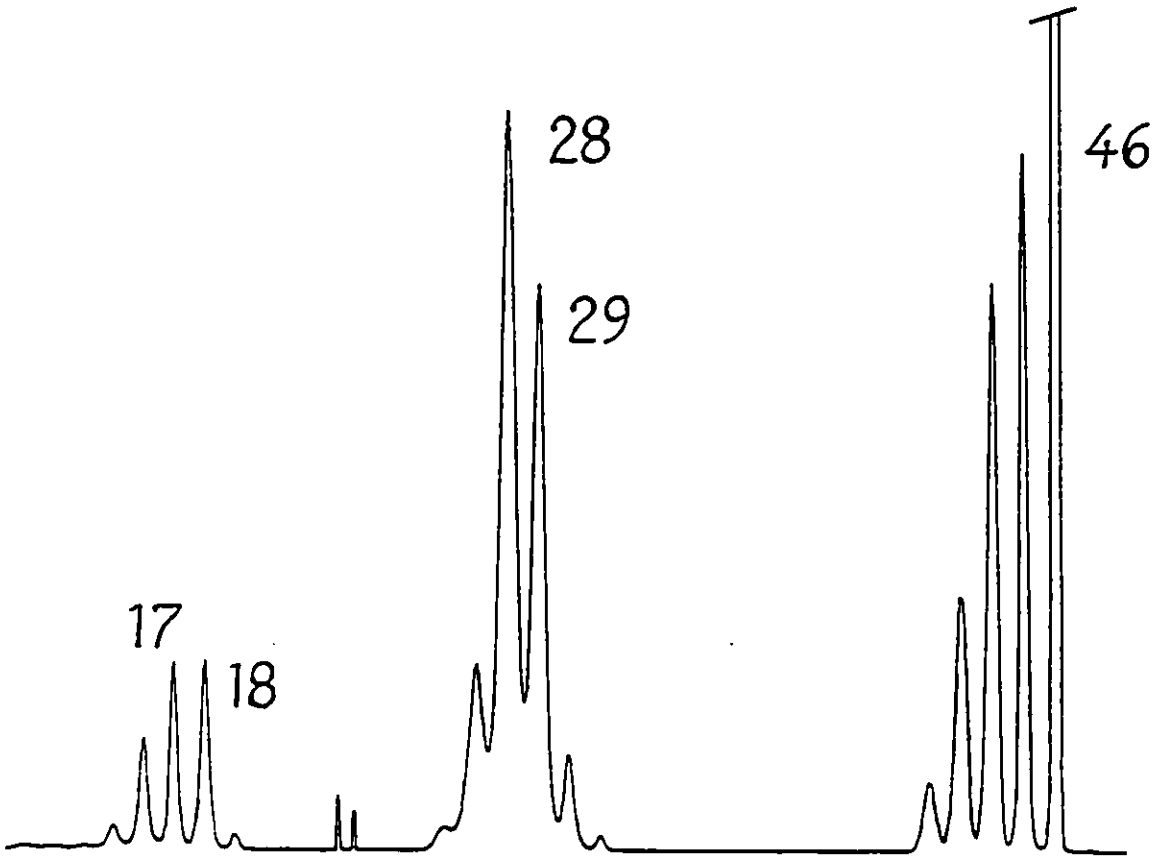

Fig. 2.1 CA mass spectrum of the CH_4NO^+ ions generated by loss of $HCO^{\bullet}$ from ionized methyl carbamate, $H_2NCOOCH_3^{\bullet+}$.

TABLE 2.1 ENTHALPIES (from ref. 20 a) OF PRODUCTS FOR CH_4NO^+ DISSOCIATIONS

m/z	PRODUCTS			$\Sigma\Delta H_f$ (kcal/mol)
17	$NH_3^{+\bullet}$	+	$HCO^\bullet$	234
18	NH_4^+	+	CO	125
28	$HCNH^+$	+	H_2O	168
29	HCO^+	+	NH_3	186
29	$HCNH_2^+$	+	$OH^\bullet$	267
30	$HCOH^{+\bullet}$	+	$NH_2^\bullet$	275

There are intense peaks at m/z 29, m/z 28, and also at m/z 17. The CA mass spectrum is compatible with ion **a**, which is expected to dissociate to $H\text{-}C{=}O^+$ (which can fragment further to $CO^{+\bullet}$) and to $NH_3^{+\bullet}$. However, there are also clear signals at m/z 27, (probably $HNC^{+\bullet}$), at m/z 16 (NH_2^+) and at m/z 30 (loss of $NH_2^\bullet$) indicative of structure **b**. The NR spectrum of the CH_4NO^+ ions is shown in Figure 2.2a. Two important observations are that (1) there is a recovery signal at m/z 46 of considerable intensity and (2) the NR mass spectrum is very similar to the CA mass spectrum (m/z 18 is much less intense in the NR mass spectrum as this peak arises from the slow dissociation of the reionized species). These observations indicate that the neutralized species is stable for at least 0.5 μs and this argues against ions **a** which are not expected to survive neutralization.

Further evidence for this assignment comes from the NR mass spectrum of the $CH_2D_2NO^+$ ions generated by $D\text{-}C{=}O^\bullet$ loss (no $H\text{-}C{=}O^\bullet$ loss is observed) from the OCD_3 labelled carbamate, shown in Figure 2.2b. If we were dealing with **a** type ions these ions could be $H_2DN\text{-}CD{=}O^+$ and/or $HD_2N\text{-}CH{=}O^+$. However, since m/z 19 is very weak (compare the intensity of m/z 17 in Figure 2.2a) the latter structure can be discarded and so the species would have to be $H_2DN\text{-}CD{=}O^+$. This ion, after NR, should yield $D\text{-}C{=}O^+$ followed by loss of $D^\bullet$ to produce peaks at m/z 30 and 28, but no peak at m/z 29 is

expected, in sharp contrast with the experimental findings (Figure 2.2b). The m/z 29 peak then must be the result of HDO loss and so about 40 % of m/z 28 in the unlabelled ion's NR and CA spectra is not $CO^{+\bullet}$ but rather $HNCH^+$ formed by loss of H_2O. These findings are compatible with the proposal that the daughter ions are indeed $H_2N\text{-}CH\text{-}OH^+$, **b**, which incidentally can produce m/z 29 $HCNH_2^+$ ions via a simple bond cleavage reaction (see Table 2.1). That loss of H_2O is observed at all is not so surprising considering the products' enthalpies. The labelled $CH_2D_2NO^+$ daughter ions are then $H_2N\text{-}CD\text{-}OD^+$ (as also evidenced by the clean shift of m/z 30 to m/z 32, $CDOD^{+\bullet}$).

Note that the CA mass spectrum of $H_2N\text{-}CH\text{-}OH$ (Figure 2.1) contains weak signals at m/z 19 and m/z 31. These signals could well arise from a trace of ethanol [14a]: the corresponding signals are absent in the CA mass spectrum of the labelled species (not shown). We mention this because a trace amount of ethanol may render the interpretation of the m/z 46 appearance energy value questionable (see below).

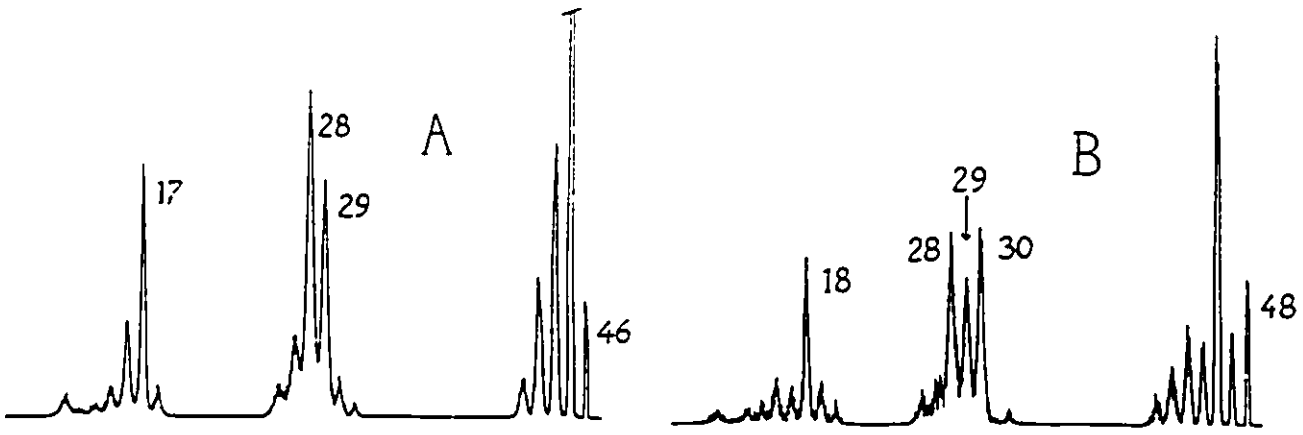

Fig. 2.2 (A) [Xe, O_2] NR mass spectrum of the CH_4NO^+ ions generated by loss of $HCO^\bullet$ from ionized methyl carbamate, $H_2NCOOCH_3^{\bullet+}$; (B) NR mass spectrum of the $CH_2D_2NO^+$ ions generated by loss of $DCO^\bullet$ from the labelled ester, $H_2NCOOCD_3^{\bullet+}$.

To obtain more information on the mechanism of HCO• and CO loss the MI and CA mass spectra of several labelled molecules were investigated and the results are summarized as follows :

$H_2N\text{-}C(=O)\text{-}O\text{-}CD_3^{+\bullet}$	loses	$DCO^{\bullet}$	and	CO
$H_2N\text{-}C(=O)\text{-}O\text{-}^{13}CH_3^{+\bullet}$	loses	$H^{13}CO^{\bullet}$	and	^{12}CO
$H_2N\text{-}C(=O)\text{-}^{18}O\text{-}CH_3^{+\bullet}$	loses	$HC^{18}O^{\bullet}$	and	$C^{16}O$
$H_2N\text{-}C(=O)\text{-}^{18}O\text{-}^{13}CH_3^{+\bullet}$	loses	$H^{13}C^{18}O^{\bullet}$	and	$^{12}C^{16}O$

Both rearrangement/dissociation processes (loss of HCO• and CO) are thus atom-specific and the following reactions are established:

$$H_2N\text{-}C(=O)\text{-}^{\bullet}O\text{-}^{\bullet}CH_3^{+\bullet} \rightarrow {}^{\bullet}CH_2={}^{\bullet}O\cdots HNH_2^{+\bullet} + C{=}O \quad (1)$$

$$\rightarrow H_2N\text{-}CH\text{-}OH^{+} + H\text{-}{}^{\bullet}C={}^{\bullet}O^{\bullet} \quad (2)$$

Energetic measurements

The ionization energy (IE) and appearance energy (AE) values were measured using monochromatic electrons [17]. IE $[H_2NCOOCH_3]$ = 10.44 ±0.05 eV, yielding ΔH_f $[H_2NCOOCH_3]^+$ = 141 kcal/mol using ΔH_f $[H_2NCOOCH_3]$ = -100 kcal/mol. The AE for m/z 46 was measured as 10.82 ±0.05 eV, which is only 0.35 eV above the IE of ethanol [20a]. Since we had noted above that a trace of ethanol could well be present, it is conceivable that the measured value is too low. To remove this ambiguity the AE of the *metastable* peak for loss of HCO• was measured by the comparative method described in ref. 19, AE = 11.20 ±0.1 eV. The AE of the metastable peak for loss of CO was also measured by this method, AE = 11.15 ±0.1 eV. The latter AE value was found to be identical with that obtained using monochromatic electrons (AE =11.16 ±0.05 eV), which gives credence to the metastable measurements. Therefore we propose that the activation energies for loss of HCO• and CO are the same within experimental error.

ΔH_f $[H_2N\text{-}CH\text{-}OH^+]$ as derived from the above AE measurement, 149 kcal/mol, is much higher than that of protonated formamide, 123 kcal/mol. This leads to the

conclusion that the loss of HCO• from 1 is associated with a significant energy barrier (~1.1 eV) for the reverse reaction. Note that this is not reflected in the magnitude of the kinetic energy release: <T> is only 77 meV. This point will be addressed later. The formation of the hydrogen-bridged species $[CH_2{=}O{\cdots}H{\cdots}NH_2]^{+\bullet}$, too, may involve a barrier for the reverse reaction and so the experimentally determined ΔH_f (184 kcal/mol [12b]) must be regarded as an upper limit.

At slightly higher energies, AE = 11.24 eV, another process comes into play, namely dissociation into m/z 44 $H_2N{-}C{=}O^+$ ions and the 31 dalton neutrals, $^\bullet CH_2OH$ (ΔH_f = -6.2 kcal/mol [20a]) or $CH_3O^\bullet$ (ΔH_f = +3.7 kcal/mol [20a]). Depending on the structure of the neutral lost, the apparent ΔH_f of the m/z 44 $H_2N{-}C{=}O^+$ ions is 155 kcal/mol (for loss of $CH_3O^\bullet$) and 165 kcal/mol (for loss of $^\bullet CH_2OH$). Since ΔH_f [$H_2N{-}C{=}O^+$] has been established as 161 kcal/mol [20b] it follows that at threshold the radical eliminated is $^\bullet CH_2OH$ and not $CH_3O^\bullet$.

At still higher energies (AE = 11.44 eV) a fourth reaction, loss of $CH_2{=}O$, comes into play. This process could lead to the ionized carbene $H_2N{-}C{-}OH^{+\bullet}$ or to the distonic ion $H_3N{-}C{=}O^{+\bullet}$. The NR mass spectrum of the labelled daughter ion $CH_2DNO^{+\bullet}$ formed from the OCD_3 labelled carbamate is shown in Figure 2.3. It is observed that the recovery signal is base peak and that intense signals are present at m/z 16, (NH_2^+) and m/z 18, (OD^+). Since the hypervalent species $H_2DN{-}C{=}O^{+\bullet}$ is not expected to survive it is proposed that the daughter ions are $H_2N{-}C{-}OD^{+\bullet}$, which upon neutralization yield the stable carbene $H_2N{-}C{-}OD$. The daughter ions are thus $H_2N{-}C{-}OH^{+\bullet}$ and not $H_3N{-}C{=}O^{+\bullet}$, in agreement with our theoretical calculations which predict that the N-C bond strength in $H_3N{-}C{=}O^{+\bullet}$ is only 0.8 kcal/mol (see below). Barring a reverse term, ΔH_f [$H_2N{-}C{-}OH^{+\bullet}$] is assessed at 190 kcal/mol.

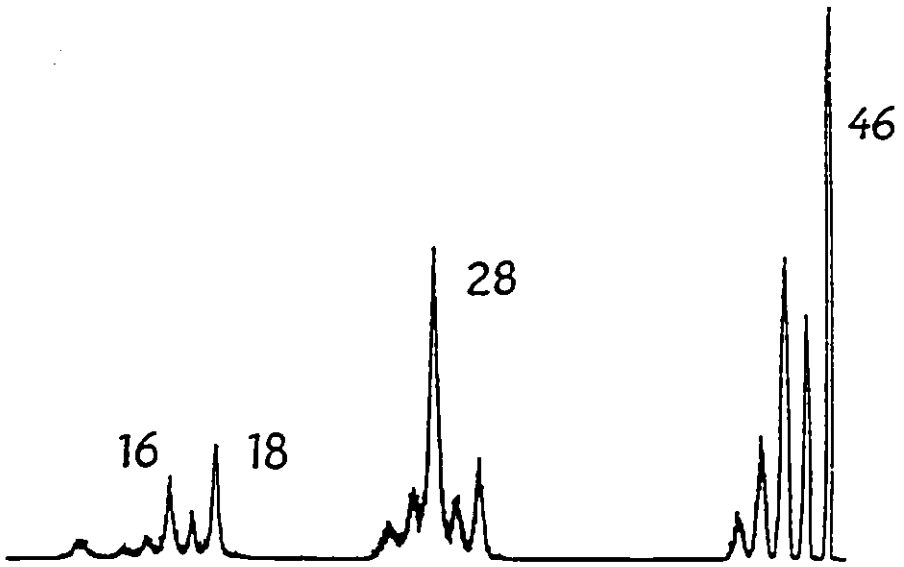

Fig. 2.3 [Xe, O_2] NR mass spectrum of the CH_2DNO^+ ions generated by loss of CD_2O from the labelled ester, $H_2NCOOCD_3^{\bullet+}$.

The higher energy losses of $CH_2{=}O$ and $^{\bullet}CH_2OH$ (or $CH_3O^{\bullet}$) give rise to prominent peaks in the CA mass spectrum [12b]. These reactions too appeared atom-specific: the $H_2N\text{-}C(=O)\text{-}^{18}O\text{-}^{13}CH_3$ labelled carbamate loses exclusively $^{13}CH_2{}^{18}O$ and $^{13}CH_3{}^{18}O^{\bullet}$ and/or $^{13}CH_2{}^{18}OH^{\bullet}$. Thus for the collision induced dissociations the following reactions are established :

$$H_2N\text{-}C(=O)\text{-}^{\bullet}O\text{-}^{\bullet}CH_3^{+\bullet} \rightarrow H_2N\text{-}C\text{-}OH^{+\bullet} + {}^{\bullet}CH_2{=}{}^{\bullet}O$$

$$\rightarrow H_2N\text{-}C{=}O + {}^{\bullet}CH_3{}^{\bullet}O^{\bullet}/{}^{\bullet}CH_2{}^{\bullet}OH^{\bullet}$$

It is remarkable that whereas the AE for loss of $^{\bullet}CH_2OH$ is only slightly higher than the AE for loss of $HCO^{\bullet}$ and CO, no loss of $^{\bullet}CH_2OH$ is observed in the MI mass spectrum: the signal at m/z 44 is at least a factor of 400 less intense than that at m/z 46 (loss of $HCO^{\bullet}$) and in addition it may well result from collision induced dissociation by residual background gas.

That the losses of CO and $HCO^{\bullet}$ compete in the microsecond time frame indicates

that their activation energies are almost, if not exactly, the same; the latter will be so if these reactions proceed via the same rate-determining barrier (see below).

Theoretical methods

Standard LCAO-MO-SCF calculations were performed with the program GAMESS [21] employing restricted Hartree-Fock (RHF) procedures. The isomers, transition states (TS) and dissociation products which have been examined are given in Scheme 2.1.

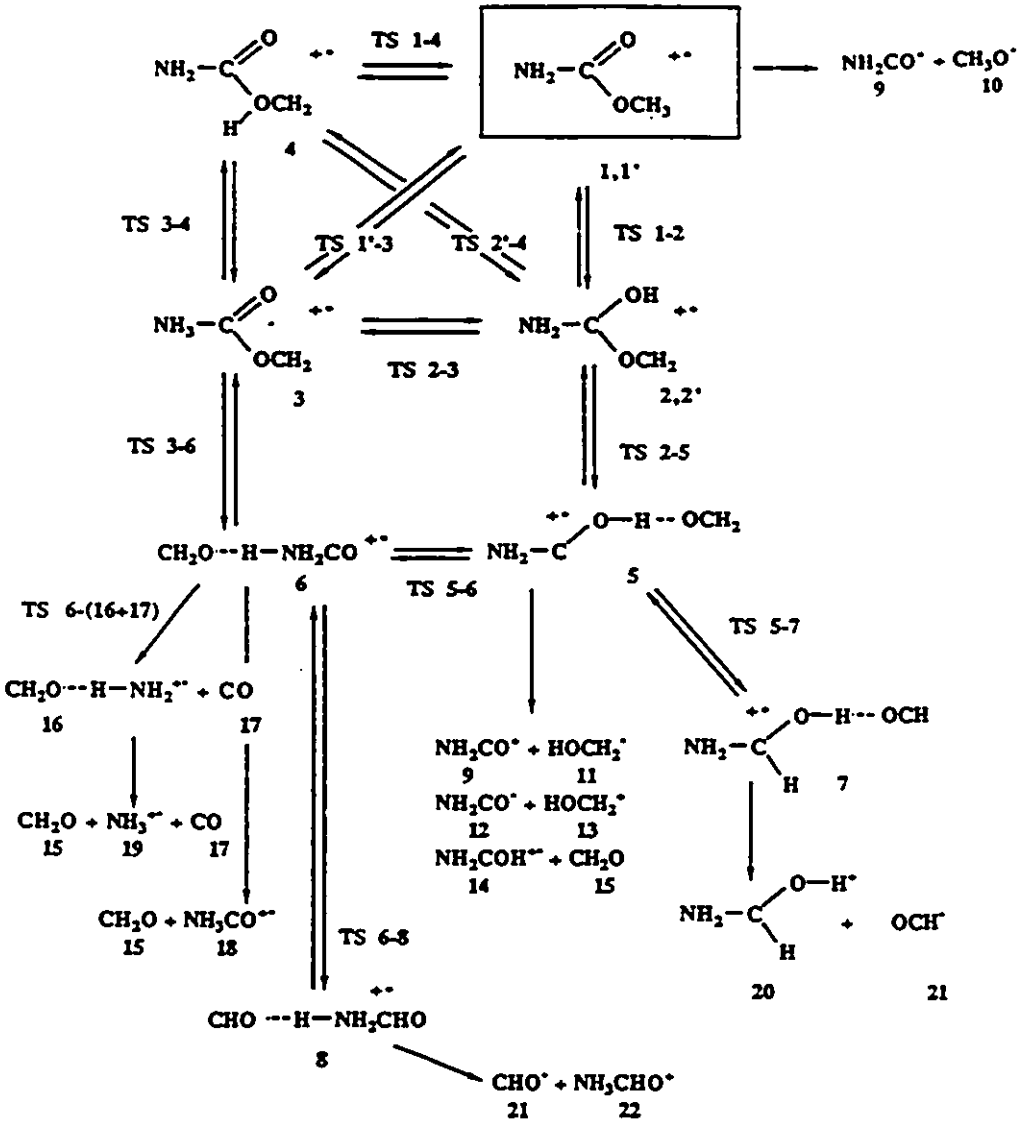

Scheme 2.1

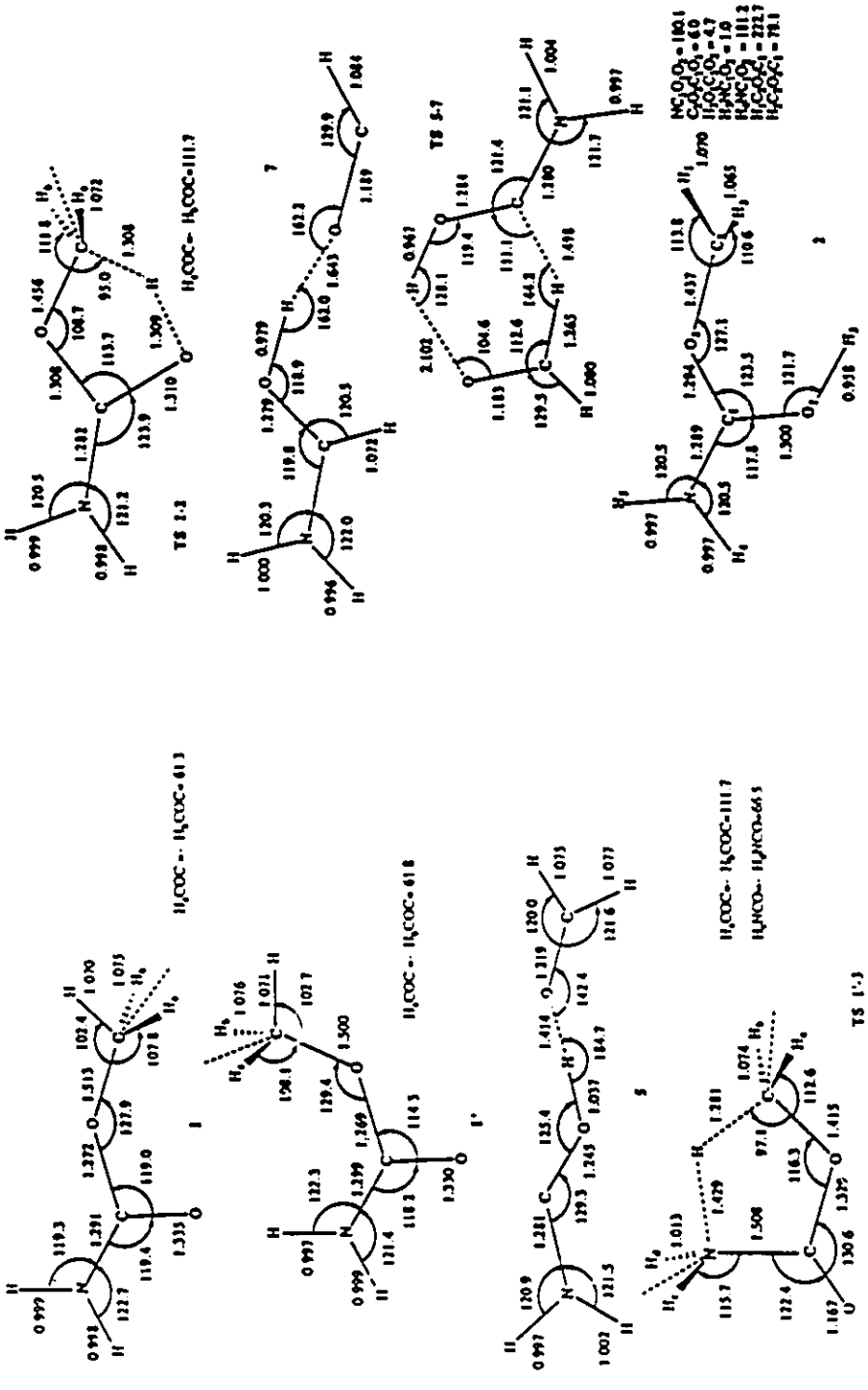

Fig. 2.4 Geometries of $C_2H_5NO_2^{+\bullet}$ isomeric ions and some Transition States optimized at the SCF/4-31G'' level of theory.

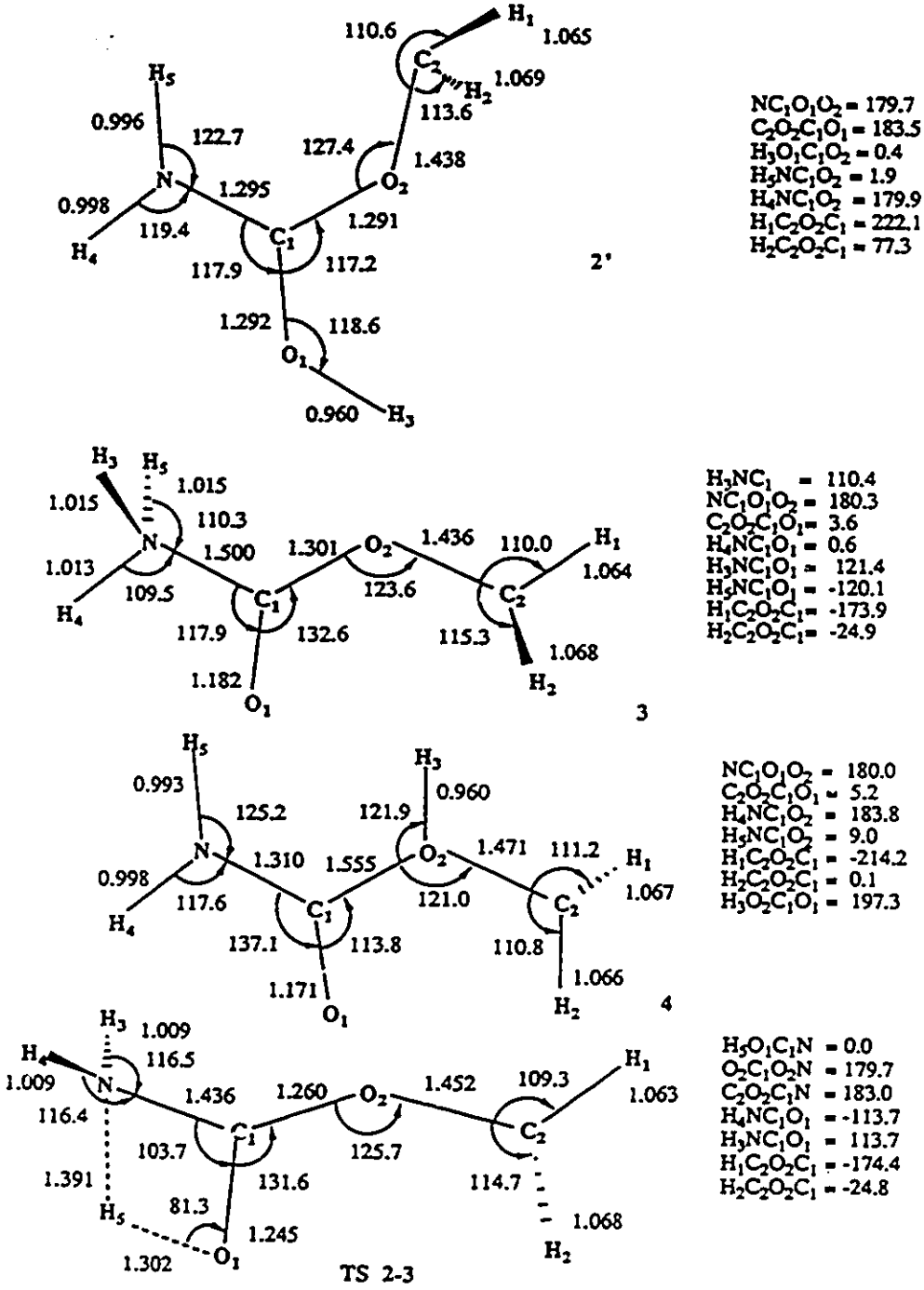

Fig. 2.4 continued

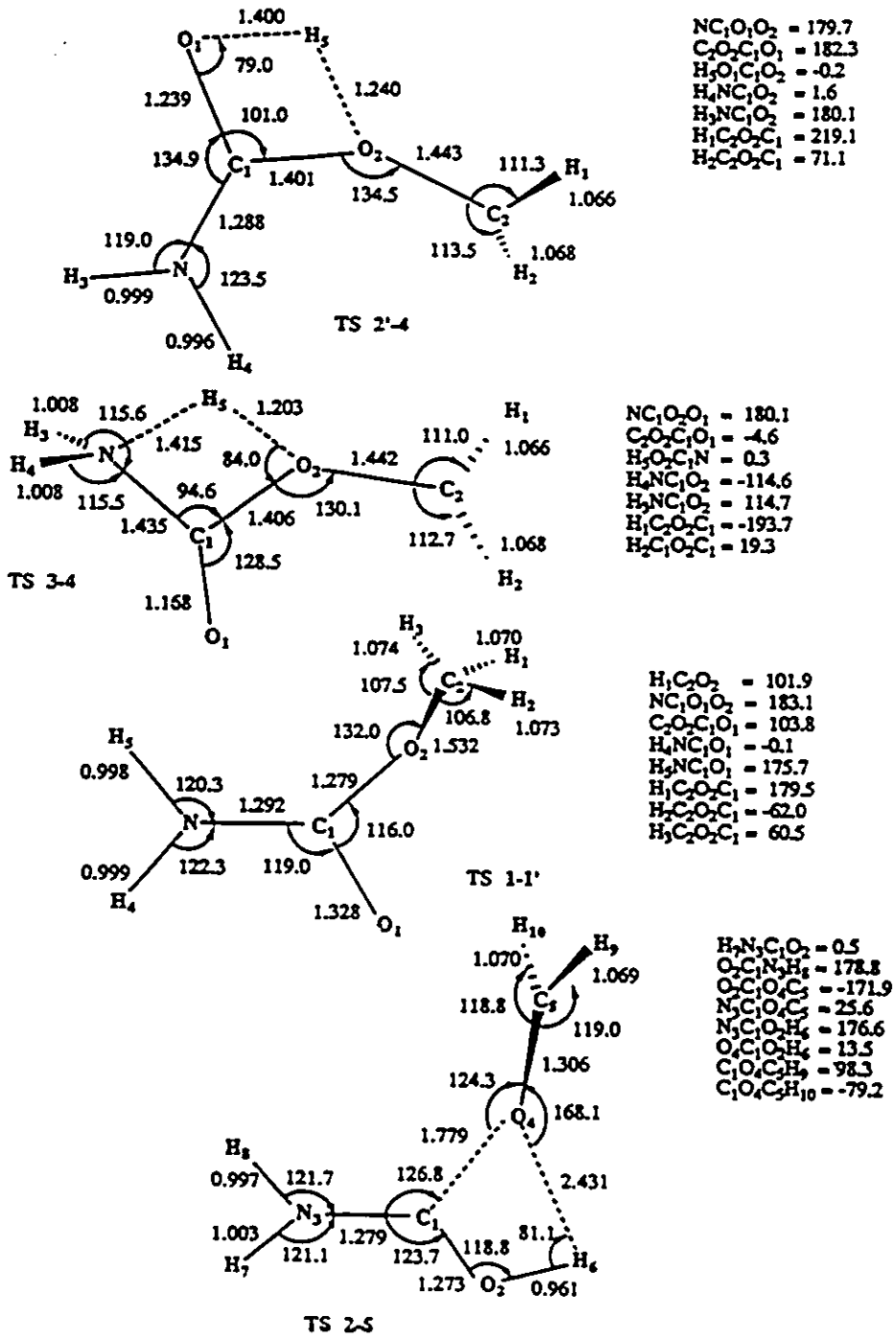

Fig. 2.4 continued

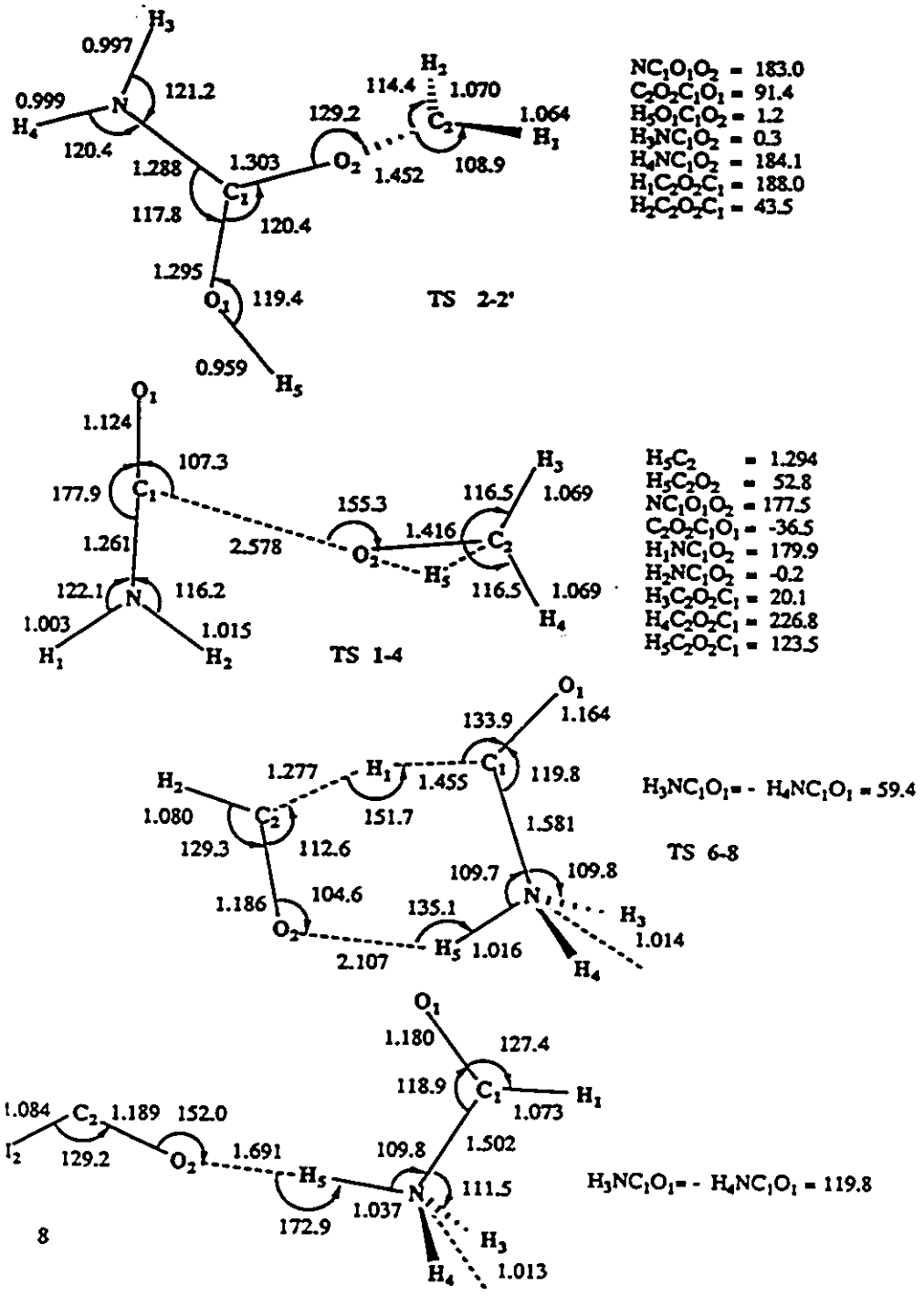

Fig. 2.4 continued

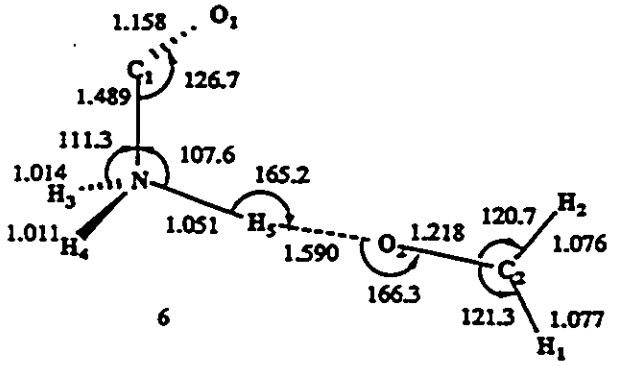

6

H_4NC_1 = 110.6
$H_3NC_1O_1$ = -23.0
$H_4NC_1O_1$ = -145.2
$H_5NC_1O_1$ = 96.4
$O_2H_5NC_1$ = -0.9
$C_2O_2H_5N$ = -171.4
$H_1C_2O_2H_5$ = 176.6
$H_2C_2O_2H_1$ = 180.0

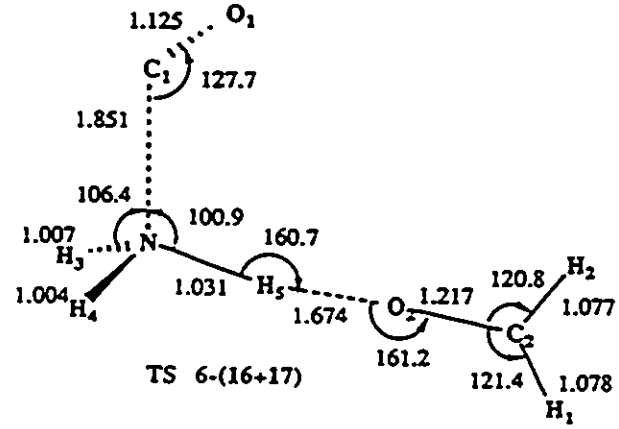

TS 6-(16+17)

H_4NC_1 = 105.2
$H_3NC_1O_1$ = -51.7
$H_4NC_1O_1$ = -172.3
$H_5NC_1O_1$ = 68.3
$O_2H_5NC_1$ = 2.6
$C_2O_2H_5N$ = -175.6
$H_1C_2O_2H_5$ = 178.9
$H_2C_2O_2H_1$ = 180.0

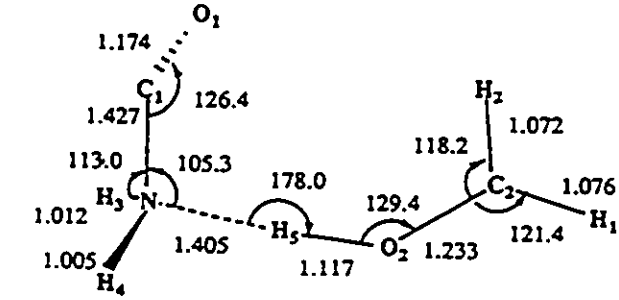

TS 5-6

H_4NC_1 = 112.9
$H_3NC_1O_1$ = -59.9
$H_4NC_1O_1$ = 174.4
$H_5NC_1O_1$ = 53.6
$O_2H_5NC_1$ = -43.1
$C_2O_2H_5N$ = 13.7
$H_1C_2O_2H_5$ = 180.0
$H_2C_2O_2H_1$ = 180.0

Fig. 2.4 continued

Table 2.2

Calculated total energies (hartrees) , zero-point vibrational energies (kcal/mol) and relative energies (kcal/mol) for isomers and components of ionized methyl carbamate

Species	Point group	State	RHF/4-31G// 4-31G	RHF/6-31G**// 4-31G	Pople/6-31G**// 4-31G	ZPVE 4-31G a)	E_{rel}
1	C_S	$^2A'$	-282.11727	-282.54499	-283.32871	48.0	0.
1'	C_S	$^2A'$	-282.11127	-282.54028	-283.32309	48.1	3.6
2	C_1	^2A	-282.12129	-282.55630	-283.34766	47.3	-12.6
2'	C_1	^2A	-282.12419			47.4	
3	C_1	^2A	-282.09446	-282.53260	-283.33567	47.5	-4.9
4	C_1	^2A	-282.07479	-282.49841	-283.29903	46.1	16.7
5	C_S	$^2A'$	-282.10309	-282.53057	-283.32719	45.3	-1.7
6	C_1	^2A	-282.06938	-282.50513	-283.31557	45.8	6.0
7	C_S	$^2A'$	-282.12184	-282.55292	-283.35072	46.1	-15.7
8	C_S	$^2A'$	-282.08043	-282.51570	-283.32376	45.3	0.4
TS 1-1'	C_1	^2A	-282.10438			47.6	
TS 2-2'	C_1	^2A	-282.11255			47.2	
TS 1-2	C_S	$^2A'$	-282.04093	-282.48412	-283.30594	45.3	11.6
TS 1'-3	C_S	$^2A'$	-282.00160	-282.45001	-283.28028	44.6	27.0
TS 2-3	C_1	^2A	-282.00813	-282.45582	-283.26723	43.9	34.5
TS 1-4	C_1	^2A	-281.98368	-282.42355	-283.24373	41.9	47.2
TS 2'-4	C_1	^2A	-282.02086	-282.45257	-283.26192	43.8	37.7
TS 3-4	C_1	^2A	-282.01800	-282.44667	-283.26090	43.9	38.5
TS 5-6	C_1	^2A	-282.05807	-282.49663	-283.30602	43.9	10.2
TS 6-(16+17)	C_1	^2A	-282.05463	-282.48989	-283.30957	44.0	8.0
TS 5-7	C_S	$^2A'$	-282.02916	-282.46888	-283.29304	43.5	17.9
TS 6-8	C_S	$^2A'$	-281.99844	-282.44246	-283.27881	42.8	26.1
9 + 10			-282.05347	-282.48274	-283.27413	43.7	30.0
9 + 11			-282.03356	-282.47677	-283.27966	43.3	26.1
12 + 13			-282.03379	-282.47395	-283.27459	44.9	30.9
14 + 15			-282.05404	-282.49146	-283.29055	44.5	20.5
16 + 17			-282.08952	-282.52336	-283.31274	40.7	2.7
15 + 18			-282.02327	-282.46915	-283.28732	44.6	22.6
15 + 19 + 17			-282.04349	-282.48615	-283.27749	39.3	23.4
20 + 21			-282.08580	-282.52626	-283.33184	44.6	-5.4
22 + 21			-282.04675	-282.49118	-283.30787	44.1	9.2

a) The zero-point vibrational energies include scaling by a factor 0.9.

The geometries of the isomers were determined using analytical gradient and numerical second derivative optimization procedures with the 4-31G basis set. These are displayed in Figure 2.4. The calculated energies are shown in Table 2.2. The relative energies presented in the Table were obtained by performing single + double configuration interaction (SD-CI) calculations in the 4-31G optimized geometries using the 6-31G** basis set with the help of the DIRECT CI program [22] .The SDCI results were size consistency corrected using Pople's formula [23]. The Pople size consistency corrected results were corrected for the scaled (0.9) contribution of zero-point vibrational energies (ZPVE). The ZPVE's [21] in Table 2.2 were calculated for the 4-31G optimized geometries employing the 4-31G basis set.

The unimolecular chemistry of methylcarbamate ions

Since we believed [12b] that we had indications for the participaticn of ion **3** in the loss of CO from **1**, we first calculated its relative energy and the barrier separating it from **1**. At our highest level of theory (see Table 2.2) **3** is favoured over **1** by 4.9 kcal/mol, and so the ion is thermodynamically accessible. However, the barrier for its formation (from **1'**) turned out to be surprisingly high, 26.9 kcal/mol, i.e. 11 kcal/mol higher than the experimentally derived activation energy (16 kcal/mol). Considering the level of our calculations and the generally good agreement between experiment and theory at comparable levels of theory found for other systems [7,11,12] we conclude that the isomerization **1** → **3** does not take place, at least not prior to the spontaneous loss of CO or that of HCO^+.

How then does the loss of CO and also that of HCO^+ occur? Previous theoretical calculations on methyl esters indicate that a 1,4-hydrogen shift to the oxygen atom requires only 11-15 kcal/mol. In the case of methyl carbamate TS **1** → **2** lies only 11.6 kcal/mol above **1** and isomer **2**, the distonic ion $H_2N\text{-}C(OH)\text{-}OCH_2^{+\bullet}$, is 12.6 kcal/mol more stable than **1**. Thus it is clear that the transformation **1** → **2** can take place below the

minimum energy required for the losses of CO and HCO$^{\bullet}$; by contrast the transformation **1** → **3** cannot take place below the minimum dissociation energy. Hence we conclude that the distonic ion **2** is accessible. That TS **1'** → **3** is much higher in energy than TS **1** → **2** may be traced to the fact that the NCOO π-electron system in **1** is not affected by the transition **1** → **2**, whereas in TS **1'** → **3** the π-electron delocalisation does not extend to the N-atom. However, for ion **2** to serve as a key intermediate in the losses of CO and HCO$^{\bullet}$ it must be able to undergo rearrangement reactions whose energy requirement are below that for the direct bond cleavage reaction **2** → $H_2NCOH^{+\bullet}$ + CH_2=O, (**14** + **15**). An attractive pathway which satisfies this requirement involves isomerisation into the very stable hydrogen-bridged isomer **5** as the first step:

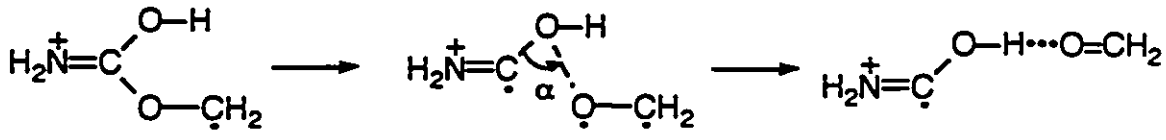

2 **TS 2 → 5** **5**

A similar isomerisation has been proposed to occur in the distonic ions H-C(OH)-$OCH_2^{+\bullet}$ (generated from ionized methyl formate) and CH_3-C(OH)-$OCH_2^{+\bullet}$ (generated from ionized methyl acetate): calculations [6,11,12a] have shown that in these ions stretching of the formaldehyde-carbene bond does not immediately lead to dissociation but to a situation where, well below the dissociation limit, isomerization can occur to the stable hydrogen-bridged isomer R-C=O···H···O=$CH_2^{+\bullet}$ [R = H or CH_3.

Using the SCF method, however, we were not able to find a saddle point for the transition state (TS **2** → **5**). A number of partial geometry optimizations were then performed for fixed values of the angle α (< OOC) as the reaction coordinate. These calculations indicated that for α = 45° *two* SCF solutions exist : one which is characterized by a *single* C-O bond in the formaldehyde moiety (as in ion **2**) and one in which this bond is a *double* C=O bond (as in ion **5**). The two solutions correspond with

valleys in the potential energy surface which are not separated by a saddle point but by an intersecting line, as indicated in Figure 2.5.

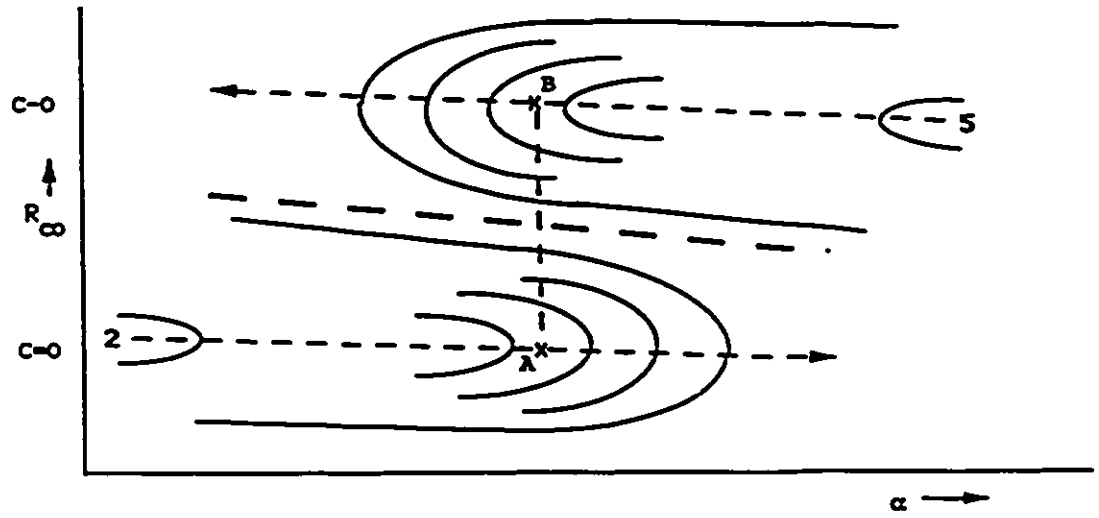

Fig. 2.5 Schematic Representation of the SCF potential energy surface for the isomerization 2 → 5.

Additional SCF calculations were performed for several C-O bond lengths between the two partial SCF minima (A and B in Figure 2.5) for a fixed angle $\alpha = 45°$. These calculations show a discontinuity in the energy gradient of the formaldehyde C-O bond resulting in an intersecting line between the two valleys (the dotted line in Figure 2.5). This discontinuity will disappear when the two SCF solutions are superimposed into a CASSCF wavefunction. In the case of a CASSCF calculation one selects an active orbital space which consists of occupied and unoccupied (virtual) orbitals. Within the active space all excitations are allowed, so a full confuguration interaction (CI) calculation is done for the active orbital space chosen. In our case we need three active orbitals for the three electrons (one on each of the two C atoms and one on the O atom) which are directly involved in the 2 → 5 isomerisation reaction. Using an interpolated geometry with $\alpha = 45°$ and $R_{CO} = 1.45$ Å as the starting point we were thus able to locate the transition state (TS 2 → 5). Computation of the activation energy was performed at the

CASSCF/4-31G level of theory and the same level of theory was used for optimizing the geometries of the ions **2** and **5**. According to these calculations, the transition state, TS **2** → **5**, corresponds to both the breaking of the (N)C–O(C) bond in ion **2** and the breaking of one $(H_2)C=O$ bond in ion **5**. In TS **2** → **5** there are essentially three radical electrons, localized on the two O atoms and on the formaldehyde C atom. In the SCF method two of these electrons are forced to occupy the same MO. The character of the SCF wave function is determined by the $(H_2)C=O$ bond length; for intermediate CO bond lengths there is an instability with respect to localization of the radical electron on either of the two C atoms, leading to a discontinuity in the energy gradient of the CO bond.

The final results of our CASSCF calculations which, because of the large computational expense involved, had to be restricted to the CASSCF/4-31G level of theory, are as follows: ion **2**, E = -282. 14122; ion **5**, E = -282. 11974; and TS **2** → **5**, E = -282.08514 Hartree. This is equivalent with TS **2** → **5** being 35 kcal/mol higher in energy than **2**, or 22.4 kcal/mol above **1** (see Figure 2.6). From the results in Table 2.2, it can be seen that enlarging the basis set with polarization functions generally has little effect on the activation energies. However, electron correlation effects are much more important for the transition states than for the stable isomeric ions and their inclusion results in a decrease of the activation energies for the isomerizations. Since inclusion of the ZPVE's is expected to have the same effect we propose that the calculated activation energy for the isomerization step **2** → **5** may be an upper limit. In any case, the calculated relative energy for TS **2** → **5** is in satisfactory agreement with the experimental observations: it lies below the dissociation limit for **2** → $H_2NCOH^{+\bullet}$ + $CH_2=O$, (**14** + **15**) and it may well represent the (rate determining) second isomerisation step in the mechanism for the losses of CO and $HCO^{\bullet}$.

The fate of ions **5** is intriguing: in marked contrast to the related species CH_3-C=O···H···O=$CH_2^{+\bullet}$ and H-C=O···H···O=$CH_2^{+\bullet}$ which dissociate by simple bond cleavage to their components, our calculations indicate that ions **5** can undergo two

rearrangement reactions below or close to the dissociation limit. The energy diagram presented in Figure 2.6 shows the results of our *ab initio* calculations. For comparison this diagram also contains the experimentally derived activation energies for loss of $HCO^{\bullet}/CO$ (16 kcal/mol), $CH_2{=}O$ (23 kcal/mol) and $CH_3O^{\bullet}/CH_2OH^{\bullet}$ (18.5 kcal/mol).

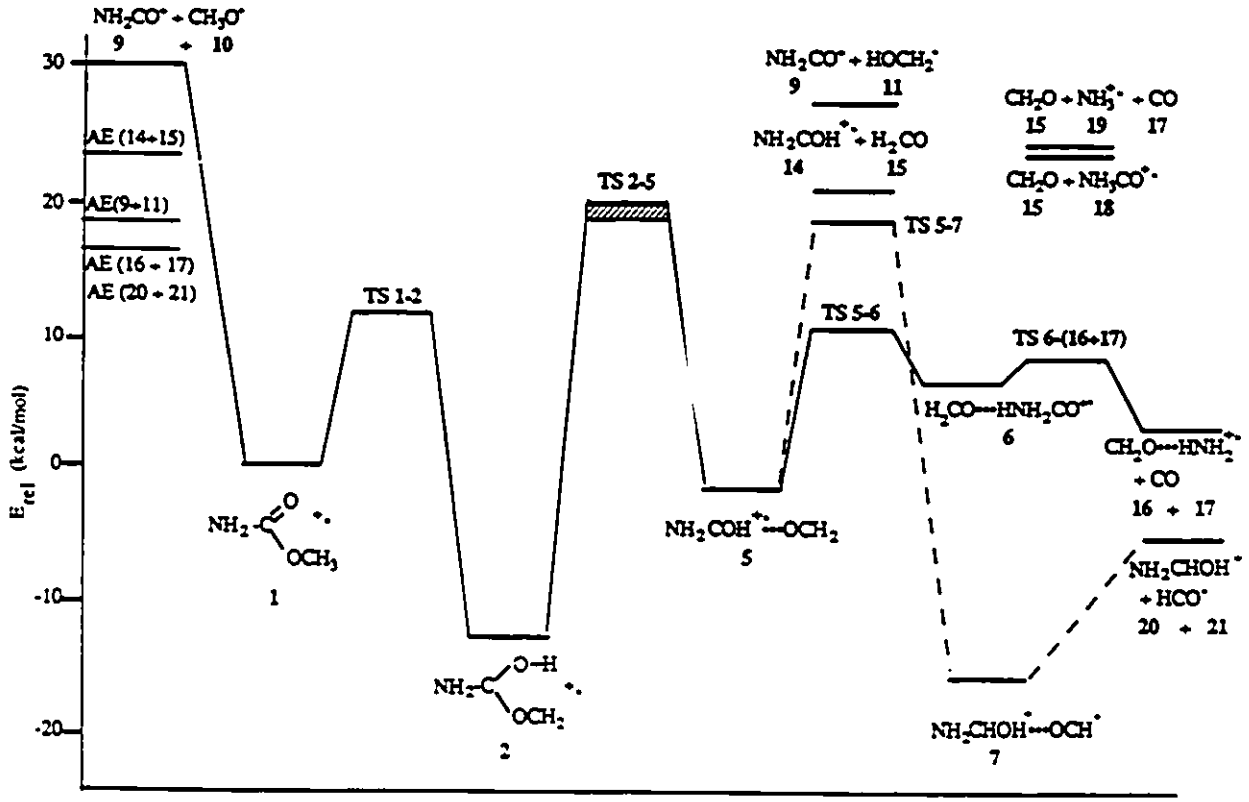

Fig. 2.6 Theoretically derived energy diagram for the dissociation reactions of ionized methyl carbamate, $H_2NCOOCH_3^{\bullet+}$.

The first possibility is that the formaldehyde molecule in **5** attracts the hydroxyl hydrogen. The incipient $^{\bullet}CH_2OH$ radical subsequently moves within the electrostatic field of the $H_2N{=}C{=}O^+$ ion towards the N atom to form, via TS **5** → **6**, the hydrogen-bridged species $H_2C{=}O{\cdots}H{\cdots}NH_2CO^{+\bullet}$, **6**:

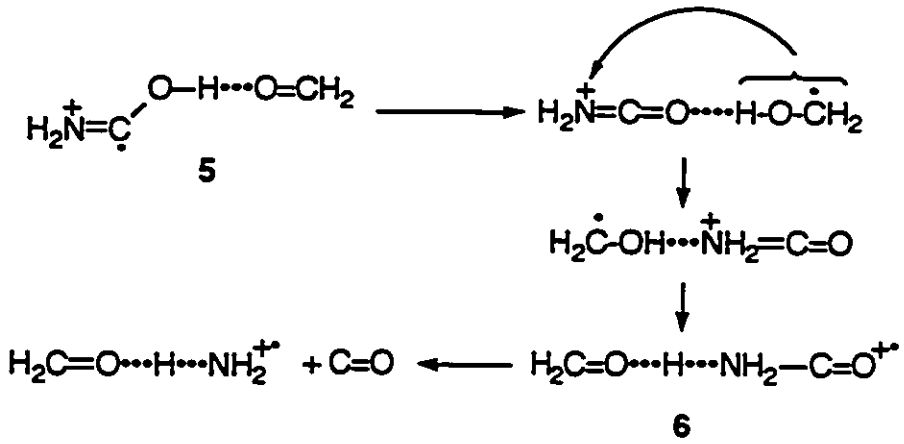

Thus, in agreement with our previous proposal [12b], it is indeed ion **6** from which the loss of CO occurs. However, this ion is *not* formed via the simple pathway proposed previously, but via a more complex route. According to the calculations these ions lie in a shallow well only and they dissociate by loss of CO to produce the hydrogen-bridged product ion $[H_2C{=}O{\cdots}H{\cdots}NH_2]^{+\bullet}$, in agreement with experiment. Note that the dissociation limit for the reaction **6** → $H_3N{-}C{=}O^{+\bullet} + CH_2{=}O$ is much higher in energy, i.e. the N-C bond in **6** is much weaker than the -O···H···N- hydrogen-bridged ion-dipole interaction.

Alternatively, instead of accepting a hydrogen the formaldehyde molecule in **5** may *donate* a hydrogen to the carbon atom of the $H_2N{-}C{-}OH^{+\bullet}$ ion, forming via TS **5** → **7** the most stable $C_2H_5NO_2$ isomer, $[H_2NCHOH^+{\cdots}O{=}C^{\bullet}{-}H]$, in which the $NH_2{-}CH{-}OH^+$ ion interacts with the formyl dipole. Loss of $HCO^{\bullet}$ occurs directly therefrom as shown below.

Are the results of the calculations, as summarized in the energy diagram shown in Figure 2.6, in agreement with experiment? First of all, theory predicts that metastable ions **1** will lose $HCO^{\bullet}$ and CO, as is observed experimentally. Secondly, theory predicts the correct structures for the daughter ions, i.e. $NH_2{-}CH{-}OH^{+\bullet}$ and $H_2C{=}O{\cdots}H{\cdots}NH_2^{+\bullet}$

respectively.

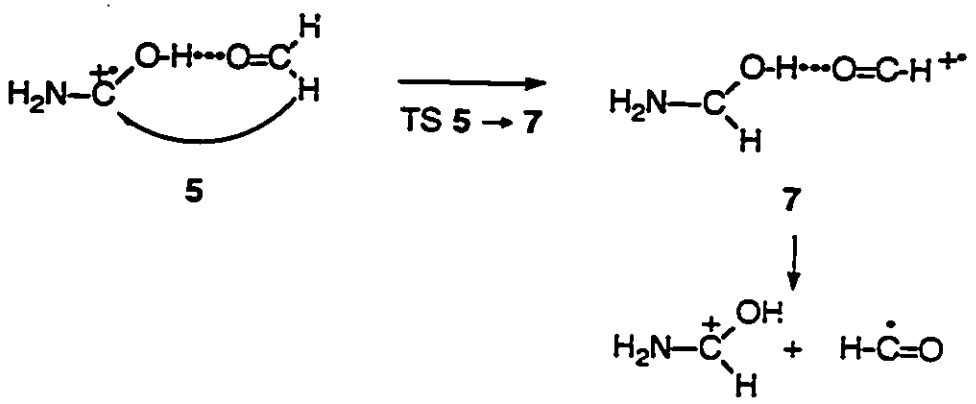

Furthermore, for the labelled species theory predicts atom-specific behaviour and it also predicts the correct isotopic positions in the products (see above), notably the observation that H_2N-C(O)-^{18}O-$^{13}CH_3$ cleanly eliminates $H^{13}C^{18}O$ and $^{12}C^{16}O$.

In addition, we had shown earlier [12b] that the dissociative neutralization of the OCD_3 labelled carbamate generated, among other products, largely $^{\bullet}CD_2OD$ (together with some $^{\bullet}CD_2OH$). Dissociative neutralization, not collisional activation, was chosen to prevent post-collisional isomerization [12b]. Had low energy methyl carbamate ions rearranged to **3** then mostly $^{\bullet}CD_2OH$ would have been generated. This is strong support for the rearrangement **1** → **2** → **5** after which dissociative neutralization to $^{\bullet}CD_2OD$ takes effect.

The small amount of $^{\bullet}CD_2OH$ formed after the neutralization indicates that in **2** the formaldehyde molecule may also migrate to the N atom generating $[CH_2{=}O{\cdots}H{\cdots}NH\text{-}C\text{-}OH]^{+\bullet}$, but this was not further investigated. Note that formation of $^{\bullet}CD_2OH$ cannot be ascribed to the transformation **1** → **3** as low energy ions are sampled in the NR experiment. The partially labelled ion $H_2NC(O)OCD_2H^{+\bullet}$ in the μs time frame loses $DCO^{\bullet}$ and $HCO^{\bullet}$ in a ratio of 2:1. This is precisely what our calculations predict, provided that no isotope effects operate in the steps **1** → **2** and **5** → **7** and so we conclude that not these steps, but the transformation **2** → **5** is rate-determining as was the case with ionized methyl acetate [12a].

The calculated relative energies and the experimental values, where they overlap, compare favourably except for the energy difference, Δ, between **1** and its dissociation products H_2N-C=O + $^{\bullet}CH_2OH$, (**9** + **11**): experiment (this work), Δ = 18 kcal/mol vs. theory Δ = 26 kcal/mol. The reason for this large discrepancy is not well understood although it should be noted that in general dissociation energies are more difficult to accurately establish than the relative energies of a set of isomeric ions.

There is particularly good agreement between the experimentally and theoretically derived magnitude of the reverse term for loss of $HCO^{\bullet}$: 26 kcal/mol (experiment) vs. 24 kcal/mol (theory). Note however that the average kinetic energy release, <T> is small and non-specific; <T> =1.77 kcal/mol and so only about 7 % of the energy is released as kinetic energy. Similar effects have been observed previously in the dissociation of other hydrogen-bridged radical cations [11, 14a]. Similarly the loss of CO has a calculated reverse term, E_{rev} , of ~15 kcal/mol, but <T> is only 1.07 kcal/mol (~ 7% of E_{rev}). The observation that the $[CD_2{=}O{\cdots}D{\cdots}NH_2]^{+\bullet}$ daughter ions formed from the OCD_3 labelled carbamate generate upon collisional activation a 2:1 mixture of $^{+}CD_2OH$ and $^{+}CD_2OD$ ions and upon dissociative electron capture a 2:1 ratio of $^{\bullet}CD_2OH$ and $^{\bullet}CD_2OD$ radicals can be rationalized by allowing the formaldehyde dipole to (freely) rotate around the ammonia ion, i.e. $[CD_2{=}O{\cdots}D{\cdots}NH_2]^{+\bullet} \rightarrow [CD_2{=}O{\cdots}H{\cdots}NDH]^{+\bullet}$.

Finally there are two questions related to the ion chemistry of ionized methyl carbamate which we are currently investigating. The first question concerns the possible participation of the isomeric ion H-N=C(OH)-$OCH_3^{+\bullet}$, **1a**, the "iminol" analogue of methyl acetate, in the isomerisation behaviour of **1**. This iminol type ion, which according to preliminary calculations is quite a stable species, could be formed from ions **2** by a 1,4-Hydrogen shift (a 1,3-hydrogen shift in ions **1** is probably energetically prohibitive [12d]). However, if this isomerisation reaction occurs then ions **1a** cannot isomerize back to **2** because the labelled ion H_2N-C(=O)-$OCD_3^{+\bullet}$ specifically loses $DCO^{\bullet}$. Ion **1a** was expected to be generated from R-CH=N-N(H)-C(=O)-OCH_3, R = {H, CH_3} by a McLafferty-type

rearrangement:

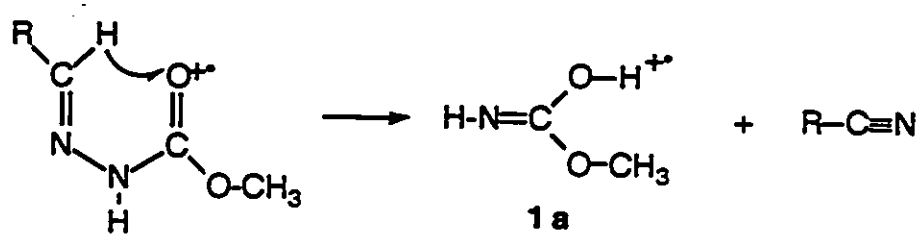

1a

but surprisingly the MI, CA and NR mass spectra of the abundant m/z 75 $C_2H_5NO_2$ ions generated from these precursor molecules were very close to those of the keto ion **1**. We are currently investigating other means of generating **1a** and also establishing the height of the barriers for its (inter)conversion with ions **1** and **2** by *ab initio* calculations. The second question concerns the following: if one of the amino hydrogen atoms of methyl carbamate is substituted by an NH_2 group (yielding methyl carbazate, H_2N-N(H)-$COOCH_3$) an unexpected and totally different dissociation behaviour ensues [25]. Methyl carbazate ions dissociate to, among other products, the immonium ion H_2N-N(H)=CH_2^+ by expulsion of $^{\bullet}COOH$ in a one step process [25]. Based on a variety of experiments the following mechanism was proposed:

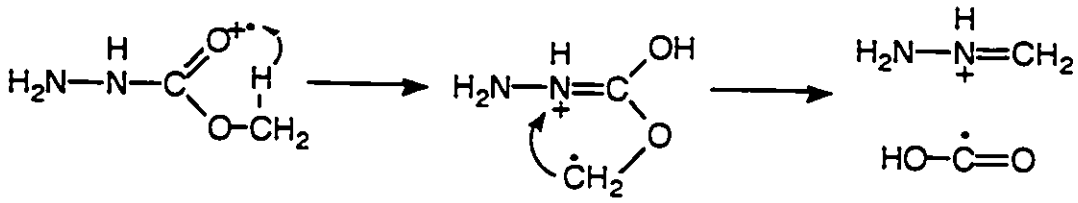

According to this proposal, in the intermediate distonic ion, which can be considered as the analogue of **2**, a methylene unit is transferred to the charged centre. In case of ion **2**, a similar reaction would lead to the very stable immonium ion $^{+}CH_2NH_2$ and $^{\bullet}COOH$ whose combined enthalpies ($\Sigma\Delta H_f$ [$CH_2NH_2^+$ + $^{\bullet}COOH$] = 125 kcal/mol [20a]) are lower than those for the observed reaction products. From the start of the present study we were, in fact, surprised that methyl carbamate ions do not expel $^{\bullet}COOH$.

Conclusion

The results of our study provide a detailed insight into the unimolecular chemistry of ionized methylcarbamate. Although its chemistry (loss of HCO$^{\bullet}$ and CO) would superficially appear to be totally different from that of ionized methyl acetate (losses of $CH_3O^{\bullet}$ and $^{\bullet}CH_2OH$), the first two of the three isomerization steps are in fact the same (molecular ion → distonic ion → hydrogen-bridged ion).

However, in contrast with ionized methyl acetate, the resulting hydrogen-bridged radical cation $H_2N\text{-}C\text{-}OH\cdots O{=}CH_2^{+\bullet}$, **5**, can undergo two further rearrangement reactions. The first process involves rearrangement into the hydrogen-bridged ion-dipole complex $H_2C{=}O\cdots H\cdots NH_2\text{-}C{=}O^{+\bullet}$, **6**, which leads to the loss of CO by a simple bond cleavage. The second process involves isomerization into another hydrogen-bridged ion-dipole complex, the most stable $C_2H_5NO_2^{+\bullet}$ isomer $H_2NCHOH^{+}\cdots\cdot O{=}C\text{-}H$, **7**, which is the immediate precursor for loss of HCO$^{\bullet}$. Thus it appears that the participation of hydrogen-bridged ion-dipole complexes in isomerizations is even more important in the unimolecular chemistry of ionized methyl carbamate than ionized methyl acetate. This is largely due the combination of stability and flexibility in these ions.

Finally we note that, as was the case with methyl acetate [12a], a coherent description of the chemistry of solitary methyl carbamate ions could not have been achieved by the analysis of experimental data only.

References

1 (a) H. Budzikiewicz, C. Djerassi and D.H. Williams, Mass Spectrometry of Organic Compounds, Holden-Day Inc.: London (1967); (b) F.W. McLafferty, Mass Spectrometry of Organic Ions, Academic press: New York (1963).

2 R.I.Reed, Quarterly Rev. 20 (1966) 527.

3 K. Biemann, in Mass Spectrometry, Organic Chemical Applications, McGraw-Hill, New York (1967), p. 102.

4 (a) R.G. Cooks, J.H. Beynon, R.M. Caprioli and G.R. Lester, Metastable Ions, Elsevier: Amsterdam (1973); (b) K. Levsen, Fundamental Aspects of Organic Mass Spectrometry, Verlag Chemie: Weinheim (1978).

5 (a) C. Wesdemiotis and F.W. McLafferty, Chem. Rev. 87 (1987) 485; (b) J.K. Terlouw and H. Schwarz, Angew. Chem., Int. Ed. Engl. 26 (1987) 805; *ibid.* Angew. Chem. 99 (1987) 799; (c) J.K. Terlouw, Adv. Mass Spectrom. 11 (1989) 984; (d) J.L. Holmes, Mass Spectrom. Rev. 8 (1989) 513.

6 For a detailed computational and experimental study see: N. Heinrich, T. Drewello, P.C. Burgers, C. Morrow, J. Schmidt, W. Kulik, J.K. Terlouw and H. Schwarz, J. Am. Chem. Soc. 114 (1992) 3776.

7 For a recent review see: P.C. Burgers and J.K. Terlouw, in Specialist Periodical Reports : Mass Spectrometry, M.E. Rose (ed.), The Royal Society of Chemistry: London (1989), Vol. 10, Chapter 2.

8 P.C. Burgers, C.E.C.A. Hop, J.K. Terlouw and J.L. Holmes, Org. Mass Spectrom. 21 (1986) 549.

9 see for example: C.E. Hudson, T. Lin and D.J. McAdoo, Org. Mass Spectrom. 22 (1987) 311.

10 (a) A.N.H. Yeo, J. Chem. Soc. D (1970) 1154; (b) J.L. Holmes, P.C. Burgers and J.K. Terlouw, Can. J. Chem. 12 (1981) 1805; (c) L. Freiser-Monteiro, M.L. Freiser- Monteiro, J.L. Butler and T. Baer, J. Phys. Chem. 86 (1982) 752.

11 N. Heinrich and H. Schwarz, in Ion and Cluster Ion Spectroscopy and Structure, J.P. Maier (Ed.), Elsevier: Amsterdam (1989), p. 329.

12 (a) N. Heinrich, J. Schmidt, H. Schwarz and Y. Apeloig, J. Am. Chem. Soc. 109 (1987) 1317 and references cited therein; (b) P.C. Burgers, C. Lifshitz, P.J.A. Ruttink, G. Schaftenaar and J.K. Terlouw, Org. Mass Spectrom. 24 (1989) 579; (c) W. Hehre, L. Radom, P. v. R. Schleyer and J.A.

Pople, Ab Initio Molecular Orbital Theory, John Wiley and Sons: New York (1986); (d) B. Yates and L. Radom, J. Am. Chem. Soc. 109 (1987) 2910.

13 (a) S. Hammerum, Mass Spectrom. Rev. 7 (1988) 123; (b) B.F. Yates, W.J. Bouma and L. Radom, Tetrahedron 22 (1986) 6225.

14 (a) P.C. Burgers, J.L. Holmes, C.E.C.A. Hop, R. Postma, P.J.A. Ruttink and J.K. Terlouw, J. Am. Chem. Soc. 109 (1987) 7315; (b) B.L.M. van Baar, P.C. Burgers, J.L. Holmes and J.K. Terlouw, Org. Mass Spectrom. 23 (1988) 355; (c) P.C. Burgers, J.L. Holmes, J.K. Terlouw and B.L.M. van Baar, Org. Mass Spectrom. 20 (1985) 202.

15 (a) D.J. McAdoo, Mass Spectrom. Rev. 7 (1988) 363; (b) R. Postma, P.J.A. Ruttink, B.L.M. van Baar, J.K. Terlouw, J.L. Holmes and P.C. Burgers, Chem. Phys. Lett. 123 (1986) 409.

16 D. Bethel and V. Gold, Carbonium Ions - An Introduction, Academic Press: New York (1967), p. 205.

17 F.P. Lossing and J.C. Traeger, Int. J. Mass Spectrom. Ion Phys. 19 (1976) 9.

18 A.M. Paquin, Z. Naturforschg. 1 (1946) 518.

19 P.C. Burgers and J.L. Holmes, Org. Mass Spectrom. 17 (1982) 123.

20. (a) S.G. Lias, J.E. Bartmess, J.F. Liebman, J.L. Holmes, R.D. Levin and W.G. Mallard, J. Phys. Chem. Ref. Data 17, supplement 1 (1988); (b) C.E.C.A. Hop, J.L. Holmes, P.J.A. Ruttink, G. Schaftenaar and J.K. Terlouw, Chem. Phys. Lett. 156 (1989) 251: this paper shows that ΔH_f° $[H_2N\text{-}C{=}O]^+$ as quoted in ref. 20a (167 kcal/mol) is probably in error.

21 M. Dupuis, D. Spangler and J. Wendolowski, NRCC Software Catalog 1, Program No QG01, GAMESS (1980); M.F. Guest and J. Kendrick, GAMESS User Manual, An Introductory Guide,CCP/86/1, Daresbury Laboratory (1986).

22 V.A. Saunders and J.H. van Lenthe, Mol. Phys. 48 (1983) 923.

23 J.A. Pople, R. Seeger and N.R. Krishan, Int. J. Quantum Chem. 11 (1977) 149.

24 J.A. Pople, H.B. Schlegel, R. Krishan, D.J. DeFrees, J.S. Binkley, M.J. Frisch, R.A. Whiteside, R.F. Hout, Jr. and W.J. Hehre, Int. J. Quantum Chem. 15 (1981) 269.

25. P.C. Burgers, T. Drewello, H. Schwarz and J.K. Terlouw, Int. J. Mass Spectrom. Ion Processes 95 (1989) 157 .

CHAPTER 3

The gas phase chemistry of the methyl carbamate radical cation $H_2NCOOCH_3^{+\bullet}$. II . A test case for ion structure assignment.

Introduction

In this chapter the unimolecular chemistry of the methyl carbamate radical cation, $H_2NCOOCH_3^{+\bullet}$, **1**, is further investigated by tandem mass spectrometric (metastable ion (MI), collisional activation (CA), and neutralization-reionization (NR) mass spectrometry), MS/MS/MS "double collision" and ^2H labelling labelling experiments.

The difficulties faced in ion structure assignment are clearly illustrated in our attempts to generate the isomeric "iminol" ion $H\text{-}N{=}C(OH)\text{-}OCH_3^{+\bullet}$, **1a** by loss of CH_3CN from $CH_3CH{=}N\text{-}NHCOOCH_3$. Ab initio MO calculations were used to evaluate the stability of **1a** and the hydrogen-bridged radical cation $[H_2C{=}O\cdots H\cdots N(H)COH]^{+\bullet}$, **6a**, as well as the barriers for their formation from **1** and the key distonic ion $H_2N\text{-}^+C(OH)OCH_2^\bullet$, **2**.

This material was previously published in a paper having the same title:

G.A. McGibbon, C.A. Kingsmill, J.K. Terlouw and P.C. Burgers,

Org. Mass Spectrom. 27 (1992) 126.

Our earlier [1,2] investigations of methylcarbamate radical cations $H_2NCOOCH_3^{+\bullet}$,**1**, raised the question of whether or not the iminol isomer $H\text{-}N{=}C(OH)\text{-}OCH_3^{+\bullet}$, **1a**, plays a role in the isomerization behavior of ion **1**. We anticipated, as proposed in ref. 3, that an ion of structure **1a** would result from a McLafferty-type rearrangement of precursors $RCH{=}NNHCOOCH_3$ (R= H, CH_3). Surprisingly however, the metastable ion (MI), collisional activation (CA) and neutralization-reionization (NR) mass spectra of the resultant m/z 75 $C_2H_5NO_2^{+\bullet}$ ions were very similar to the spectra of ion **1**.

With regard to ion structure assignment, Holmes [4] has critically assessed the methods and techniques available for the assignment of ion structures and he also discussed the hidden dangers associated with the interpretation of the results, notably those obtained from CA experiments. On the topic of CA he writes, "Far too many reported CA mass spectra have been assigned to single ion structures, the assignment being based solely on unsubstantiated assumptions as to the mechanism of the reaction which generates the ion." This chapter presents a test case of structure assignment and it shows that unequivocal structure assignment can indeed be far from straightforward. This work constitutes the third part of a study of the intriguing unimolecular chemistry of the methyl carbamate $H_2NCOOCH_3$ radical cation and a summary of previous work [1,2] is given below as an appropriate introduction to this chapter on the detailed chemistry of $C_2H_5NO_2^{+\bullet}$ ions.

The methyl carbamate radical cation is a case *par excellence* of a species which dissociates via the intermediacy of distonic ions [5], hydrogen-bridged [1,2,6] radical cations and flexible ion-dipole complexes [5c,7]. Metastable $H_2NCOOCH_3^{+\bullet}$ fragments by loss of $HCO^{\bullet}$ (96%) and by loss of CO (4%). The product ion formed by loss of $HCO^{\bullet}$ has the structure $H_2N\text{-}CH\text{-}OH^+$, a carbenium ion stabilized by two powerful electron donating groups; the product ion generated by loss of CO is the hydrogen-bridged radical cation $[CH_2{=}O\cdots H\cdots NH_2]^{+\bullet}$ which is best viewed as $NH_3^{+\bullet}$ interacting with the formaldehyde dipole. By combining results from mass spectrometric experiments and state-of-the-art

ab initio calculations the mechanisms shown in Scheme 3.1 were derived for $HCO^{\bullet}$ and CO loss [2]:

SCHEME 1

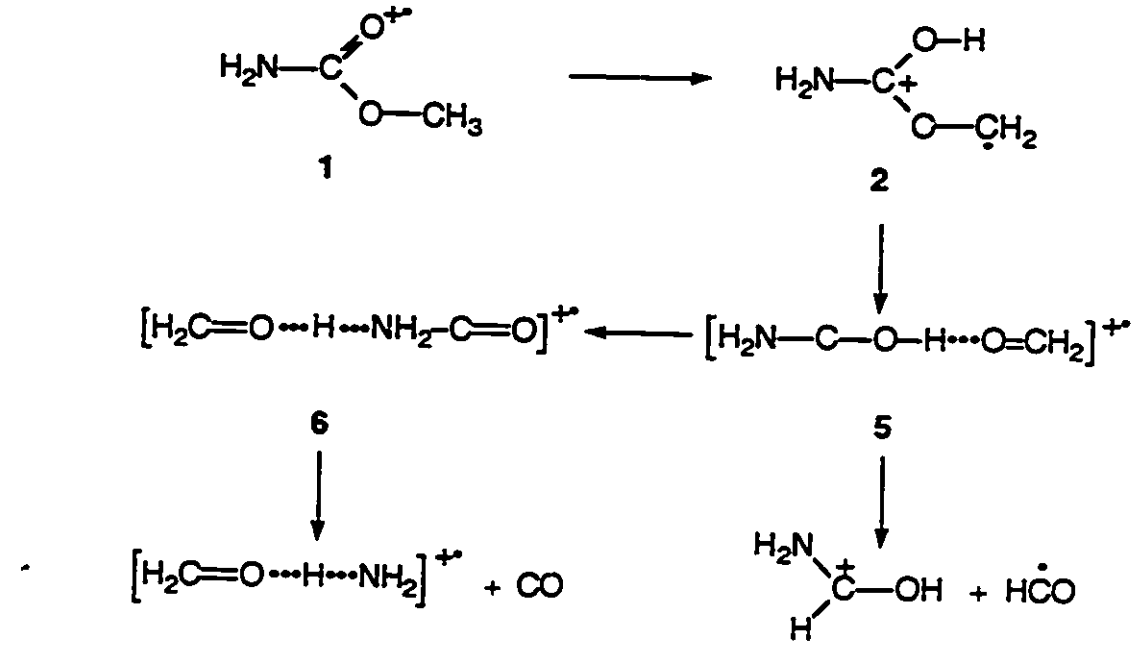

Scheme 3.1

The reaction commences with a 1,4-hydrogen shift to produce the distonic ion **2**. Next, upon elongation of the C-OCH_2 bond the formaldehyde dipole moves within the electrostatic field of the aminohydroxycarbene ion to generate the hydrogen-bridged species **5**. The formaldehyde can then donate a hydrogen ("1,5-hydrogen" shift) to the H_2N-C-$OH^{+\bullet}$ ion followed by loss of $HCO^{\bullet}$, or it can attract the bridge hydrogen whereupon a subsequent migration of the incipient $CH_2OH^{\bullet}$ within the electrostatic field of the protonated isocyanic acid $H_2N{=}C{=}O^{+}$, ion **6** is produced which then sheds CO. The transformation **5** → **6** can be viewed as the formaldehyde catalyzed 1,3-hydrogen shift H_2N-C-$OH^{+\bullet}$ → H_3N-C-$O^{+\bullet}$. We note here that the unimolecular chemistry of ionized methyl carbamate, notably the transition **1** → **2** → **5** is very similar to that of ionized methyl acetate [8] and methyl formate [9]; even the associated enthalpy changes are very similar (see Table 3.1).

However, in contrast to methyl acetate, methyl carbamate shows atom-specific behaviour, i.e. there are no H/D exchange reactions for $H_2N\text{-}C(=O)OCD_3^{+\bullet}$, whereas $H_3C\text{-}C(=O)OCD_3^{+\bullet}$ shows isotopic exchanges almost to the statistical limit.

Table 3.1. Relative Energies (kJ/mol) for Transformation of $X\text{-}C(=O)OCH_3^{+\bullet}$ with X = H, CH_3, NH_2.

X	$X\text{-}C(=O)OCH_3^{+\bullet}$ 1	TS1→2	$X\text{-}C(OH)OCH_2^{+\bullet}$ 2	TS1→5	$[XC{=}O\cdots H\cdots O{=}CH_2]^{+\bullet}$ 5	Ref.
H	0	64	-48	99	-4	[9]
CH_3	0	47	-51	71	-2	[8]
NH_2	0	49	-53	94	-7	[2]

For methyl acetate the equilibria keto ⇔ distonic ⇔ enol [8]:

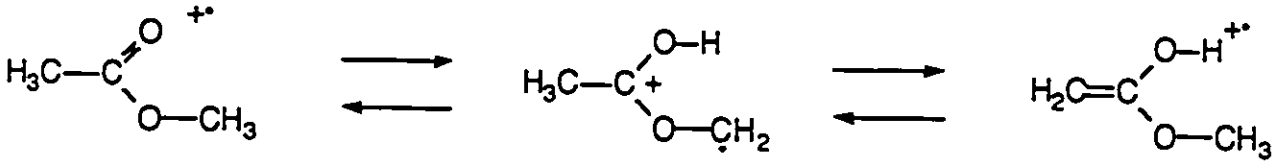

keto distonic enol

accounts for the loss of positional identity, but such reversible reactions clearly do not occur for methyl carbamate ions, i.e. there is no interconversion with the corresponding iminol ion:

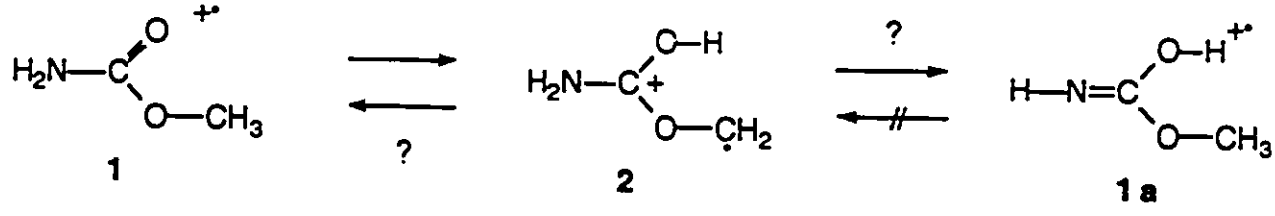

1 2 1a

keto distonic iminol

When the starting ions $H_2N\text{-}C(O)\text{-}OCH_3^{+\bullet}$ are collisionally activated two other processes (i.e. in addition to $HCO^\bullet$ and CO losses) are observed, viz. loss of $CH_2{=}O$ and $CH_2OH^\bullet$; that the latter radical is $CH_2OH^\bullet$ and not $CH_3O^\bullet$ was deduced from neutralization-reionization experiments [2]. It was concluded that the distonic ion **2** is the reacting configuration for $CH_2{=}O$ loss and that the hydrogen bridged ion **5** sheds $CH_2OH^\bullet$. With regard to the latter fragmentation it was observed, unexpectedly, that the labelled ion $H_2N\text{-}C(=O)OCD_3^{+\bullet}$ generates $CD_2OH^\bullet$ in admixture with the expected $CD_2OD^\bullet$ and it was proposed that the formaldehyde dipole in **2** could also migrate to the NH_2 group to produce $[D_2C{=}O\cdots H\cdots N(H)COD]^{+\bullet}$ which then sheds $CD_2OH^\bullet$.

To more fully understand the intriguing unimolecular chemistry (be it spontaneous or by activation) of ionized methyl carbamate we have undertaken a combined study of mass spectrometry based experiments and *ab initio* calculations. In particular we wish to understand why there are no hydrogen exchange reactions, as mentioned above, in what would otherwise appear to be a very flexible system.

Theoretical methods

Standard *ab initio* MO calculations were performed with the GAUSSIAN 90 series of programs [10] employing unrestricted Hartree-Fock (UHF) procedures. Optimized geometries, harmonic frequencies and zero-point vibrational energies (ZPVE) were calculated with the split-valence 4-31G basis set [11]. The force constant matrices for the stationary points were checked to have the correct number of negative eigenvalues. Single-point calculations of the 4-31G geometries were performed with the 6-31G* basis set [11,12]. Electron correlation was included by using Møller-Plesset perturbation theory terminated at third order (MP3) [13]. The vibrational frequencies were scaled by a factor of 0.9 [14]. The isomers and transition states are displayed in Figure 3.1.

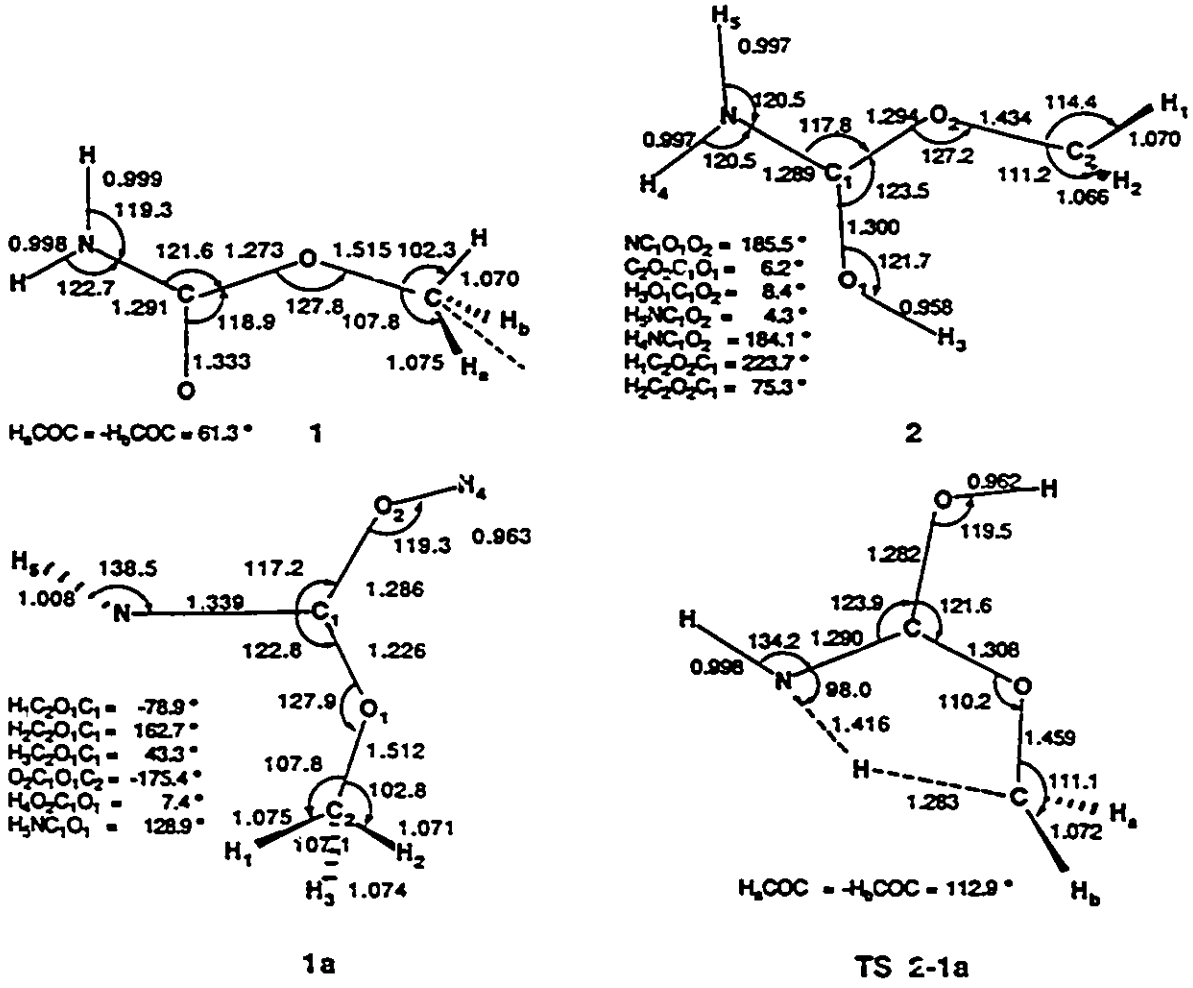

Fig. 3.1 Geometries of $C_2H_5NO_2^{+\bullet}$ isomeric ions and some Transition Statesoptimized at the 4-31G level of theory.

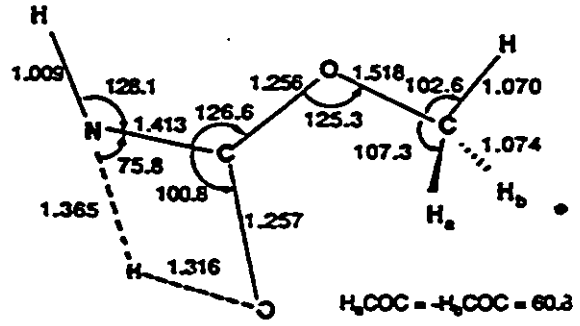

TS 1-1a

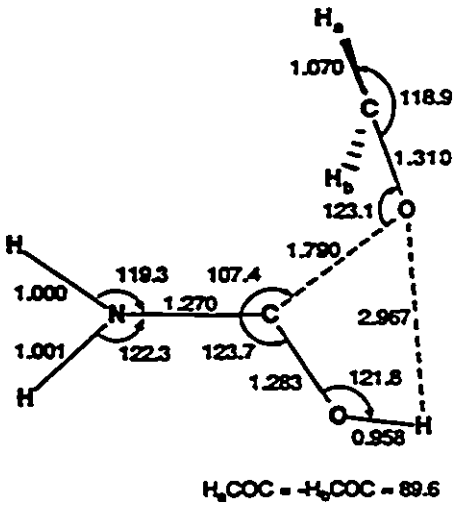

TS 2-5

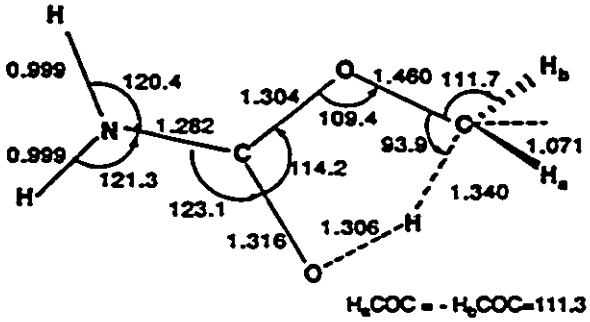

TS 1-2

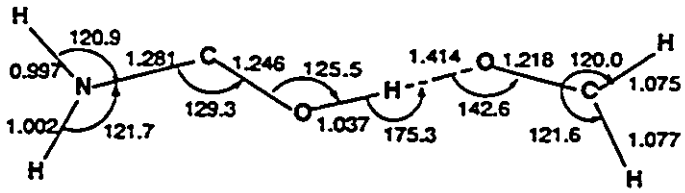

5

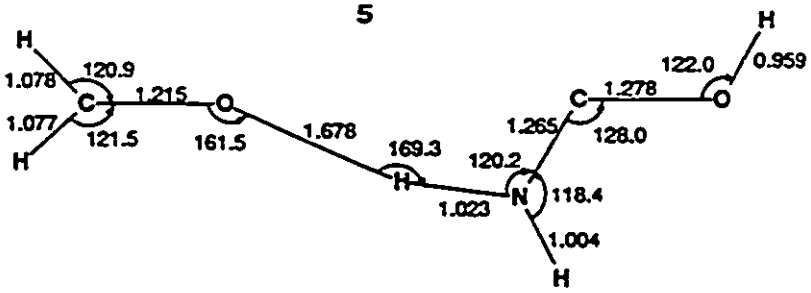

6a

Fig. 3.1 continued

The calculated energies are shown in Table 3.2 and the corresponding energy diagram is given in Figure 3.2.

Table 3.2. Total energies (Hartrees), zero-point vibrational energies [ZPVE] and relative energies E[rel]* (kJ/mol) for isomers and components of the $C_2H_5NO_2^+$ system.

STRUCTURE	POINT GROUP	STATE	UHF/4-31G	6-31G*//4-31G	MP3/6-31G*// 4-31G	ZPVE	E[rel]*
1	C_S	$^2A'$	-282.11920	-282.53595	-283.27144	201	0
2	C_1	^2A	-282.12388	-282.54064	-283.28851	197	-50
1a	C_1	^2A	-282.08664	-282.51571	-283.25733	193	30
5	C_S	$^2A'$	-282.10550	-282.51301	-283.26337	190	10
6a	C_S	$^2A'$	-282.09281	-283.23476	-283.25260	190	39
TS **1** → **1a**	C_S	$^2A'$	-282.00332	-282.43504	-283.19511	182	181
TS **2** → **1a**	C_S	$^2A'$	-282.03523	-282.46240	-283.22433	185	108
TS **1** → **2**	C_S	$^2A'$	-282.05360	-282.47963	-283.24376	189	61
TS **2** → **5**	C_S	$^2A'$	-282.05734	-282.46099	-283.20932	187	150
H_2NCO^+ + $CH_2OH^•$			-282.03845	-282.46124	-283.21212	181	135
$H_2NCOH^{+•}$ + CH_2O			-282.05663	-282.47540	-283.22325	185	111
$NH_2C(H)OH^+$ + $HCO^•$			-282.08912	-282.51140	-283.26468	186	3

* The relative calculated energies include scaled (0.9) zero-point vibrational contributions. The spin contamination was acceptable for the even electron species ($\langle s^2 \rangle$ values were 0.0) and also for the odd electron species ($\langle s^2 \rangle$ values ranged from 0.75 to 0.79) with the exception of the TS 2→ 5 radical cation which had an unacceptably high $\langle s^2 \rangle$ value of 1.0, and so its total energy is overestimated [see ref.2 for further details].

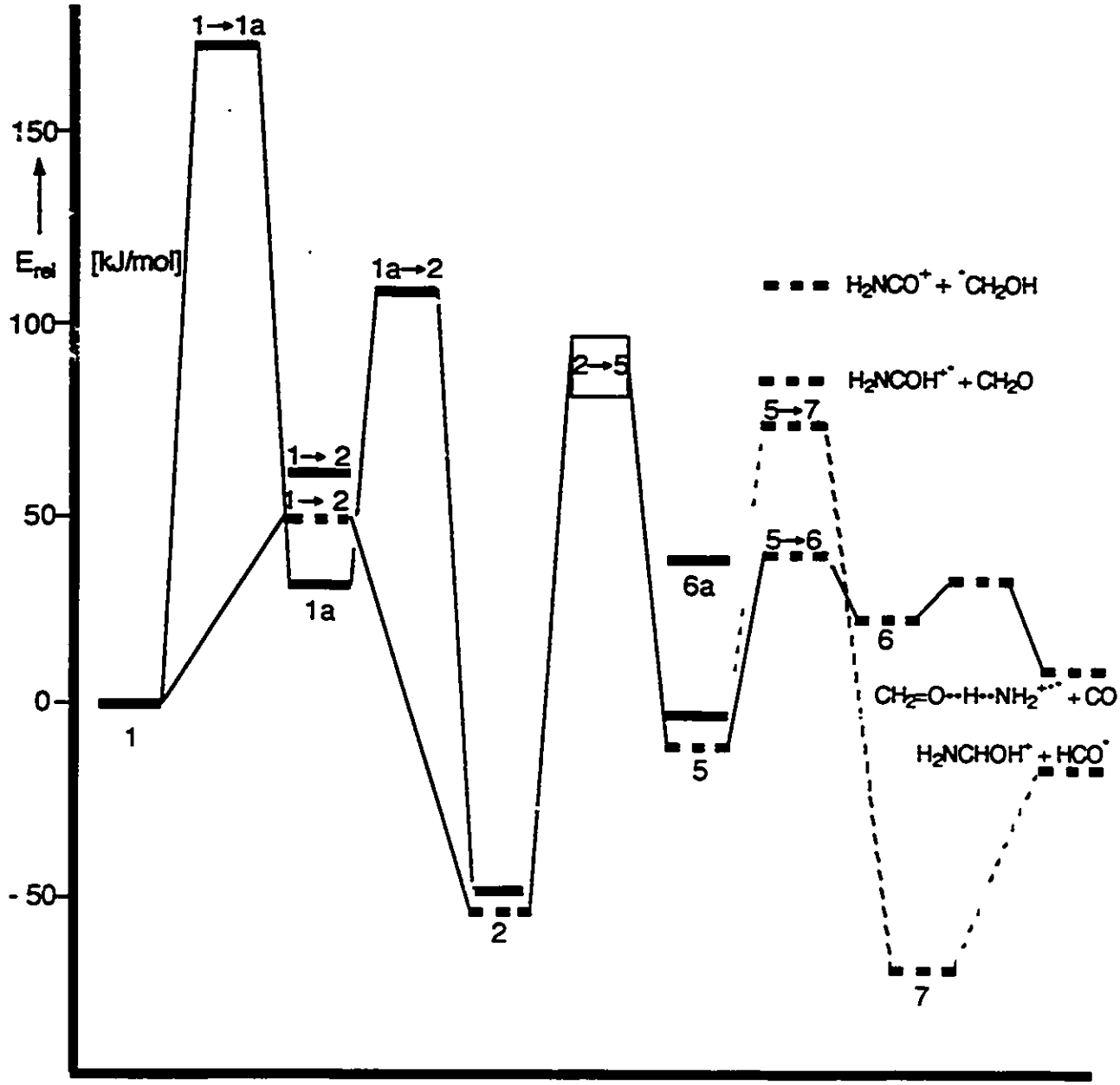

1 = $H_2N\text{-}COOCH_3^{+\bullet}$ **5** = $H_2N\text{-}C{=}O{\cdots}H{\cdots}O{=}CH_2^{+\bullet}$ **7** = $NH_2CHOH{\cdots}OCH^{+\bullet}$

1a = $HN{=}C(OH)\text{-}OCH_3^{+\bullet}$ **6** = $H_2CO{\cdots}H{\cdots}NH_2\text{-}CO^{+\bullet}$

2 = $H_2N\text{-}C(OH)\text{-}OCH_2^{+\bullet}$ **6a** = $H_2CO{\cdots}H{\cdots}N(H)\text{-}COH^{+\bullet}$

Fig. 3.2 Calculated energy diagram for the dissociation reactions of ionized methyl carbamate, **1**. Not included are isomers **3** and **4**, which have been discussed before [2]. The UHF/MP3/6-31G*//4-31G energy levels are designated by the thick solid lines. The RHF/SDCI/6-31G**//4-31G levels designated by the thick dashed lines are taken from Ref.2.

The spin contamination is within acceptable range except for the TS **2**→**5** radical cation, which has a $\langle s^2 \rangle$ value of 1, and therefore its total energy is overestimated. Previous [2] CASSCF calculations (in which all excitations are allowed) had indicated that TS **2**→**5** is essentially a triradical cation and so we have used the previously obtained CASSCF result (see Figure 3.2). Our calculations indicate that, apart from the hydrogen-bridged species $[H_2N\text{-}C{=}O\cdots H\cdots O{=}CH_2]^{+\bullet}$, **5**, another related hydrogen-bridged species is energetically accessible, viz. $[H_2C{=}O\cdots H\cdots N(H)COH]^{+\bullet}$, **6a**. Thus we propose that the formaldehyde dipole in excited **2** can also migrate towards the NH_2 group and this provides a rationale for the observation that $H_2N\text{-}C(=O)OCD_3^{+\bullet}$ generates, in CA and NR experiments, $CD_2OH^{\bullet}$ (in admixture with $CD_2OD^{\bullet}$ from **5**). This parallels observations being presently made [15] for ionized methyl formate where, in the corresponding distonic ion $H\text{-}C(OH)OCH_2^{+\bullet}$, the formaldehyde not only moves towards the OH group to generate $[H\text{-}C\text{-}O\cdots H\cdots O{=}CH_2]^{+\bullet}$ [9] but also to the H-C group to generate the O···H···C bridged ion $[H_2C{=}O\cdots H\cdots C\text{-}O\text{-}H]^{+\bullet}$.

Results and Discussion

The unimolecular chemistry of ionized methyl carbamate

Where our calculations overlap with those of Schaftenaar et. al., [2] agreement is excellent. The calculations predict that below the dissociation limit ionized methyl carbamate can freely interconvert with the distonic ion **2**, as was the case with methyl acetate. Obviously such an equilibrium will not be evident when starting from labelled methyl carbamate ions (hidden hydrogen rearrangement [16]); the equilibrium will only reveal itself when starting from a specifically labelled distonic ion **2** (see later).

Our calculations indicate that the iminol ion **1a** is quite a stable species, but in contrast to the related keto-enol system the iminol ion lies higher in energy than the carbamate ion. It is separated from **1** by a barrier of 152 kJ/mol and so the (inter)conversion **1**→**1a** will play no role in metastable ions. However the barrier connecting **1a** and **2** is much lower

(79 kJ/mol) and lies at about the same level as the rate determining step (TS 2 → 5) in the dissociation of **1**. To ascertain whether **1a** is involved in the unimolecular chemistry of **1** we attempted to generate **1a** via an independent pathway and to assign its structure. We attempted to generate **1a** via a McLafferty type rearrangement of acetaldehyde N-methoxycarbonylhydrazone, **I**, as proposed earlier for a higher homologue [3]:

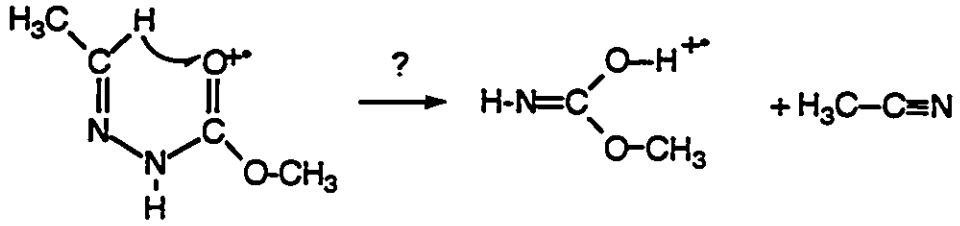

I **1a**

Compound **I** indeed shows an intense metastable peak for the loss of CH_3CN; the reaction is atom-specific (not necessarily site specific, see below), i.e. both CH_3-CD=N-N(H)-$COOCH_3$ and CH_3-CH=N-N(D)-$COOCH_3$ molecular ions specifically lose CH_3CN.

Table 3.3. Metastable ion spectra of $C_2H_5NO_2$ ions [a]

PRECURSOR ION	DAUGHTER ION (m/z)			
	44	45	46	47
$H_2NC(=O)OCH_3$	-	-	100	5.6
H_3C-CH=NN(H)$COOCH_3$	0.1	6.3	100	6.3

a) Base peak = 100, values ± 0.5.

The MI mass spectrum of the product ion generated from **I** (see Table 3.3) is virtually identical to that of methyl carbamate except that the product ion shows an additional small (6%) peak for loss of $H_2C=O$. The CA mass spectrum of these ions is shown in Figure 3.3a, together with that of methyl carbamate (Figure 3.3b). If the signals

at m/z 46 and m/z 47 (metastable peaks) are ignored the two spectra are identical. The NR mass spectra (Figure 3.4) are also virtually identical, although methyl carbamate has a slightly more intense survivor signal.

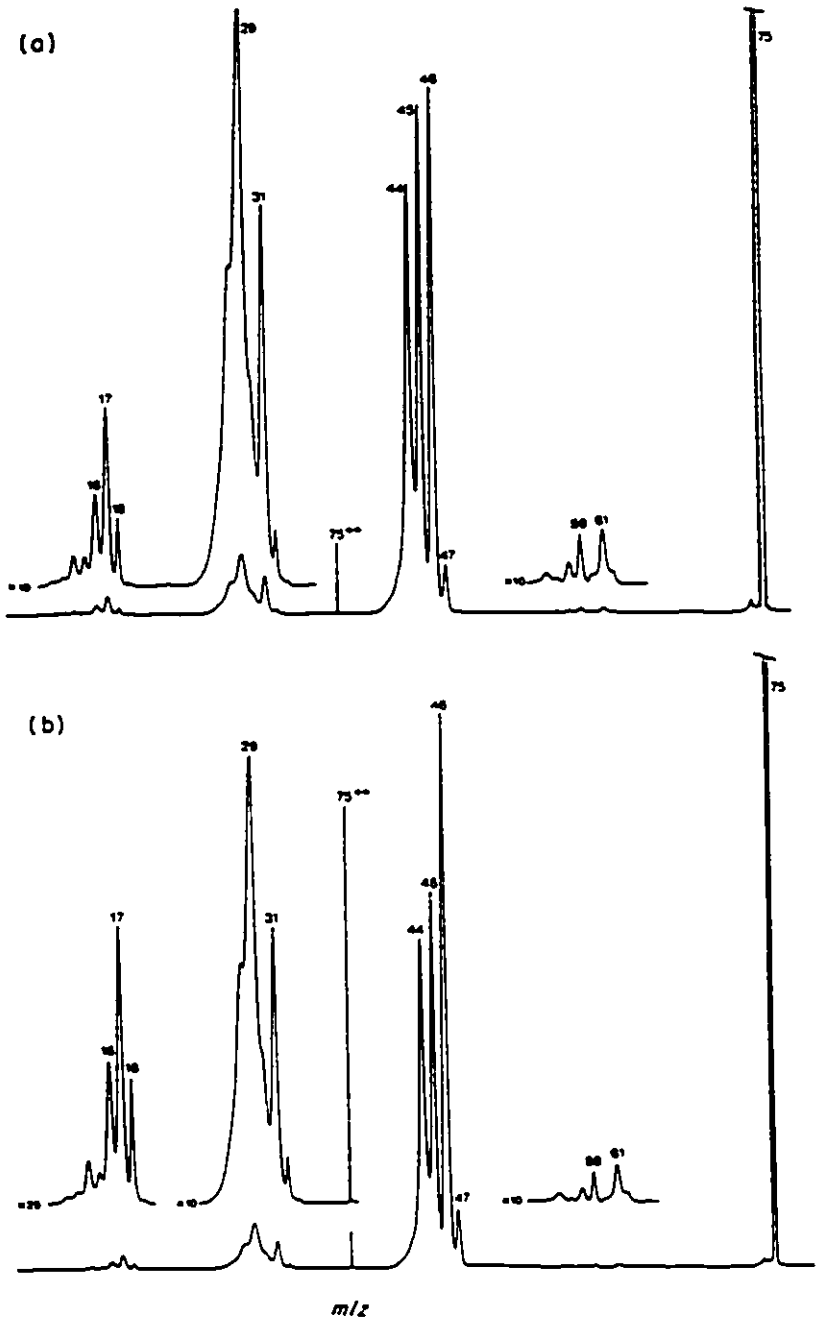

Fig. 3.3 CA mass spectra of the $C_2H_5NO_2^{+\bullet}$ ions generated by CH_3CN loss from CH_3-CH=NN(H)COOCH$_3$ (a) and by direct ionization of methyl carbamate (b).

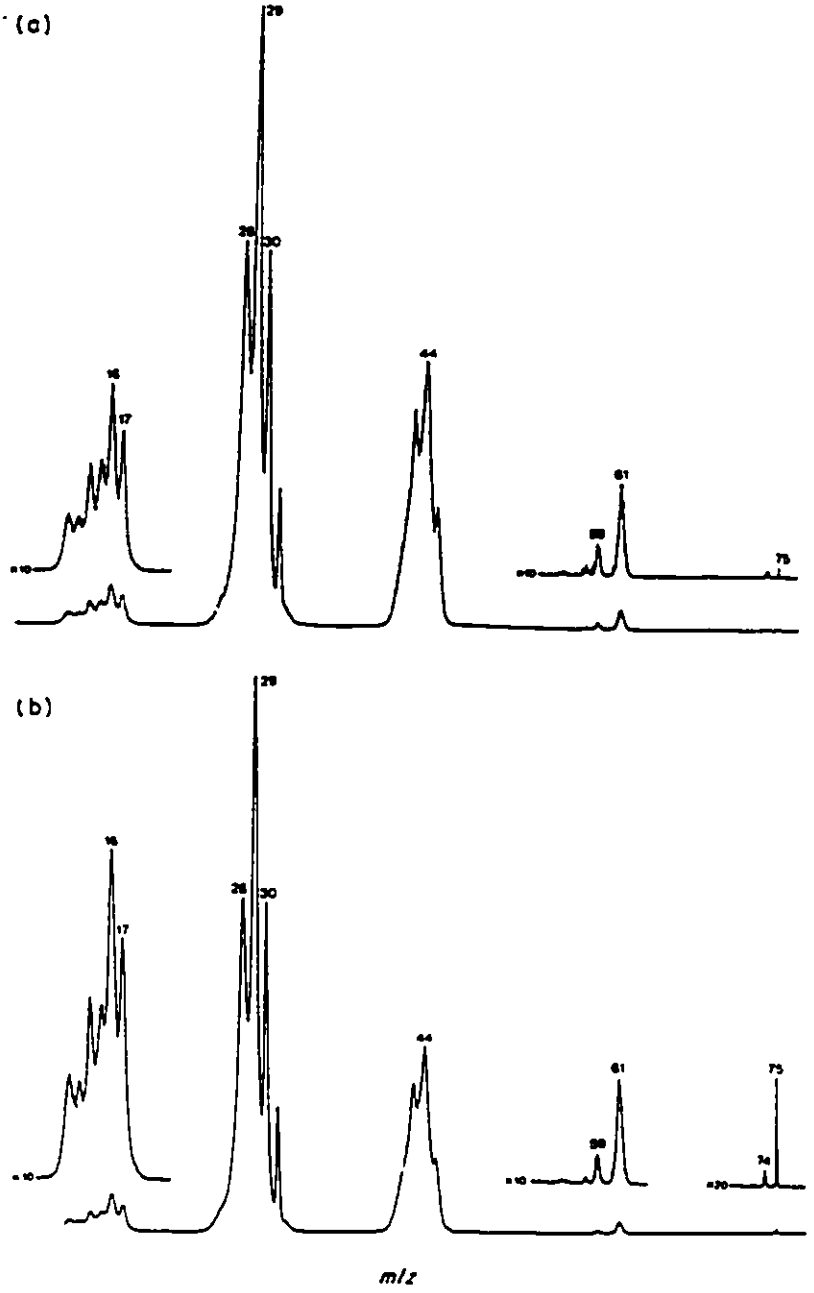

Fig. 3.4 NR mass spectra of the $C_2H_5NO_2^{+\bullet}$ ions generated by CH_3CN loss from CH_3-CH=NN(H)$COOCH_3$ (a) and by direct ionization of methyl carbamate (b).

These results could indicate that (i) the product ion actually is methyl carbamate or (ii) the initially formed product ions are the distonic ions 2 and these, as shown by the calculations, interconvert with ionized methyl carbamate or (iii) the product ion initially formed has the iminol structure but prior to or after activation it rearranges to 1 and/or 2. Note the small but highly characteristic peak at m/z 61 in the CA and NR mass spectra, which, it is argued, corresponds to loss of CH_2 from 2. It was observed, (see below) that the CH_2 lost always contained the original hydrogen atoms. To distinguish between the above possibilities various isotopomers were studied.

Holmes warning [4] notwithstanding, we must begin our analysis by some simple mechanistic assumptions. From CH_3-CD=N-N(H)-$COOCH_3$ the most likely iminol structure is H-N=C(OD)-$OCH_3^{+\bullet}$ (see above); if the product ions are 1 then the most likely connectivity is HDN-C(=O)$OCH_3^{+\bullet}$ via a 1,3-D shift and if the product ions have the distonic structure they are most likely HDN-C(OH)-$OCH_2^{+\bullet}$ and/or H_2N-C(OD)-$OCH_2^{+\bullet}$ formed as shown below :

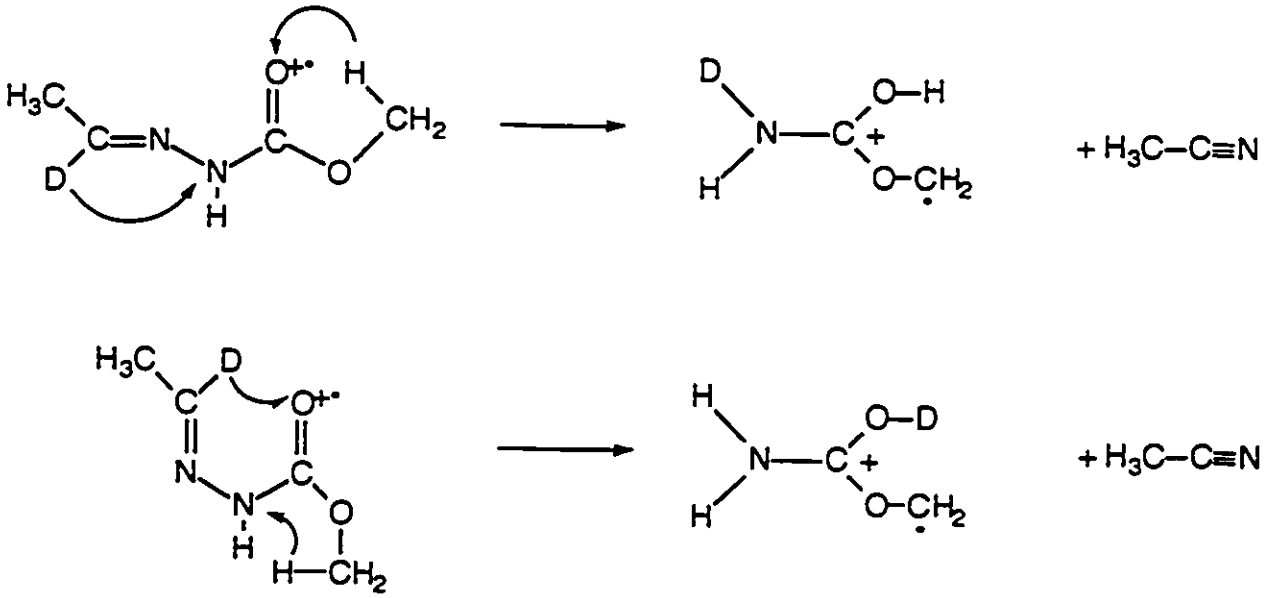

Scheme 3.2

Now one of the most intense signals in the CA mass spectrum Figure 3.3 is due to loss of H_2C=O (m/z 45). If the iminol ion is formed then our ab initio calculations (Figure

3.2) indicate that after activation the ion will rearrange to 5 and then fragment to H_2N-C-OD$^{+\bullet}$; by contrast the keto ions 1 will produce HDN-C-OH$^{+\bullet}$. The distonic ions may form either H_2N-C-OD$^{+\bullet}$ or HDN-C-OH$^{+\bullet}$ or a mixture of these two ionized carbenes. The CA mass spectrum of the $CH_2DNO^{+\bullet}$ ions generated from collisionally activated precursor ions, in a "double collision" MS/MS/MS-type experiment (see Section 1.2 in the INTRODUCTION to the thesis) is shown in Figure 3.5a, together with that of the unlabelled compound (Figure 3.5b).

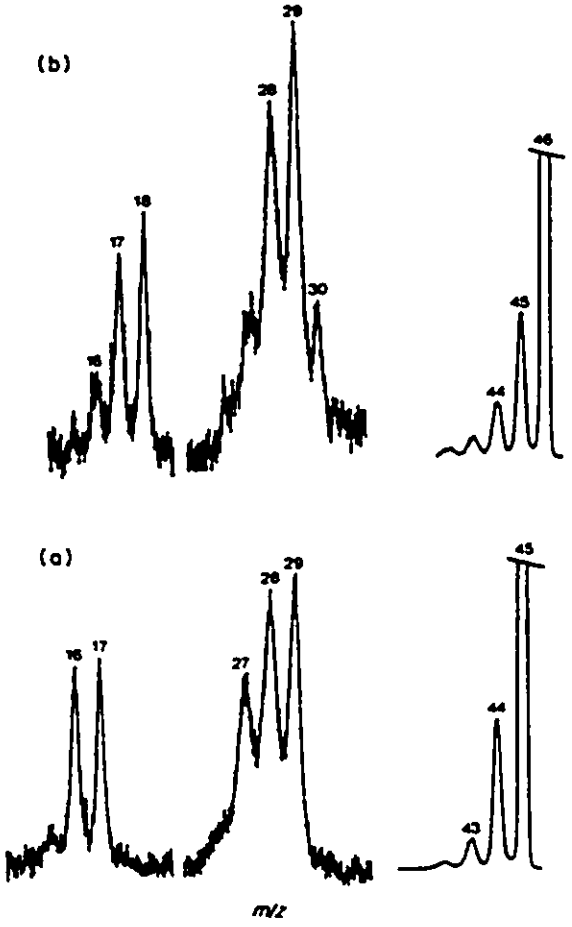

Fig. 3.5 MS/MS/MS mass spectra of $CH_3NO^{+\bullet}$ product ions from $H_2NCOOCH_3^{+\bullet}$ (a) and of the $CH_2DNO^{+\bullet}$ product ions generated from CH_3-CD=NN(H)COOCH$_3$ (b).

The processes we consider are the following (ΔH_f values cf. ref. 17):

$H_2NCOH^{+\bullet}$	→	COH^+	+	$NH_2^\bullet$	$\Sigma\Delta H_f =$	1155 kJ/mol	(m/z 29)
	→	H_2NC^+	+	$OH^\bullet$	$\Sigma\Delta H_f =$	1146 kJ/mol	(m/z 28)
	→	HNC^+	+	H_2O	$\Sigma\Delta H_f =$	1163 kJ/mol	(m/z 27)

The simple bond cleavage processes (m/z 28 and m/z 29) have identical activation energies and so peaks of equal intensity are observed (Figure 3.5b). Now the ion HDN-C-OH$^{+\bullet}$ cannot generate m/z 30 and the ion H_2N-C-OD$^{+\bullet}$ cannot generate m/z 29 directly. Since both signals are present in Figure 3.5a it follows that the spectrum results from a mixture of (60%) HDN-C-OH$^{+\bullet}$ and (40%) H_2N-C-OD$^{+\bullet}$ (when a 60/40 ratio is used it is found that the calculated intensity of m/z 28 is too high and that of m/z 27 is too low; however an isotope effect of unexceptional magnitude in H_2O loss will operate against formation of $HNC^{+\bullet}$, m/z 27, and in favour of $DNC^{+\bullet}$, m/z 28). The above results can most simply be explained in terms of formation of HDN-C(OH)-$OCH_2^{+\bullet}$ and H_2N-C(OD)-$OCH_2^{+\bullet}$ directly from the molecular ion of D labelled **I** (see Scheme 3.2), but it is still possible that initially a mixture of H-N=C(OD)-$OCH_3^{+\bullet}$ and HDN-C(=O)$OCH_3^{+\bullet}$ is formed which prior to or after activation rearrange to the distonic forms. Definitive evidence comes from MI mass spectrometry. The MI mass spectrum of methyl carbamate and the $C_2H_5NO_2^{+\bullet}$ product ions from **I** are shown in Table 3.3. Both spectra are dominated by $HCO^\bullet$ loss, but the $C_2H_5NO_2^{+\bullet}$ product ions from **I** also lose a small amount of CH_2=O (see above).

In Table 3.4 are shown the MI mass spectra of the $C_2H_4DNO_2^{+\bullet}$ ions generated from HDN-C(=O)OCH_3, CH_3-CH=N-N(D)-$COOCH_3$ and CH_3-CD=N-N(H)-$COOCH_3$. It can be seen, compare appropriate entries in Tables 3.3 and 3.4, that the product ions generated from CH_3-CH=N-N(D)-$COOCH_3$ (putatively HDN-C(OH)-$OCH_2^{+\bullet}$) behave as expected, with clean shifts. However, the $C_2H_4DNO_2^{+\bullet}$ product ions generated from CH_3-CD=N-N(H)-$COOCH_3$ give rise to significant peaks at m/z 46 and m/z 45. Now, if the product ion has the structure H_2N-C(OD)-$OCH_2^{+\bullet}$ as opposed to the structure H-N=C(OD)-$OCH_3^{+\bullet}$ or HDN-C(=O)$OCH_3^{+\bullet}$ then

our theoretical calculations predict that the OD deuterium and the CH_2 hydrogen atoms will become positionally equivalent due to the equilibrium 2 ⇔ 1 (see Figure 3.2). Thus for *metastable* ions a mixture of H_2N-C(OD)-$OCH_2^{+\bullet}$, H_2N-C(=O)$OCH_2D^{+\bullet}$ and H_2N-C(OH)-$OCHD^{+\bullet}$ will ensue. The latter ion will eliminate CHD=O (leading to m/z 45) but it will also shed DC=O$^\bullet$ [2] leading to m/z 46. In fact, by using the observed intensity distributions it can be calculated that about 50% of the product ions have the starting structure H_2N-C(OD)-$OCH_2^{+\bullet}$ and 50% then have the starting connectivity HDN-C(OH)-$OCH_2^{+\bullet}$ and/or HDN-C(=O)$OCH_3^{+\bullet}$ which do *not* undergo H/D exchange reactions and eliminate only HCO$^\bullet$ and CH_2=O. The latter two ions are in fact indistinguishable. Note the similarity of these calculated fractions with those derived from MS/MS/MS experiments (see above). Another possibility is that 50% of the product ions are H_2N-C(=O)$OCH_2D^{+\bullet}$, and not H_2N-C(OD)-$OCH_2^{+\bullet}$ but we note that in the CA and NR mass spectra specific loss of CH_2 is observed, ruling out H_2N-C(=O)$OCH_2D^{+\bullet}$. (Although these ions are not present as stable ions, they are formed by isomerization of the *metastable* ions, see above). We have now established that at least 50% of the product ions have the distonic structure, the other 50% being ionized methyl carbamate and/or the distonic ion. We propose that *only* the more stable distonic ions are produced according to Scheme 3.2.

Table 3.4. Metastable ion spectra of $C_2H_4DNO_2$ ions [a]

PRECURSOR ION	DAUGHTER ION (m/z)				
	44	45	46	47	48
HDNC(=O)OCH_3	-	-	2.0[b]	100	6.1
H_3C-CH=NN(D)COOCH_3	-	0.1	7.5	100	8.2
H_3C-CD=NN(H)COOCH_3	-	3.7	24.7	100	7.6

a) Base peak = 100, values ±0.5; b) This peak arises from interference from $[MD_2\text{-}H]^+$

Further evidence for the above comes from small but significant differences in the CA mass spectra of the $C_2H_4DNO_2^{+\bullet}$ product ions, ($HDN\text{-}C(OH)\text{-}OCH_2^{+\bullet}$) generated from $CH_3\text{-}CH{=}N\text{-}N(D)\text{-}COOCH_3^{+\bullet}$ and ($H_2N\text{-}C(OD)\text{-}OCH_2^{+\bullet}$ and $HDN\text{-}C(OH)\text{-}OCH_2^{+\bullet}$) generated from $CH_3\text{-}CD{=}N\text{-}N(H)\text{-}COOCH_3^{+\bullet}$, see Figure 3.6b and 3.6c respectively, compare with Figure 3.6a, the unlabelled product ion. The interpretation of Figure 3.6a follows from our earlier work [1,2], i.e. m/z 47, loss of CO (m^*); m/z 46, loss of $HCO^\bullet$ (m^*); m/z 45, loss of $H_2C{=}O$; and m/z 44, loss of $H_2COH^\bullet$ (not $^\bullet OCH_3$) as indicated by NR experiments [2]. We will concentrate on the loss of $H_2COD^\bullet$ for which [2] there are two reaction pathways, A and B, as shown in Scheme 3.3.

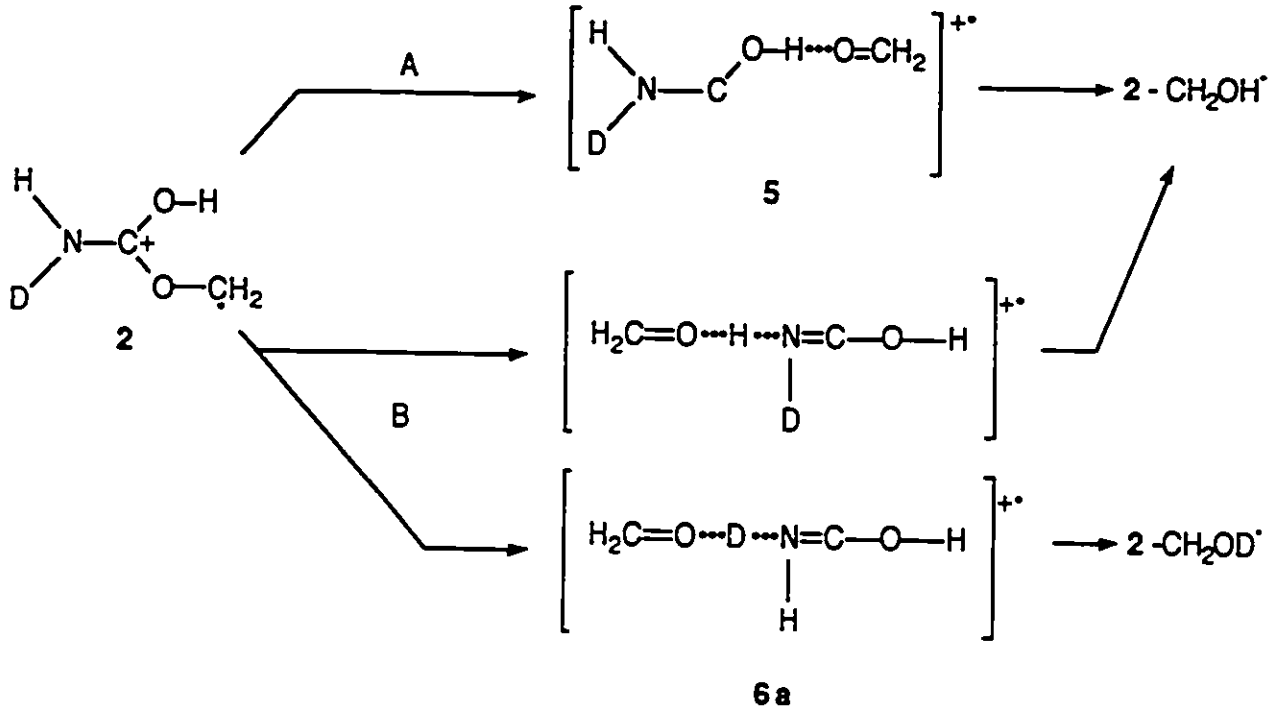

Scheme 3.3

Thus for the ion $HDN\text{-}C(OH)\text{-}OCH_2^{+\bullet}$ generated from $CH_3\text{-}CH{=}N\text{-}N(D)\text{-}COOCH_3$ we observe a small signal at m/z 44 (loss of $H_2COD^\bullet$ via path B, see Figure 3.6b), but the major signal (m/z 45) arises by path A. Now, if $H_2N\text{-}C(OD)\text{-}OCH_2^{+\bullet}$ is cogenerated, as is the case in Fig 3.6c, then it is predicted that these ions will lose $CH_2OD^\bullet$, via path A, to

generate m/z 44, which explains the more intense signal at m/z 44 in Figure 3.6c, compared to that in Fig 3.6b.

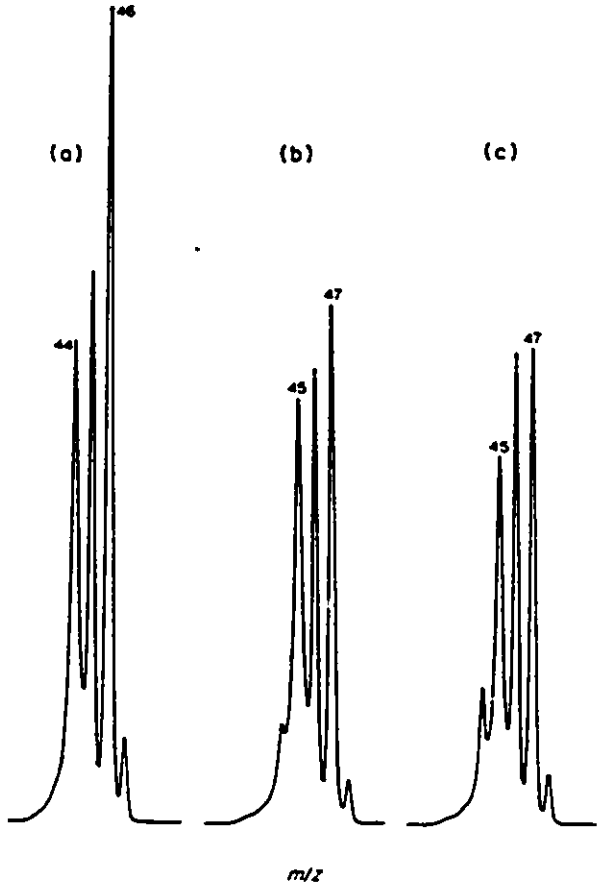

Fig. 3.6 Partial CA mass spectra of ionized methyl carbamate (a) and of the $C_2H_4DNO_2^{+\bullet}$ ions generated from CH_3-CH=NN(D)$COOCH_3$ (b) and from CH_3-CD=NN(H)$COOCH_3$ (c) .

In summary , we have shown by this test case that ion structure assignment can be exceedingly difficult. In the present case this is so because the distonic ion **2** can rearrange, below the dissociation limit, to ionized methyl carbamate and it does so to an equilibrium mixture. At the same time this very equilibrium revealed the generation of the distonic ion when labelled material was investigated. That is, the equilibrium **1** ⇔ **2** lies unsuspected when starting from **1**, because the CH_3 hydrogen atoms in **1** are obviously already equivalent, but it becomes manifest when specifically labelled ions **2** are studied. It may well be that other distonic ions having dissociation characteristics similar to those of their conventional counterparts have, for this reason been misidentified as their conventional isomers.

As far as the dissociations of ionized methyl carbamate are concerned, we have shown that the distonic ion $H_2N\text{-}C(OH)\text{-}OCH_2^{+\bullet}$ is the key intermediate. However, the iminol ion $H\text{-}N{=}C(OH)\text{-}OCH_3^{+\bullet}$ is not involved in the rearrangement/dissociation reactions of ionized methyl carbamate as indicated by our calculations and experiments. The fate of the distonic ion is quite intriguing: elongation of the $C\text{-}OCH_2$ bond does not immediately lead to dissociation, but instead the incipient formaldehyde dipole moves within the electrostatic field of the $H_2N\text{-}C\text{-}OH^{+\bullet}$ ion towards either the OH group to generate the hydrogen-bridged species $[H_2N\text{-}C{=}O\cdots H\cdots O{=}CH_2]^{+\bullet}$ or to the NH_2 group to generate $[H_2C{=}O\cdots H\cdots N(H)COH]^{+\bullet}$. These species then lead to the products observed in MI and CA mass spectrometry.

References

1. P.C. Burgers, C. Lifshitz, P.J.A. Ruttink, G. Schaftenaar and J.K. Terlouw, Org. Mass Spectrom. 24 (1989) 579.
2. G. Schaftenaar, R. Postma, P.J.A. Ruttink, P.C. Burgers, G.A. McGibbon and J.K.Terlouw , Int. J. Mass Spectrom. Ion Proc. 100 (1990) 521.
3. H. Budzikiewicz, C. Djerassi and D.H. Williams, Mass Spectrometry of Organic Compounds, Holden-Day Inc.: London (1967).
4. J.L. Holmes, Org. Mass Spectrom. 20 (1985) 169.
5. (a) B.F. Yates, W.J. Bouma and L. Radom, Tetrahedron 22 (1986) 6225; (b) S. Hammerum, Mass Spectrom. Rev. 7 (1988) 123; (c) P.C. Burgers and J.K. Terlouw, in Specialist Periodical Reports: Mass Spectrometry, M.E. Rose (ed.), Vol. 10, The Royal Society of Chemistry: London (1989) Chapter 2; (d) N. Heinrich and H. Schwarz, in Ion and Cluster Spectroscopy and Structure, J.P. Maier (ed.), Elsevier: Amsterdam (1989) p. 329.
6. (a) P.C. Burgers, J.L. Holmes, C.E.C.A. Hop, R. Postma, P.J.A. Ruttink and J.K. Terlouw, J. Am. Chem. Soc. 109 (1987) 7315; (b) B.L.M. van Baar, P.C. Burgers, J.L. Holmes and J.K. Terlouw, Org. Mass Spectrom. 23 (1988) 355.
7. D.J. McAdoo, Mass Spectrom. Rev. 7, (1988) 363.
8. N. Heinrich, J. Schmidt, H. Schwarz and Y. Apeloig, J. Am. Chem. Soc. 109 (1987) 1317.
9. N. Heinrich, Th. Drewello, P.C. Burgers, J.C. Morrow, J. Schmidt, W. Kulik, J.K. Terlouw and H. Schwarz , J. Am. Chem. Soc. 114 (1992) 3776.
10. Gaussian 90: M.J. Frisch, M. Head-Gordon, G.W. Trucks, J.B. Foresman, H.B. Schlegel, K. Raghavachari, M.A. Robb, J.S. Binkley, C. Gonzales, D.J. DeFrees, D.J. Fox, R.A. Whiteside, R. Seeger, C.F. Melius, J. Baker, R.L. Martin, L.R. Kahn J.J.P. Stewart, S. Topiol and J.A. Pople, Gaussian, Inc., Pittsburgh PA, 1990.
11. W.J. Hehre, R. Ditchfield and J.A. Pople, J. Chem. Phys. 56 (1972) 2257.
12. P.C. Harihan and J.A. Pople, Theor. Chim. Acta, 28 (1973) 213.
13. (a) C. Møller and M.S. Plesset, Phys. Rev. 46 (1934) 618; (b) J.A. Pople, R. Seeger and

R. Krishnan Int. J. Quantum Chem., Quantum Chem. Symp. 11 (1977) 149.

14. (a) J.A. Pople, H.B. Schlegel, R. Krishnan, D.J. DeFrees, J.S. Binkley, M.J. Frisch, R.A.Whiteside, R.F. Hout and W.J. Hehre, Int. J. Quantum Chem., Quantum Chem Symp. 15 (1981) 269.

15. P.C. Burgers and J.K. Terlouw, personal communication.

16. H. Schwarz, Org. Mass Spectrom. 15 (1980) 491.

17. S.G. Lias, J.E. Bartmess, J.F. Liebman, J.L. Holmes, R.D. Levin and W.G. Mallard, J. Phys. Chem. Ref. Data 17, Supplement 1 (1988).

CHAPTER 4

The gas phase chemistry of N-methyl-O-methyl carbamate radical cations, $CH_3N(H)COOCH_3^{\bullet+}$.

Introduction

In this chapter the unimolecular chemistry of N-methyl-O-methyl carbamate radical cations $CH_3N(H)COOCH_3^{+\bullet}$, **1** has been studied by a variety of MS/MS and MS/MS/MS techniques (metastable ion (MI) mass spectrometry and (multiple) collision experiments) in combination with extensive D, ^{13}C and ^{18}O labelling experiments.

Section 4.1 focusses on the surprising spontaneous dissociation reaction of metastable $CH_3N(H)COOCH_3^{+\bullet}$ ions: loss of a methyl radical. A mechanism which involves two isomeric distonic ions $CH_3N(H)\text{-}^{+}C(OH)OCH_2^{\bullet}$ and $CH_2{=}^{+}N(H)\text{-}^{\bullet}C(OH)OCH_3$ is proposed. In addition, the heats of formation of the molecular ion and the $C_2H_4NO_2^+$ product ion have been estimated by additivity methods.

Section 4.2 describes a "double collision" MS/MS/MS-type experiment which was used to generate and characterize the elusive O-protonated isocyanic acid (isoformylaminylium) ion, $HNCOH^+$. This ion is not easy to make any other way since the N-protonated isocyanic acid (aminoformylium) ion, $H_2N\text{-}C{=}O^+$, is thermodynamically the most stable $[H_2,C,N,O]$ isomer.

4.1 How does ionized N-methyl-O-methyl carbamate, $CH_3N(H)COOCH_3^{\bullet+}$, lose a methyl group? Unimolecular equilibration with two distonic isomers.

Many solitary organic radical cations undergo dissociations that could, in principle, be formulated as simple cleavage reactions, but which are actually the result of more or less extensive rearrangement processes. Such processes can best be described as "hidden" rearrangements [1]. A recently published [2] and surprising case is that of dimethylsulfoxide, CH_3-S(=O)$CH_3^{\bullet+}$, which at rate-constants < 10^6 s^{-1} sheds $^{\bullet}CH_3$ to produce CH_2=S=OH^+ not CH_3-S=O^+ expected from a simple bond cleavage reaction. The rearrangement process will occur if: (i) the product ion formed by rearrangement is more stable thermodynamically than the isomer which would have been formed by direct bond cleavage; (ii) the barrier towards isomerization of the molecular ions lies below the threshold for direct dissociation (although the isomerized ion need not be more stable than the molecular ion) and; (iii) sufficient time is available for rearrangement. In the case of dimethylsulfoxide the unexpected rearrangement was uncovered by experiment and supported by theory however, simple thermochemical considerations may often cast doubt on what would otherwise appear to be a straightforward bond cleavage reaction. A case in point is ionized N-methyl-O-methyl carbamate, $CH_3N(H)COOCH_3^{\bullet+}$, **1**, which abundantly sheds $^{\bullet}CH_3$ at both high and low rate constants. It is highly unlikely that this process (especially when it occurs on the microsecond time-scale) is a simple cleavage process because both nitrenium ($R_1R_2N^+$) and oxonium (RO^+) ions are highly unstable entities [3].

During the last few years distonic ions [4] have been identified as important intermediates of radical cation fragmentations. This followed the realization (mainly from ab initio molecular orbital calculations [5]) that distonic ions can be as, or even more, stable thermodynamically and kinetically than isomeric ionized molecules. Thus many reactions have been rationalized in terms of stepwise interconversion between distonic

ions and the molecular ion of conventional structure [6]. For example, the prototype ester distonic ion $H\text{-}^{+}C(OH)OCH_2^{\bullet}$ has been found [7] to be responsible for many of the reactions displayed by ionized methylformate. Indeed, the successful unravelling of the mechanisms of reactions involving distonic ions rests heavily upon a combination of isotopic labelling, ab initio computations and experiments aimed towards identifying product ion structures [8].

In this section we have investigated in detail the fragmentation of ionized N-methyl-O-methyl carbamate using a combination of D, ^{13}C and ^{18}O isotopic labelling and metastable ion, collisional activation and neutralization-reionization mass spectrometric experiments. Metastable molecular ions equilibrate with at least two distonic ions, one of which serves as the precursor for methyl radical elimination. The structure of the daughter ion was also established.

Results and Discussion

Dissociation characteristics of the molecular ion, $CH_3N(H)COOCH_3^{\bullet+}$

The Metastable Ion (MI) mass spectrum of $CH_3N(H)COOCH_3^{\bullet+}$, **1**, is dominated by loss of $^{\bullet}CH_3$ (98%) with minor processes leading to m/z 58 (loss of $CH_3O^{\bullet}$ and/or $CH_2OH^{\bullet}$), m/z 59 (loss of $CH_3NH^{\bullet}$ and/or $CH_2{=}O$) and m/z 60 (loss of $HCO^{\bullet}$), see Figure 4.1a. The kinetic energy release, measured at half height, $T_{0.5}$ for loss of $^{\bullet}CH_3$ is 315 meV and this large value is indicative of a large reverse term. The reverse barrier could be the result of an energy demanding rearrangement step, but it could also indicate that the dissociation step involves an O-C or an N-C bond cleavage which are known to have large reverse terms [9]. It was observed that for O-methyl-N-ethyl carbamate, $CH_3CH_2N(H)COOCH_3^{\bullet+}$ loss of $^{\bullet}CH_3$ was again an important peak in the normal electron ionization (EI) mass spectrum, whereas that for elimination of $^{\bullet}C_2H_5$ was weak. This may well indicate that for **1** it is the O-CH_3 methyl group which is lost. To unambiguously identify the eliminated carbon and hydrogen atoms, a variety of labelled ions were

studied, see Table 4.1.

TABLE 4.1. Intensity distributions[a] for loss of methyl radical isotopologues[b] from ^{13}C and D labelled N-methyl-O-methyl carbamate molecular ions.

Precursor molecule	Spectrum Type	Radical lost				
		$^{13}CH_3$	CH_3	CH_2D	CHD_2	CD_3
$CH_3N(H)COO^{13}CH_3$	MI	100				
$CH_3N(D)COOCH_3$	MI		100			
$CH_3N(H)COOCD_3$	MI		15	51	31	3
	CA		11	43	36	10
	EI		4	25	48	22
	NR		2	11	42	45
	calc.		5	45	45	5
$CD_3N(H)COOCH_3$	MI		9	47	40	4
	CA		13	47	36	4
	EI		31	47	23	3
	NR		36	47	16	1
	calc.		5	45	45	5
$CH_3N(H)COOCD_2H$	MI		25	57	18	
	CA		18	53	29	
	EI		10	40	51	
	NR		7	34	60	
	calc.		20	60	20	

a Intensities relative to sum = 100 %; MI = metastable ion mass spectrum; CA = collisional activation mass spectrum; EI = normal electron ionization (70eV) mass spectrum; NR = neutralization-reionization mass spectrum; calc. = calculated assuming complete H/D exchange of the methylic hydrogen atoms.

b For a definition of nomenclature see ref. 20.

It can immediately be seen from the MI mass spectra that $CH_3N(H)COO^{13}CH_3^{\bullet+}$, as well as $CH_3N(H)CO^{18}O^{13}CH_3^{\bullet+}$, exclusively eliminate a $^{13}CH_3$ radical and that $CH_3N(D)COOCH_3^{\bullet+}$ exclusively sheds $^{\bullet}CH_3$. These processes remain specific for higher energy ions, for example those dissociating in the ion source. Hence, it is the methoxy carbon which is lost, whereas the N-H hydrogen does not appear in the eliminated methyl radical (in fact, see below, it fulfills a spectator's role). However, the CD_3-N, O-CD_3 and O-CD_2H labelled ions all showed losses of all possible isotopologues to the statistical limit (see later) for exchange of all six methyl H and D atoms, see Table 4.1. This may well indicate that prior to dissociation an equilibrated mixture of ions exists. Such exchanges are generally reduced at higher rate constants (i.e. higher internal energies) and indeed (see Table 4.1), the EI mass spectrum shows less exchange reactions and more specificity for the loss of the methoxy hydrogens; for example, for $CH_3N(H)COOCD_3^{\bullet+}$ there is a clear preference for the specific loss of $^{\bullet}CD_3$, relative to complete scrambling. Note that a similar effect is observed in the CA mass spectra (see Table 4.1), but here two separate factors are responsible for this efect. First, in CA experiments, ions of low internal energy are sampled and these ions may not have sufficient evergy to surmount the barrier for H/D exchange reactions, leading to reduced scrambling. Secondly, upon collisional activation these "cold" ions are forced to dissociate rapidly and this too, see above, suppresses scrambling reactions.

In an interesting study, Drinkwater and McLafferty [10] have observed that isotopic scrambling can be significantly reduced in the NR mass spectrum (compared to the CA mass spectrum) when the neutralization step is highly exothermic. They observed that when labelled toluene ions are neutralized by Cs vapour to form excited (5 eV) toluene molecules, the latter rapidly dissociate, thus reducing isotopic scrambling. It can be seen from Table 4.1 that in the NR mass spectra of the labelled carbamates a significant reduction (compared to that observed in the CA mass spectra) in isotopic scrambling is also observed, but we believe that in our case a different mechanism to the one

proposed by Drinkwater and McLafferty must be operative. The ionization energy (IE) of the neutralization agent (N,N-dimethylaniline) is 7.13 eV [11], whereas, the IE of $CH_3N(H)COOCH_3$ is estimated at 10 eV (see later) and considering the great number (87) of vibrational degrees of freedom involved, it is highly unlikely that neutralization which is exothermic by 2.9 eV would lead to fast dissociation of the $CH_3N(H)COOCH_3$ molecule. Rather, in our case, we attribute the reduced scrambling to the same factors responsible for reduced scrambling in the CA mass spectra: neutralization samples even lower energy ions than collisional activation and after reionization excited ions are formed which will dissociate rapidly and these combined effects lead to reduced scrambling.

All of the above findings are perfectly compatible with specific loss of the O-CH_3 methyl group at high energies (EI mass spectrum); at lower energies (MI mass spectrum) **1** interconverts to an equilibrium extent with other isomeric ions leading to exchange of the methyls' hydrogen atoms. As evidenced by the reduced scrambling in the CA and NR mass spectra, compared to the MI mass spectra, energy barriers are associated with the interconversion of **1** with its isomeric forms.

The structure of the $[C_2H_4N,O_2]^+$ product ions

The MI spectrum of m/z 74 $[M - {}^{\bullet}CH_3]^+$ is dominated by loss of CO_2 ($T_{0.5}$= 273 meV) leading to the stable $H_2C{=}NH_2^+$ ions. This is the process of lowest energy requirement [11]. The CA mass spectrum of m/z 74 is shown in Figure 4.2a. In addition to the metastable process there are now peaks at m/z 45, 29 and 28. The m/z 45 fragment ion was shown by MS/MS/MS experiments (see below) to correspond to $HOCO^+$, not to a $[C,H_3,N,O]^+$ ion, with the reciprocal ion, $CH_2{=}NH^{\bullet+}$, most likely producing the peak at m/z 29. The CA mass spectrum of m/z 77 generated by loss of ${}^{\bullet}CH_3$ from $CD_3N(H)COOCH_3$ (Figure 4.2b) shows intense peaks at m/z 46 ($DOCO^+$), m/z 33 (loss of CO_2) and m/z 31 ($CHD{=}NH^{\bullet+}$ or $CH_2{=}ND^{\bullet+}$), which represent clean mass shifts. However, m/z 29 of the unlabelled ion (Figure 4.2b) is now split into m/z 29 and m/z 30 in a ratio of 1 : 0.7. Thus,

part of m/z 29 and likely all of m/z 30 may have arisen from sequential decomposition of m/z 33 (CD_2=$NHD^{\bullet+}$), which is formed from metastable ions via its most favourable pathways (i.e. losses of HD and D_2, via 1,2-eliminations [12]. Hence, ignoring the low energy dissocation path (loss of CO_2) and sequential dissociations, the CA mass spectrum of the $[M - {}^{\bullet}CH_3]^+$ product ion is characterized by CH_2=$NH^{\bullet+}$ and $HOCO^+$, and assuming that these collision induced reactions are simple cleavage processes, the most logical product ion structure would seem to be that of the (N-carboxyl)-methyliminium ion, CH_2=N(H)-$COOH^+$, **5**. This is an immonium ion, substituted by the electronegative COOH functionality; such species have been referred to as "destabilized" ions [13] and should have elevated reactivities. However, we have shown that a similar "destabilized" ion, CH_2=N(H)-$COCH_3^+$, (N-acetyl)methyliminium is a stable entity which can be generated in the gas phase [14]. Moreover, it has also been inferred from a combination of ab initio calculations and energetic data, that the -COOH functionality behaves as a hydrogen atom, that is to say its destabilization effect is close to zero [15]. Hence, CH_2=N(H)-$COOH^+$ may well be energetically accessible but we do not rule out the possibility that **5** could undergo ring closure to **6** or **7**, which would alleviate any destabilizing inductive effects but at the expense of additional ring strain energies.

The NR mass spectrum of **5** is shown in Figure 4.2c. An intense survivor signal is present and apart from the metastably generated CO_2 molecules, this NR mass spectrum is very close to the CA mass spectrum (Figure 4.2a). Not only does this indicate that the radical $^{\bullet}CH_2$-N(H)-COOH is a stable species which does not isomerize, it also shows that loss of a methyl radical from **1** yields essentially only one ionic form, rather than a mixture of isomers **5**, **6** and/or **7**.

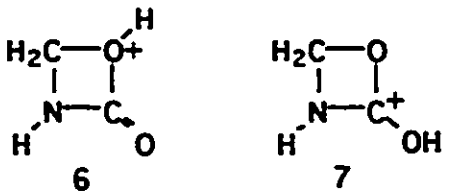

6 **7**

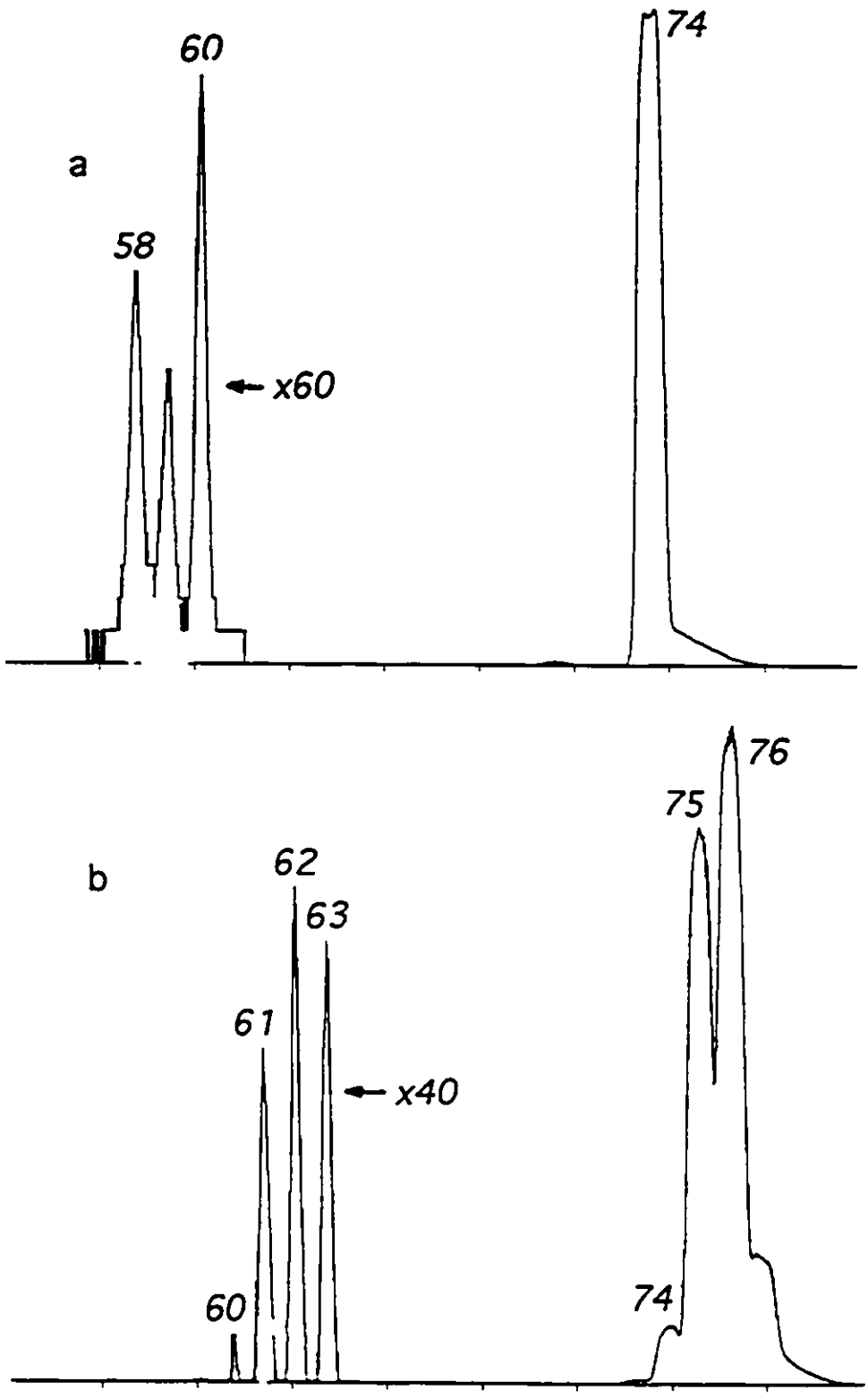

Fig. 4.1 Metastable ion mass spectra of (a) CH_3-N(H)-$COOCH_3$ and (b) CD_3-N(H)-$COOCH_3$.

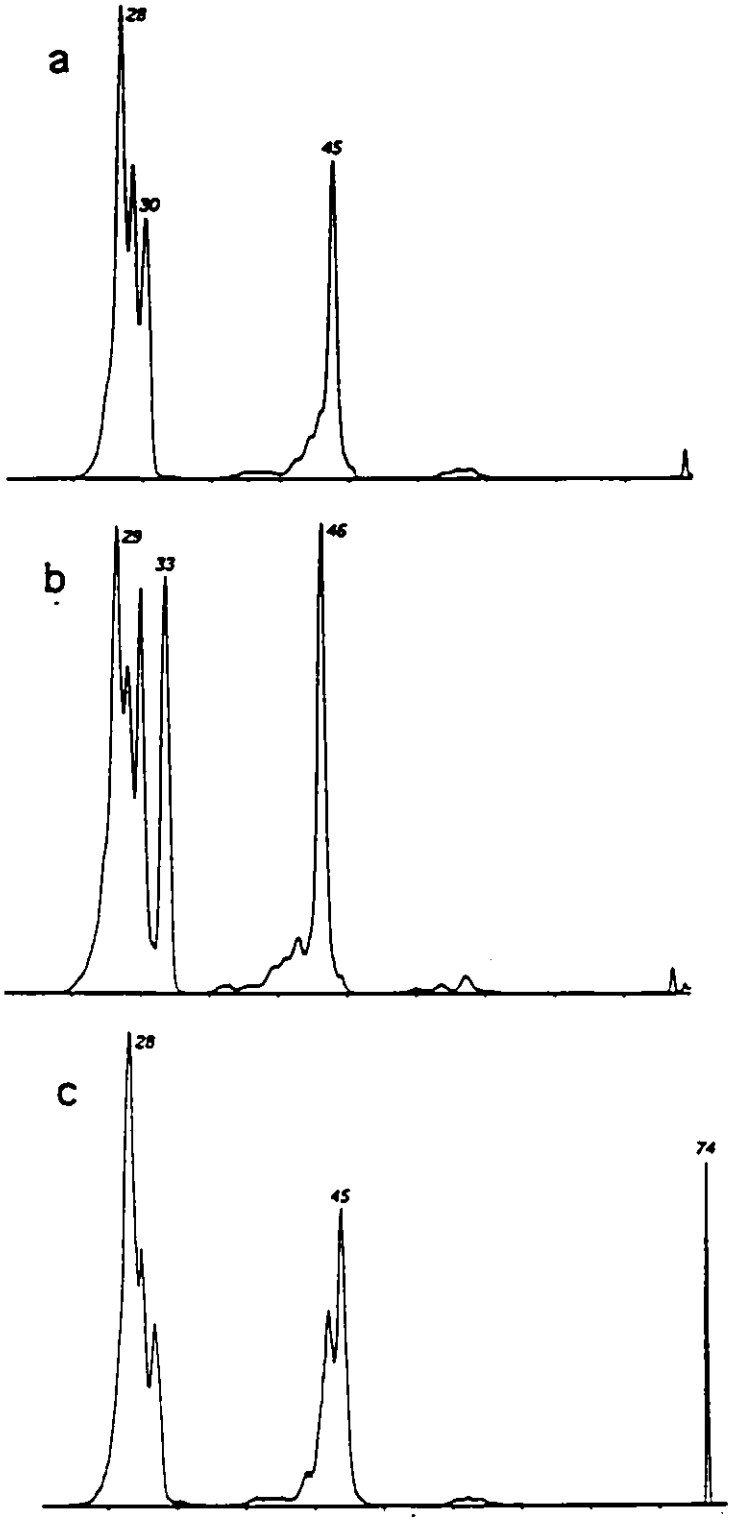

Fig. 4.2 (a) Collision Activation (CA) mass spectrum of the $[M\text{-}CH_3]^{\bullet+}$ ions generated from $CH_3\text{-}N(H)\text{-}COOCH_3$, (b) CA mass spectrum of the $[M\text{-}CH_3]^+$ ions generated from $CD_3\text{-}N(H)\text{-}COOCH_3$, (c) Neutralization-Reionization mass spectrum of the $[M\text{-}CH_3]^+$ ions generated from $CH_3\text{-}N(H)\text{-}COOCH_3$.

A mechanism for loss of $^{\bullet}CH_3$ from $CH_3N(H)COOCH_3^{\bullet+}$

First, the mechanism of the high energy (specific) elimination of $^{\bullet}CH_3$ is now discussed. This loss can be rationalized most simply by the two pathways shown scheme 4.1, both of which involve 1,4-hydrogen shifts:

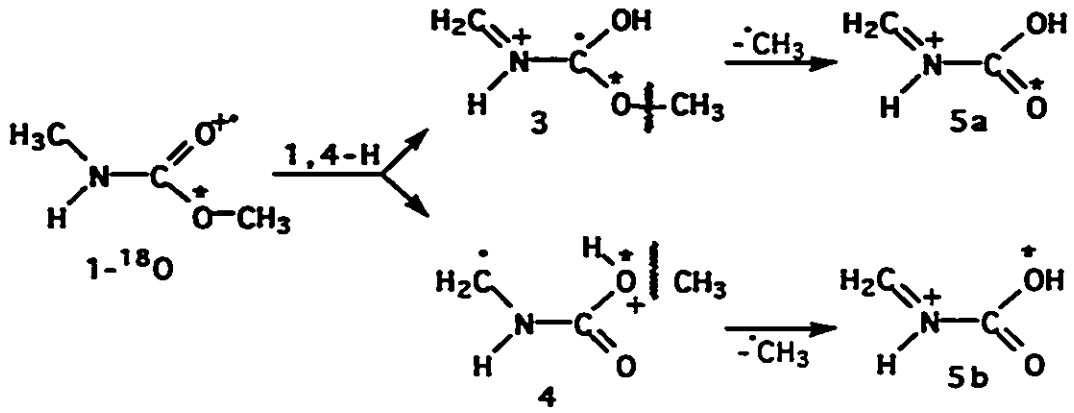

Scheme 4.1

The * indicates the fate of the O-CH_3 oxygen atom for both mechanisms. As mentioned above, the CA mass spectrum of the product ions contains a characteristic peak for $HOCO^+$. The $HOCO^+$ ion, when collisionally activated produce signals at m/z 17 (OH^+), m/z 28 ($CO^{\bullet+}$) and m/z 29 (COH^+) [16]. If the asterixed oxygen is selectively labelled with ^{18}O then for the ion from **5a**, signals are thus expected at m/z 17 (OH^+), m/z 30 ($C^{18}O^{\bullet+}$) and m/z 29 (COH^+) whereas that from **5b** should lead to signals at m/z 19 ($^{18}OH^+$), m/z 28 ($CO^{\bullet+}$) and m/z 31 ($C^{18}OH^+$).

To differentiate between the two pathways, the following MS/MS/MS (CA/CA) experiment was performed. First, the labelled ion $CH_3N(H)CO^{18}OCH_3^{\bullet+}$ was allowed to lose $^{\bullet}CH_3$ in the ion source. The resulting m/z 76 daughter ions were selected by B and induced to decompose to m/z 47 ($H^{18}OCO^+$ or $HOC^{18}O^+$). The m/z 47 ions were then selected by E_1 and were collisionally dissociated; the products were scanned by E_2 and the resulting CA mass spectrum of these m/z 47 ions is shown in Figure 4.3.

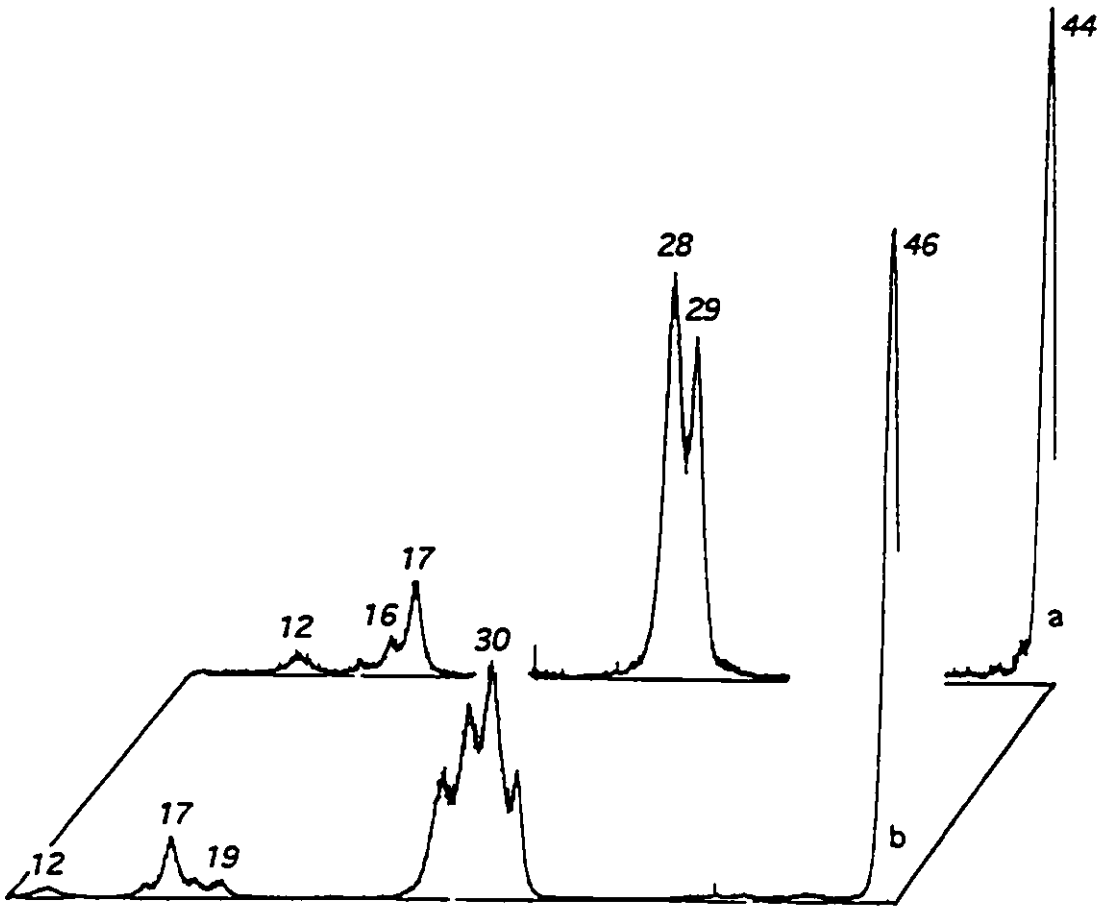

Fig. 4.3 (a) Collision Activation (CA) mass spectrum of the $HOCO^+$ ions generated from collisionally activated CH_2=N(H)$COOH^+$, (b) CA mass spectrum of the $[C, H, O, {}^{18}O]^+$ ions generated from collisionally activated ^{18}O labelled CH_2=N(H)$COOH^+$ ions.

It can immediately be seen, especially from the region at m/z 16 - 20, that the majority of ions 1 dissociate via ion 3. Moreover, we have evidence from ab initio MO calculations [17] that the $HOC^{18}O^+$ ion can, below the threshold for its least energy demanding dissocation reaction, undergo a slow degenerate isomerization to $OC^{18}OH^+$ via triplet $HCO^{18}O^+$ which may explain the presence of peaks corresponding to $^{18}OH^+$, $CO^{+\cdot}$ and $C^{18}OH^+$ in the CA mass spectrum of $HOC^{18}O^+$. We conclude from these results that fast loss of $^{\cdot}CH_3$ from 1 proceeds via a 1,4-hydrogen shift to the keto-oxygen followed by O-C cleavage. Note that an alternative pathway which would also explain the ^{18}O labelling results, namely:

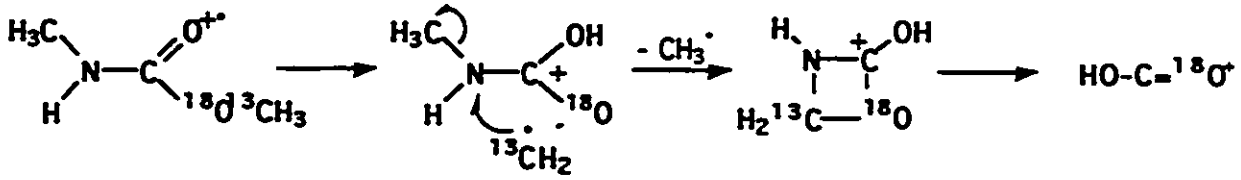

1 -^{18}O,^{13}C 2-^{18}O,^{13}C 7 -^{18}O,^{13}C

can be ruled out since $CH_3N(H)CO^{18}O^{13}CH_3$ cleanly eliminates a ^{13}C containing methyl radical (see above).

As mentioned above, ions 1 of low internal energy content can exchange, to the statistical limit, all the methyls' hydrogen atoms. One way that this can be achieved requires the participation of another isomer of 1, that is the distonic ion $CH_3N(H)$-$^+C(OH)OCH_2^{\cdot}$, 2. Although, as shown above, 2 does not serve as the direct precursor for the methyl loss, it could still participate in hydrogen transfer reactions which precede the O-C bond cleavage process. Distonic ions of the type 2 are known to exist (see Introduction); of particular importance for the present study is that the lower distonic homologue of 2, H_2N-$^+C(OH)OCH_2^{\cdot}$ has been identified (see chapters 2 and 3) as the key intermediate in the unimolecular decay of ionized methyl carbamate, $H_2NCOOCH_3^{\cdot+}$ [18]. The observed H/D exchanges can be explained by the equilibria 1↔3↔2. However, the direct interconversion 1↔2 is also a 1,4-hydrogen transfer and

thus the exchanges could also be rationalized by the equilibria 1↔2↔3. In fact, the most simple explanation for the labelling results observed for the low energy ions (Table 4.1) is probably provided by the equilibria shown in Scheme 4.2.

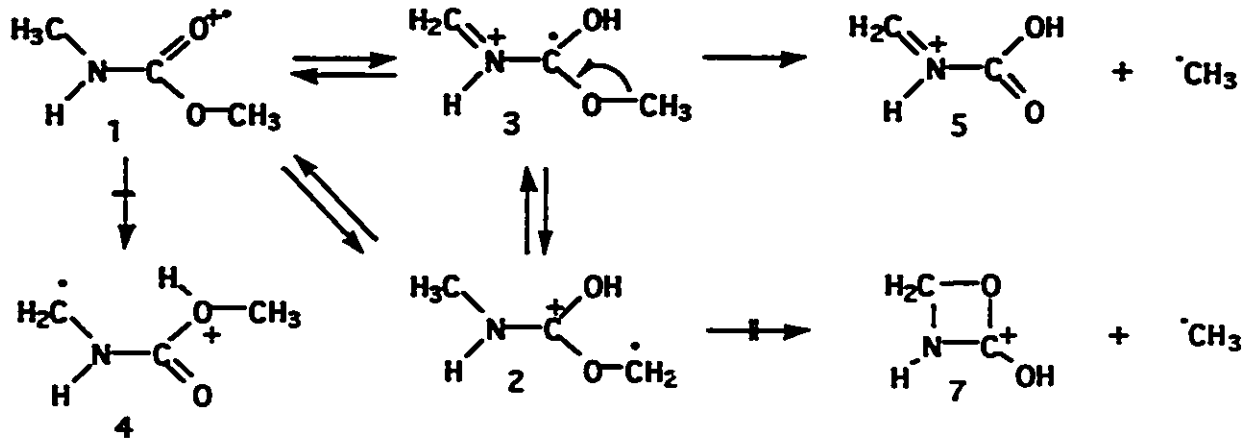

Scheme 4.2

Standard ab initio calculations executed at the 4-31G level of theory indicate that 1, 2 and 3 have comparable energies, while ion 4 lies considerably higher (by c. 60 kJ/mol), in agreement with our experimental results. Note that for the D-labelled ions, in particular for $^{\bullet}CH_3N(H)COOCD_3^{\bullet+}$ (see Table 4.1), the slight but significant preference over the statistical limit for loss of $^{\bullet}CH_3$ (and to a lesser extent $^{\bullet}CH_2D$). This may be rationalized by introducing small isotope effects for the 1,4-hydrogen shifts, i.e. 1↔2 and 1↔3 (but not for the 1,5-hydrogen shifts, 2↔3); in this way in the statistical limit the methoxy carbon will become enriched with hydrogen atoms. That isotope effects should be associated with 1,4-hydrogen shifts and not with the 1,5-hydrogen shifts is precisely what is expected as 1,4-hydrogen shifts invariably have higher activation energies than 1,5-hydrogen shifts [4a]. If the methyl hydrogens of the molecular ion undergo scrambling to the statistical limit prior to loss of methyl, then the positional identity of these atoms should also remain lost in the $[M - {}^{\bullet}CH_3]^+$ product ions. This is indeed what is

observed. In Figure 4.4a is shown the CA mass spectrum of the $[M - {}^{\bullet}CD_2H]^+$ ions generated from $CH_3N(H)COOCD_3^{\bullet+}$.

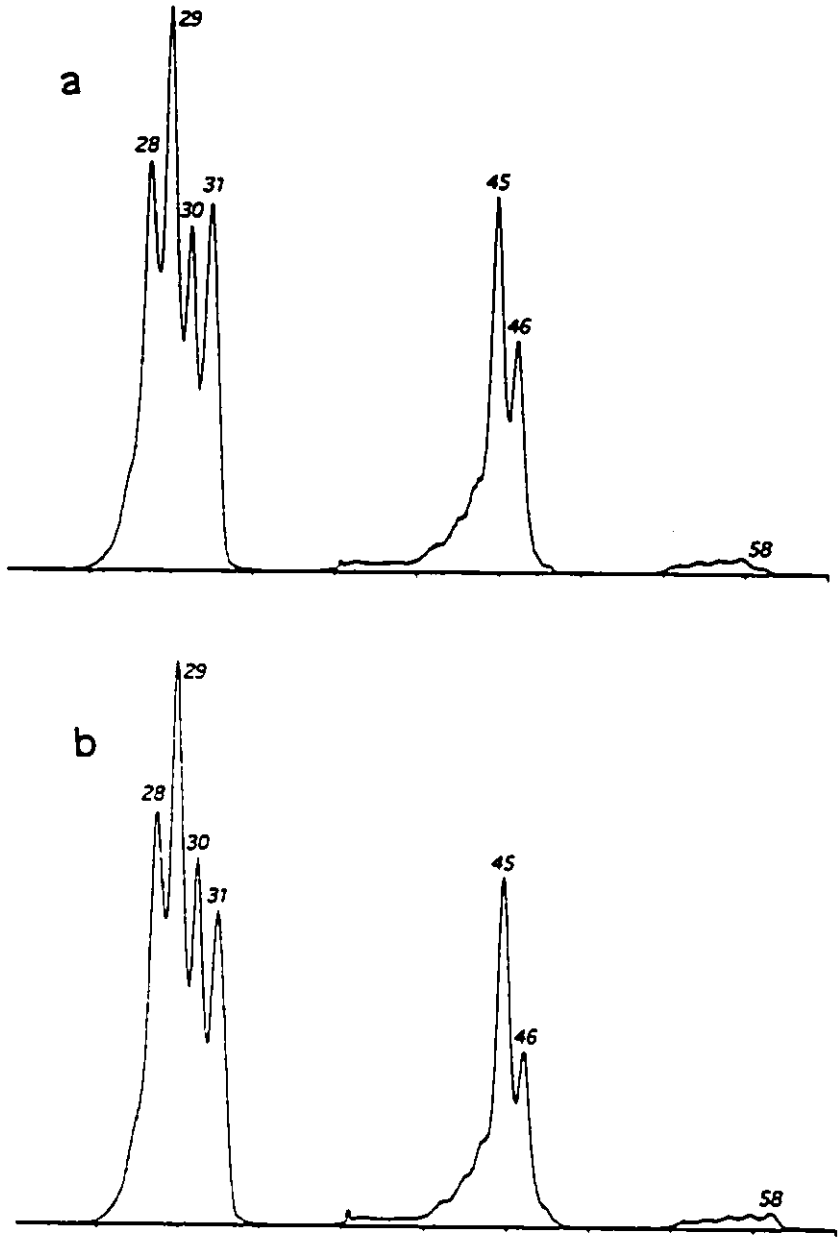

Fig. 4.4 (a) Collision Activation (CA) mass spectrum of the $[M\text{-}CO_2H]^+$ ions generated from $CH_3\text{-}N(H)\text{-}COOCD_3^{\bullet+}$. (b) CA mass spectrum of the $[M\text{-}CH_2D]^+$ ions generated from $CH_3\text{-}N(H)COOCD_2H^{\bullet+}$.

If the methyl hydrogen and deuterium atoms have become indistinguishable, the product ions should consist of a 1:2 mixture of CH_2=N(H)-COOD$^+$ and CHD=N(H)-COCH$^+$ and this is indeed borne out by the 1:2 intensity ratio of the DOCO$^+$: HOCO$^+$ peaks (Figure 4.4a). The peaks at m/z 28 to m/z 31 are predicted to have the distribution m/z 28 : 29 : 30 : 31 = 30 : 25 : 20 : 25, in reasonable agreement with experiment (24 : 33 : 21 : 22). Note also, see Figure 4.4b, that the CA mass spectrum of the [M - $^\bullet CH_2D$]$^+$ ion from $CH_3N(H)COOCD_2H^{\bullet+}$ is virtually identical to that for the [M - $^\bullet CD_2H$]$^+$ ion from $CH_3N(H)COOCD_3^{\bullet+}$, Figure 4.4a, again attesting to complete H/D exchange reactions.

As mentioned above (see Figure 4.1), the MI mass spectrum of 1 contains small peaks at m/z 58 (loss of $CH_3O^\bullet$/$CH_2OH^\bullet$), m/z 59 (loss of CH_3NH and/or CH_2=O) and m/z 60 (loss of HCO$^\bullet$). If these processes are truly unimolecular, significant H/D exchange reactions may be expected for these losses just as was observed for loss of methyl.

In Figure 4.1b is given the MI mass spectrum of $CD_3N(H)COOCD_3^{\bullet+}$. No loss of CH_3NH (to m/z 59) is observed and so m/z 59 in Figure 4.1a corresponds wholly to CH_2=O loss. Interestingly, the m/z 60 - 63 intensity ratio in Figure 4.1b could only be reconstructed from the corresponding distribution in Figure 4.1a by assuming that the losses of HCO$^\bullet$ and H_2C=O are associated with complete exchange of the methyls' hydrogens and that significantly less exchange reactions are associated with the loss of $CH_3O^\bullet$/$CH_2OH^\bullet$, i.e. loss of $CH_3O^\bullet$/$CH_2OH^\bullet$ involves to a large extent the original methoxy hydrogens. Interestingly, it was observed that m/z 58 and m/z 59 in Figure 4.1a were very sensitive to the collision gas presssure and these peaks are prominent in the CA mass specturm (not shown). Analysis of the CA mass spectrum of $CH_3N(H)CO^{18}O^{13}CH_3^{\bullet+}$ revealed that 60% of the m/z 59 peak in the CA mass spectrum of 1 corresponds to loss of CH_3NH, with the remainder being loss of CH_2=O). This parallels previous observations [19] that m/z 59 in the EI mass spectrum of 1 is a doublet due to losses of CH_3NH and CH_2=O. The latter produces the carbene ion $CH_3N(H)$-C-OH$^{\bullet+}$, very likely from ion 2 [19].

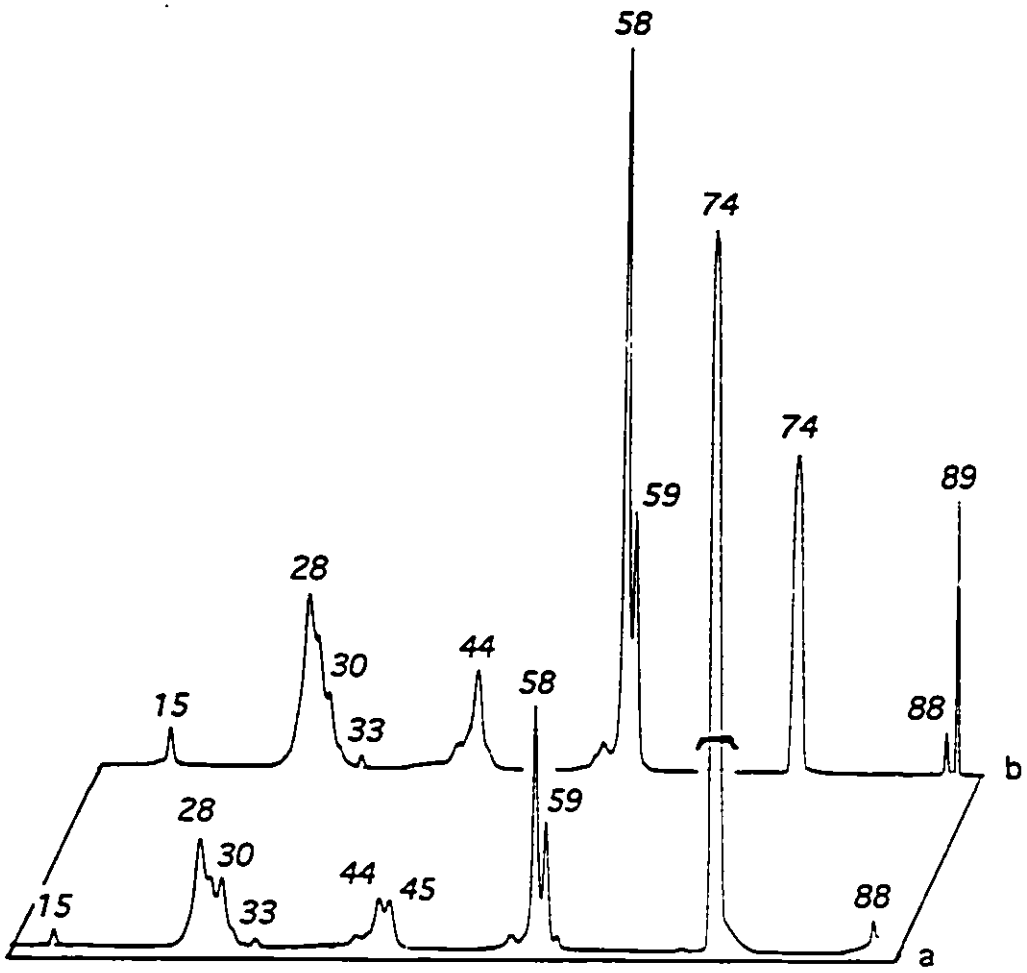

Fig. 4.5 Collisional Activation (a) and Neutralization-Reionization (b) mass spectra of CH_3-N(H)COCCH$_3$.

It now becomes clear, by integrating all of the above results, that all true metastable processes, including the minor losses of $HCO^{\bullet}$ and $CH_2{=}O$ are preceded by complete randomization of the methyls' hydrogens, whereas for the collision induced reactions, the specific process is seen. Hence, again, in the CA experiments ions **1** are sampled that do not have sufficient energy to surmount the barriers for the isomerizations **1↔2↔3↔1**. Thus, the CA mass spectrum of **1** (see Figure 4.5a) should represent to a large extent unrearranged ions **1**. A more pronounced effect if reduced scrambling is seen in the NR mass spectra (see above and Table 4.2). Thus, the NR mass spectrum of **1** too, should only represent ions **1** and so it should be very close to the CA mass spectrum which, compare Figure 4.5a and 4.5b, is indeed the case.

Thermochemistry of methyl loss

All heats of formation for the following estimates are taken from ref. 11 unless otherwise stated. The heat of formation of $CH_3N(H)COOCH_3^{\bullet+}$, ΔH_f (**1**), may be estimated in two ways. First, ΔH_f ($CH_3N(H)CHO^{\bullet+}$) is known, 181 kcal/mol; the difference between ΔH_f ($H_2NCHO^{\bullet+}$) and ΔH_f ($H_2NCOOCH_3^{\bullet+}$) = 190 - 141 = 49 kcal/mol, making ΔH_f (**1**) = 132 kcal/mol. Alternatively, using ΔH_f ($H_2NCOOCH_3^{\bullet+}$) = 141 kcal/mol [18] and the difference between ΔH_f ($H_2NCOOCH_3^{\bullet+}$) and ΔH_f ($CH_3N(H)COCH_3^{\bullet+}$) = 165 - 158 = 7 kcal/mol gives ΔH_f ($CH_3N(H)COOCH_3^{\bullet+}$) = 134 kcal/mol, hence on average ΔH_f (**1**) = 133 kcal/mol.

The heat of formation of $CH_2{=}N(H)\text{-}COOH^+$, ΔH_f (**5**) may also be estimated in two ways. ΔH_f ($CH_2{=}N(H)\text{-}COCH_3^+$) has been assessed as 131 kcal/mol [14] and by using the difference between ΔH_f ($CH_3CH_2COCH_3$) and ΔH_f (CH_3CH_2COOH) = -57.5 - (-107) = +49.5 kcal/mol, one obtains ΔH_f (**5**) = 81.5 kcal/mol. This method assumes that the acetyl and $^{\bullet}COOH$ functionalities have the same (de)stabilizing effect on the iminium ion $CH_2{=}NH_2^+$.

Another way to estimate ΔH_f (**5**), which requires an estimation for the stabilization energy (SE) of the -N(H)COOH functionality, is by isodesmic substitution, Eq. (4.1).

$^{+}CH_3 + CH_3\text{-}N(H)COOH \rightarrow CH_4 + {}^{+}CH_2\text{-}N(H)COOH\ (5) + SE$ (Eq. 4.1)

$^{+}CH_3 + CH_3NH_2 \rightarrow CH_4 + {}^{+}CH_2\text{-}NH_2 + SE$ (Eq. 4.2)

$^{+}CH_3 + CH_3\text{-}N(H)COCH_3 \rightarrow CH_4 + {}^{+}CH_2\text{-}N(H)COCH_3 + SE$ (Eq. 4.3)

For Eq. 4.2 the SE is calculated at 95 kcal/mol. For Eq. 4.3 the SE is calculated at 90 kcal/mol, using ΔH_f (CH_3-N(H)$COCH_3$) = - 56 kcal/mol and ΔH_f (CH_2-N(H)$COCH_3^+$) = 131 kcal/mol [14]. Considering the above very similar SE values for the -NH_2 and -N(H)$COCH_3$ substituents, it seems reasonable to use an SE value of 95 kcal/mol for the -N(H)COOH functionality. Next is needed ΔH_f (CH_3N(H)COOH), which can be estimated from the known ΔH_f (H_2NCOCH_3) = -100 kcal/mol [14], the difference in enthalpy between CH_3COOCH_3 and CH_3COOH (-98 - (-103) = + 5 kcal/mol), and the ΔH_f differential of H_2NCOCH_3 and CH_3N(H)$COCH_3$ which is, -57 - (-56) = +1 kcal/mol. Hence, ΔH_f (CH_3N(H)COOH) = -104 kcal/mol obtains. Inserting the appropriate values into Eq. 4.1 gives ΔH_f (5) = 83 kcal/mol.

Thus, loss of $^{\bullet}CH_3$ (ΔH_f = 35 kcal/mol) is exothermic by ~15 kcal/mol. In addition, loss of $^{\bullet}CH_3$ from the reacting configuration 3 must be associated with a significant forward barrier because as shown by labelling experiments, 3 can rearrange back to 1 and 2. Invariably endothermic O-C bond cleavages are associated with large reverse terms (c. 20 kcal/mol) [9] and so in spite of the fact that the dissociation of 3 is an exothermic reaction a significant forward barrier exists. The combination of these two effects rationalizes the observed large kinetic energy release.

4.2 The elusive $HN{=}C{-}OH^+$ ion characterized by a double collision experiment in the mass spectrometer.*

The technique of Collisional Activation (CA) [21], whereby stable gas phase ions are induced to decompose to often characteristic products has been a key method in the development of gas phase ion chemistry [22]. In particular, CA experiments in concert with or inspired by state of the art *ab initio* calculations [23] have revealed that many a species, which does not exist in the uncharged state, is stable as the oxidized form. Indeed, the answer to the question posed by Chanon et al. [24], "one electron less. What does it change? " very often is that oxidation may have a profound effect on the stability of the species. However, several unconventional cationic species predicted to exist by theory have never even been observed in the laboratory, like for example the simplest ionized true carbohydrate COH_2^+ [25].

In the case of $[H_2,C,N,O]^+$ ions [26] four out of six isomers investigated by theory [26b,c,d,f] have been generated, *viz.* the ubiquitous $H_2N{-}C{=}O^+$ ion, **1**, $HCNOH^+$, H_2CNO^+ and the nitrenium ion $HNC(H){=}O^+$, a transient species [26a]. However, the isomer $HN{=}C{-}OH^+$, **2**, has thus far eluded observation. This ion, formally O-protonated isocyanic acid, is predicted to be only 75 kJ/mol higher in energy [26e] than the most stable member of the set the N-protonated isocyanic acid, **1**.

A search of the literature unearthed an unverified proposal that parabanic acid [7] would yield $[H_2,C,N,O]^+$ ions with the connectivity of the missing isomer **2** (see below).

---

* This material has been published already in a communication with the same name:

G.A. McGibbon, J.K. Terlouw and P.C. Burgers,

Rapid Commun. Mass Spectrom. 7 (1993) 138-141.

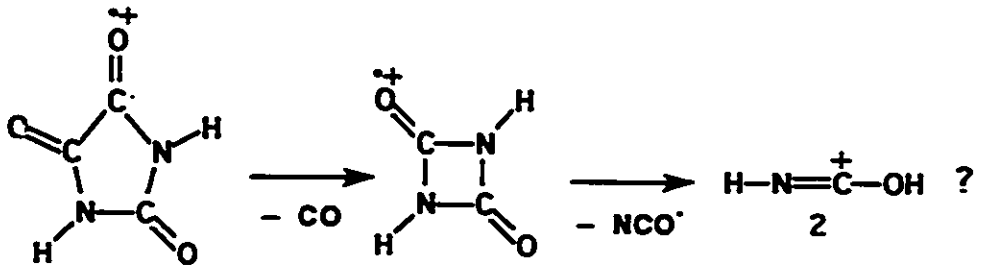

However, from a comparison of the CA mass spectrum of this ion with that of the reference spectra in ref. 26e it follows that parabanic acid generates isomer **1** rather than **2** and this inspired us to look for an alternative strategy for the generation of **2**. Such a strategy has become available with the advent of multisector mass spectrometers which allow mass selected fragment ions from collision-induced dissociations to be used as progenitors for species having interesting structures [8]. We report here the successful application of this approach for the generation and identification of the missing isomer **2**.

Results and Discussion

In the context of our studies on isomerization reactions involving distonic ions and hydrogen-bridged species in ionized carbamates [29], we noted that one of the primary dissociation reactions of $CH_3N(H)COOCH_3^{\bullet+}$ involves the loss of 30 daltons leading to m/z 59 (25 % of base peak m/z 58). The peak at m/z 59 is a doublet consisting of $[H_5C_2N,O]^+$ (via loss of formaldehyde) and $CH_3O\text{-}C{=}O^+$ [30]. For collision experiments these ions were separated by an appropriate isotopic substitution, e.g. $CD_3N(H)COOCH_3^{\bullet+} \rightarrow$ m/z 62 + $CH_2{=}O$ (but not $CH_3N(D)COOCH_3^{\bullet+}$, see below).

Collision experiments on this m/z 62 ion and on other isotopomers indicate that we are dealing with methylamino-hydroxycarbene ions $CD_3N(H)COH^{\bullet+}$, formed via a 1,4-H shift to oxygen and **not** $(CD_3)(H)_2N\text{-}C{=}O^{\bullet+}$ which could have been formed after a 1,4-H shift to nitrogen. The CA mass spectrum of $CD_3N(H)COH^{\bullet+}$ is dominated by loss of $CD_3^{\bullet}$

yielding m/z 44 ions which we suspected would have the connectivity $HNCOH^+$ that is, of isomer 2:

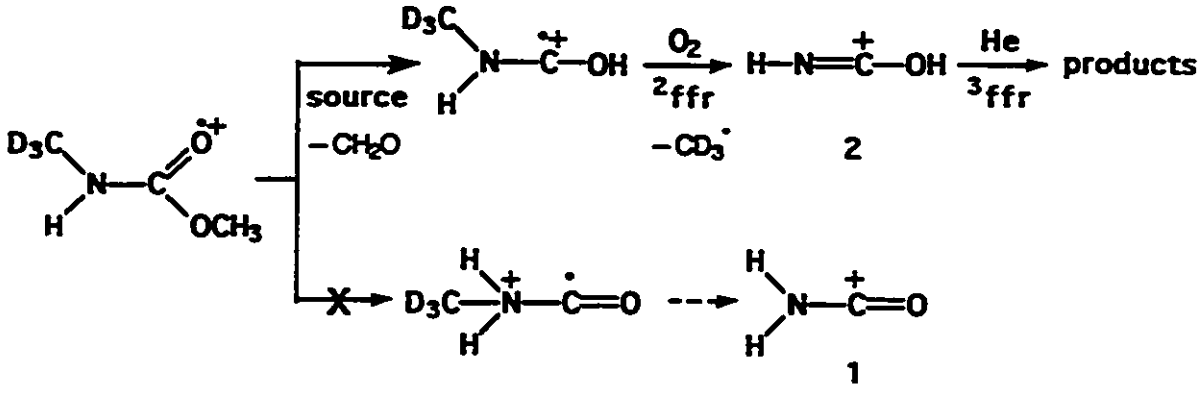

Accordingly, we performed a double collision experiment [28] wherein m/z 44 ions, formed by collision induced dissociation of $CD_3N(H)COH^{\bullet+}$ in the second field free region (2FFR) of the instrument, were subjected to CA in the third field free region (3FFR). The resulting CA mass spectrum (Fig. 4.6a) is markedly different from that of the more stable H_2NCO^+ ion 1 (Fig. 4.6b) (which for comparative purposes was made by the collision induced loss of $CH_3^{\bullet}$ from ionized acetamide) and also from the other reported isomers [26a,d,e]. Ion 1 predominantly dissociates to m/z 28 ($[H_2,C,N]^+$ and/or $CO^{\bullet+}$) and m/z 16 (NH_2^+ and/or O^+), whereas 2 chiefly fragments to m/z 27 (which can only be $[H,C,N]^+$, m/z 28 and m/z 29 (which can only be $[H,C,O]^+$). From the CA mass spectra of the ions $HDNCO^+$, $DNCOH^+$ and $HNCOD^+$ (see Figures 4.7a - c respectively), it follows that m/z 28 largely is $CO^{\bullet+}$ and that m/z 16 (which is not shown) is NH_2^+, in agreement with previous high resolution data [6a]. Note that ions $HNCOH^+$ can produce HNC^+ and COH^+ via direct cleavages and similarly that H_2NCO^+ can produce NH_2^+ and $CO^{\bullet+}$ via simple fissions ; this lends strong support for the assigned structures. The observation that $HNCOH^+$ can produce NH_2^+ and $CO^{\bullet+}$ we take as showing that $HNCOH^+$ can isomerize into H_2NCO^+. This reaction could occur at internal energies slightly below the threshold for the dissociation of lowest energy requirement: $\Sigma\Delta Hf\ [NH_2^+ + CO] = 481$ kJ/mol [26e,11]

whereas the isomerization barrier 1 → 2 derived from theory is > 400 kJ/mol [26e]. Also labelling experiments show that the weak peak at m/z 30 in the spectra of 1 and 2 (Fig. 4.6a,b) is NO^+ and so complex rearrangements (probably of the activated ions) can take place.

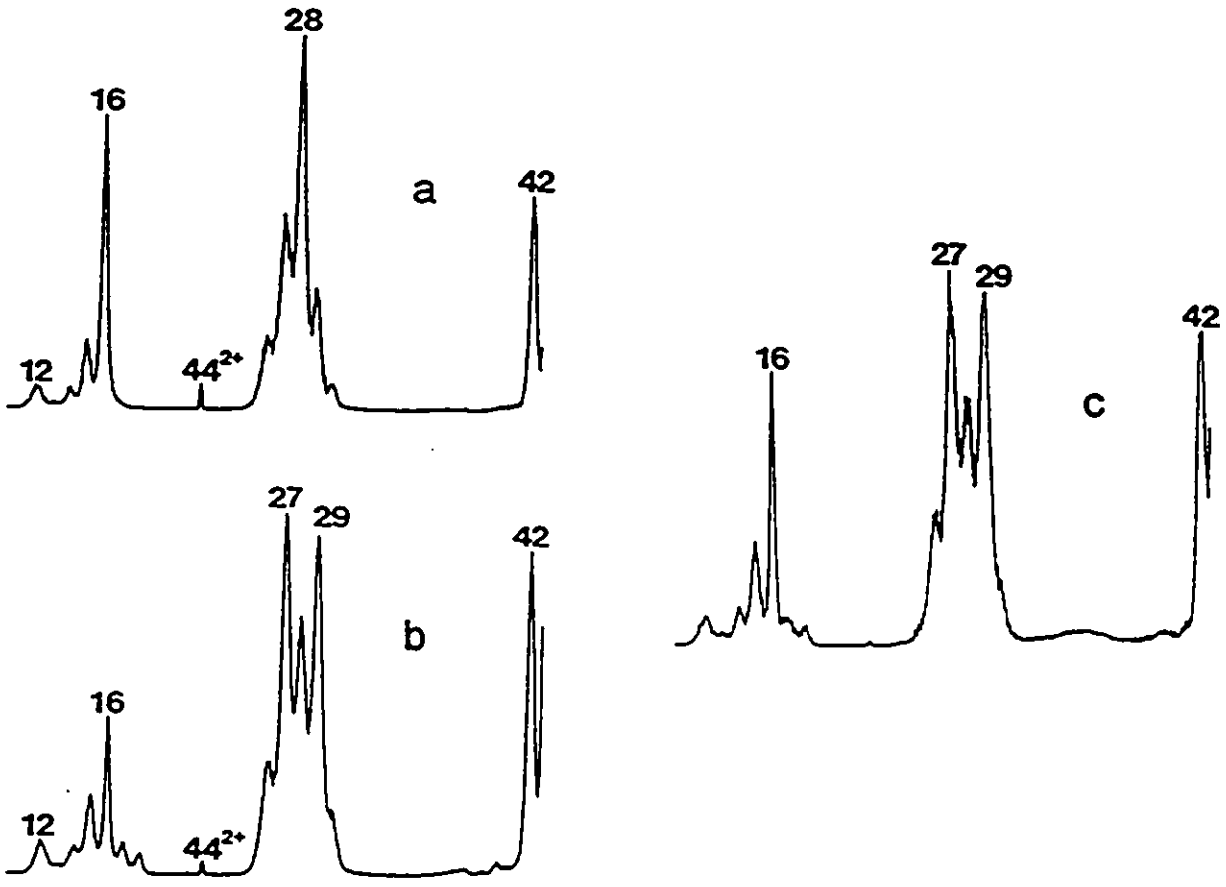

Fig. 4.6 Partial [3FFR,He] CA mass spectra of (a) ions 2, $HN{=}C{-}OH^+$, generated by the collision induced dissociation of $CH_3N(H)COH^{\bullet+}$ [2FFR,O_2] . (b) ions 1, $H_2N{-}C{=}O^+$, generated by the [2FFR,O_2] collision induceddissociation of $H_2NCOCH_3^{\bullet+}$ and (c) the $[H_2,C,N,O]^+$ ions generated by the [2FFR,O_2] collision induced dissociation of $CH_3(H)N{-}C(H){=}O^{\bullet+}$.

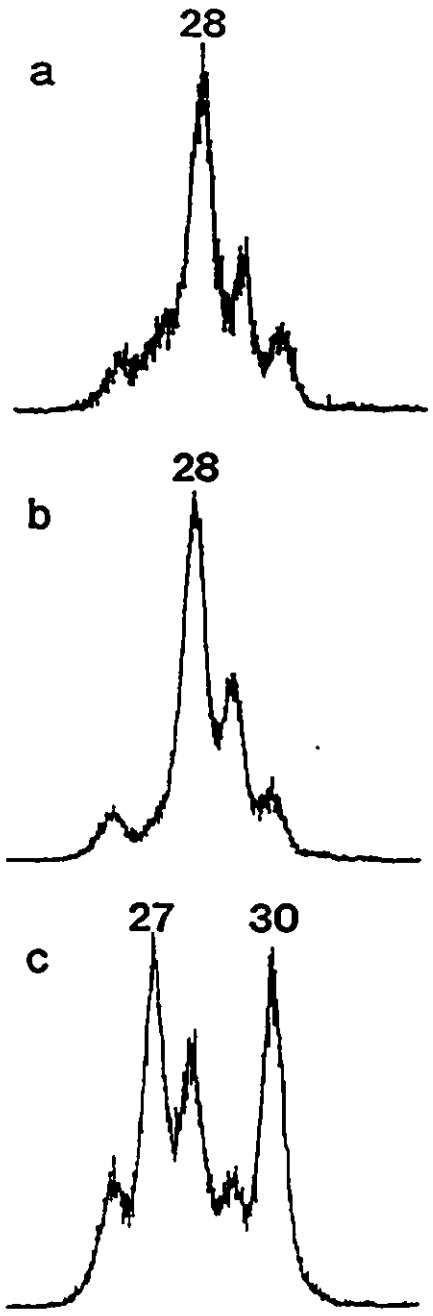

Fig. 4.7 Partial [3FFR,He] CA mass spectra of (a) ions $HDN\text{-}C{=}O^+$, generated by the [2FFR,O_2] collision induced dissociation of $HDNCOCH_3^+$, (b) ions $DNCOH^+$, generated by the [2FFR,O_2] collision induced dissociation of $CH_3N(D)COH^{+\bullet}$ and (c) ions $HNCOD^+$, generated by the [2FFR,O_2] collision induced dissociation of $CH_3N(H)COD^{+\bullet}$.

Compared with the unlabelled $HNCOH^+$ species, for the ion $DNCOH^+$ m/z 27 ($HNC^{\cdot+}$) shifts to m/z 28 ($DNC^{\cdot+}$), whereas m/z 28 ($CO^{\cdot+}$) does not shift and thus by coincidence the CA mass spectrum of $DNCOH^+$ (Fig. 4.7a) is very similar to that of $HDNCO^+$ (Fig. 4.7b). Now we mentioned above that unlabelled $CH_3N(H)COOCH_3^{\cdot+}$ produces the isobaric species $CH_3N(H)COH^{\cdot+}$, the precursor for **2** and $CH_3O\text{-}C{=}O^+$ and that interference by the latter can be eliminated by isotopic substitution. Had the first (reasonable) choice been $CH_3N(D)COOCH_3$ (obtained by a simple H/D exchange experiment with $CH_3N(H)COOCH_3$) it might have been erroneously concluded , see Figs. 4.8a and 4.8b, that the product ions actually have the connectivity of **1**.

The most intense peak in the CA mass spectrum of **1** and **2** is the loss of $H^{\cdot}$. The labelled ion $HDN\text{-}C{=}O^+$ loses $H^{\cdot}$ and $D^{\cdot}$ and double collision experiments showed that both losses lead to the same product ions, ionized isocyanic acid. The observed CA ratio (peak areas) for the loss of $H^{\cdot}$ vs $D^{\cdot}$ is 1.6 $\pm$ 0.1, compatible with a primary isotope effect [31a] approaching c. $\sqrt{2}$, the ratio of the N-H and N-D stretching frequencies [31b]. The labelled ions $DN{=}C\text{-}OH^+$ and $HN{=}C\text{-}OD^+$ both lose $H^{\cdot}$ and $D^{\cdot}$ in ratio's of 2.6 : 1 and 1.1 : 1 respectively. Although CA mass spectra permitting the identification of the daughter ion structures could not be obtained with our instrumentation, the above ratios are compatible with c. 50 % direct cleavage yielding $H\text{-}N{=}C{=}O^{\cdot+}$ and 50 % rearrangement to the H/D symmetrical ion $HDN\text{-}C{=}O^+$ (see above), giving $H\text{-}N{=}C{=}O^{\cdot+}$ and $D\text{-}N{=}C{=}O^{\cdot+}$.

The above identification of **2** by CA mass spectrometry prompted us to briefly re-examine the experimental evidence [26a,e] for the formylnitrenium ion $HNC(H){=}O^+$, **3**. According to *ab initio* molecular orbital calculations [26e] the most stable form is a triplet ion-dipole complex **3a** lying 377 kJ/mol above **1**; the most stable singlet state is the strained carbenium ion **3b**, lying 449 kJ/mol above **1**, with singlet $HNC(H){=}O^+$, **3c**, lying even higher: 549 kJ/mol above **1**. The latter species may even be unstable towards dissociation by direct bond cleavage, considering that the dissociation limit for HCO^+ + NH, calculated from thermochemical data [11], lies only 527 kJ/mol above **1**.

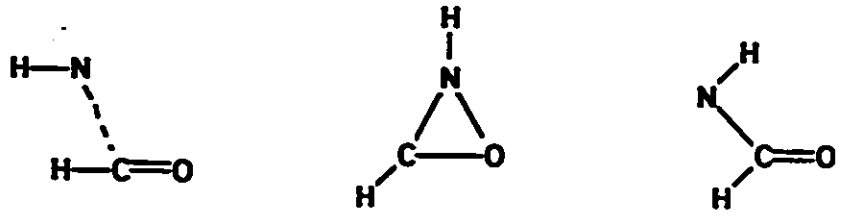

3a 3b 3c

Ions of connectivity **3** have been made by Charge Reversal (CR) [12,32] of $HNC(H)=O^-$ but it was concluded from an elegant experiment that the resulting nitrenium ion is unstable and rapidly (10^{-5} s) transforms to **1** [26a]. Another way to generate ions of putative structure **3** involves the (minor) loss of $CH_3^\bullet$ from ionized N-methylformamide, i.e. $CH_3(H)N\text{-}C(H)=O^{\bullet+} \rightarrow HNC(H)=O^+$. Although it was noted [26a] that the CA mass spectrum of the $[H_2,C,N,O]^+$ ions thus formed was markedly different from the CR mass spectrum of $HNC(H)=O^-$, ions **3** were nevertheless proposed to be generated from the amide [26e]. The 3FFR CA mass spectrum we obtained from the m/z 44 $[H_2,C,N,O]^+$ ions generated by the collision induced loss of $CH_3^\bullet$ from $CH_3(H)N\text{-}C(H)=O^{\bullet+}$ in the 2FFR is shown in Figure 4.6c. From a comparison of the results shown in Figure 4.7 and the data in refs. 26a and 26e, we propose that loss of $CH_3^\bullet$ from $CH_3(H)N\text{-}C(H)=O^{\bullet+}$ does not yield the high energy species **3** but rather, that predominantly **2** is formed and that some **1** may be co-generated.

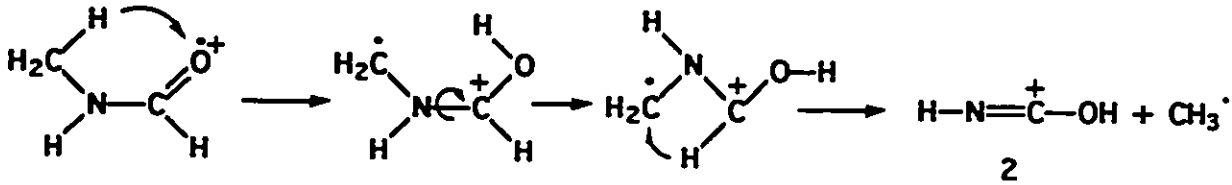

2

The formation of ions **2** from the amide can be rationalized by the mechanism shown above which is analogous to that proposed for the formation of $HO\text{-}C=O^+$ from ionized methyl formate, $HC(=O)OCH_3^{\bullet+}$ [3].

References

1. (a) H. Schwarz, Org. Mass Spectrom. 15 (1980) 491; (b) H. Schwarz, Topics Curr. Chem. 97 (1981) 1.
2. G.A. McGibbon, P.C. Burgers and J.K. Terlouw, Chem. Phys. Letters 218 (1994) 499.
3. P.C. Burgers, A.A. Mommers and J.L. Holmes, J. Am. Chem. Soc. 105 (1983) 5976.
4. (a) B.F. Yates, W.J. Bouma and L. Radom, Tetrahedron 22 (1986) 6225; (b) S. Hammerum, Mass Spectrom. Rev. 7 (1988) 123.
5. L. Radom, Org. Mass Spectrom. 26 (1991) 359.
6. H.-F. Grützmacher, Int. J. Mass Spectrom. Ion Processes 118/119 (1992) 825
7. N. Heinrich, T. Drewello, P.C. Burgers, J.C. Morrow, J. Schmidt, W. Kulik, J.K. Terlouw and H. Schwarz, J. Am. Chem. Soc. 114 (1992) 3776.
8. J.L. Holmes, Org. Mass Spectrom. 20 (1985) 169.
9. (a) P.C. Burgers, J.L. Holmes and J.K. Terlouw, J. Chem. Soc. Chem. Commun. (1984) 642; (b) W.J. Bouma, P.C. Burgers, J.L. Holmes and L. Radom, J. Am. Chem. Soc. 108 (1986) 1767.
10. D.E. Drinkwater and F.W. McLafferty, Org. Mass Spectrom. 28 (1993) 378.
11. S.G. Lias, J.E. Bartmess, J.F. Liebman, J.L. Holmes, R.D. Levin and W.G. Mallard, J. Phys. Chem. Ref. Data 17, supplement 1 (1988).
12. K.F. Donchi, B.A. Rumpf, G.D. Willet, J.R. Christie and P.J. Derrick, J. Am. Chem. Soc. 110 (1988) 347.
13. A.-M. Dommröse and H.-F. Grützmacher, Int. J. Mass Spectrom. Ion Processes 76 (1987) 95.
14. P.C. Burgers, C.A. Kingsmill, G.A. McGibbon and J.K. Terlouw, Org. Mass Spectrom. 27 (1992) 398.
15. D. Suh, C.A. Kingsmill, P.J.A. Ruttink, J.K. Terlouw and P.C. Burgers, Org. Mass Spectrom. 28 (1993) 378.
16. (a) P.C. Burgers and J.L. Holmes, Chem. Phys. Letters 97 (1983) 236; (b) A.J. Illies, M.F. Jarrold and M.T. Bowers, J. Chem. Phys. 77 (1982) 5847; (c) A.J. Illies, M.F. Jarrold and M.T. Bowers, J. Am. Chem. Soc. 105 (1983) 2562.
17. P.J.A. Ruttink, G.A. McGibbon, P.C. Burgers and J.K. Terlouw, in preparation.
18. G. Schaftenaar, R. Postma, P.J.A. Ruttink, P.C. Burgers, G.A. McGibbon and J.K. Terlouw, Int. J.

Mass Spectrom. Ion Proc. 100 (1990) 521.

19. G.A. McGibbon, J.K. Terlouw and P.C. Burgers, Rapid Commun. Mass Spectrom. 7 (1993) 138.

20. J.I. Seeman, H.V. Secor, R. Disselkamp and F.R. Bernstein, J. Chem. Soc., Chem. Commun. 713 (1992)

21. see for example : (a) K. Levsen, Fundamental Aspects of Organic Mass Spectrometry, Verlag Chemie: New York (1978); (b) Collision Spectroscopy, R.G. Cooks (ed.), Plenum: New York (1978); (c) K. Levsen and H. Schwarz, Mass Spectrom. Rev. 2 (1983) 77; (d) J. Bordas-Nagy and K. R. Jennings, Int. J. Mass Spectrom Ion Processes 100 (1990) 105.

22. J.L. Holmes, Org. Mass Spectrom. 20 (1985) 169.

23. W.J. Hehre, L. Radom, P. v. R. Schleyer and J.A. Pople, Ab Initio Molecular Orbital Theory, Wiley-Interscience: New York (1986).

24. M. Chanon, M. Rajzmann and F. Chanon, Tetrahedron 46 (1990) 6193.

25. W.J. Bouma, P.C. Burgers, J.L. Holmes and L. Radom, J. Am. Chem. Soc. 108 (1986) 1767.

26. (a) J.P. Kiplinger, A.T. Maynard and M. M. Bursey, Org. Mass Spectrom. 22 (1987) 534; (b) J.R. Bews and C. Glidewell, J. Mol. Struct. 67 (1980) 141, 151; (c) S. Green, J. Phys. Chem. 85 (1981) 1676; (d) H. Egsgaard, L. Carlsen and S. Elbel, Ber. Bunsenges. Physik. Chem. 90 (1986) 369; (e) C.E.C.A. Hop, J.L. Holmes, P.J.A. Ruttink, G. Schaftenaar and J.K. Terlouw, Chem. Phys. Lett.156 (1989) 251; (f) J. Hrusak, M.C. Holthausen, N. Goldberg, M. Iraqi, W. Koch and H. Schwarz, Israel J. Chem. 33 (1993) 277.

27. R. A. Corral, O. O. Orazi and J. Zinczuk, Org. Mass Spectrom. 14 (1979) 470.

28. see for example: S. Villeneuve and P.C. Burgers, Org. Mass Spectrom. 21 (1986) 733.

29. (a) P.C. Burgers, C. Lifshitz, P.J.A. Ruttink, G. Schaftenaar and J.K. Terlouw, Org. Mass Spectrom. 24 (1989) 579; (b) G. Schaftenaar, R. Postma, P.J.A. Ruttink, P.C. Burgers, G.A. McGibbon and J.K. Terlouw, Int. J. Mass Spectrom. Ion Processes 100 (1990) 521; (c) G.A. McGibbon, C.A. Kingsmill, J.K. Terlouw and P.C. Burgers, Org. Mass Spectrom. 27 (1992) 126; (d) G.A. McGibbon, J.K. Terlouw and P.C. Burgers, in preparation (see section 4.1).

30. M.C. Blanchette, J.L. Holmes, C.E.C.A. Hop, F.P. Lossing, R. Postma, P.J.A. Ruttink and J.K.

Terlouw, J. Am. Chem. Soc. 108 (1986) 7589.

31. (a) P.J. Derrick, Mass Spectrom. Rev. 2 (1983) 285; B.J. Wang and E.R. Thornton, J. Am. Chem. Soc. 90 (1968) 1216.

32. M.M. Bursey, Mass Spectrom. Rev. 9 (1990) 555.

CHAPTER 5

Aspects of the CH_5N_2 potential energy surface: ions CH_3NHNH^+, $CH_3NNH_2^+$ and $CH_2NHNH_2^+$ and radicals $CH_2NHNH_2^{\bullet}$ studied by theory and experiment.

Introduction

In this chapter the $CH_5N_2^+$ system is investigated by high level ab initio computations and mass spectrometric experiments. AE measurements and theory are used to (re)-evaluate the heats of formation of the title ions. Theoretical methods were also used to calculate their 1,2- and 1,3-H shift interconversion energy barriers and to evaluate the stabilities of two other isomers: the ring-closed form of CH_2=NH-NH_2^+ and the hydrogen-bridged entity CH_2=N$\therefore$H$\therefore$$NH_2^+$. Mechanisms are proposed for the metastable dissociation reactions of $CH_5N_2^+$ ions to $HCNH^+ + NH_3$ and to $HC{\equiv}N + NH_4^+$; the latter rationalized in terms of a dissociating $[HC{\equiv}N\cdots NH_4]^+$ ion-dipole complex. It should be noted that a lower energy pathway for this reaction has since been located (Nguyen and Vanquickenbourne, J. Chem. Soc. Perkin Trans. 2 (1993) 1969, see appendix). This demonstrates that keen chemical intuition is crucial in the search for low energy reaction pathways and that computations are not a panacea for gas phase ion chemistry problems.

Triple collision (collision activation of neutralization-reionization *survivor* ions, NR/CA or NR/CID) experiments were used to assess the stability of the neutral CH_2=NH-$NH_2^{\bullet}$ and the fate of most of the neutralized CH_2=NH-NH_2^+ ions is considered in light of the computed geometry differences between the CH_2=NH-NH_2 ion and radical.

The work that is described here has already been published under the above title:

H.F. Van Garderen, P.J. A. Ruttink, P.C. Burgers, G.A. McGibbon and J.K. Terlouw

Int. J. Mass Spectrom. Ion Processes 121 (1992) 159-182.

The generation and identification of CH_5N_2 radicals, cations and dication radicals was reported in a recent paper [1]. Ions of putative structure CH_3-NH=NH^+, 1^+, CH_3-N=NH_2^+, 2^+ and CH_2-NH-NH_2^+, 3^+, the diazapropylium ions, were generated by appropriate simple bond fissions. By integration of results obtained from collisional activation (CA) mass spectrometry [2], neutralization-reionization (NR) mass spectrometry [3] and deuterium labelling experiments, it was concluded [1] that the above ions are stable species and that the barriers for their interconversion are high. The hydrazyl radicals CH_3-NH=$NH^\bullet$ and CH_3-N=$NH_2^\bullet$ were generated by gas-phase reduction of 1^+ and 2^+ respectively.

From Appearance Energy (AE) measurements the heat of formation of the above ions could be assessed: ΔH_f (1^+) $\leq$ 188 kcal/mol, ΔH_f (2^+) = 183.5 kcal/mol and ΔH_f (3^+) = 195 kcal/mol. A fourth isomer, CH_2=N-NH_3^+, 4^+, was not independently generated, but results from CA and Charge Stripping-Electron Capture Induced Decomposition [4] (CS/ECID [1]) mass spectroscopy indicated that ions 4^+ are formed following a slow (10^{-5} s^{-1}) isomerization of ions 3^+. Thus, for the non-decomposing ions the relationships shown in Scheme 5.1 were derived.

In fact, the possibility was entertained that ions 3^+ and 4^+ collapse to the bridged entity shown in Scheme 5.1. Metastable diazapropylium ions decompose to NH_4^+ + HC≡N (not HNC) and to the conjugate base/acid pair NH_3 + $HCNH^+$ [1] and so metastable $CH_5N_2^+$ ions rearrange prior to decay. For all $CH_5N_2^+$ isomers, the metastable ion characteristics for loss of HC≡N were almost the same, as were those for the loss of NH_3 and so it was concluded that the $CH_5N_2^+$ ions rearrange to (a) common intermediate(s). It was proposed that 3^+ was the reacting configuration for de-amination and that 4^+ reacts to give protonated ammonia. However, despite many experiments, a detailed description of the rearrangement /dissociation processes of the $CH_5N_2^+$ ions could not be given.

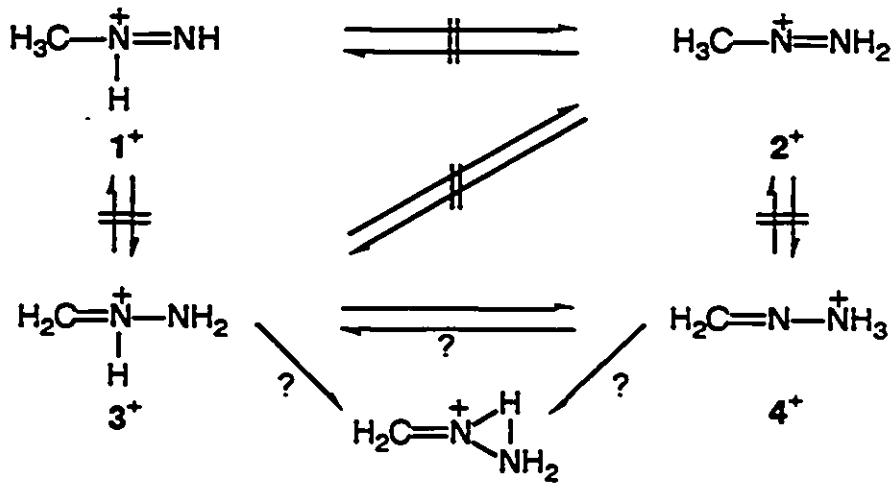

Scheme 5.1

The purpose of the present paper is to examine in some detail the $CH_5N_2^+$ potential energy surface by high level ab initio molecular orbital (MO) calculations. We will show that such calculations can lead to a proper description of the rearrangement/dissociation processes which could not have been achieved by analysis of experimental data only. Since the relative stabilities of the ions 1^+ - 3^+ predicted by theory differed from our previously published experimental results, we will also discuss some new experimental results aimed at resolving this discrepancy. New experimental and theoretical results are also reported pertaining to the stability and the dissociation characteristics of the $^{\bullet}CH_2$-NH-NH_2 radical $3^{\bullet}$, which will be shown to be more stable than originally proposed.

Theoretical methods

Standard LCAO-MO-SCF calculations were performed with the program GAMESS [5] employing restricted Hartree-Fock (RHF) procedures. The isomers, transition states and dissociation products which have been examined are given in Scheme 5.2.

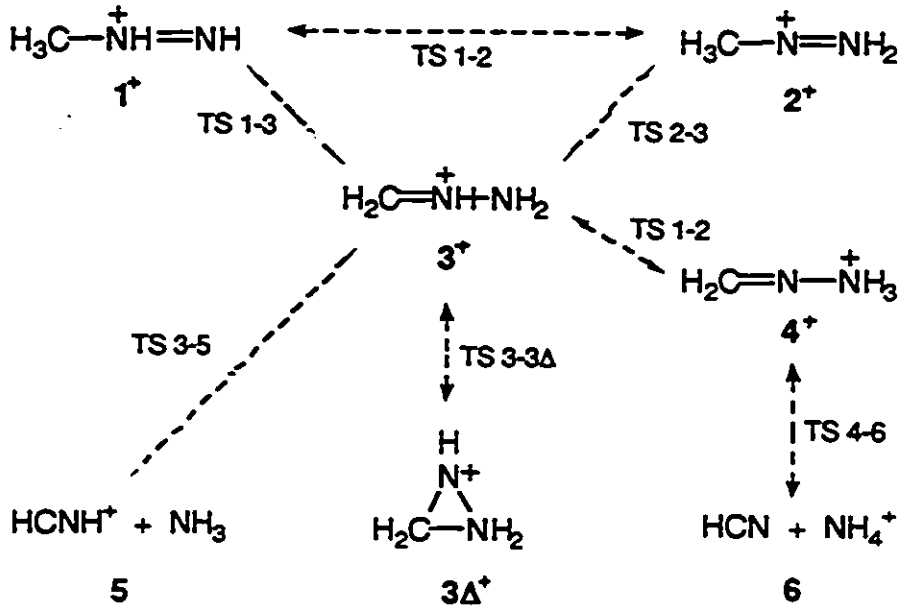

Scheme 5.2

The geometries, harmonic frequencies and zero-point vibrational energies (ZPVE) were calculated with the split-valence 6-31G** basis set. The force constant matrices for the stationary points were checked to have the correct number of negative eigenvalues. Single-point calculations of the 6-31G** geometries were performed with the 6-31G** basis set with the help of the direct CI program [6]. The SDCI results were size-consistency corrected using the formula of Pople et al. [7a], and the resulting data were corrected for the scaled (0.9) contribution of ZPVEs (RHF/6-31G**) [8]. The optimized geometries of the isomers and transition states are displayed in Figure 5.1. The calculated energies are shown in Table 5.1 and an energy diagram derived therefrom is presented in Figure 5.2.

The same computational procedure was used to obtain the proton affinities (PA's) of HN=NH, CH_3N=NH and CH_3N=NCH_3. These results are shown in Table 5.2.

Ions 1^+, 2^+ and 3^+ and the neutral radical $3^\bullet$ were also treated using the CASSCF method for optimizing geometries [9] and the Multi-Reference CI method (including the Pople-type correction for size consistency [7b]) for obtaining final energies. In these

calculations the active space consists of the highest bonding and lowest anti-bonding π MO's. For the ions, the relative energies differ by less than 1 kcal/mol from the SDCI values (see Table 5.3) indicating that in spite of the π-π^* near degeneracy effect, the electronic correlation does not affect the relative stabilities significantly.

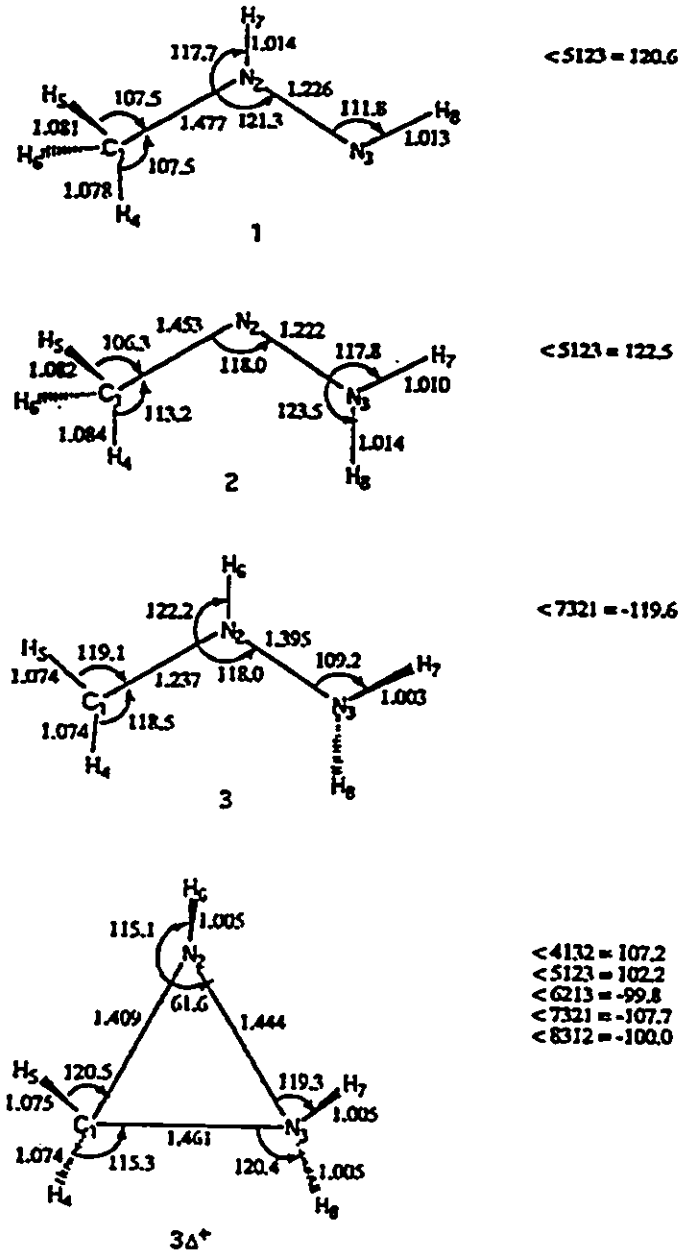

Fig. 5.1 Geometries of $CH_5N_2^+$ isomeric ions and transition states optimized at the SCF/6-31G** level of theory.

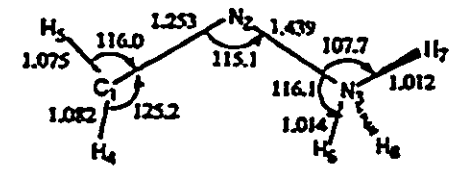

4

<7321 = -122.3

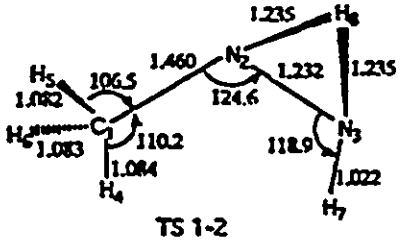

TS 1-2

<238 = 60.0
<328 = 60.1
<612 = 107.0

<4123 = 128.3
<5123 = -115.3
<6123 = 6.4
<7321 = 1.9
<8321 = -144.9

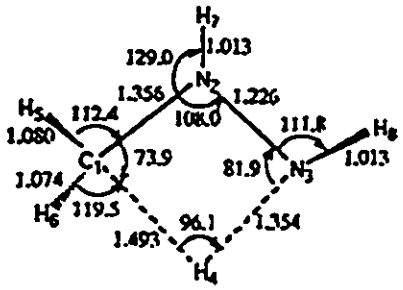

TS 1-3

<4123 = 3.0
<5123 = 71.4
<6123 = -144.1
<7213 = 177.9
<8321 = -147.1

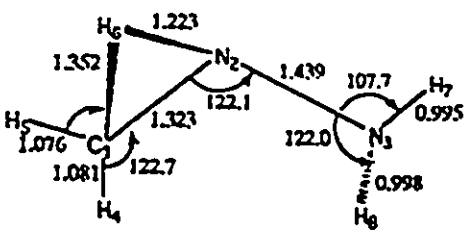

TS 2-3

<512 = 115.5
<621 = 64.0
<612 = 54.4

<4123 = -4.6
<5123 = -174.8
<6123 = 88.2
<7321 = -177.9
<8321 = 12.2

Fig. 5.1 continued

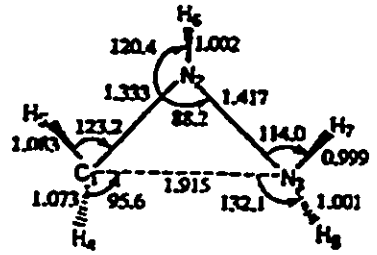

<4132 = 122.8
<5123 = 112.3
<6213 = -120.0
<7321 = -97.8
<8312 = -78.8

TS 3-3 Δ

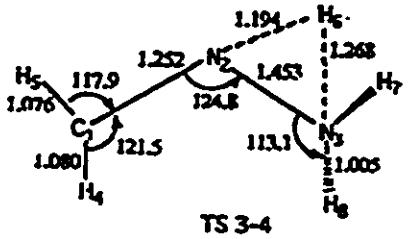

<236 = 51.5
<326 = 56.2
<6321 = 180
<7321 = -67.5

TS 3-4

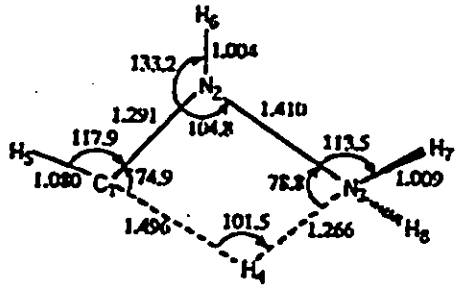

<4123 = 0
<7321 = -110.1

TS 3-5

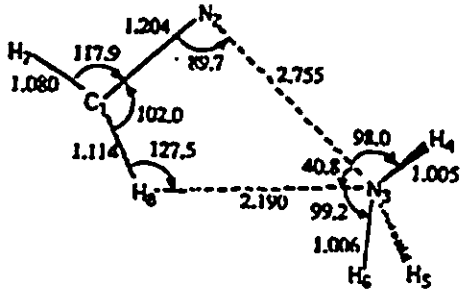

<438 = 119.2
<4381 = 66.2

TS 4-6

Fig. 5.1 continued

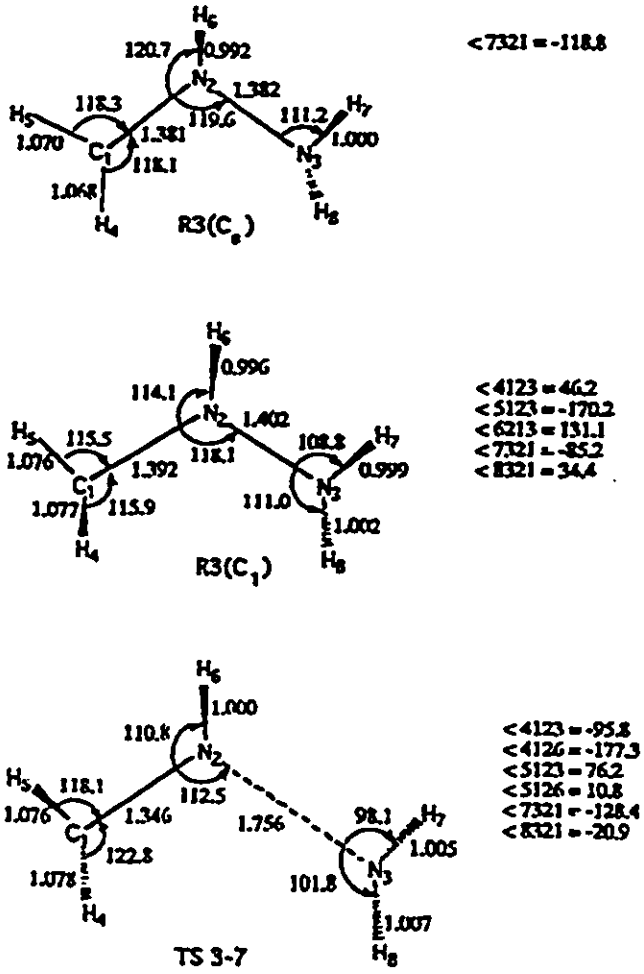

Fig. 5.1 continued

Table 5.1. Calculated total energies (hartrees), ZPVEs and relative energies [a] (E_{rel}, kcal/mol) for the isomers, transition structures (TS) and dissociation products of the $CH_5N_2^+$ system.

	Point Group	RHF/6-31G** //6-31G**	SDCI + Pople	ZPVE [b]	E_{rel} [c]		
					I	II	III
Ions							
1	C_s	-149.37385	-149.87849	43.0	8.8	7.4	- 6.9
2	C_s	-149.37739	-149.87944	42.7	7.9	6.7	-11.5
3	C_s	-149.39612	-149.89341	43.5	0.0	0.0	0.0
3Δ	C_1	-149.36392	-149.86788	44.5	16.7	15.0	
4	C_s	-149.38556	-149.89003	43.7	2.4	0.8	
TS							
TS 1-2	C_s	-149.24901	-149.76582	38.0	74.6	70.5	
TS 1-3	C_1	-149.21935	-149.75582	39.5	82.4	81.0	
TS 2-3	C_1	-149.30082	-149.80688	39.5	50.2	49.0	
TS 3-4	C_s	-149.28501	-149.79855	39.1	55.0	53.3	
TS 3-3Δ	C_1	-149.32046	-149.81989	42.3	44.9	43.3	
Dissociation TS							
TS 3-5	C_s	-149.28961	-149.79725	40.6	57.3	56.2	
TS 4-6	C_s	-149.29048	-149.78321	36.7	62.4	63.3	
Dissociation products							
NH_3	C_{3v}	-56.19554	-56.39858	20.7			
$HCNH^+$	$C_{\infty v}$	-93.16530	-93.46019	17.1			
Total		-149.36094	-149.85877	37.8	16.0	17.2	+20.1
NH_4^+	T_d	-56.45888	-56.75091	29.9			
HCN	$C_{\infty v}$	-92.73193	-93.17340	10.1			
Total		-149.19081	-149.92431	40.0	-22.9	-20.6	-11.9

a) The SDCI/6-31G**//6-31G** relative energies given in column I are calculated from the Pople/CI values, with ion 3^+ taken as zero. All values are corrected with the ZPVE.

b) The zero-point vibrational energies include scaling by a factor of 0.9.

c) The E_{rel} values in column II are obtained from SDCI/6-31G**//4-31G calculations, the values in column III are based upon the experimental values reported in ref. 1

For the radical $^{\bullet}CH_2$-NH-NH_2, **3**$^{\bullet}$, the relative energies of three different geometries were obtained. Considering that neutralization is a vertical process, we first calculated the relative energy of neutral **3**$^{\bullet}$ in the (optimized) geometry of the ion. However, the resulting structure is not at a stationary point on the potential energy surface (PES), hence the ZPVE cannot reliably be obtained. We therefore optimized the geometry of the radical within C_S symmetry and performed a ZPVE calculation for the resulting $^2A''$ structure. Finally, the symmetry constraints on the internal coordinates were relaxed and a full geometry optimization of the radical was performed. For these CASSCF calculations three active space MO's were used. As indicated by the unrestricted Hartree-Fock (UHF) $\langle s^2 \rangle$ values in Table 5.4, the transition state for the dissociation **3**$^{\bullet}$ → CH_2=NH + $NH_2^{\bullet}$ is indeed sensitive to electronic correlation effects, in contrast to the situation with the ions.

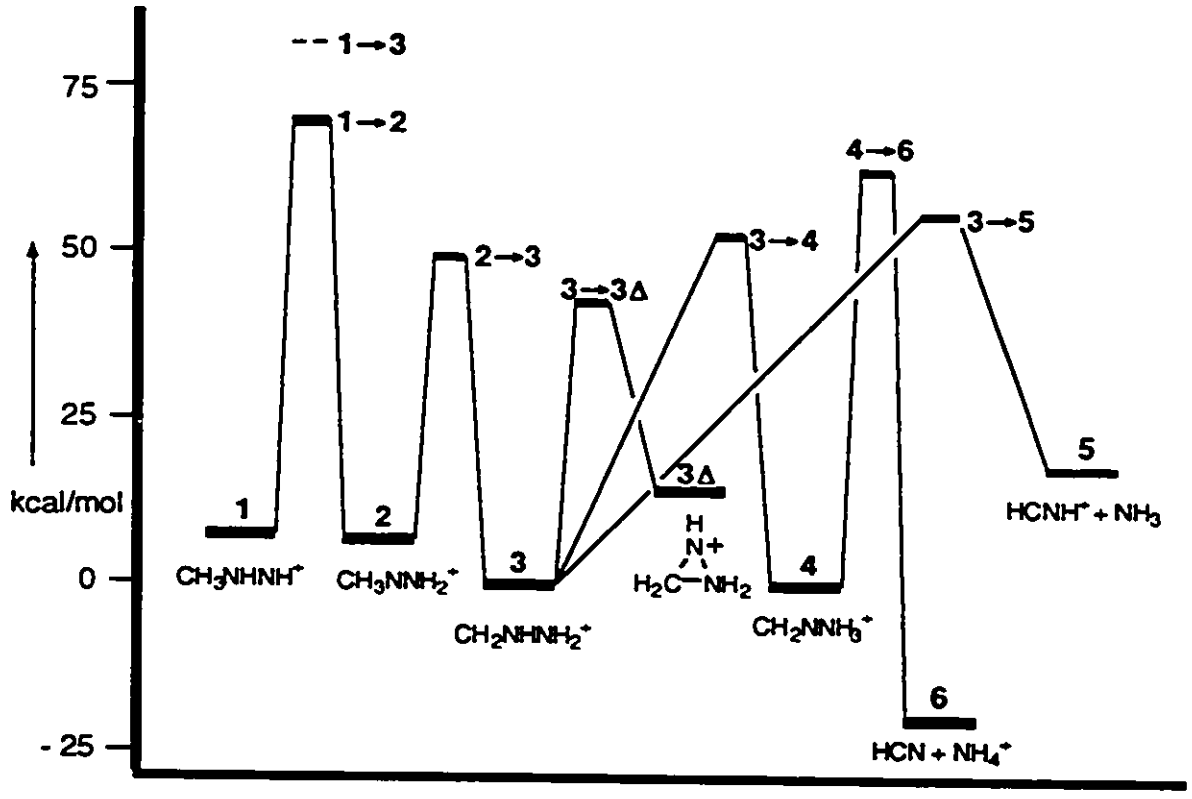

Fig 5.2 Calculated energy diagram for the $CH_5N_2^+$ ions

Table 5.2. Proton Affinities (PA, kcal/mol) for HN=NH, CH_3N=NH and CH_3N=NCH_3 calculated from (SDCI + Pople)/6-31G**//6-31G** energies [a]

Mol/Ion	Point Group	RHF/6-31G** //6-31G**	SDCI + Pople [b]	ZPVE [c]	PA (Mol)
HN=NH	C_{2h}	-109.99037	-110.34743	17.4	
$HN=NH_2^+$	C_S	-110.31744	-110.66647	26.0	192 [d]
CH_3N=NH	C_S	-149.04059	-149.54489	34.7	
$CH_3NH=NH^+$	C_S	-149.37385	-149.87849	43.0	201
$CH_3N=NH_2^+$	C_S	-149.37739	-149.87944	42.7	202
$CH_3N=NCH_3$	C_{2h}	-188.07845	-188.73788	51.3	
$CH_3NH=NCH_3^+$	C_S	-188.42919	-189.08719	59.5	211

a) The PA values were calculated from the relationship PA(Mol) = E(Mol) + E(H^+) - E(Ion) using the (SDCI + Pople) Energies corrected for the ZPVE.
b) SDCI calculations corrected using the size-consistency formula of Pople et al. [7a]
c) The zero-point vibrational energies include scaling by a factor of 0.9.
b) Using the CASSCF - Multireference CI procedure PA (HN=NH) becomes 187 kcal/mol.

Table 5.3. Calculated total energies (hartrees), ZPVEs and relative energies (E_{rel}, kcal/mol) for the $CH_5N_2^+$ isomers 1^+- 3^+ and TS 2-3 using the CASSCF – Multi-Reference CI method [a]

Ion	Group	CASSCF	MCCI + Pople	ZPVE [b]	E_{rel}
1	C_S	-149.41220	-149.88809	43.0	7.4
2	C_S	-149.41017	-149.88796	42.7	7.2
3	C_S	-149.42318	-149.90043	43.5	0.0
TS 2-3	C_1	-149.31949	-149.81417	39.5	50.2

a) see Theoretical Methods for further details.

b) The ZPVE values are corrected with a factor of 0.9.

Results and Discussion

The stabilities of ions 1+, 2+ and 3+: discord between theory and experiment?

We have located four equilibrium structures with a CNN backbone, viz. CH_3-NH=NH$^+$, **1**$^+$, CH_3-N=NH_2^+, **2**$^+$, CH_2-NH=NH_2^+, **3**$^+$ and CH_2=N-NH_3^+, **4**$^+$ (see Table 5.1). Our calculations show that another related $CH_5N_2^+$ isomer exists, *viz.* the ring-closed valence isomer of **3**$^+$, **3Δ**$^+$, which lies only 16.7 kcal/mol above **3**$^+$; the possible formation of **3Δ**$^+$ by an appropriate dissociative ionization will be discussed later.

The bridged species CH_2N^{+}H-NH$^+$ is not a minimum on the PES but a transition state lying 55.0 kcal/mol above **3**$^+$ and so our earlier proposal [1] that **3**$^+$ and **4**$^+$ rapidly transform to this species needs to be revised. Our theoretical calculation that the bridged species is not stable parallels earlier observations on the structure of azonium cations R_1-N=N(H)-R_2^+ [15]. Thus, according to theory and in contrast to our previous proposal [1] ions **3**$^+$ *do not spontaneously* rearrange to **4**$^+$. These matters will be discussed later; first we address a serious discrepancy between experiment and theory concerning the relative stabilities of ions **1**$^+$, **2**$^+$ and **3**$^+$. According to theory, ions **1**$^+$ and **2**$^+$ lie substantially above ions **3**$^+$ but according to experiment (AE measurements) they lie substantially beneath **3**$^+$. The discrepancy between theory and experiment for the set of ions **1**$^+$, **2**$^+$ and **3**$^+$ is unacceptably large, for example 19.4 kcal/mol for ions **2**$^+$ and **3**$^+$. Now the experimental evidence leaves no doubt that ions **1**$^+$, **2**$^+$ and **3**$^+$ do have the structures indicated above, so the possibility that we are dealing with other isomeric forms in the experiments can be ruled out. Could our theoretical calculations then be the culprit, in particular the lack of electron correlation in the geometry determinations? Table 5.2 gives the calculated energies of the isomers **1**$^+$, **2**$^+$ and **3**$^+$ using electron correlation in the geometry determinations (CASSCF type calculations, see theoretical methods). It can be seen that the relative energies change only slightly and thus the discrepancy remains. In fact, at various levels of theory including SDCI/6-31G**//4-31G type calculations without polarization functions in the geometry determinations (see

Table 5.1, column II) the large discrepancy is about the same. In order to determine whether the experimental heat of formation (ΔH_f) values of 1^+, 2^+ and/or 3^+ may be incorrect we have critically examined existing AE data on hydrazines.

For discussion purposes we begin with the homologous $C_2H_7N_2^+$ system. For the AE of the $[M-H]^+$ ion generated by electron impact ionization of 1,1-dimethyl -hydrazine two values have been reported: 10.2 ±0.2 eV [16a] and 10.08 ±0.1 eV [16c]. Both are reasonably close to that, 9.9 ±0.1 eV, obtained in a photoionization study [16b]. Using ΔH_f ($(CH_3)_2NNH_2$) = 20.0 kcal/mol [17] the ΔH_f of the $C_2H_7N_2^+$ ion is then calculated to lie between 196 - 203 kcal/mol. Foner and Hudson [16c], assuming that this ion had the structure $(CH_3)_2N{=}NH^+$, $\mathbf{1a}^+$, combined its ΔH_f with the IE of the $(CH_3)_2N{=}NH^\bullet$ radical $\mathbf{1a}^\bullet$ - obtained from a high intensity crossed molecular beam experiment between $(CH_3)_2NNH_2$ and oxygen atoms - and derived ΔH_f ($\mathbf{1a}^\bullet$) = 48–55 kcal/mol. This result is in poor agreement with the value, 81 kcal/mol, obtained in ref. 16a from AE (CH_3^+) for the reaction $(CH_3)_2NNHCH_3 \rightarrow CH_3^+ + (CH_3)_2N{=}NH^\bullet$. Note that the latter ΔH_f ($\mathbf{1a}^\bullet$) value in combination with its IE (6.4 ±0.2 eV), would yield ΔH_f ($\mathbf{1a}^+$) = 228 kcal/mol.

On the other hand, we previously established [1] that the product ion generated in the reaction $CH_3NHNHCH_3 \rightarrow CH_5N_2^+ + CH_3^\bullet + e^-$ has the structure $CH_3{-}NH{=}NH^+$, i.e. $\mathbf{1}^+$, and based on an (monoenergetic) electron impact AE value of ≤ 8.69 eV, we proposed that its ΔH_f would be ≤ 188 kcal/mol. This would imply that the ΔH_f of $\mathbf{1}^+$, is *lower* than that of its methyl substituted homologue $\mathbf{1a}^+$, which does not seem possible. We observed that metastable $(CH_3)_2NNH_2^{\bullet+}$ ions undergo two dissociations namely loss of $CH_3^\bullet$ (to generate $CH_5N_2^+$) and loss of $H^\bullet$. Furthermore, the labelled ion $(CH_3)_2NND_2^{\bullet+}$ only lost $H^\bullet$ to the exclusion of $D^\bullet$ loss. These simple cleavage reactions all take place close to threshold and thus $H^\bullet$ loss from the unlabelled ion yields $CH_2{=}N(CH_3){-}NH_2^+$, $\mathbf{3a}^+$, not $\mathbf{1a}^+$. This implies that ΔH_f ($\mathbf{1a}^+$) is greater than ΔH_f ($\mathbf{3a}^+$),196 - 203 kcal/mol (see above), and that the ΔH_f of the mono-methyl-substituted ion $\mathbf{1}^+$ may reasonably be expected to be even larger.

The above conclusion that the previously reported ΔH_f (1^+) value must be too low is reinforced by the finding that the experimentally determined proton affinity (PA) of $CH_3N{=}NCH_3$ (206.9 kcal/mol [16e]), yields 194 kcal/mol as the ΔH_f value of the symmetrically methyl substituted analogue of 1^+, $CH_3NH{=}NCH_3^+$, $\mathbf{1b}^+$.

A further inconsistency concerns the ΔH_f value of the m/z 45 $CH_5N_2^+$ ion generated by the reaction $(CH_3)_2NNH_2^{\bullet+} \rightarrow CH_3\text{-}N{=}NH_2^+$ (2^+) + $CH_3^\bullet$. The structure of the daughter ion was established in our previous study and its ΔH_f value was calculated as 183.5 kcal/mol from an AE value of 8.60 eV obtained from a measurement using monochromatic electrons. This AE value is close to that (8.7 ± 0.2 eV) obtained in the photoionization study of ref. 16b but it differs greatly from the one reported in the electron ionization study of ref. 16a: AE = 9.7 ± 0.2 eV yielding ΔH_f (2^+) = 209 kcal/mol (using $\Delta H_f(CH_3^\bullet)$ = 35 kcal/mol [16a] and $\Delta H_f((CH_3)_2NNH_2)$ = 20 kcal/mol [17]). Although ΔH_f values derived from AE measurements using a conventional electron impact source are often higher than the more accurate and precise values derived from photoionization or electron impact methods using monochromatic electrons, this discrepancy is nevertheless anomalously large.

In order to resolve the discrepancy between these experimental values, and to verify the prediction from the ab initio calculations that the $CH_5N_2^+$ isomer 3^+ is more stable than its isomers 1^+ and 2^+, we examined the structure of the $CH_5N_2^+$ ion generated by loss of $H^\bullet$ from ionized methylhydrazine, $CH_3NHNH_2^{\bullet+}$. Loss of $H^\bullet$ therefrom could *a priori* lead to 1^+, 2^+ or 3^+. The AE for this reaction has been measured and the two electron impact derived AE values - 10.2 ± 0.1 eV [16a], 10.18 ± 0.1 eV [16b] - are reasonably close to that obtained by photoionization; 9.8 ± 0.2 eV, [16c]. The derived ΔH_f values (using $\Delta H_f(CH_3NHNH_2)$ = 22.6 kcal/mol [17]) lie in the range 197 - 206 kcal/mol and this value has been proposed to correspond with ions of structure $CH_3\text{-}NH{=}NH^+$, 1^+.

Our experiments show that the MI mass spectrum of $CH_3NHNH_2^{\bullet+}$ is dominated by a

gaussian shaped peak ($T_{0.5}$ = 75 meV) at m/z 45. The (2FFR) CA mass spectrum of this $CH_5N_2^+$ product ion is shown in Fig. 5.3a.

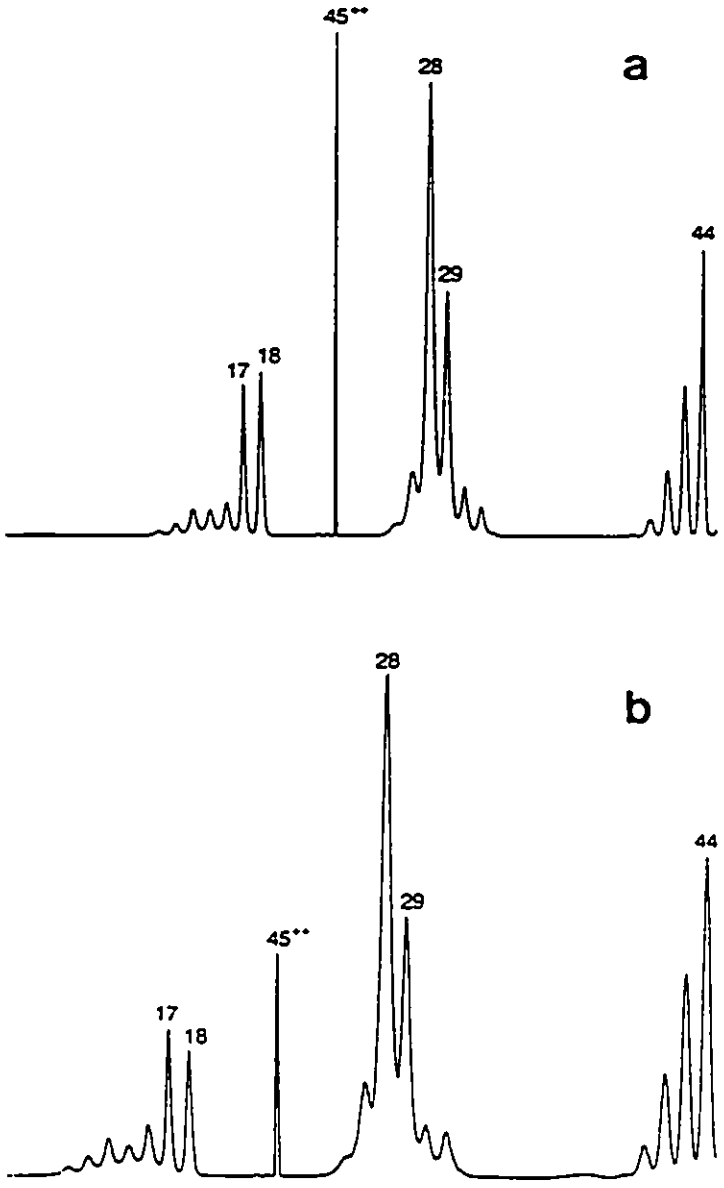

Fig. 5.3 (a) CA mass spectrum of $CH_5N_2^+$ ions generated in the ion source from $CH_3NHNH_2^{\bullet+}$ ions, (b) CA mass spectrum of $CH_5N_2^+$ ions generated from metastable $CH_3NHNH_2^{\bullet+}$ ions. The lower intensity level of the charge stripping peak at m/z 22.5 in Figure b is due to the lower resolving power of the second electric sector compared to the first.

Comparison of this spectrum with those of the reference ions 1^+, 2^+, and 3^+ previously reported [1] leaves no doubt that we are dealing with ions of structure 3^+. In addition, the 3FFR CA mass spectrum of the $CH_5N_2^+$ ions generated from metastable $CH_3NHNH_2^{\bullet+}$ ions dissociating in the 2FFR of our three sector instrument was also obtained, see Fig. 5.3b. It again is only compatible with the formation of ions of structure 3^+. Thus the $H^\bullet$ loss from $CH_3NHNH_2^{\bullet+}$ involves *solely* the *methylic* hydrogen atoms and this observation provides evidence that among ions 1^+, 2^+, and 3^+, the isomer CH_2=NH-NH_2^+, 3^+, is *the ion of lowest energy*, in agreement with the theoretical predictions.

Of course this argumentation is only valid if cleavage of the N-H bond(s) is not associated with a large reverse energy term. Thus ions 1^+ and 2^+ could lie below 3^+ but only if a large barrier - on top of the thermochemical energy requirement - prevents their formation from $CH_3NHNH_2^{\bullet+}$. Previous work [18] has shown that cleavage of an X-R bond, where X is a heteroatom attached to a carbenium center and R is H or CH_3, is invariably associated with a significant reverse term leading to large kinetic energy releases (KERs). However, the above mentioned loss of $CH_3^\bullet$ from $(CH_3)_2NNH_2^{\bullet+}$ is associated with a small KER ($T_{0.5}$ = 9 meV) and hence cleavage of the C-N bond in $(CH_3)_2NNH_2^{\bullet+}$ does not seem to have a significant reverse activation energy. This provides evidence that the fissions of the N-H bonds in $CH_3NHNH_2^{\bullet+}$ are not associated with significant reverse terms. Further support for this conclusion comes from an ab initio calculation of the barrier for the recombination reaction $H^\bullet$ + H-N=NH_2^+ → H_2N-$NH_2^{\bullet+}$; at the SDCI/6-31G**//6-31G** level of theory a barrier of only 2.7 kcal/mol is obtained.

Our measurements therefore show that the ΔH_f values of 197 - 206 kcal/mol obtained from AE measurements on CH_3NHNH_2 are really those for ion 3^+. In our previous study [1] the AE of metastable ions 3^+ generated in the reaction $HOCH_2CH_2NHNH_2^{\bullet+}$ → 3^+ + $^\bullet CH_2OH$ was measured using the method of Burgers and Holmes [14] and this yielded ΔH_f (3^+) = 195 kcal/mol. We have repeated this

measurement on the KRATOS MS 902 mass spectrometer for which this method was developed. A somewhat higher AE was obtained, 9.5 ± 0.2 eV , and from this new value ΔH_f (3^+) becomes 204 ± 5 kcal/mol. Using ΔH_f (3^+) = 204 kcal/mol, the energy differences between 3^+ and its dissociation products NH_4^+ + HCN and NH_3 + $HCNH^+$ are calculated from thermochemical data [16e] to be −21 and +11 kcal/mol respectively.These values compare well with the energy differences derived from the ab initio calculations, −22.9 and +16.0 kcal/mol respectively. We conclude that the measured ΔH_f (3^+) = 204 ±5 kcal/mol, although not precise, is reliable and also that tne AE values for the loss of $CH_3^\bullet$ from the dimethylhydrazines previously reported [1,16b] are in error.

A likely source of error is the following: hydrazines in the presence of moisture and air have been reported to undergo various catalytic decomposition reactions on glass inlet lines thereby producing, among other products, trace quantities of amines [19]. Thus, for example, $(CH_3)_2NNH_2$ may decompose to $(CH_3)_2NH$ which is isobaric with CH_5N_2. Now the IE of $(CH_3)_2NH$ is 8.23 eV [16e], much lower than the $CH_5N_2^+$ ion's AE of 9.8 eV calculated for the reaction $(CH_3)_2NNH_2 \rightarrow CH_3\text{-}N{=}NH_2^+$ (2^+) + $CH_3^\bullet$, using ΔH_f (2^+) = ΔH_f (3^+) + 7.2 = 211 kcal/mol (see Table 5.3), ΔH_f ($(CH_3)_2NNH_2$) = 20.0 ± 0.5 kcal/mol [17] and ΔH_f ($CH_3^\bullet$) =35 kcal/mol [16e]. Therefore, a trace of dimethylamine is sufficient to lead to erroneously low values in the AE experiments.

Interferences from amines may also be responsible for discrepancies in the heat of formation of the $N_2H_3^+$ ion. We previously proposed [1] ΔH_f ($N_2H_3^+$) = 214 kcal/mol based on AE = 9.82 eV for $N_2H_3^+$ ions generated by the loss of $CH_3^\bullet$ from $CH_3NHNH_2^{\bullet+}$. The linear extrapolation value quoted in the photoionization study of ref.16b is 10.4 ±0.1 eV whereas the onset value is much lower: 9.5 ±0.1 eV. The long low energy tail in this experiment is probably due to interference from methylamine and the ΔH_f ($N_2H_3^+$) value, 228 kcal/mol, based on the linear extrapolation AE value, is probably the more reliable one. This is because the photoionization AE for loss of $H^\bullet$ from H_2NNH_2, where such an

"amine" interference does not occur, yields ΔH_f ($N_2H_3^+$) = 226 kcal/mol [16b].

We assess ΔH_f ($N_2H_3^+$) therefore at 227 kcal/mol and make use of this value in an evaluation of ΔH_f (1^+) and ΔH_f (2^+) based on the PA's calculated by ab initio methods for the following reactions:

(E)-N_2H_2	+ H^+	→	$N_2H_3^+$	+ PA	[a]
(E)-CH_3N=NH	+ H^+	→	CH_3-NH=NH^+ (1^+)	+ PA	[b]
(E)-CH_3N=NH	+ H^+	→	CH_3-N=NH_2^+ (2^+)	+ PA	[c]
(E)-CH_3N=NCH_3	+ H^+	→	CH_3-NH=N-CH_3^+	+ PA	[d]

Calculations were performed at the SDCI/6-31G**//6-31G** level of theory as for the ions in in Table 5.1. We obtained the following PA's (see Table 5.2): reaction [a], 192 kcal/mol; reaction [b], 202 kcal/mol; reaction [c], 201 kcal/mol; reaction [d], 211 kcal/mol (the difference in PA's of reactions [b] and [c] correspond of course to the energy differences in 1^+ and 2^+ in Table 5.1). Combining the PA's for reactions [a] and [d] with the experimentally available ΔH_f values for the neutral species (ΔH_f (N_2H_2) = 51 kcal/mol and ΔH_f (CH_3-N=N-CH_3) = 36 kcal/mol [16e]) yields ΔH_f ($N_2H_3^+$) = 225 kcal/mol and ΔH_f (CH_3-NH=N-CH_3^+) = 192 kcal/mol, in excellent agreement with the experimentally derived values of 227 and 194 kcal/mol for $N_2H_3^+$ and CH_3-NH=N-CH_3^+ [16e]. The consistency of experiment and theory for reactions [a] and [d] lends strong credence to the use of reactions [b] and [c] for the calculation of ΔH_f (1^+) and ΔH_f (2^+). We find ΔH_f (1^+) = 209 kcal/mol, and consequently ΔH_f (2^+) = 208 kcal/mol, see Table 5.1, using the *estimated* value ΔH_f (CH_3-N=N-CH_3) = 45 ±2 kcal/mol quoted in ref. 16e. This number is again consistent with that derived from experiment and the high level computational results in Table 5.3, i.e. ΔH_f (1^+) = ΔH_f (3^+) +7 = 211 kcal/mol.

In conclusion, we have provided evidence that the reported AE values for loss of $CH_3^\bullet$ from 1,1- and 1,2-dimethylhydrazine and from methylhydrazine are not reliable because of interferences from traces of amines. This raises the possibility that, for this reason, other AE values for hydrazines [16d] might also be in error. From AE

measurements not affected by these interferences, ΔH_f (3^+) is proposed to be 204 ±5 kcal/mol from which theory leads us to recommend ΔH_f values of 211 ±5 kcal/mol for 1^+ and 2^+.

Finally, we note that these large discrepancies were uncovered by high level ab initio calculations and thus it is indeed "a good rule not to put overmuch confidence in the observational results that are put forward until they are confirmed by theory" [20]

The Unimolecular Chemistry of the 1,2-diazaprop-3-yl radicals 3•

In our previous study [1] we had concluded that ions 3^+ rearrange spontaneously to 4^+. This proposal was based on two observations: (i) Ions of putative structure 3^+ abundantly form $NH_3^{\bullet+}$ after activation, and (ii) Ions of putative structure 3^+ do not survive neutralization, a finding compatible with the unstable hypervalent species CH_2=N-$NH_3^{\bullet}$ and not with $^{\bullet}CH_2$-NH-NH_2. However, our calculations clearly show, see Fig. 5.2, that the barrier $3^+ \rightarrow 4^+$ is very large, ruling out spontaneous rearrangement.

Do we have experimental evidence that 3^+ cannot spontaneously rearrange to 4^+? The most intense peak in the CA mass spectrum of 3^+ is that for the doubly charged species. This ion spontaneously dissociates to $HCNH^+ + NH_3^{\bullet+}$ and to a lesser extent to $CH_2^{+\bullet} + N_2H_3^+$ [1]. If ion 3^+ could spontaneously rearrange to 4^+ prior to oxidation, the deuterium labelled isotopomer CH_2=ND-ND_2^+, $3(N\text{-}d_3)^+$, ought to form CH_2=N-ND_3^+, $4(N\text{-}d_3)^+$, and the latter, after oxidation should yield $HCNH^+ + ND_3^{\bullet+}$; by contrast, ions $3(N\text{-}d_3)^+$ should give $HCND^+ + ND_2H^{\bullet+}$. It was observed that the $(N\text{-}d_3)$-labelled doubly charged ions predominantly generated $HCND^+ + ND_2H^{\bullet+}$ indicating that 3^+ does not spontaneously rearrange to 4^+. That ions 3^+ form $NH_3^{\bullet+}$ after activation, point (i) above, is now interpreted in terms of a post-collisional isomerization.

That ions 3^+ hardly survive neutralization, point (ii) above, could indicate that the geometries of the cation and radical are very different so that after reduction a vibrationally excited neutral is formed which then dissociates.The [Xe,O_2] NR mass

spectrum of CH_2=ND-ND_2^+, 3(N-d_3)$^+$, remeasured on the ZAB-R instrument is shown in Figure 5.4a (the labelled ions were investigated to eliminate interference of $C_2H_5O^+$ and $(CH_3)_2NH^{\cdot+}$).

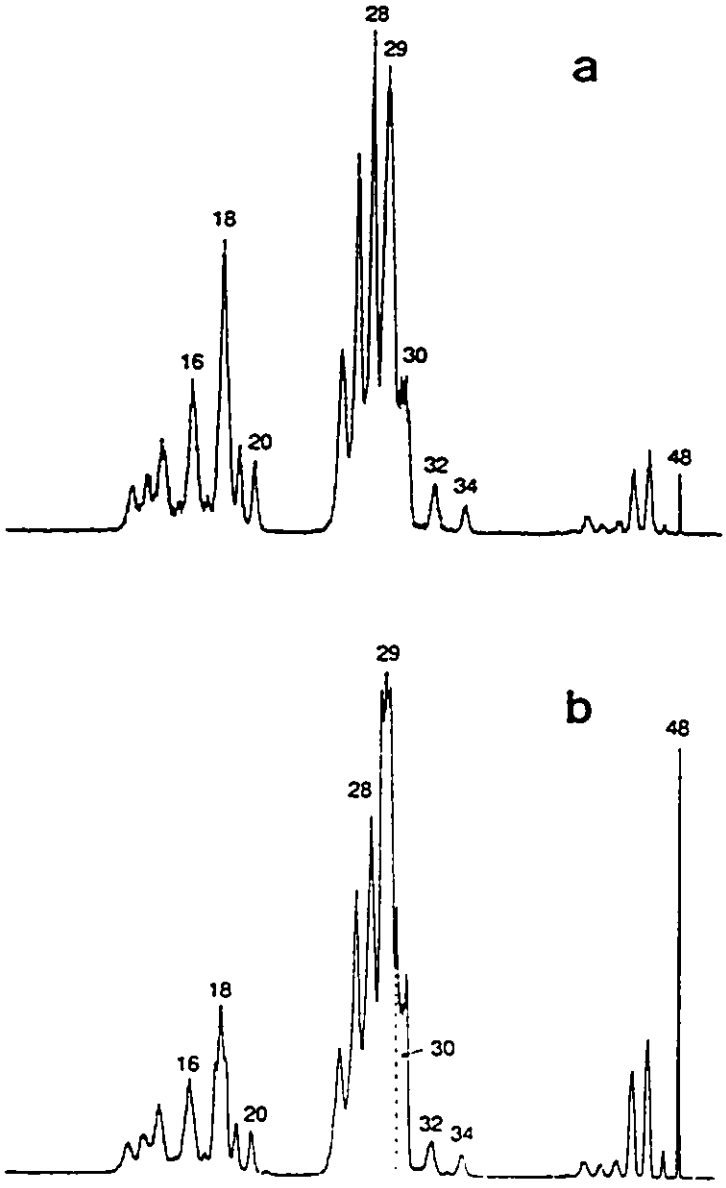

Fig. 5.4 (a) NR mass spectrum of CH_2=ND-ND_2^+. Neutralization agent Xe and oxidation agent O_2. (b) as (a), but neutralization agent N,N-dimethylaniline, see text. (c) CA mass spectrum of CH_2=ND-ND_2^+, collision gas O_2. (d) CA-NR spectrum of CH_2=ND-ND_2^+; triple collision experiment (see text). Neutralization agent N,N-dimethylaniline, oxidation agent O_2 and collision gas O_2.

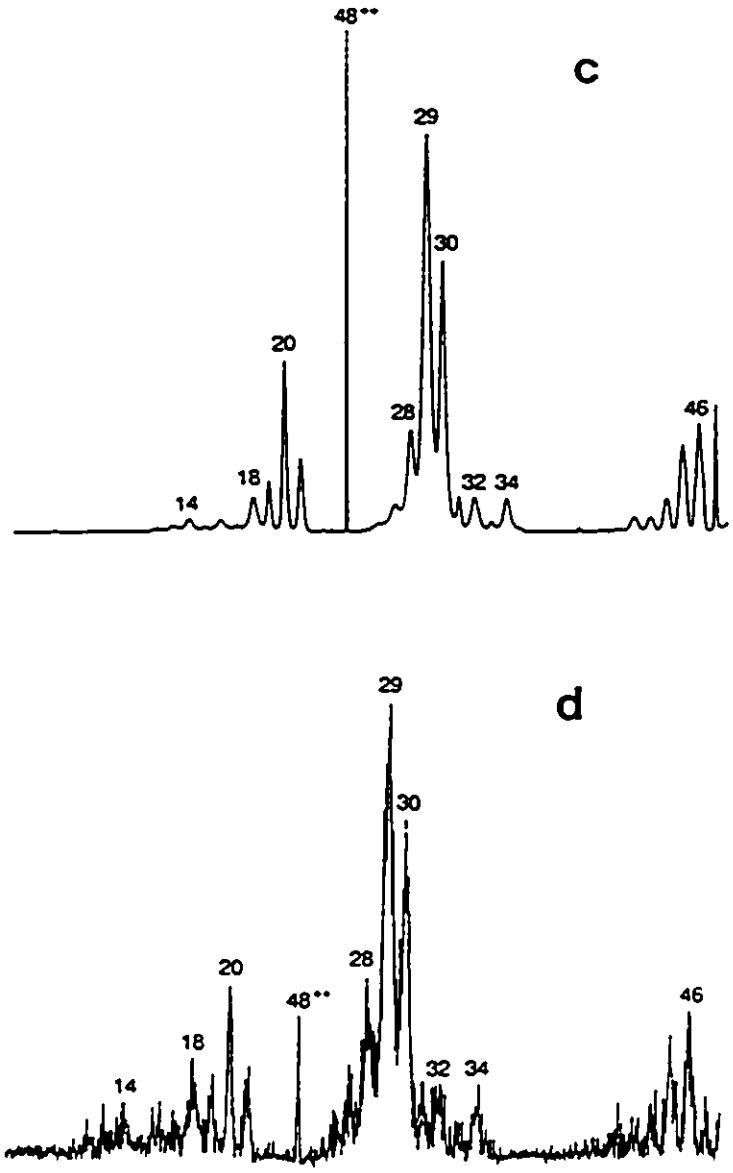

Fig. 5.4 continued

As can be seen, the survivor signal at m/z 48 is very weak, in agreement with previous results [1]. Neutralization with N,N-dimethylaniline (DMA) [12] gives a more intense spectrum (Fig. 5.4b) and also the intensity of the survivor signal is now greatly enhanced (see below). This NR mass spectrum shows three broad signals which are associated with large KER's *viz.* m/z 30, CH_2=N-D$^{\bullet+}$, m/z 29, HCND$^+$ and m/z 18, ND_2^+. This we take as showing that excited $^{\bullet}CH_2$-ND-ND_2 radicals **3**$^{\bullet}$ are formed which dissociate to CH_2=N-D and to $ND_2^{\bullet}$ with a large KER. The molecule CH_2=N-D can then dissociate further to HCND$^{\bullet}$ + H$^{\bullet}$ and since CH_2=N-D is formed with a large KER, the products derived therefrom will display broad peaks in the NR mass spectrum (see Figure 5.4b). Thus, in agreement with our earlier results a significant fraction of the radicals dissociate. The structure of the stable radicals was probed in a triple collision (NR/CA) experiment: neutralization and reionization took place in the 2FFR, the survivor ions were selectively transmitted through the first electric sector (E_1) and were collisionally dissociated in the 3FFR with the products being analysed by scanning the second electric sector (E_2). The resulting NR/CA mass spectrum (Figure 5.4d) is almost superimposable with the conventional CA mass spectrum (Figure 5.4c).

To test our proposal that a significant fraction of radicals **3**$^{\bullet}$ are formed in a vibrationally excited state, we have performed ab initio calculations on the radical $^{\bullet}CH_2$-NH-NH_2 its dissociation products CH_2=NH + $NH_2^{\bullet}$ and the corresponding transition state as described under theoretical methods. The results are presented in Table 5.4. It can be seen that the ground state (C_1 symmetry) of **3**$^{\bullet}$ lies above CH_2=NH + $NH_2^{\bullet}$ but there exists a significant barrier for this bond cleavage, so that **3**$^{\bullet}$ is kinetically stable. However, when the radical is formed by vertical neutralization, it posesses the geometry of the ion (C_S symmetry) and enters the PES, as depicted in Figure 5.5, *above* the transition state for dissociation and it will rapidly dissociate. Note in particular that the KER associated with this dissociation (ca. 20.8 kcal/mol, from the half height width of the broad component of the m/z 18 peak) is very close (see Figure 5.5) to the calculated

E_{rel} value for neutral 3• having the geometry of the ion (see Table 5.4). That more non-dissociating $^{\bullet}CH_2$-NH-NH_2 radicals are formed by neutralization with DMA than with xenon may indicate that with DMA neutralization is closer to resonance (IE (DMA) = 7.37 eV [16e], IE (Xe) =12.2 eV [16e] and IE (3•) ≈ 5.3 eV, from the data in Tables 5.3 and 5.4) and/or that neutralization with a large organic molecule need not strictly lead to a vertical transition.

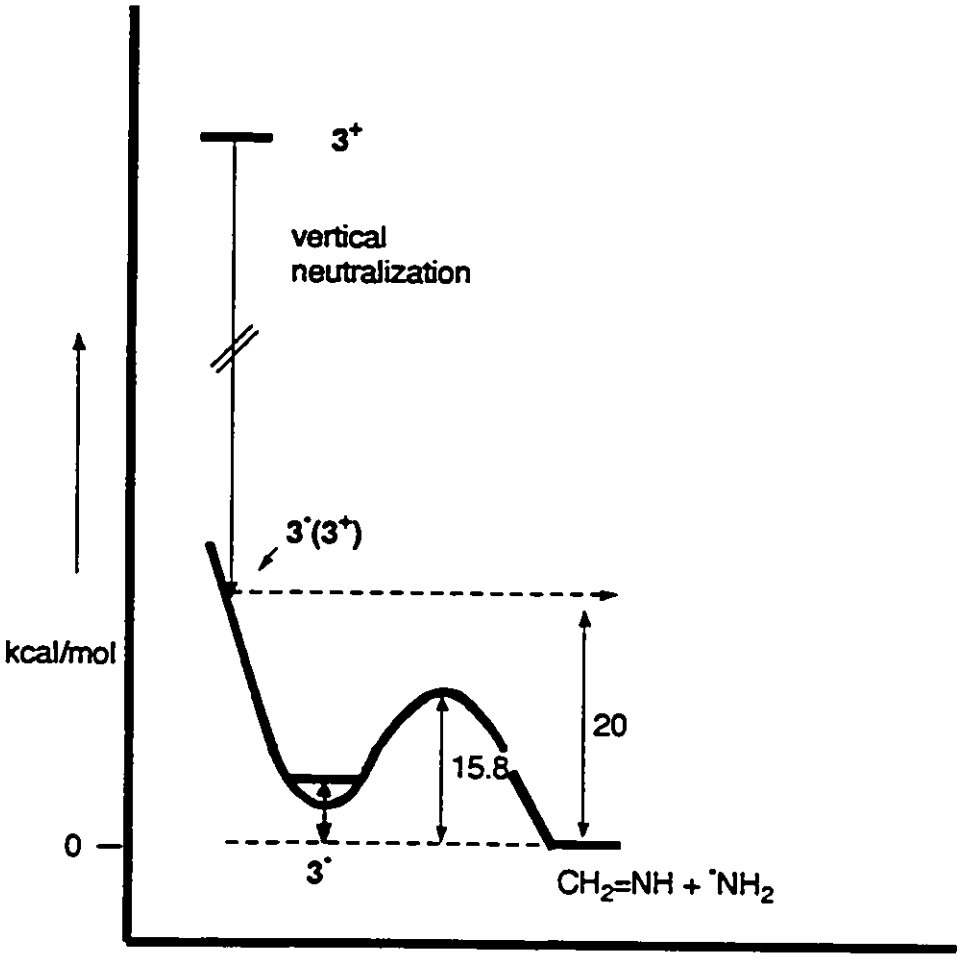

Fig. 5.5 Calculated energy diagram for the generation and dissociation of $^{\bullet}CH_2$-NH-NH_2, 3•, in a Neutralization-Reionization experiment.

Table 5.4. Calculated total energies (hartrees), ZPVEs and relative energies (E_{rel}, kcal/mol) for the $CH_5N_2^{\bullet}$ radical **3**$^{\bullet}$ and its dissociation products CH_2=NH + $^{\bullet}NH_2$ using the CASSCF – Multi-Reference CI method [a]

Structure	Group	UHF (<s^2>)	CASSCF	MCCI+Pople	ZPVE[b]	E_{rel}
R3/3$^+$ [c]	C_S	-149.57043 (.76)	-149.57259	-150.07245	40.1	20.5
R3/C_S	C_S	-149.58362 (.76)			39.5	20.1
R3/C_1	C_1	-149.59122 (.76)	-149.60524	-150.09477	41.2	7.6
TS 3-7 [d]	C_1	-149.56415 (.96)	-149.58758	-150.07772	38.7	15.8
CH_2NH		-94.03569 (.0)	-94.06833	-94.36897	24.3	
NH_2		-55.56482 (.76)	-55.56063	-55.72924	11.5	
Total		-149.60051 (.76)	-149.62896	-150.09821	35.8	0

a) see Theoretical Methods for further details.
b) The ZPVE values are corrected with a factor of 0.9.
c) R3/3$^+$ is the $^{\bullet}CH_2NHNH_2$ radical **3**$^{\bullet}$ with the geometry of ion **3**$^+$, for R3/C_S the geometry of the radical was optimized within C_S symmetry, for R3/C_1 the geometry of **3**$^{\bullet}$ was allowed to relax to C_1 symmetry.
d) TS 3-7 is the transition state for the dissociation **3**$^{\bullet}$ → CH_2=NH + $^{\bullet}NH_2$.

The unimolecular chemistry of the diazapropylium ions 3$^+$

It can be seen from Table 5.1 that the least energy demanding isomerization reactions of the diazapropylium ions are 1,2-hydrogen shifts, not 1,3-hydrogen shifts. This is the opposite of what has been found from ab initio calculations [21] for unbranched primary alkylamine radical cations. That for **3**$^+$ a 1,3-hydrogen shift is less facile than a 1,2-hydrogen shift is, we propose, the result of the rigidness of the C-N-N skeleton, the bending of which requires considerable energy. In agreement with earlier conclusions [1], the ion CH_2=NH-NH_2^+, **3**$^+$, is the reacting configuration for formation of $HCNH^+$ + NH_3, and the ion CH_2=N-NH_3^+, **4**$^+$, reacts to produce HC≡N + NH_4^+; starting from **1**$^+$, three consecutive 1,2-hydrogen shifts lead eventually to the hydrazonium ion **4**$^+$; this species then loses HC≡N via an intriguing pathway, see below :

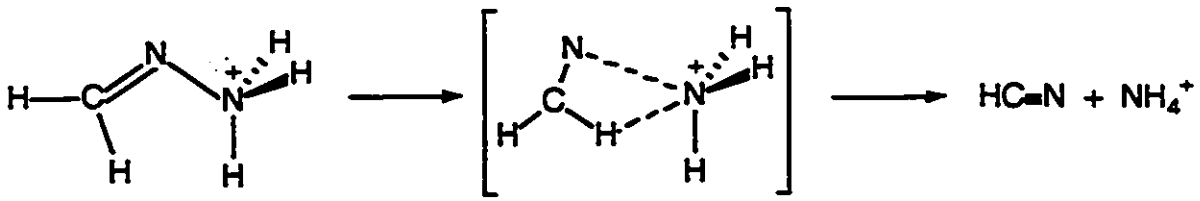

The reaction commences with stretching of the N–N bond in 4^+. In the transition state the N···N and the C···NH_3 distances are both 2.8 Å, almost the sum of the van der Waals' radii (~3 Å) and so, in the transition state, the NH_3 and CH_2=N^+ moieties just touch each other; we can thus view the transition state as an ion-dipole state. Note that CH_2=N^+ is not an equilibrium structure on the singlet surface but rather a transition state [22] towards $HCNH^+$ (the experimentally observed CH_2=N^+ species [23] most likely is in a triplet state [24]). Next, a highly exothermic (85.3 kcal/mol) proton transfer takes effect leading to the formation of HC≡N + NH_4^+. This exothermicity however is not reflected in the KER which is only 9 kcal/mol [1]; this we rationalize in terms of ion-dipole attraction in the dissociating complex $[HC{\equiv}N{\cdots}NH_4]^+$, leading to a relatively small recoil velocity of the products. At the 6-31G**/RHF level of theory the stabilization energy (SE) of $[HC{\equiv}N{\cdots}HNH_3]^+$ relative to HC≡N + NH_4^+ was computed to be 19.2 kcal/mol. The calculated dipole moment (μ) of HC≡N is 3.20 D (the experimental value is 2.98 D). The ion-dipole distance, R, was calculated to be 3.53 Å and so the electrostatic contribution to the stability of the ion-dipole complex is calculated as SE = μ/R^2 = 17.8 kcal/mol .

Starting from 1^+ the reaction sequence is: CH_3-NH=NH^+ → CH_3-N=NH_2^+ → CH_2-NH=NH_2^+ → CH_2=N-NH_3^+, i.e. 1^+ → 2^+ → 3^+ → 4^+. Previous labelling experiments gave inexplicable results: the ions CH_3-ND=ND^+, $1(N\text{-}d_2)^+$, and CH_3-N=ND_2^+, $2(N\text{-}d_2)^+$, showed atom-specific behaviour whilst extensive H/D randomization reactions were observed for CH_2=ND-ND_2^+, $3(N\text{-}d_3)^+$, i.e. losses of HCN, DCN, NH_2D, NHD_2 and ND_3. It appears however that the metastable peaks for ion 3^+ are very sensitive to the presence of residual collision gas (this can also be inferred from Figure 5.3, where the contributions from the

metastable peaks in the CA mass spectrum of Figure 5.3a are very small) and a careful analysis of the MI mass spectrum of $3(N\text{-}d_3)^+$ showed that the peaks at m/z 28 and 30 are largely of collision induced origin and that $3(N\text{-}d_3)^+$ loses specifically NHD_2 (along with HCN and DCN). According to our calculations, the transition $2^+ \rightarrow 3^+$ is the least energy demanding and we allow this transition to be an equilibrium. Then for $3(N\text{-}d_3)^+$ a 1 : 2 mixture of $CH_2{=}ND\text{-}ND_2^+$ and $CHD{=}NH\text{-}ND_2^+$ ensues and the expected ratio of NHD_2 vs ND_3 loss is 2 : 1, but an isotope effect in the final step will operate against ND_3 loss. Similarly the ratio of HCN vs DCN loss is calculated to be 2 : 1 (experimental ratio ~1 : 1 [1]) but an isotope effect in the final step operates against HCN loss. By inspection, very large isotope effects reproduce the experimental results reasonably well.

We had observed previously [1] that methylcarbazate ions $H_2NNHC(=O)OCH_3^{\bullet+}$ abundantly lose $^{\bullet}COOH$ to produce ions 3^+ and the following mechanism was proposed:

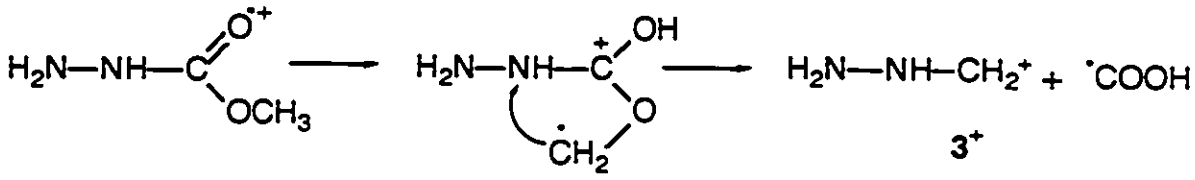

However it was subsequently observed [25] that ionized methylcarbamate does *not* lose $^{\bullet}COOH$ although this is the reaction of lowest calculated enthalpy change :

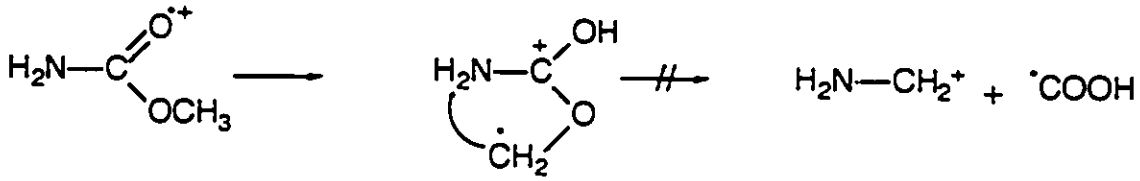

Note that the first step does take place [25]. One explanation for this marked difference is that for methylcarbazate, the intermediate cyclic immonium ion $H_2N\text{-}\underline{NH\text{-}C(OH)\text{-}OCH_2}^+$ is sufficiently stabilized by the electron donating NH_2 group that it can be formed below the dissociation limit. Our caiculations point to another possibility, namely, the daughter ions

could actually be the cyclic ion $3\Delta^+$ formed as follows:

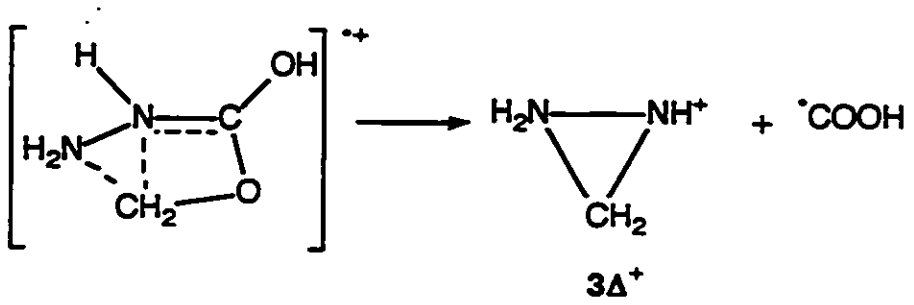

$3\Delta^+$

relieving some of the ring strain energy of the transition state. The CA mass spectrum of the $CH_5N_2^+$ daughter ions formed from $H_2NNHC(=O)OCH_3^{\bullet+}$ was identical to that of the $CH_5N_2^+$ ions generated from $HOCH_2CH_2NHNH_2^{\bullet+}$ but since the CA spectra of 3^+ and $3\Delta^+$ may well be identical the question must remain open.

Stability of hydrazonium ions

Smith and co-workers [26] reported that aldehydes may be converted to nitriles in a one-pot synthesis by converting the aldehyde to a hydrazonium salt which then undergoes a base-induced elimination to generate the nitrile [27]. For the simplest case the reaction sequence is $CH_2{=}O \rightarrow CH_2{=}N\text{-}NH_3^+$; $CH_2{=}N\text{-}NH_3^+ + OH^- \rightarrow HC{\equiv}N + NH_3 + H_2O$.

Using H_2O and NH_3 as model bases the decay of $CH_2{=}N\text{-}NH_3^+$ to $HC{\equiv}N$ was studied theoretically by Nguyen et al. [27] and they showed that the elimination is syn-periplanar. Experimentally [27], it is known that hydrazonium ions are stable in neutral solvents. As we have shown above, the formation of $HC{\equiv}N$ from isolated $CH_2{=}N\text{-}NH_3^+$ is exothermic but there exists a large barrier towards this decomposition (see Figure 5.2) and so although hydrazonium ions are thermodynamically unstable, they are stable kinetically and this explains their persistence in the gas-phase and in neutral solvents.

References

1. P.C. Burgers, T. Drewello, H. Schwarz and J.K. Terlouw, Int. J. Mass Spectrom. Ion Proc. 95 (1989) 157.
2. K. Levsen, Fundamental Aspects of Organic Mass Spectrometry, Verlag Chemie, Weinheim,1978.
3. Reviews: (a) C. Wesdemiotis, F.W. McLafferty, Chem. Rev., 87 (1987) 485; (b) J.K. Terlouw, H. Schwarz, Angew. Chem. Int. Ed. Engl. 26 (1987) 805; (c) H. Schwarz, Pure Appl. Chem. 61 (1989) 685; (d) J.L. Holmes, Adv. Mass Spectrom.11 (1989) 53; (e) J.K. Terlouw, Adv. Mass Spectrom. 11 (1989) 984; (f) J.L. Holmes, Mass Spectrom. Rev. 8 (1989) 513; (g) F.W. McLafferty, Science, 247 (1990) 990; (h) F.W. McLafferty, Adv. Mass Spectrom. 12 (1992) in press.
4. (a) K. Vekey, A.G. Brenton and J.H. Beynon, J. Phys. Chem. 90 (1986) 3569; (b) R.G. Kingston, A.G. Brenton and J.H. Beynon, Int. J. Mass Spectrom. Ion Processes,77 (1987) 223 ; (c) J.M. Curtis, D. Vekey, A.G. Brenton and J.H. Beynon, Org. Mass Spectrom. 22 (1987) 289.
5. M. Dupuis, D. Spangler and J. Wendolowski, NRCC Software Catalog 1, Program No QG01, GAMESS, 1980; M.F. Guest and J. Kendrick, GAMESS User Manual, An Introductory Guide, CCP/86/1, Daresbury Laboratory, 1986.
6. V.A. Saunders and J.H. van Lenthe, Mol. Phys. 48 (1983) 923.
7. (a) J.A. Pople, R. Seeger and N.R. Krishnan, Int. J. Quantum Chem. 11 (1977) 149; (b) MCCI ref-PJAR
8. J.A. Pople, H.B. Schlegel, R. Krishnan, D.J. DeFrees, J.S. Binkley, M.J. Frisch, R.A. Whiteside, R.F. Hout Jr. and W.J. Hehre, Int. J. Quantum. Chem. 15 (1981) 269.
9. B.O. Roos, P.R. Taylor and P.E.M. Siegbahn, Chem. Phys. 4 (1988) 157.
10. R.P. Morgan, J.H. Beynon, R.H. Bateman and B.N. Green, Int. J. Mass Spectrom. Ion Phys. 28 (1978) 171.
11. T. Wong, J.K. Terlouw, T. Weiske and H. Schwarz, Int. J. Mass Spectrom. Ion Proc. 113 (1992) R23.
12. For the use of organic neutralization agents whose ionization energy is close to that of the recombination energy of the target ion see : (a) M-Y Zhang and F.W. McLafferty, J. Am. Soc. Mass Spectrom. 3 (1992) 108 ; (b) ref.11
13. S. Villeneuve and P.C. Burgers, Org. Mass Spectrom. 21 (1986) 733.
14. P.C. Burgers and J.L. Holmes, Org. mass Spectrom. 17 (1982) 123.

15. E. Haselbach and E. Heilbronner, Tetrahedron Lett. 46 (1967) 4531.

16. (a) V.H. Dibeller, J.L. Franklin and R.M. Reese, J. Am. Chem. Soc. 81 (1959) 68; (b) M.E. Akopyan and F.I. Vilesov, Kinetics Catalysis (USSR), 4 (1963) 32, the values quoted from this study are the authors' linear extrapolation values, not the ionization threshold numbers quoted in ref. 13d; (c) S.N. Foner and R.L. Hudson, J. Chem. Phys. 53 (1970) 4377; (d) H.M. Rosenstock, K. Draxl, B.W. Steiner and J.T. Herron , J. Phys. Chem. Ref. Data, Vol. 6, Suppl. 1, 1977; (e) S.G. Lias, J.E. Bartmess, J.F. Liebman, J.L. Holmes, R.D. Levin and W.G. Mallard, J. Phys. Chem. Ref. Data 17, Supplement 1 (1988).

17. J.B. Pedley, R.D. Naylor and S.P. Kirby, Thermochemical Data of Organic Compounds, 2nd Ed., Chapman and Hall: London (1986).

18. (a) G. Frenking, N. Heinrich, W. Koch and H. Schwarz, Chem. Phys. Letters (1984) 490; (b) P.C. Burgers, J.L. Holmes and J.K. Terlouw, J. Chem. Soc., Chem. Comm. (1984) 642.

19. (a) L.F. Audrieth and B. Ackerson, The Chemistry of Hydrazine, John Wiley & Sons: New York (1951) Chapter 6; (b) W.R. McBride and H.W. Kruse, J. Am. Chem. Soc. 79 (1957) 572; (c) I.P. Fisher and E. Henderson, Trans. Faraday Soc. 63 (1967) 1342.

20. Sir Arthur Stanley Eddington, in H. Judson, New Yorker, 4 December (1978) p. 132.

21. B.F. Yates, W.J. Bouma and L. Radom, J. Am. Chem. Soc. 109 (1987) 2250.

22. (a) T.K. Ha and M.T. Nguyen, Chem. Phys. Lett. 97 (1983) 503; (b) H.F. Schaefer III, Acc. Chem. Res. 12 (1979) 288.

23. P.C. Burgers, J.L. Holmes and J.K. Terlouw, J. Am. Chem. Soc., 106 (1984) 2762.

24. D.J. DeFrees and A.D. McLean, J. Am. Chem. Soc. 107 (1985) 4350.

25. G. Schaftenaar, R. Postma, P.J.A. Ruttink, P.C. Burgers, G.A. McGibbon and J.K. Terlouw, Int. J. Mass Spectrom. Ion Proc. 100 (1990) 521.

26. (a) R.F. Smith and E.D. Otremba, J. Org. Chem. 27 (1962) 879; (b) R.F. Smith and L.E. Walker, J. Org. Chem. 27 (1962) 4372.

27. M.T. Nguyen, L.F. Clarke and A.F. Hegarty, J. Org. Chem. 55 (1990) 6177.

Appendix

In 1993 Nguyen and Vanquickenborne [J. Chem. Soc., Perkin Trans. 2, (1993) 1969] published a computational study on 'The mechanism of the Beckmann rearrangement of formaldehyde oxime and formaldehyde hydrazone in the gas phase'. According to their ab initio calculations at the MP4SDTQ/6-311++G(d,p)//MP2/6-31G(d,p) + ZPE level of theory, the total energies of CH_2-NH-NH_2^+ and CH_2-N-NH_3^+ were -149.96780 and -149.96367 with scaled (0.9) HF/6-31G(d,p) ZPE's of 182 kJ/mol and 183kJ/mol, respectively. The energy corresponding to the transition state structure [HC$^{\cdot\underline{H}\cdot}$N-$NH_3^+$] of C_s symmetry relative to CH_2-N-NH_3^+ was 189 kJ/mol. The reaction to the separated products HCN +NH_4^+ is exothermic by 120 kJ/mol. However, the intermediate ion-dipole complex [HCN··H·NH_3^+] is even more stable, -202 kJ/mol relative to the educt. In the complex the proton is shared unequally, being 1.051 Å from the ammonia nitrogen atom (only slightly longer than the other H-N bonds of 1.019 Å) and 1.754 Å from the cyanide nitrogen atom. The authors did not calculate the energy barrier for the 1,2-*cis*-elimination pathway proposed in our paper and thus the values for the two pathways (189 kJ/mol and 251 kJ/mol [our work]) cannot be compared directly. Nevertheless, given the large difference between the values and the level of sophistication of the two calculations it is predicted that the Beckman rearrangement CH_2-N-NH_3^+ → [HC$^{\cdot\underline{H}\cdot}$N-$NH_3^+$] → [HCN··H··$NH_3^+$] → HCN +$NH_4^+$ will be the preferred route for dissociation of ion **4**$^+$ to HCN +NH_4^+. This would undoubtedly also represent the final step in the dissociation of the metastable $CH_5N_2^+$ ions **1**$^+$ - **3**$^+$ to HCN +NH_4^+.

Note added after submission of thesis: Nguyen reaffirms this prediction and also finds that the ion-dipole complex serves as the key intermediate for both metastable processes in a subsequent study of the "Hydrogen cyanide loss from $[CH_5N_2]^+$ cations: 1,2-elimination versus Beckmann rearrangement" [Int. J. Mass Spectrom. Ion Processes 136 (1994) 45].

CHAPTER 6

Deacetylation of gaseous amidoalkylating reagents (N-acyliminium ions) via iminium/ketene complexes; an unprecedented isotope effect.

Introduction

In this chapter a mechanism for unimolecular deacetylation of the N-acetylmethyl-iminium ion, $CH_3C(=O)\text{-}N(H)=CH_2^+$ (1), to $CH_2NH_2^+$ and $CH_2=C=O$, is proposed. The role of the hydrogen-bridged complex $O=C=CH_2\cdots H\cdots N(H)=CH_2^+$ (2) is discussed, with emphasis placed on the observation of large isotope effects and exceedingly small translational energy releases as indications of the intermediacy of ion-molecule complexes. In addition, several other isomeric ions, e.g. $H_2C=C=O\cdots H\cdots N(H)=CH_2^+$ (3), $CH_2\text{-}O\text{-}C\text{-}N(H)\text{-}CH_3^+$ (4), $CH_2=C(OH)\text{-}N(H)\text{-}CH_2^+$ (5), $H_2N\text{-}CH_2\text{-}CH_2\text{-}C=O^+$ (6), $CH_3C(OH)=N=CH_2^+$ (7) and protonated azetidin-2-one (8), were also briefly examined and characterized by metastable ion (MI) and collisional activation (CA) mass spectrometry as well as D-labelling experiments and/or ab initio molecular orbital calculations.

The work described here has appeared before in a manuscript of the same title:

P.C. Burgers, C.A. Kingsmill, G.A. McGibbon and J.K. Terlouw

Org. Mass Spectrom. 27 (1992) 398-405.

Amidoalkylation, whereby a new bond is formed by replacement of X (X = OH, OR, OCOR, halogen etc.) from the electrophilic reagent R_1-C(=O)-N(R_2)-C(R_3)(R_4)X, is an important reaction in organic chemistry and interest in its practical application is considerable [1,2]. Amidoalkylation may be a convenient way to synthesize substances which are otherwise difficult to prepare. For example, aminomethylphosphonous acid, the prototype of a class of important intermediates for the synthesis of biologically active compounds, can be conveniently prepared using a simple amidoalkylation procedure [3]. The intermediate in the amidoalkylation is the N-acyliminium ion [R_1-C(=O)-N(R_2)-C(R_3)(R_4)]$^+$ (amidoalkylating reagent), which because of the electron-withdrawing carbonyl group is more reactive than the corresponding Mannich reagent, the highly stable iminium ion [(R_1)(R_2)N=C(R_3)(R_4)]$^+$; N-acyliminium ions can therefore be regarded as "destabilized" [4] iminium ions, by analogy to "destabilized" carbenium ions, extensively studied by Grützmacher and co-workers [4b-d]. Because of their limited stability, N-acyliminium ions are for synthetic purposes invariably generated *in situ* [1]. It is not surprising that relatively little is known about the intrinsic properties of the amidoalkylating reagent. For example, are N-acyliminium ions, in the absence of solvent stable species or do they rapidly rearrange to more stable isomers or even do they decompose, for instance by deacetylation to the stable Mannich ion? Previous studies [4,5] on "destabilized" carbenium ions (such as the "push-pull" carbenium ion CH_3-CH_2-CH-COOH$^+$) have shown that such species can be generated in the gas phase and that they exhibit a rich and intriguing unimolecular chemistry. In particular, they may rearrange via a multi-step pathway to hydrogen-bridged complexes [6] which then become responsible for significant dissociations leading to intense peaks in the Electron Ionization (EI) mass spectra. Inspired by these results and spurred by the call of Speckamp and Hiemstra [1] for more research on amidoalkylating reagents, we have generated in the gas-phase the prototype amidoalkylating reagent, the

N-acetylmethyliminium ion **1**, and have studied its intriguing unimolecular chemistry by a combined approach of mass spectrometry-based experiments (metastable ion (MI), collisional activation (CA) and D-labelling) and *ab initio* molecular orbital calculations.

Results and Discussion

$C_3H_6NO^+$ ions of putative structure **1** can be generated from N-alkylacetamides [7]. Thus loss of $C_2H_5^\bullet$ from N-(*n*-propyl)acetamide, CH_3-C(=O)-NH-$CH_2CH_2CH_3$ (**I**) yields an important fragment in the 70 eV EI mass spectrum. This process is not the reaction of lowest energy requirement, because the m/z 72 $C_3H_6NO^+$ ion is not present in the MI mass spectrum of **I**; instead an intense signal is observed for loss of $CH_3^\bullet$. The labelled ion CD_3-C(=O)-NH-$CH_2CH_2CH_3$ (**I-d$_3$**) specifically loses $CH_3^\bullet$, consistent with rationalizations given in previous papers [7b,c] and this process was not further investigated.

The MI mass spectrum of **1** is dominated by a very narrow metastable peak at m/z 30 ($CH_2NH_2^+$), resulting from deacetylation (see Figure 6.1), with a very small kinetic energy release, $T_{0.5}$ = 0.3 meV (0.03 kJ/mol): thus the products $CH_2NH_2^+$ and CH_2=C=O recoil with a velocity corresponding to only 4 K. Such extremely small kinetic energy releases (a factor of 100 less than what is usually encountered [8] for reactions having a negligible reverse energy term) have been linked to dissociation of ion-dipole complexes [9]. The above deacetylation process has been proposed to occur via a simple 1,3-hydrogen shift [7b,c]; indeed we observe that metastable CH_3-C(=O)-N(D)=CH_2^+ (**1-d$_1$**) specifically forms CH_2=NHD$^+$ + CH_2=C=O and CD_3-C(=O)-N(D)=CH_2^+ (**1-d$_4$**) specifically generates CH_2=ND_2^+ + CD_2=C=O as expected. However, the labelled ion CD_3-C(=O)-N(H)=CH_2^+ (**1-d$_3$**) dissociates to totally unexpected products: it does not form, as would have been expected from the above, CH_2=NHD$^+$ + CD_2=C=O, but it almost specifically (>95%) generates CH_2=ND_2^+ + CHD=C=O.

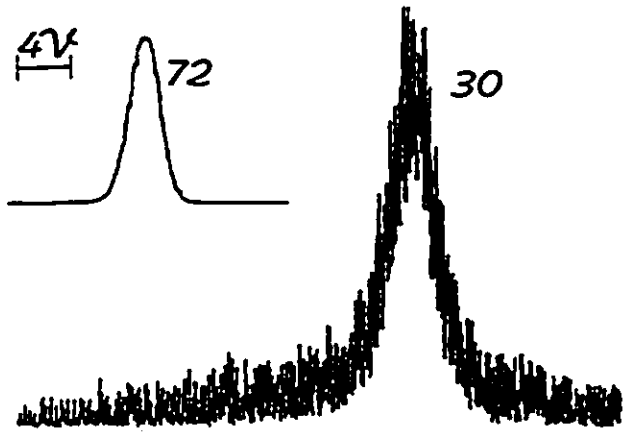

Fig. 6.1 Metastable peak for CH_3-C(=O)N(H)=CH_2^+ → $CH_2NH_2^+$ + CH_2=C=O. Inset : main beam with energy scale as indicated.

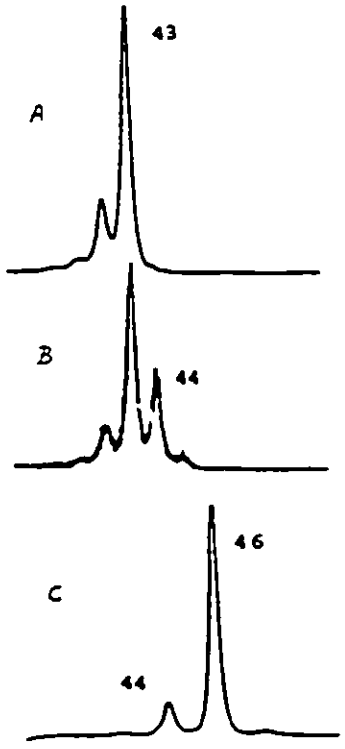

Fig. 6.2 Partial CA mass spectra of CH_3-C(=O)N(H)=CH_2^+ , A, CH_3-C(=O)N(D)=CH_2^+ , B, and CD_3-C(=O)N(D)=CH_2^+, C.

Hence the following reactions are established:

CH_3-C(=O)-N(D)=CH_2^+ **1-d_1** ⟶ CH_2=NHD^+ + CH_2=C=O

CD_3-C(=O)-N(H)=CH_2^+ **1-d_3** ⟶// CH_2=NHD^+ + CD_2=C=O

1-d_3 ⟶ CH_2=ND_2^+ + CHD=C=O

The latter reaction requires at least three H/D transfers. Clearly, an "all-or-nothing" [10] isotope effect of as yet unknown origin is operative in the deacetylation process. The minimum energy requirement for deacetylation and a number of related processes which are **not** observed in the MI spectrum are shown in Table 6.1.

Table 6.1. Potential CH_3-C(=O)-N(D)=CH_2^+ dissociation products and their enthalpies.

1 →	CH_2=NH_2^+	+	CH_2=C=O	$\Sigma\Delta H_f$ = 701	kJ/mol [a]	[11]
	CH_2=$NH_2^{\bullet}$	+	CH_2=C=$O^{+\bullet}$	$\Sigma\Delta H_f$ = 1038	kJ/mol	[11]
	CH_3=NH^+	+	CH_2=C=O	$\Sigma\Delta H_f$ = 757	kJ/mol	[11]
	CH_2=NH	+	CH_3-C=O^+	$\Sigma\Delta H_f$ = 722	kJ/mol	[11,12]
	CH_3-NH-CH_2^+	+	CO	$\Sigma\Delta H_f$ = 584	kJ/mol	[11]

a) Metastable process

The direct bond cleavage reaction 1 → CH_2=NH + CH_3-C=O^+ has a minimum energy requirement which is only 21 kJ/mol higher than that for the rearrangement process 1 → CH_2=NH_2^+ + CH_2=C=O, yet m/z 43 ions are not present in the MI mass spectrum. However, they give rise to an intense signal in the CA mass spectrum, see Table 6.2; the partial CA mass spectrum is shown in Figure 6.2.

Since formation of CH_3-C=O^+ has significant bearing on the discussion concerning the deacetylation of metastable ions 1 we will discuss it in some detail. The partial CA mass spectrum of CH_3-C(=O)-N(D)=CH_2^+, **1-d_1** , given in Figure 6.2b. shows that m/z 43 has partially shifted to m/z 44, CH_2D-C=O^+. On the other hand, see Figure 6.2c, the labelled ion CD_3-C(=O)-N(D)=CH_2^+,**1-d_4**, specifically generates CD_3-C=O^+ without any

CH_2D-C=O$^+$. We take these results as showing that prior to formation of CH_3-C=O$^+$ from 1 the CH_3- and N–H hydrogen atoms undergo exchange reactions, and that the CH_2=N hydrogens are not involved in these scrambling reactions. If the exchange reactions occur to the statistical limit then the ratio m/z 43 : 44 in Figure 6.2b should be 1 : 3, compared with the observed ratio of ~ 2 : 1. Clearly, for ions sampled by CA, the H/D randomizations are not complete. However, H/D exchange reactions invariably become more extensive in metastably dissociating ions [13] and so we will assume that prior to the deacetylation of metastable ions 1 the CH_3 and N–H hydrogens become positionally indistinguishable, i.e. for these hydrogen atoms H/D exchanges occur to the statistical limit. We therefore propose the following: prior to metastable deacetylation of $CD_3C(=O)$-N(H)=CH_2^+ (**1-d_3**), there exists a freely interconverting mixture of **1-d_3** and $CD_2HC(=O)$-N(D)=CH_2^+ (**1'-d_3**) and **only** ions **1'-d_3** dissociate, by loss of CHD=C=O but **not** CD_2=C=O.

Upon collisional activation however, both $CH_2ND_2^+$ and CH_2NHD^+ are formed in a ratio of 1.2 : 1 (see Table 6.3), consistent with complete H/D exchange, i.e. **1-d_3** ⇔ **1'-d_3** and a much smaller isotope effect, approaching unity. Hence the isotope effect rapidly diminishes at higher internal energies. At even higher energies (normal EI mass spectrum, see Table 6.3) the major product is CH_2NHD^+ so that at these higher energies H/D reactions play only a minor role. It can be seen from Table 6.3 that in going from MI to EI the intensity ratio m/z 32 : 31 decreases by a factor of at least 300, hence for slow dissociations the major product is $CH_2ND_2^+$ and for fast dissociations the major product is CH_2NHD^+.

The following experimental and computational work concentrates on the question: of whether ion 1 prior to deacetylation communicate with other stable isomers and if so whether this communication provides a basis for the rationalization of the exchange mechanism, the very small kinetic energy release and the remarkable isotope effect.

TABLE 6.2 Collisional Activation Mass Spectra of $C_3H_6NO^+$ Ions

ION	m/z→	58	57	56	55	54	44	43	42	72^{++}	30	29	28	18	15	14
1		-	-	-	-	-	-	100	29	-	360	21	29	-	4	-
4		41	3	7	3	4	34	44	100	12	31	24	70	-	10	5
6		-	1	-	5	2	4	100	73	3	720	27	45	1	4	3
7		-	22	16	7	6	32	100	28	19	62	28	35	5	2	7
8		-	-	1	64	125	100	64	66	32	84	32	90	7	3	8

a) Peaks normalized to base peak in CA spectrum = 100 % ; peaks containing contributions from metastable processes underlined.

TABLE 6.3 $CH_2ND_2^+/CH_2NHD^+$ peak intensity ratios in $CD_3C(=O)NHCH_2^+$ spectra.

SPECTRUM	$CH_2ND_2^+/CH_2NHD^+$	
MI	> 25	[a]
CA	1.2	
EI	0.09 0.16	[b]

a) the small peak at m/z 31, CH_2NHD^+, is partly collision induced; b) from ref. 7b

The isomeric ions considered by experiment and/or theory (ab initio molecular orbital calculations at the MP3/6-31G*//4-31G level) are:

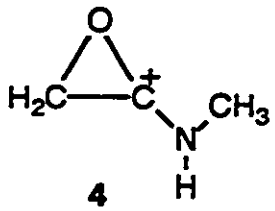

4

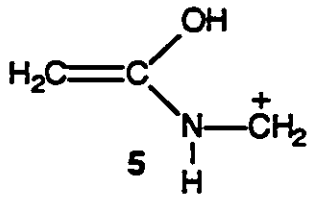

5

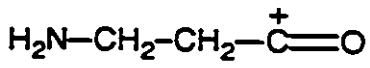

6

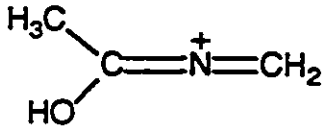

7

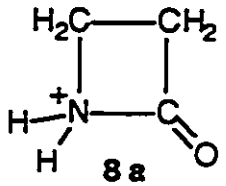

8a

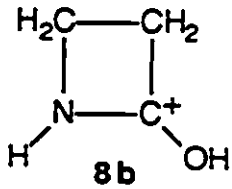

8b

The experimental results (CA mass spectra) are summarized in Table 6.2 and the computational results are found in Figure 6.3, Table 6.4 and Figure 6.4.

Table 6.4. Total energies [Hartrees], zero-point vibrational energies [ZPVE] and relative calculated energies E_{rel} [kJ/mol] for isomers and components of the $C_3H_6NO^+$ system.

STRUCTURE	POINT GROUP	UHF/4-31G	6-31G*//4-31G	MP3/6-31G*//4-31G	ZPVE	E_{rel} [a,b]	
1	C_s	-245.78713	-246.15590	-246.88112	234	0	[0]
2	C_s	-245.75434	-246.11889	-246.84360	225	90	[88]
3	C_s	-245.77379	-246.12780	-246.85056	225	72	
4	C_1	-245.71828	-246.10545	-246.83990	234	109	
5	C_s	-245.77630	-246.12933	-246.85958	236	59	
6	C_1	-245.75003	-246.12208	-246.84906	231	81	
TS 1-2	C_1	-245.73013	-246.10041	-246.83304	212	105	
TS 1-4	C_1	-245.66664	-246.04130	-246.77097	220	276	[275]
TS 1-5	C_s	-245.62806	-245.99537	-246.73941	220	358	
CH_3-C=O$^+$							
CH_2=NH		-245.70052	-246.08618	-246.80831	215	173	[175]
CH_2=C=O							
$CH_2NH_2^+$		-245.74457	-246.10689	-246.82199	221	143	[129]

a) The relative calculated energies include scaled (0.9) zero-point vibrational contributions.
b) Values in brackets refer to MP3/6-31G*//6-31G* calculations.

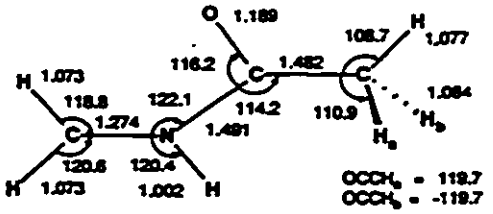

ISOMER *a*

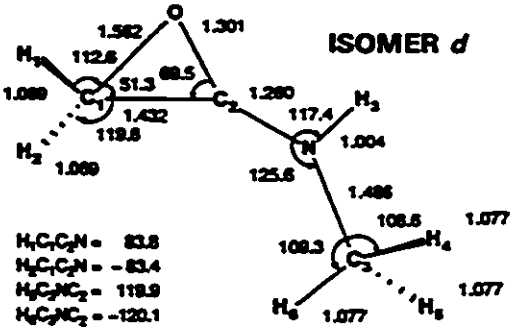

ISOMER *d*

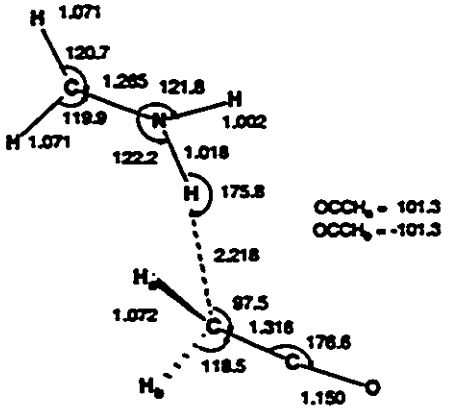

ISOMER *b*

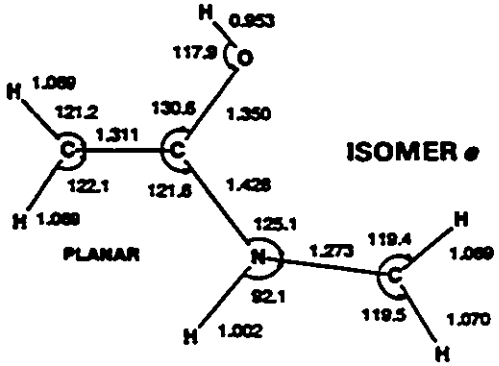

ISOMER *e*

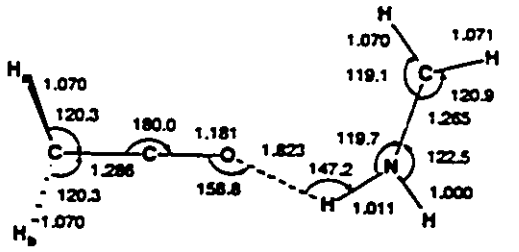

ISOMER *c*

OCCH$_5$ = 90.0
OCCH$_6$ = -90.0

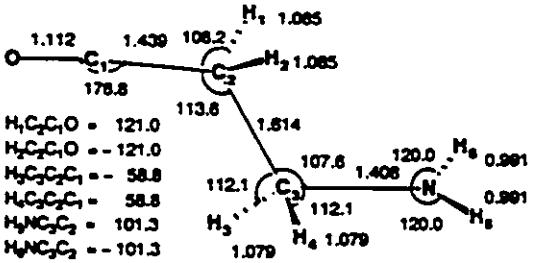

ISOMER *f*

Fig. 6.3 Geometries of $C_3H_6NO^+$ isomeric ions and some Transition States at the MP3 /6-31G*//4-31G level of theory.

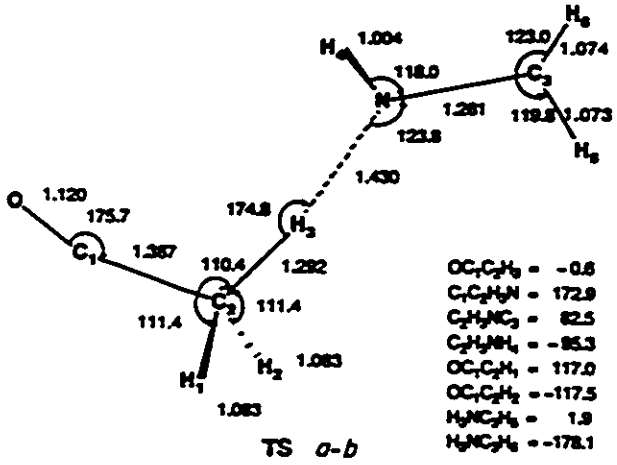

TS *a-b*

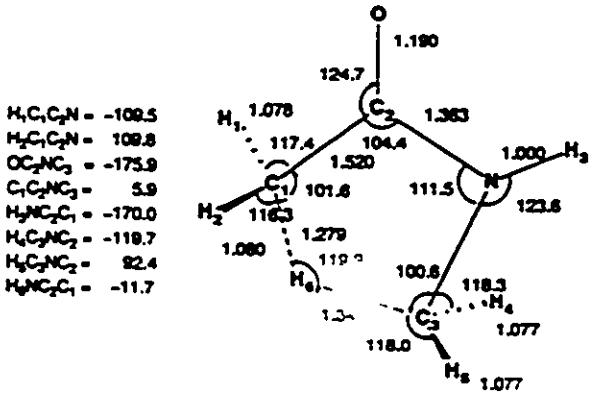

TS *a-d*

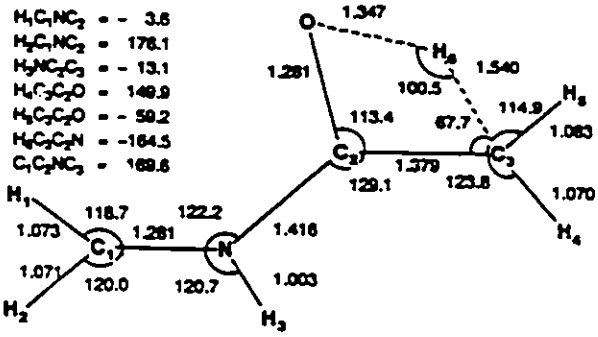

TS *a-e*

DISSOCIATION PRODUCTS

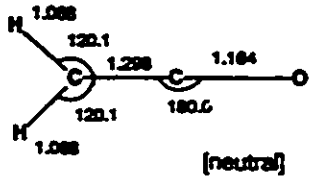

[neutral]

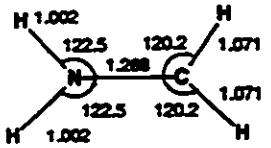

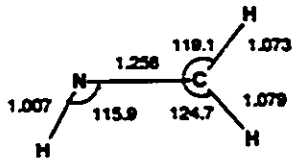

[neutral]

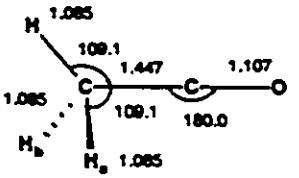

$OCCH_a$ = -120.0
$OCCH_b$ = 120.0

Fig. 6.3 continued

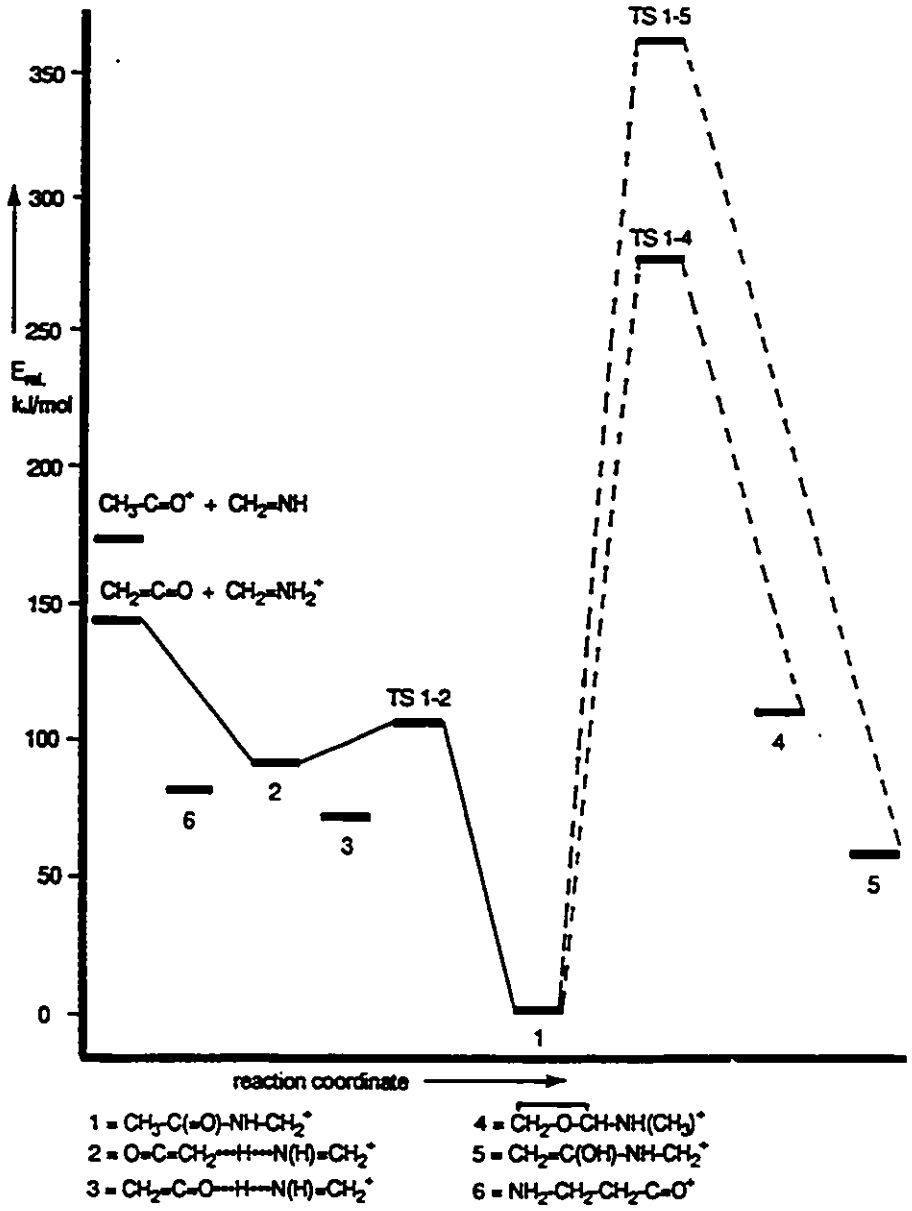

Fig. 6.4 The calculated $C_3H_6NO^+$ potential energy surface.

Loss of I$^{\bullet}$ from ionized I-$CH_2C(=O)NH-CH_3$ yields $C_3H_6NO^+$ ions which form the base peak in the 70 eV mass spectrum. Our calculations predict that the ion does not have the structure $^+CH_2C(=O)NH-CH_3$ (**4a**) but rather that it is the (methylamino)oxiranyl cation **4**. The ring-opened form of **4** is not a stable species and it collapses to **4**: when the calculation was started with a **4a** geometry, convergence to the epoxide type structure **4** took place. Such a conversion has also been proposed for the CH_2-$C(=O)OH^+$ ions generated by loss of I$^{\bullet}$ from ionized I-CH_2COOH [14]. The calculations further show (see Table 6.4 and Figure 6.4) that isomer **4** lies below the dissociation threshold for $CH_2=NH_2^+ + CH_2=C=O$, but that the barrier for its formation from **1** is very high. Thus ions **4** are not expected to be involved in the unimolecular chemistry of **1**. In agreement with this, ions **4** display a characteristic CA (and MI) mass spectrum which bears no relationship with that of ion **1** (see Table 6.2).

No experimental information on the isomeric enol ion **5** has been reported and we were not able to find a suitable precursor molecule for its generation. The ab initio calculations show that it is a minimum on the $C_3H_6NO^+$ potential energy surface but the barrier for isomerization into **1** is very high, indicating that **5** is not involved in the deacetylation of **1**. Odd-electron enol cations are generally more stable than the corresponding oxo forms [15]. Theory predicts the even-electron enol ion **5** to be less stable than the keto form, by 60 kJ/mol.

Ion **6** was generated from the methyl ester of β-alanine, $NH_2CH_2CH_2COOCH_3$. The CA mass spectrum of the m/z 72 ions is close to but not identical with that of ion **1**: compare the peaks at m/z 55, 42, 36 (72^{2+}) and 18 in Table 6.2. However, the base peak in the MI mass spectrum is a very narrow peak at m/z 30 , $CH_2NH_2^+$ and the associated very small kinetic energy release for the reaction **6** → $CH_2NH_2^+ + CH_2=C=O$ is the same as that observed for the dissociation of **1**. This suggests that metastable ions **6** may well communicate with ions **1**. If this is true, then the labelled isotopomer $NH_2-CH_2-CD_2-C=O^+$ is expected to show a pronounced isotope effect as in **1-d_3**. This

prediction has not yet been verified nor were further calculations on the interconversion **1** → **6** performed since in this study we have focussed on an explanation of the isotope effect and the exchange reactions of **1** which communication with **6** does not explain. ΔH_f (**6**) can be reliably estimated as 623 kJ/mol (assuming that the effect of NH_2 substitution on a CH_3 hydrogen atom in CH_3-CH_2-C=O$^+$ is identical with that on $CH_3CH_2CH_2CH_3$ and using the appropriate thermochemical data from ref. [11]). Combining this estimate for **6** with its E_{rel} from Table 6.4 yields ΔH_f (**1**) = 542 kJ/mol. This value is gratifyingly close to the 549 kJ/mol derived by subtracting the appropriate E_{rel} from the enthalpy of formation of the dissociation products CH_3-C=O$^+$ and CH_2=NH given in Table 6.1.

Budzikiewicz and co-workers [7b] have proposed that ions of structure **7** are generated from ionized N-ethyl-N-acetyl-cyclohexylamine by the consecutive loss of $CH_3^\bullet$ and cyclo-C_6H_{10}. We obtained the CA mass spectrum of the m/z 72 ion from this amine and it is very different from that of **1** (see Table 6.2). Ab initio calculations on this enol-type ion have not been performed.

The gas-phase protonation of azetidin-2-one could yield two different cyclic ions, **8a** and/or **8b**. Considering the preferred site of protonation of formamide [16] it seems most likely that carbonyl protonation occurs. From the CA mass spectra resulting from protonation in Chemical Ionization experiments using CH_4 or CH_3OH as the protonating agent (see Table 6.2), it follows that the protonated azetidin-2-one ion is not related to ion **1**. In view of this and considering that the heat of formation, the site of protonation and the proton affinity (PA) of azetidin-2-one are unknown, ab initio calculations were not been performed on these ions.

It is clear that the above isomeric ions are not responsible for the H/D exchange reactions in **1**. We therefore embarked on further computations of isomers on the $C_3H_6NO^+$ potential energy surface to ascertain whether ion **1** can rearrange to another species not easily accessible by experiment. Since we have reasons to believe that the

deacetylation is ion-dipole mediated (see above), we have concentrated on the hydrogen-bridged complex $[O{=}C{=}CH_2{\cdots}H{\cdots}N(H){=}CH_2]^+$, **2**, and its isomer $[CH_2{=}C{=}O{\cdots}H{\cdots}N(H){=}CH_2]^+$, **3**.

The mechanism of the deacetylation of the N-acetyliminium ions

The C···H···N and O···H···N hydrogen-bridged ions **2** and **3** are minima at both the 6-31G* and the 4-31G levels of geometry optimization. Ion **3** is the more stable isomer and its stabilization energy (SE) with respect to its components $CH_2{=}NH_2^+/CH_2{=}C{=}O$ is calculated to be 71 kJ/mol. Using the empirical relationship [17] for the estimation of the SE in O···H···N bridged species, SE = 126 – 0.26 ΔPA (kJ/mol), where ΔPA is the difference in proton affinity of $CH_2{=}C{=}O$ (at oxygen) and of $CH_2{=}NH$ (at nitrogen), 172 kJ/mol [11,12], the estimated SE becomes 81 kJ/mol, in good agreement with our ab initio value. The SE of the C···H···N bridged species **2** , for which we do not have a reliable rule of thumb to estimate its SE, is calculated from the results in Table 6.4 to be lower, 53 kJ/mol. The hydrogen bond distances of structure **2** are not indicative of a "shared" hydrogen, it being much closer to the nitrogen atom than to the carbon atom. To check if this result was due to the choice of the starting geometry, several other geometries were considered but they all converged to the geometry shown in Figure 6.3. In this context, it is of interest to note that similar structures were found in a study dealing with the participation of $[CH_3{-}C{=}O^+{\cdots}CH_2{=}C{=}O]$ ion neutral complexes in the dissociation of the ion $CH_3COCH_2CO^+$ [18].

Ion **2** cannot be envisaged as a conventional ion-dipole complex, because as viewed, the dipole vector of ketene points away from the charge and the species should be destabilized by ion-dipole repulsion. However, a Mulliken population analysis (MP3/6-31G*//4-31G) indicated that the nitrogen and the carbon atoms of the H-bridge in **2** are actually negatively charged, –0.69 and –0.72 e^-, respectively, with the "bridging" hydrogen being considerably positive (+ 0.49 e^-) and the rest of the positive charge

distributed over the peripheral hydrogen atoms. We tentatively propose that in species **2** electrostatic interactions (charge alternations) are a dominant factor governing its stability, as in dications [19].

Next, the transition state between **1** and **2** was located and its final geometry (**TS 1-2**) is shown in Figure 6.3. Using the internal reaction coordinate analysis option within the Gaussian 90 program, **TS 1-2** could be shown to connect ions **1** and **2**. We now have a mechanism for deacetylation: stretching of the C(=O)-NH bond in **1** does not immediately lead to dissociation, but instead the CH_2=NH molecule can migrate within the electrostatic field of the CH_3-C=O$^+$ cation. When, at 105 kJ/mol, the structure **TS 1-2** is reached, proton transfer takes effect to generate **2**. All attempts to locate a TS for the transition **1** → **3** lying below the energy level of the dissociation products failed and we therefore propose that ion **3** may only communicate with **1** via the reaction sequence **1** → **2** → **3**. The latter interconversion is likely but because it is not immediately required for the explanation of the experimental observations it was not further studied computationally.

From our experiments, we can derive an upper limit for **TS 1-2**. In the microsecond time frame there is no loss of CH_2=NH, and thus **TS 1-2** must lie below the threshold for the products CH_3-C=O$^+$ and CH_2=NH. The kinetic energy release for the dissociation of CH_2=NH_2^+ and CH_2=C=O is so exceedingly small that there will be no detectable reverse activation energy, and also, the excess term will be very small, ~0.1 kJ/mol [9d]. Therefore, **TS 1-2** must lie even lower, i.e. at or below the level for the products CH_2=NH_2^+ + CH_2=C=O.

The calculations indicate that **TS 1-2** lies below the threshold for dissociation, as does **2** itself, and so the reaction **1** → **2** may be reversible. Considering that **2** is an ion-molecule complex, we expect that the incipient Mannich ion, CH_2=NH_2^+, is able to rotate along the ketene C-C-O axis. Although we have not performed the appropriate calculations, such a rotation is not expected to require more energy than the complex's

SE (53 kJ/mol). We therefore propose the exchange mechanism shown in Scheme 6.1.

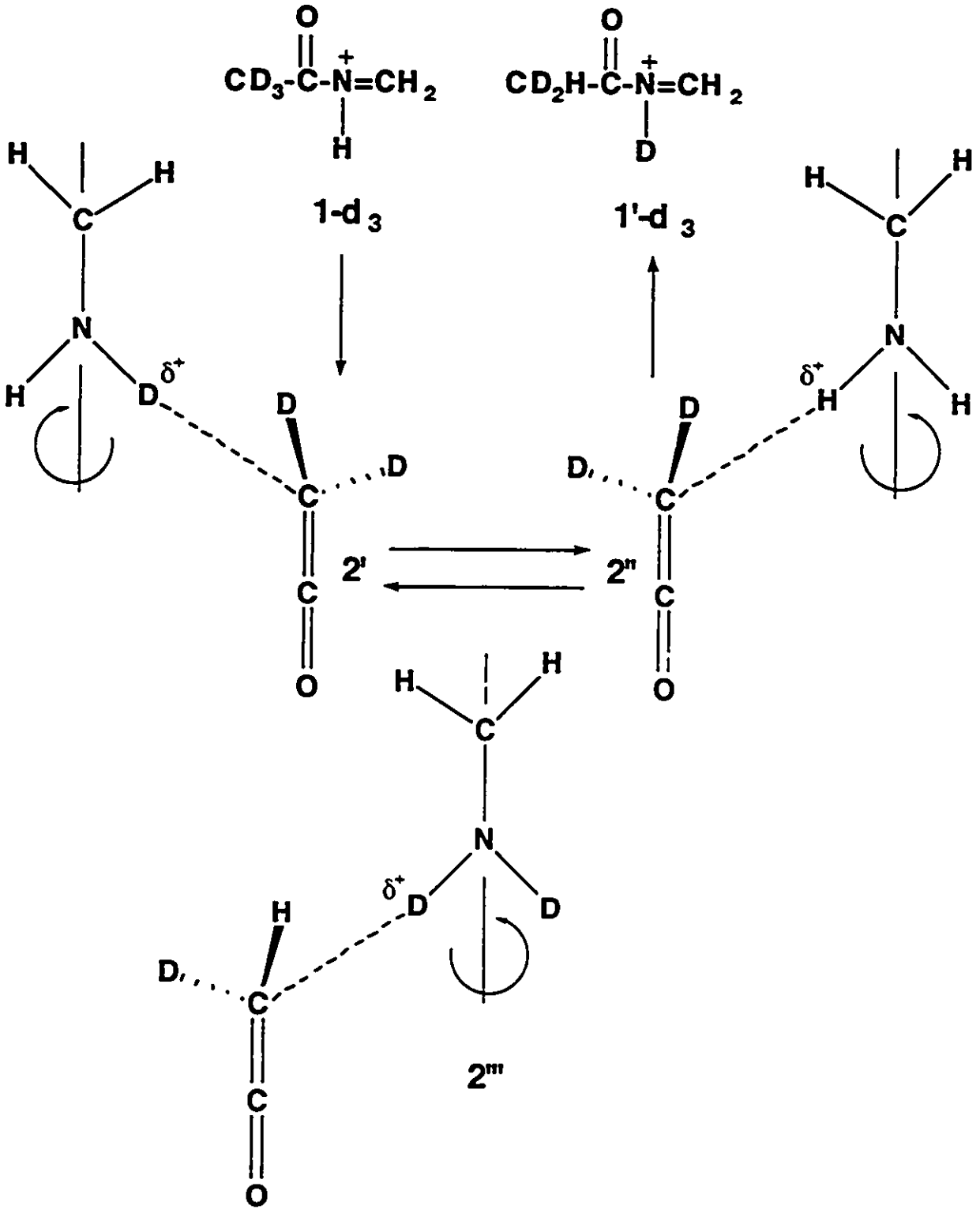

Scheme 6.1

After one more cycle the associated ion **2'''** is formed. The question then arises: why do **2'** and **2''** remain associated in the microsecond time frame, whereas **2'''** dissociates? One interpretation is that the D atoms "prefer" the N-D position in the $CH_2{=}NH_2^+$ over the C-D position in ketene. The N-H bond is shorter and stronger than the C-H bond (see Figure 6.3) and more importantly, the stretching frequencies of the former are larger. At the UHF/4-31G level of theory the calculated N-H symmetric and asymmetric stretch frequencies are 3806 and 3703 cm^{-1} respectively, compared with 3465 and 3369 cm^{-1} for C-H. The calculated (UHF/4-31G) ZPVE's for the dissociation products from **2'** and **2''**, *viz.* $CH_2{=}NHD^+$ and $CD_2{=}C{=}O$ and for those from **2'''** are 197.5 and 195.8 kJ/mol, respectively (including a scaling factor of 0.9). Although small, the difference in ZPVE's, 1.7 kJ/mol, in favour of $CH_2{=}ND_2^+$ and CHD=C=O, is about 60 times the translational energy release, 0.03 kJ/mol, and is thus more than sufficient to guarantee that only $CH_2{=}ND_2^+$ and CHD=C=O are formed. The deuterium "prefers" the short and strong N-D bond , because the resulting decrease in ZPVE is larger for the N-D bond, strong bonds having higher vibrational frequencies, see above.

A similar effect has been observed in ESR spectroscopy: at 4 K (= 0.04 kJ/mol) the $CH_2D_2^+$ cation prefers the C_{2v} symmetry, with short C-D bonds and long C-H bonds [19]. In this case the differences in ZPVE's were approximately 2.5 kJ/mol, "more than sufficient" [20] to guarantee that only one isomer exists at 4 K.

The observed isotope effect for the N-acyliminium ion is not an equilibrium isotope effect as encountered in solution chemistry [21,22], but rather it is a kinetic isotope effect. It is clear from this work that the isotope effect results from very small differences in zero-point energies. Hence such isotope effects will especially be observed for dissociations taking place at threshold, i.e. for ion-molecule dissociations. We especially anticipate that such zero-point effects should be observable in low-temperature ion-molecule reactions.

Theoretical methods

Standard *ab initio* MO calculations were performed with the GAUSSIAN 90 series of programs [23] employing unrestricted Hartree-Fock (UHF) procedures. Optimized geometries, harmonic frequencies and zero-point vibrational energies (ZPVE) were calculated with the split-valence 4-31G basis set [24]. The force constant matrices for the stationary points were checked to have the correct number of negative eigenvalues. Single-point calculations of the 4-31G geometries were performed with the 6-31G* basis set [24,25]. Electron correlation was included by using Møller-Plesset perturbation theory terminated at the third order (MP3) [26].The vibrational frequencies were scaled by a factor of 0.9 [27]. The isomers and transition states are displayed in Figure 6.3, and all isomers are minima on the potential energy surface (no negative eigenvalues) and all transition states are saddle points (one negative eigenvalue which corresponds to the correct reaction coordinate).The system studied consists of even-electron species where the UHF wavefunctions tend to become RHF, which is evident in that the spin contamination $\langle s^2 \rangle$, is zero for all isomers and transition states.

References

1. W.N. Speckamp and H. Hiemstra, Tetrahedron 41 (1985) 4367; see also: A. Bolognese, M.V. Diurno, O. Mazzoni and F. Giordano, Tetrahedron, 47 (1991) 7417 where N-acyliminium ions are proposed as intermediates in the Staudinger reaction.
2. H.E. Zaug, Synthesis 85 (1984).
3. D. Grobelny, Syn. Commun. 19 (1989) 1177.
4. (a) Th.T. Tidwell, Angew. Chem. 96 (1984) 16 ; (b) A-M. Dommröse and H-Fr. Grützmacher, Int. J. Mass Spectrom. Ion Processes 76 (1987) 95; (c) R. Wolf, A-M. Dommröse and H-Fr. Grützmacher, Org. Mass Spectrom. 23 (1988) 26; (d) R. Wolf, and H-Fr. Grützmacher, Org. Mass Spectrom. 24 (1989) 398.
5. P.C. Burgers, K.J. van den Berg, H. Visser and J.K. Terlouw, Int. J. Mass Spectrom. Ion Processes 101 (1990) 83.
6. for reviews see: (a) P.C. Burgers and J.K. Terlouw, in Specialist Periodical Reports: Mass Spectrometry, Vol. 10, M.E. Rose (ed.), The Royal Society of Chemistry: London (1989) Chapter 2;

(b) N. Heinrich and H. Schwarz, in Ion and Cluster Spectroscopy and Structure, J.P. Maier (ed.), Elsevier: Amsterdam (1989) p. 329.

7. (a) K. Heyns and H-Fr. Grützmacher, Ann. Chemie 660 (1962) 194; (b) Z. Pelah, M.A. Kielczewski, J.M. Wilson, M. Okasi, H. Budzikiewicz and C. Djerassi, J. Am. Chem. Soc. 85 (1963) 2470; (c) H. Budzikiewicz, C. Djerassi and D.H. Williams, Mass Spectrometry of Organic Compounds, Holden-Day Inc.: London (1967).

8. J.L. Holmes, Org. Mass Spectrom. 20, 169 (1985).

9. (a) S. Hammerum, Mass Spectrom. Rev. 7 (1988) 123; (b) D.J. McAdoo, Mass Spectrom. Rev. 7 (1988) 363; (c) S. Hammerum and H.E. Audier, J. Chem. Soc. Chem. Commun. 860 (1988); (d) P.J.A. Ruttink, J. Phys. Chem. 91 (1987) 703; (e) R. Postma, S.P. van Helden, J.H. van Lenthe, P.J.A. Ruttink, J.K. Terlouw and J.L. Holmes, Org. Mass Spectrom. 23 (1988) 503; (f) R. Postma, P.J.A. Ruttink, B.L.M. van Baar, J.K. Terlouw, J.L. Holmes and P.C. Burgers, Chem. Phys. Lett. 123 (1986) 409; (g) R. Postma, P.J.A. Ruttink, J.K. Terlouw and J.L. Holmes, J. Chem. Soc. Chem. Commun. 683 (1986); (h) S. Hammerum, J. Chem. Soc. Chem. Commun. 858 (1988).

10. P.J. Derrick and K.F. Donchi, in Comprehensive Chemical Kinetics, ed. by C.H. Bamford and C.F.H. Tipper, Vol 24. Elsevier, Amsterdam (1983).

11. S.G. Lias, J.E. Bartmess, J.F. Liebman, J.L. Holmes, R.D. Levin and W.G. Mallard, J. Phys. Chem. Ref. Data 17, supplement 1 (1988).

12. ΔH_f [CH_2=N-H] from R.A.L. Peerboom, S. Ingemann, N.M.M. Nibbering and J.F. Liebman, J. Chem. Soc. Perkin Trans 2, 1825 (1990).

13. (a) R.G. Cooks, J.H. Beynon, R.M. Caprioli and G.R. Lester, Metastable Ion, Elsevier: Amsterdam, 1973; (b) K. Levsen, Fundamental Aspects of Organic Mass Spectrometry, Verlag Chemie: Weinheim, (1978).

14. M.C. Blanchette, J.L. Holmes, C.E.C.A. Hop, F.P. Lossing, R. Postma, P.J.A. Ruttink and J.K. Terlouw, J. Am. Chem. Soc. 108 (1986) 7589.

15. F. Turecek, in The Chemistry of Enols, Z. Rapoport (ed.), Wiley: New York (1990) Chapter 3.

16. G. Schaftenaar, R. Postma, P.J. A. Ruttink, P.C. Burgers, G.A. McGibbon and J.K. Terlouw, Int. J.

Mass Spectrom. Ion Processes 100 (1990) 521.

17. M. Meot-Ner (Mautner), J. Am. Chem. Soc. 106 (1984) 1257.
18. H.E. Audier, personal communication.
19. W. Kock, G. Frenking, J. Gauss and D.J. Cremer, J. Am. Chem. Soc. 108 (1986) 5808.
20. M.N. Paddon-Row, D.J. Fox, J.A. Pople, K.N. Houk and D.W. Pratt, J. Am. Chem. Soc. 107 (1985) 7696.
21. G.R. Stevenson, S.J. Peters and K.A. Reidy, Tetrahedron Letters 31 (1990) 1651.
22. M. Saunders, K.E. Laidig and M. Wolfsberg, J. Am. Chem. Soc. 111 (1989) 8989.
23. Gaussian 90 : M.J. Frisch, M. Head-Gordon, G.W. Trucks, J.B. Foresman, H.B. Schlegel, K. Raghavachari, M.A. Robb, J.S. Binkley, C. Gonzales, D.J. DeFrees, D.J. Fox, R.A. Whiteside, R. Seeger, C.F. Melius, J. Baker, R.L. Martin, L.R. Kahn, J.J.P.Stewart, S. Topiol and J.A. Pople, Gaussian, Inc., Pittsburgh PA, 1990.
24. W.J. Hehre, R. Ditchfield and J.A. Pople, J. Chem. Phys. 56 (1972) 2257.
25. P.C. Harihan and J.A. Pople, Theor. Chim. Acta 28 (1973) 213.
26. (a) C. Moller and M.S. Plesset, Phys. Rev. 46 (1934) 618; (b) J.A. Pople, R. Seeger and R. Krishnan Int. J. Quantum Chem., Quantum Chem. Symp. 11 (1977) 149.
27. (a) J.A. Pople, H.B. Schlegel, R. Krishnan, D.J. DeFrees, J.S. Binkley, M.J. Frisch, R.A.Whiteside, R.F. Hout and W.J. Hehre, Int. J. Quantum Chem., Quantum Chem Symp. 15 (1981) 269 .

PART II

ELUSIVE NEUTRALS FROM NRMS EXPERIMENTS

CHAPTER 7

The isomeric C_2NO^+ ions $NCCO^+$, $CNCO^+$, $CCNO^+$ and their neutral counterparts are stable species in the gas-phase.

Introduction

This short chapter demonstrates the use of Neutralization-Reionization (NR) mass spectrometry and Collision Induced Dissociative Ionization (CIDI) experiments for generating and characterizing isomeric neutrals, in this case the $[C_2NO]$ radicals, $NCCO^{\bullet}$, **1**$^{\bullet}$, $CNCO^{\bullet}$, **2**$^{\bullet}$, and $CCNO^{\bullet}$, **3**$^{\bullet}$. (Multiple) Collisional experiments identified the cations that they were produced from *viz.* $NCCO^+$,**1**$^+$, $CNCO^+$, **2**$^+$, and $CCNO^+$, **3**$^+$. Ab initio MO calculations were brought in to support the experimental findings.

The work has been previously communicated under the same title:

G.A. McGibbon, C.A. Kingsmill, J.K. Terlouw and P.C. Burgers

Int. J. Mass Spectrom. Ion Processes 121 (1992) R11-R18.

The recent identification of carbonyl and cyano-containing polycarbon molecules in the interstellar medium [1] has prompted molecular spectroscopists to study the properties of heteroatom cumulenes in the laboratory [2]. A promising mass spectrometric technique to study such elusive species is Neutralization-Reionization Mass Spectrometry (NRMS) [3]. Although the structure information derived from an NR spectrum is limited to the connectivity of the atoms, this versatile technique uses cations or anions and these can often uniquely be generated by dissociative electron ionization of suitable precursor molecules. A case in point forms recent NR work on O=C=C=S [4a,b], polycarbon nitride radicals $C_nN^{\bullet}$ (n = 2-5) [4c], OCCNO$^{\bullet}$ [4d] and the isobaric radicals NCCCO$^{\bullet}$ and NCCNN$^{\bullet}$ [4e,f]. Surprisingly however, the [C_2NO] system has been largely overlooked. Thermochemical data for [C_2NO] ions or neutrals are not available and apart from a brief reference to the stability of the NCCO$^+$ cation [5], ab initio calculations have not been reported on this system.

We therefore feel it expedient to report the identification by Collisional Activation (CA) mass spectrometry of the three isomeric C_2NO^+ ions NCCO$^+$, **1**$^+$, CNCO$^+$, **2**$^+$, and CCNO$^+$, **3**$^+$. NR experiments reveal that their neutral counterparts are also stable in the absence of intermolecular interactions.

The experimental findings are in accordance with our *ab initio* molecular orbital study which we confined to the calculation of the geometries and relative energies of cations and neutrals **1-3** and their dissociation (but not isomerization) reactions of lowest energy requirement.

The C_2NS system was also briefly examined but unfortunately C_2NS^+ ions from various precursor molecules which we anticipated would differ in structure produced CA mass spectra that were virtually identical. Thus no structures could be assigned to the intense survivor signals in their NR spectra.

Results and Discussion

Ions NCCO$^+$ (1$^+$), CNCO$^+$ (2$^+$) and CCNO$^+$ (3$^+$)

Ions 1$^+$ and 2$^+$ are calculated to be minima on the C_2NO^+ potential energy surface. They have $C_{\infty v}$ symmetry and are in a $^1\Sigma$ state. The optimized geometries and relative energies of 1$^+$ and 2$^+$ are shown in Fig. 7.1. Standard unrestricted Hartree-Fock (UHF) calculations on 3$^+$ indicate it is much higher in energy than the more conventional species 1$^+$ and 2$^+$. However, the UHF/6-31G* wavefunction of 3$^+$ has an internal instability [6] and we are currently trying to overcome this problem.

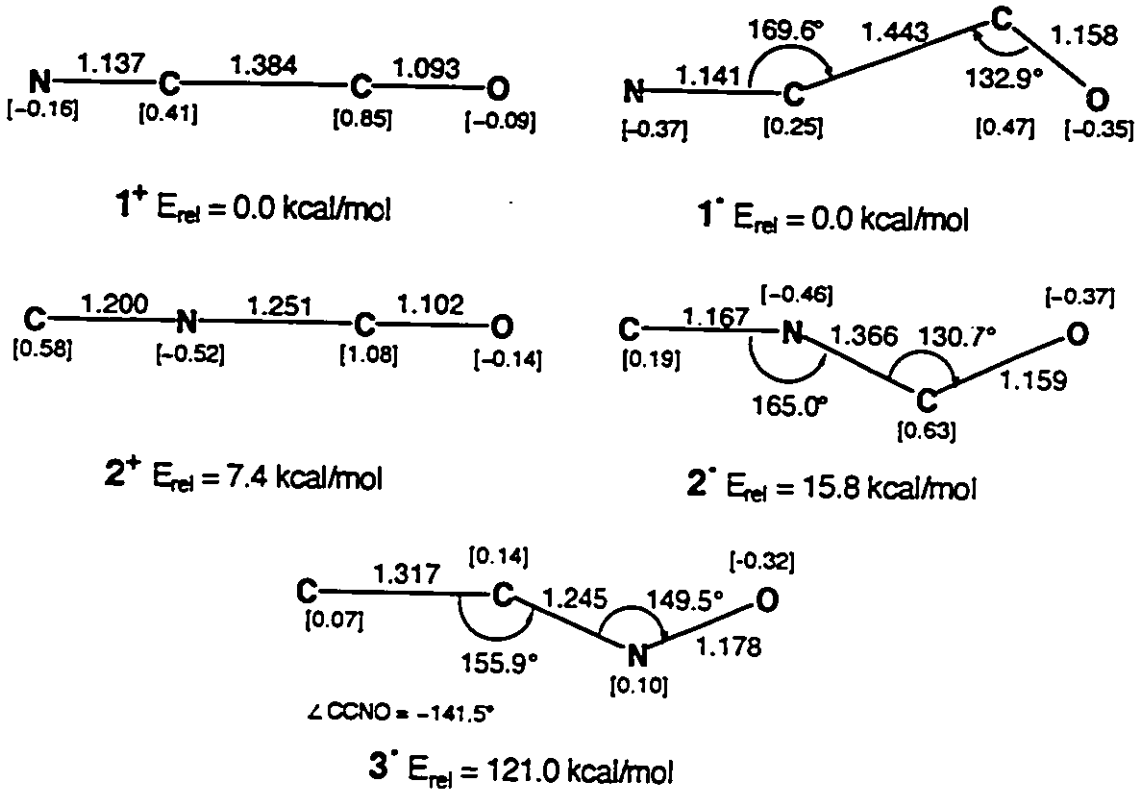

Fig. 7.1 Calculated 6-31G* geometries (bond lengths in ångstroms and E_{rel} values (kcal/mol, UMP3/6-31G* + (0.9) ZPVE) for the C_2NO cations 1$^+$ and 2$^+$ and the neutrals 2* and 3*. Numbers in brackets refer to the charge distribution (in e) derived from a Mulliken population analysis of the UMP3/6-31G*//6-31G* results.

Experimentally, the prominent m/z 54 ions in the 70 eV mass spectra of pyruvonitrile, $N{\equiv}C(C{=}O)CH_3$, and methyl cyanoformate, $N{\equiv}C(C{=}O)OCH_3$ may reasonably be expected to have the connectivity $NCCO^+$, **1**$^+$, whereas ionized methyl isocyanate, CH_3-N=C=O, yields a weak m/z 54 ion (2 % of $M^{\bullet+}$, base peak) which, unless a skeletal rearrangement precedes its formation by the consecutive losses of $H^\bullet$ and H_2 from $M^{\bullet+}$, has the connectivity of ion **2**$^+$, $CNCO^+$.

The m/z 54 ion in the EI mass spectrum of dichloroglyoxime (DCG), HO-N=C(Cl)-C(Cl)=N-OH, is expected to be $CCNO^+$, **3**$^+$, considering that the CA mass spectrum of the prominent m/z 84 ion in the mass spectrum of DCG is dominated by peaks at m/z 54 (loss of NO) and m/z 30 (loss of C_2NO). The m/z 84 ion is most likely $O{\leftarrow}N{\equiv}C{-}C{\equiv}N{\rightarrow}O^{\bullet+}$, formed by direct ionization of cyanogen di-*N*-oxide which is readily produced by the well-documented [7] thermal HCl loss from DCG. However, collision experiments indicate that the source generated m/z 54 ions are not exclusively generated from $O{\leftarrow}N{\equiv}C{-}C{\equiv}N{\rightarrow}O^{\bullet+}$ but that there is also a contribution from the reaction sequence 85^+ ($HO{-}N{=}C{-}C{\equiv}N{\rightarrow}O^+$ (?)) $\rightarrow$ 68^+ ($N{\equiv}C{-}C{\equiv}N{\rightarrow}O^+$(?)) + $OH^\bullet$ $\rightarrow$ 54^+ (C_2NO^+) + $N^\bullet$. Double collision experiments [8] on the m/z 54 ions generated by collision induced dissociation from both m/z 84 and m/z 68 ions revealed that the m/z 54 ions from m/z 84 are fully compatible with structure **3**$^+$ (see below), but those derived from m/z 68 are either a mixture of **1**$^+$ and **3**$^+$ or they represent a fourth stable (cyclic) isomer. In agreement with these observations, *source* generated C_2NO^+ ions from DCG are *not* ions of a single structure so here we confine ourselves to the analysis of the CA and NR spectra of m/z 54 ions generated by the route $84^{\bullet+} \rightarrow 54^+ + NO$ and the Collision Induced Dissociative Ionization (CIDI) [3] of the C_2NO neutral produced in the reaction $84^{\bullet+} \rightarrow NO^+ + C_2NO$. Table 7.1 shows the characteristically different CA mass spectra of the three isomers.

Table 7.1. CA mass spectra* of the C_2NO^+ isomers 1^+-3^+

ION m/z →	42	40	38	30	28	26	24	16	14	12
1^+	25	160	120	10	910	1000	30	5	20	125
2^+	60	90	120	10	870	1000	30	5	20	130
3^+	40	10	100	1000	110	120	140	-	5	30

* Peaks normalized to base peak in CA spectrum = 1000; spectra obtained in the 3FFR, collision gas He.

The direct bond cleavage reactions of lowest energy requirement from isomers 1^+ and 2^+ are $1^+/2^+ \rightarrow CO^{\bullet+} + CN^{\bullet}$ ($\Sigma\Delta H_f$ products = 403 kcal/mol [9]) and $1^+/2^+ \rightarrow CN^+ + CO$ ($\Sigma\Delta H_f$ products = 401 kcal/mol [9]) and indeed peaks at m/z 26 (CN^+) and m/z 28 ($CO^{\bullet+}$) dominate their CA spectra, see above. For 3^+ the direct bond cleavage reaction of lowest energy requirement is $3^+ \rightarrow NO^+ + C_2$ ($\Sigma\Delta H_f$ products = 434 kcal/mol [9]).This reaction accounts for the base peak in the spectrum at m/z 30 and it uniquely characterizes this isomer.

Ions 1^+ and 2^+ show structure diagnostic differences in the peak intensity ratio m/z 38 : m/z 40 : m/z 42. Without any rearrangement, ions 1^+ are expected to yield m/z 38 (CCN^+, loss of $O^{\bullet}$) and m/z 40 (C_2O^+, loss of $N^{\bullet}$) ions but not m/z 42 (loss of $C^{\bullet}$). For ions 2^+ we would expect m/z 38 (CNC^+, loss of $O^{\bullet}$) and m/z 42 (NCO^+, loss of $C^{\bullet}$) but not m/z 40 (C_2O^+, loss of $N^{\bullet}$). Although the observed ratios indicate that 1^+ and 2^+ undergo a partial (post collisional?) interconversion, possibly via intermediates akin to those proposed for $C_2N_2^{\bullet+}$ [10], they do show that the ions have largely retained their structural integrity. This is further corroborated by the NR spectra, see below. Note also that the m/z 38 : m/z 40 : m/z 42 ratio for 3^+ shows that it readily loses $O^{\bullet}$ and $C^{\bullet}$ but not $N^{\bullet}$.

We have also investigated the structures of the m/z 38 and m/z 42 ions generated in the CA spectra of ions 1^+-3^+ by performing double collision experiments. For C_2N^+

ions two stable structures are known, *viz.* CCN$^+$ and CNC$^+$ [11] whereas the Schwarz group has shown that m/z 42 ions of atom connectivity NCO$^+$ and CNO$^+$ can readily be distinguished by collision experiments [4d]. The collision induced loss of O$^\bullet$ from **1**$^+$ is expected to yield m/z 38 ions of connectivity CCN$^+$ while that from **2**$^+$ would give CNC$^+$. However, the 3FFR [He] CA spectra of m/z 38 ions generated by collisional activation of ions **1**$^+$ and **2**$^+$ were indistinguishable showing the following intensity distribution: m/z 12 [100%], m/z 14 [3%], m/z 24 [24%], m/z 26 [78%]. We observed exactly the same intensity distribution in the CA mass spectrum of the source generated C_2N^+ ions from $CH_3C{\equiv}N$ [11a] and we therefore question whether collision experiments can really distinguish the two isomers [4c,f].

In contrast, the m/z 42 ions from **1**$^+$ and **2**$^+$ could readily be identified as having the structure NCO$^+$ (m/z 12 [13%], m/z 14 [32%], m/z 16 [6%], m/z 26 [39%], m/z 28 [100%], m/z 30 [37%]) while **3**$^+$ produced CNO$^+$ (m/z 12 [9%], m/z 14 [24%], m/z 16 [4%], m/z 26 [45%], m/z 28 [75%], m/z 30 [100%])

The neutrals NCCO$^\bullet$ (1), CNCO$^\bullet$ (2) and CCNO$^\bullet$ (3)

The calculations indicate that the neutral counterparts of **1**$^+$, **2**$^+$ and **3**$^+$ are local minima on the $C_2NO^\bullet$ potential energy surface. Neutral **1**$^\bullet$ is, by 15.8 kcal/mol, more stable than **2**$^\bullet$, while **3**$^\bullet$ is much higher, 101.8 kcal/mol relative to **1**$^\bullet$. Geometrically though the ions and neutrals are quite different since the latter are all non-linear and CCNO$^\bullet$ is not even planar, see Fig. 7.1. Assuming there are no barriers for the reverse reactions, the energetically most favoured direct dissociation of the three neutrals is: **1**$^\bullet$/**2**$^\bullet$ → CO + CN$^\bullet$ and **3**$^\bullet$ → C_2 + NO. However, considering that $\Sigma\Delta H_f$ [C_2 + NO] is 143 kcal/mol [9] higher than $\Sigma\Delta H_f$ [CO + CN$^\bullet$], neutral **3**$^\bullet$ will only be a viable species if the height of the barrier for the isomerization **3**$^\bullet$ → **1**$^\bullet$/**2**$^\bullet$ exceeds 84 kcal/mol, the value for the energy difference between **3**$^\bullet$ and its dissociation products C_2 ($^1\Sigma_g$) + NO ($^2\Pi$) as derived from our *ab initio* calculations.

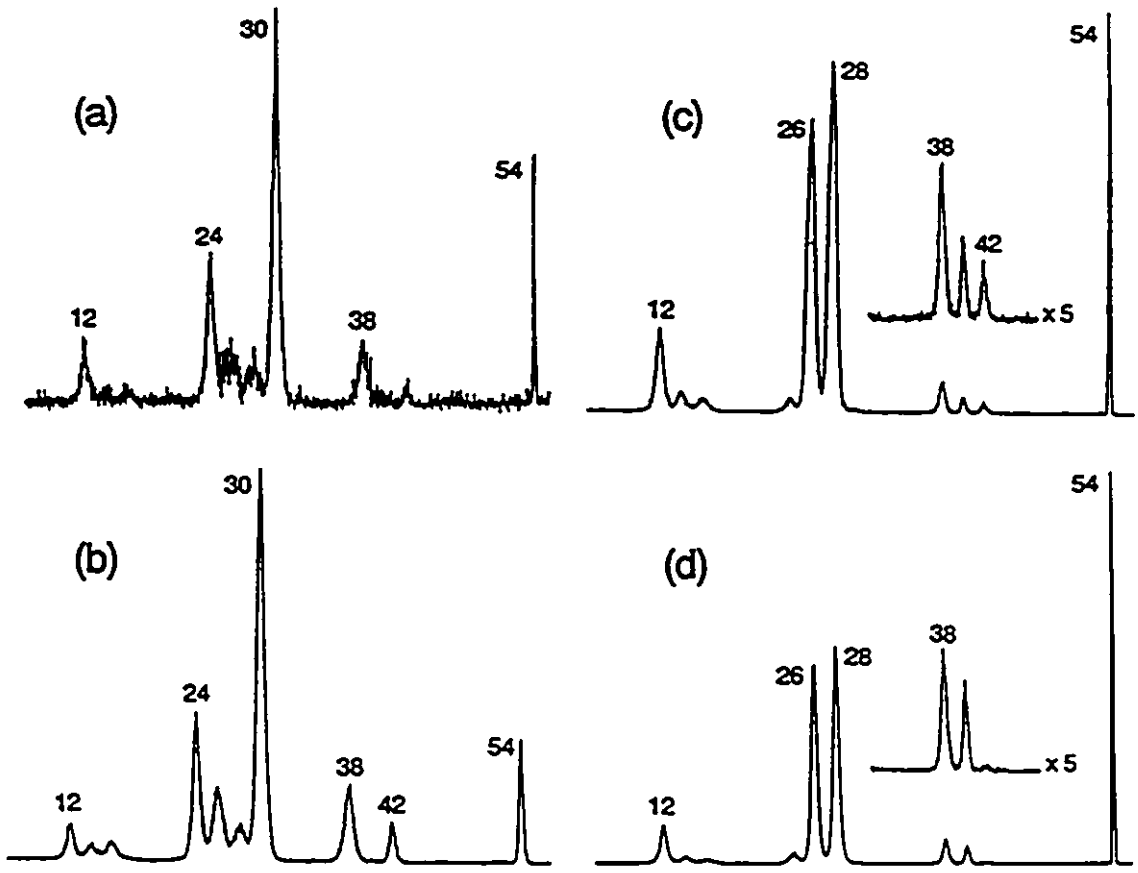

Fig. 7.2 (DMA,O_2) NR mass spectrum of product ions 3^+ from the collision induced dissociation $84^{\bullet+}$ [O←N≡C-C≡N→$O^{\bullet+}$] → $54^{\bullet+}$ [$CCNO^+$] + NO; (b) (O_2) CIDI spectrum of neutrals **3** generated by the collision induced dissociation $84^{\bullet+}$ [O←N≡C-C≡N→$O^{\bullet+}$] → $54^{\bullet}$ [$CCNO^{\bullet}$] + NO^+; (c) and (d) (DMA,O_2) NR spectra of the C_2NO^+ ions 2^+ and 1^+, generated from methylisocyanate and pyruvonitrile respectively.

That **3**• is indeed a stable neutral species follows immediately from its NR spectrum which is shown in Figure 7.2a: the spectrum (which was obtained by neutralizing the m/z 54 ions generated by the [He] collision induced dissociation of m/z 84 ions (see above) in the 1FFR of the instrument) displays an intense survivor signal and structure characteristic peaks at m/z 30 (NO^+), m/z 24 (C_2^+) , m/z 38 and m/z 42 but **not** m/z 40. Further evidence for the stability of neutral **3**• comes from the CIDI spectrum of the metastable m/z 84 ions which decompose into $NO^+ + C_2NO$ and $C_2NO^+ + NO$. The spectrum, see Fig. 7.2b, displays an intense peak at m/z 54 and the fragment ions are in keeping with the proposed CCNO connectivity of the neutral.

The NR mass spectra of **1**$^+$ and **2**$^+$ are shown in Fig. 7.2c and 7.2d respectively. Here, the survivor signal dominates the NR spectrum pointing to neutrals of high stability. Once again the ratio of the m/z 38 : m/z 40 : m/z 42 high energy dissociation products reveals that the neutrals **1**• and **2**• have largely retained their structural integrity. Note the telltale peak at m/z 42 in the two spectra : it is conspicuously weak in the NR mass spectrum of **1**$^+$, in agreement with the proposed NCCO connectivity of the neutralized ion which cannot yield $[C,N,O]^+$ ions without rearranging.

Theoretical methods

The *ab initio* MO calculations were performed using the GAUSSIAN 90 series of programs employing UHF procedures [6]. Optimized geometries, harmonic frequencies and scaled [12] zero-point vibrational energies were calculated with the 6-31G• split level basis set. [13] Correlation was included at the MP3 level of theory [14]. All UHF/6-31G• wavefunctions were tested for internal stability. For **3**•, because of spin contamination problems ($\langle s^2 \rangle = 1.535$), the relative energy ($E_{rel}$) is obtained from the projected UMP3/6-31G•//6-31G• energy value [15].

REFERENCES

1 (a) G. Winnewisser and E. Herbst, Topics in Current Chemistry, 139 (1987) 121; (b) D. Smith and N. G. Adams, J. Chem. Soc., Faraday Trans. 2, 85 (1989) 1613; (c) A. R. Newman, Anal. Chem., 62 (1990) 671A.

2 (a) M. C. L. Gerry, F. Stroh and M. Winnewisser, J. Mol. Spectrosc. 140 (1990)147; (b) H. E. Warner and T. Amano, J. Mol. Spectrosc. 145 (1991) 66; (c) A. D.Walters, M. Winnewisser, K. Lattner and B. Winnewisser, J. Mol. Spectrosc. 149 (1991) 542; (d) F. Holland and M. Winnewisser, J. Mol. Spectrosc. 149 (1991) 45.

3 Reviews: (a) C. Wesdemiotis, F.W. McLafferty, Chem. Rev. 87 (1987) 485; (b) J.K. Terlouw, H. Schwarz, Angew. Chem. Int. Ed. Engl. 26 (1987) 805; (c) H. Schwarz, Pure Appl. Chem. 61 (1989) 685; (d) J.L. Holmes, Adv. Mass Spectrom.11 (1989) 53; (e) J.K. Terlouw, Adv. Mass Spectrom. 11 (1989) 984; (f) J.L. Holmes, Mass Spectrom. Rev. 8 (1989) 513; (g) F.W. McLafferty, Science247 (1990) 990; (h) F.W. McLafferty, Adv. Mass Spectrom. 12 (1992) in press.

4 (a) D. Sülzle, J.K. Terlouw and H. Schwarz, J. Am. Chem. Soc. 112 (1990) 628; (b) D. Sülzle and H.Schwarz, in Fundamentals of Gas Phase Ion Chemistry, K. R. Jennings (ed.), Kluwer: Dordrecht (1991) p. 237; (c) D. Sülzle, K. Seemayer, B. Witulski, H. Hopf and H. Schwarz, Chem. Ber. 124 (1991) 1481; (d) D. Sülzle, P.E. O'Bannon and H. Schwarz, Chem. Ber. 125 (1992) 279; (e) C.A. Muedas, D. Sülzle and H. Schwarz, Int. J. Mass Spectrom.113 (1992) R17; (f) C.A. Muedas, D. Sülzle and H. Schwarz, Chem. Ber. 125 (1992) 1517.

5 P. Pyykkö and N. Runeburg, J. Mol. Struc. (Theochem), 234 (1991) 269.

6 Gaussian 90 : M.J. Frisch, M. Head-Gordon, G.W. Trucks, J.B. Foresman, H.B. Schlegel, K.Raghavachari, M.A. Robb, J.S. Binkley, C. Gonzales, D.J. DeFrees, D.J. Fox, R.A. Whiteside, R. Seeger, C.F. Melius, J. Baker, R.L. Martin, L.R. Kahn, J.J.P.Stewart, S. Topiol and J.A. Pople, Gaussian, Inc., Pittsburgh PA, 1990.

7 (a) C. Grundmann, V. Mini, J.M. Dean, H.-D Frommeld, Justus Liebigs Ann. Chem. 687 (1965) 191; (b) G. Maier and J.H. Teles, Angew. Chem. Int. Ed. Engl. 26 (1987) 155.

8 S. Villeneuve and P.C. Burgers, Org. Mass Spectrom. 21 (1986) 733.

9 S. G. Lias, J. E. Barthmess, J. F. Liebman, J. L. Holmes, R. D. Levin and W.G. Mallard, J. Phys. Chem. Ref. Data, Suppl. 17, 1988.

10 F. M. Bickelhaupt, R. H. Fokkens, L. J. De Koning, N. M. M. Nibbering, E. J. Baerends, S. J. Goede and F. Bickelhaupt, Int. J. Mass Spectrom. Ion Proc. 103 (1991) 157.

11 (a) J. S. Knight, S. A. H. C. G. Freeeman, M. J. McEwan, A. D. McLean and D. J. DeFrees, J. Am. Chem. Soc. 110 (1988) 5286; (b) P. W. Harland and R. G. A. R. Maclagan, J. Chem. Soc., Faraday Trans.2, 83 (11) (1987) 2133.

12. (a) J.A. Pople, H.B. Schlegel, R. Krishnan, D.J. DeFrees, J.S. Binkley, M.J. Frisch, R.A.Whiteside, R.F. Hout and W.J. Hehre, Int. J. Quantum Chem., Quantum Chem Symp. 15 (1981) 269.

13 P.C. Harihan and J.A. Pople, Theor. Chim. Acta 28 (1973) 213.

14 (a) C. Moller and M.S. Plesset, Phys. Rev. 46 (1934) 618; (b) J.A. Pople, R. Seeger and R. Krishnan Int. J. Quantum Chem., Quantum Chem. Symp. 11 (1977) 149.

15 (a) P.-O. Löwdin, Phys. Rev. 97 (1955) 1509; (b) H.B. Schlegel, J. Chem. Phys. 84 (1986) 4530.

CHAPTER 8

Elusive carbenes by neutralization-reionization mass spectrometry.

Preamble

This chapter demonstrates how two elusive prototype carbenes could be positively identified using the MS/MS/MS technique of collisional activation of neutralization-reionization *survivor* ions (NR/CA) when information from NR mass spectra was insufficient for unambiguous structure assignment to the neutral species.

NR mass spectra invariably contain contributions from other processes, see the introduction and chapter 9, which may invalidate their comparison with reference CA mass spectra. This is particularly true of systems where the CA mass spectra of isomeric ions are similar in appearance. Fortunately, it is possible to circumvent these problems by probing the structure of the *survivor* ions directly in a NR/CA experiment. This involves selectively transmitting the *survivor* ions formed in the 2FFR NR process through E_1 to the 3FFR where their CA mass spectrum is obtained by scanning E_2. The NR/CA mass spectrum reflects the behaviour of the non-decomposing neutrals. If these species do not isomerize, then the NR/CA mass spectrum should be very close to the CA mass spectrum. Conversely, if the NR/CA mass spectrum is the same as the CA mass spectrum, then it can be concluded that the neutral species is stable within the microsecond time scale of the experiment.

This technique has been applied to $H_2N\text{-}C\text{-}NH_2^{\bullet+}$ and $HO\text{-}C\text{-}OH^{\bullet+}$ in order to unambiguously identify diaminocarbene, $H_2N\text{-}\ddot{C}\text{-}NH_2$ and dihydroxycarbene, $HO\text{-}\ddot{C}\text{-}OH$.

The work that is presented here is based on a pair of recently published articles with the title of each appearing at the beginning of the appropriate section.

8.1) Experimental evidence for gaseous diaminocarbene $H_2N\text{-}\ddot{C}\text{-}NH_2$ and its radical cation.*

Introduction

Carbenes are important reactive intermediates and considerable effort has been expended to produce and study a variety of these species [1-3]. The nature of the substituents strongly influences a carbene's reactivity and stability [1,2]; the presence of electronegative or π-donating substituents stabilizing the singlet state relative to the triplet state so that (di)aminocarbenes are expected to be nucleophilic with singlet ground states [4-6].

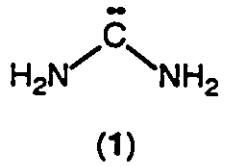

(1)

diaminocarbene

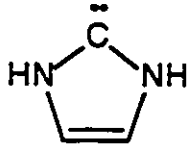

imidazol-2-ylidene

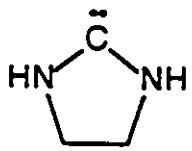

imidazolin-2-ylidene

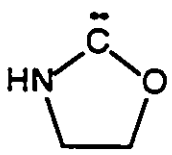

2-oxazolidinylidene

Indeed, appropriate substitution enabled Arduengo and co-workers [7] to isolate several cyclic imidazol-2-ylidene type carbenes as stable crystalline materials. Recent calculations [8] on model diaminocarbenes indicate that the reluctance of imidazol-2-ylidenes to dimerize relates to their large singlet-triplet gap ($\Delta E_{S\text{-}T}$ = 84.5 [8], 79.4 [4] kcal/mol for the prototype shown above). In contrast, the C-C saturated imidazolin-2-ylidenes, which dimerize spontaneously when generated in solution [9], have smaller gaps ($\Delta E_{S\text{-}T}$ = 69.4 kcal/mol for the prototype [8]). High reactivity is therefore anticipated for the parent diaminocarbene $H_2N\text{-}\ddot{C}\text{-}NH_2$ (1) for which $\Delta E_{S\text{-}T}$ = 58.5 [8] or 50.7 [6] kcal/mol.

* P.C. Burgers, G.A. McGibbon and J.K. Terlouw, *Chem. Phys. Letters 224 (1994) 539-543.*

This and the limited number of potential precursors [10], make the prospects for generating the simple aminocarbenes as persistent species in the condensed phase slim. On the other hand, the related "archetypal" nucleophilic carbene, dimethoxycarbene, has been observed in the condensed phase [11], but it and the previously unknown cyclic 2-oxazolidinylidene could also conveniently be generated and characterized in the dilute gas phase of a mass spectrometer [12], an excellent medium for the study of reactive species. The absence of intermolecular interactions in the gas phase has also enabled the generation and identification of several other simple carbenes, including H-$\ddot{C}$-OH [13], F-$\ddot{C}$-OH [14], H_3C-$\ddot{C}$-OH [15], and HO-$\ddot{C}$-NH_2 [16], by one-electron reduction of their corresponding radical cations using the technique of Neutralization-Reionization mass spectrometry (NRMS) [17,18]. Critical to the success of these experiments is: (i) that a beam of carbene ions free from isomeric and isobaric interferences can be obtained by dissociative ionization of some appropriate precursor molecule(s) and (ii) that substantial energy barriers restrict the carbene ion, and its neutral counterpart, from freely interconverting with their isomeric forms. Theory predicts [8] that diaminocarbenes have significant energy barriers for 1,2-hydrogen shifts, 50 kcal/mol for H_2N-$\ddot{C}$-NH_2 (1) → H_2N-C(H)=NH (2), and thus they should be kinetically stable. Moreover, our ab initio MO calculations predict that the ions H_2N-C-$NH_2^{\bullet+}$ ($1^{\bullet+}$) and H_2N-C(H)=$NH^{\bullet+}$ ($2^{\bullet+}$) are also stable and that they are separated by a significant energy barrier and criterion (ii) is thereby satisfied.

In the first section of this chapter the generation and identification of the prototype diaminocarbene H_2N-$\ddot{C}$-NH_2 from its radical cation, by Neutralization-Reionization mass spectrometry in conjunction with multiple collision experiments, is discussed.

Theoretical Section

The relative energies of $1^{\bullet+}$, $2^{\bullet+}$ and the transition state for $1^{\bullet+}$ → $2^{\bullet+}$ were calculated at the UMP3/6-31G*// HF /6-31G* + ZPVE (0, 6.4 and 59.3 kcal/mol) and MP2/6-31G*

+ ZPVE (0, 9.8 and 59.8 kcal/mol) levels of theory using the Gaussian 92 suite of programs [22]. Appropriate frequency calculations on the HF and MP2 optimized geometries gave the correct number of negative eigenvalues. In addition, GAUSSIAN-2 (G2) theory [23] energies were obtained for neutral and ion **1**, −149.71607 E_h and −149.42675 E_h respectively, from which [24] ΔH_f^0 (**1**) = 39.4 kcal/mol and ΔH_f^0 ($\mathbf{1}^{\bullet+}$) = 221.0 kcal/mol. The corresponding MP2(FULL)/6-31G* geometries (C_{2v}) are:

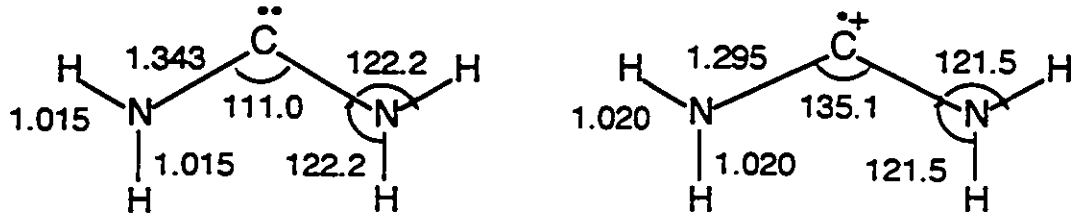

Results and Discussion

In the context of generating the carbene $H_2N\text{-}\ddot{C}\text{-}NH_2$ (**1**) and the isomeric amidine $H_2N\text{-}C(H)=NH$ (**2**), it is of interest to note that many of the carbenes generated in solution are generated from amidines: Graham oxidation [25] of an amidine yields a diazirine which, upon elimination of N_2, may form a carbene [1,2,26]. However, simple amino substituted diazirines are not stable [1,8,26] and so other precursor molecules are required for the generation of ionic or neutral **1**. A potential source of carbene ions (**1**) are the m/z 44 $CH_4N_2^{\bullet+}$ ions (25% of base peak m/z 74) found in the 70 eV mass spectrum of aminoguanidine (**I**) [27]. As indicated in Scheme 8.1, **I** could yield ions of the desired structure $H_2N\text{-}C\text{-}NH_2^{\bullet+}$ ($\mathbf{1}^{\bullet+}$) if the loss of N_2H_2 is preceded by a 1,4-H shift. However, a 1,4-H shift could, in principle, also lead to the ylid ion $H_3N\text{-}C{=}NH^{\bullet+}$ ($\mathbf{3}^{\bullet+}$) while a 1,3-H shift would yield $\mathbf{2}^{\bullet+}$.

That most or all of the m/z 44 ions formed from **I** have structure $\mathbf{1}^{\bullet+}$ follows from a comparison of their metastable ion (MI) and CA mass spectra (Figure 8.1) with those for authentic ions $\mathbf{2}^{\bullet+}$, generated from formamidine hydrochloride (**II**) as shown in Scheme

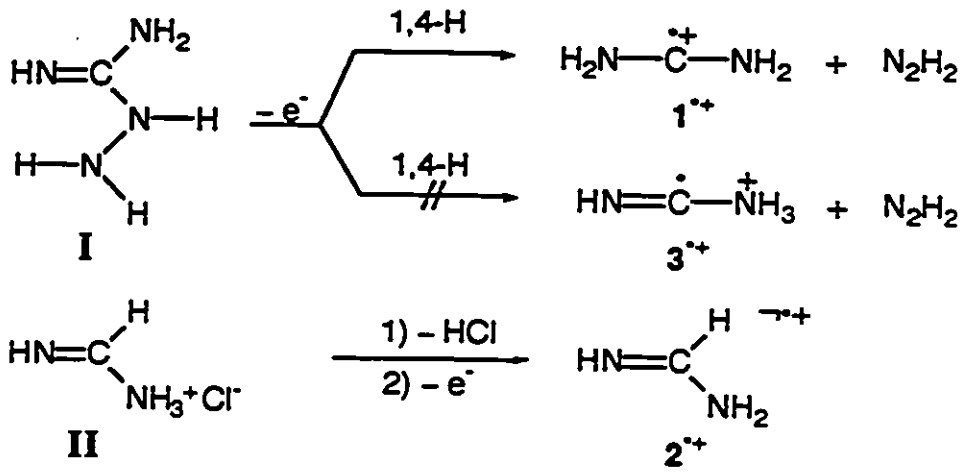

Scheme 8.1

8.1 [#1]. Considering the minimum enthalpies of formation of the potential dissociation products, see Table 8.1, it follows that the differences between the spectra of the two species are structure characteristic.

For ionized formamidine, the rearrangement reaction $2^{\bullet+} \rightarrow NH_3^{\bullet+} + HCN$ (associated kinetic energy release, $T_{0.5}$ [29] = 268 meV) is the dominant reaction of the metastable ions and even in the CA mass spectrum it competes effectively with the structure diagnostic direct cleavage process yielding $HNCH^+$ (m/z 28).

[#1] The intensity of m/z 44 has been reported [24] to be only 4% of the base peak at m/z 42. We found that m/z 44 was c. 3 times more intense than m/z 42 and c. 30 % of the base peak at m/z 36 ($H^{35}Cl^{\bullet+}$) Peaks were also observed at m/z 81 (70%), m/z 54 (50%), and 53 (20%). They originate from thermal decomposition into *s*-triazine, which does not interfere with the mass spectrometric experiments but frustrated attempts to obtain the photo-electron spectrum of 2.

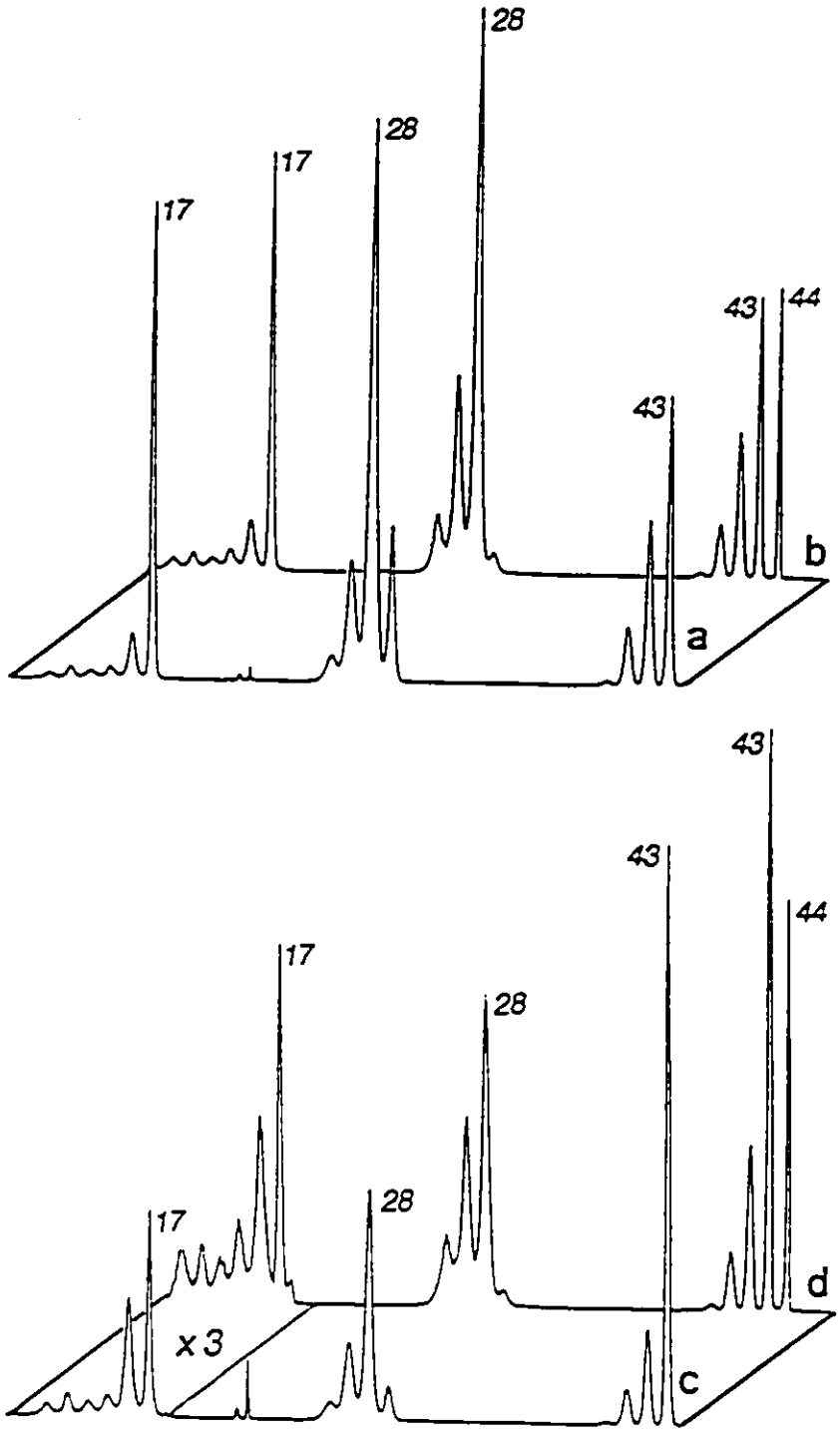

Fig. 8.1 [O_2] Collisional Activation (CA) and [NDMA/O_2] Neutralization-Reionization (NR) mass spectra (2FFR) of m/z 44 formamidine ions $1^{\bullet+}$, items **a** and **b** respectively, and m/z 44 diaminocarbene ions $2^{\bullet+}$, items **c** and **d** respectively. The m/z 12-17 region in spectra **c** and **d** has been amplified by 3x.

Table 8.1. Combined enthalpies[a] of selected $CH_4N_2^{\bullet+}$ dissociation products

m/z	ion		neutral(s)	$\Sigma\Delta H_f$
43	$H_2N\text{-}C{=}NH^+$	+	$H^\bullet$	286
42	$H_2N\text{-}CN^{\bullet+}$	+	H_2	272
29	$H_2N\text{-}CH^{\bullet+}$	+	NH	348
	$HN{=}CH_2^{\bullet+}$	+	NH	335
28	$HNCH^+$	+	$NH_2^\bullet$	271
	H_2NC^+	+	$NH_2^\bullet$	310
27	$HCN^{\bullet+}$	+	NH_3	335
	$HNC^{\bullet+}$	+	NH_3	325
18	NH_4^+	+	$CN^\bullet$	255
17	$NH_3^{\bullet+}$	+	HCN	255
	$NH_3^{\bullet+}$	+	HNC	271
16	NH_2^+	+	$HCN{+}H^\bullet$	386
	NH_2^+	+	$HNC{+}H^\bullet$	402

[a] Values in kcal/mol from ref. 30

Assuming that the latter has no reverse energy term, this rearrangement must occur below the dissociation limit for loss of $NH_2^\bullet$, situated at 271 kcal/mol. Note that an ion-dipole complex of the type $[H_3N\cdots CNH]^{\bullet+}$ in which the HCN dipole can freely rotate is probably not involved as a long-lived intermediate in the rearrangement $\mathbf{2}^{\bullet+} \rightarrow NH_3^{\bullet+} +$ HCN: such an ion is (see Table 8.1) expected to co-generate $NH_4^+ + {}^\bullet CN$, but there is virtually no m/z 18 peak in the CA mass spectrum of $\mathbf{2}^{\bullet+}$.

For the $CH_4N_2^{\bullet+}$ ion derived from **I**, the preferential loss of $H^\bullet$ observed in both its MI (loss of $H^\bullet$ 100 %, loss of HCN 5%) and its CA mass spectrum is readily rationalized in terms of the proposed carbene structure $\mathbf{1}^{\bullet+}$. Both $\mathbf{1}^{\bullet+}$ and $\mathbf{2}^{\bullet+}$ can lose $H^\bullet$ by direct bond cleavage to yield the same m/z 43 $H_2N\text{-}C{=}NH^+$ product ion. However, ion $\mathbf{2}^{\bullet+}$ preferentially loses $NH_2^\bullet$ by a competing direct bond cleavage of lower energy requirement, to yield $HCNH^+$ (m/z 28), while for $\mathbf{1}^{\bullet+}$ such a direct loss of $NH_2^\bullet$ is disfavoured since it leads to the high energy $[C,H_2,N]^+$ isomer, H_2NC^+, whose calculated minimum energy requirement lies above that for $H^\bullet$ loss, see Table 8.1. The ylid ion $\mathbf{3}^{\bullet+}$

does not contribute significantly (or at all, see below) to the $CH_4N_2^{\bullet+}$ ions generated from I since $\mathbf{3}^{\bullet+}$ is expected to yield MI and CA mass spectra that are dominated by m/z 17 ($NH_3^{\bullet+}$), the direct bond cleavage reaction of lowest energy requirement, and this is not observed. Note also that the carbene ion $\mathbf{1}^{\bullet+}$ is more susceptible to charge stripping than $\mathbf{2}^{\bullet+}$ as evidenced by the more intense narrow peak at m/z 22 ($H_2N\text{-}C\text{-}NH_2^{++}$).

As mentioned above, the products $H_2NC^+ + NH_2^{\bullet}$ are energetically less favourable than $H_2N\text{-}C{=}NH^+ + H^{\bullet}$ yet it follows from a comparison of the MI and CA mass spectra that the relative intensity of m/z 28 greatly increases upon collisional activation. The most likely explanation is that ion $\mathbf{1}^{\bullet+}$ undergoes a **post**-collisional isomerization to $\mathbf{2}^{\bullet+}$ so that it can then produce the more stable m/z 28 ($HNCH^+$) ions. To verify this proposal, the m/z 28 ions generated by collision-induced dissociation of $\mathbf{1}^{\bullet+}$ in the 2FFR were selectively transmitted through E_2 to the 3FFR where they were subjected to collisional activation. Comparison of the resulting CA mass spectra (not shown) with reference spectra [31] confirmed that the m/z 28 ions from $\mathbf{1}^{\bullet+}$ (and as expected also those from $\mathbf{2}^{\bullet+}$) indeed have the structure $HNCH^+$. These observations put the height of the tautomerization barrier $\mathbf{1}^{\bullet+} \rightarrow \mathbf{2}^{\bullet+}$ at or above the dissociation limit for loss of $H^{\bullet}$, at 286 kcal/mol, but below that for $H_2NC^+ + NH_2^{\bullet}$, at 310 kcal/mol. This result is in reasonable agreement with our quantum chemical calculations which predict that the transition state energy for the slightly endothermic isomerization $\mathbf{1}^{\bullet+} \rightarrow \mathbf{2}^{\bullet+}$ is 281 kcal/mol based on ΔH_f^0 ($\mathbf{1}^{\bullet+}$) = 221 kcal/mol obtained using G2 theory [23,24]. Thus our experiments indicate that ions $\mathbf{1}^{\bullet+}$ and $\mathbf{2}^{\bullet+}$ are distinct stable species albeit that $\mathbf{1}^{\bullet+}$ can undergo post-collisional isomerization to $\mathbf{2}^{\bullet+}$.

The NR mass spectra of $\mathbf{1}^{\bullet+}$ and $\mathbf{2}^{\bullet+}$ (Figure 8.1b and 8.1d) both show intense survivor ion signals at m/z 44 and moreover, the two spectra are considerably different. Comparison with the CA mass spectra, shows that for $\mathbf{2}^{\bullet+}$ the structure characteristic peak intensity ratios of the CA and NR mass spectra are similar [#2], thus indicating that neutral **2** has retained its structural integrity. For $\mathbf{1}^{\bullet+}$, however, the differences between

the CA and NR mass spectra are much more pronounced: the m/z 28 and m/z 41-43 peaks are relatively less intense in the NR mass spectrum and m/z 17 is more intense and this raises the question whether the neutralized ion has also retained its structure.

There are two possible explanations for the discrepancy between the CA and NR mass spectra of $1^{\bullet+}$. One is that "interference" signals, which may arise from neutrals formed from metastable ions, from collisionally activated ions or from excited neutralized precursors, significantly contribute to the NR mass spectrum. In this context we note that **2** is calculated to have an even higher barrier towards dissociation into NH_3 + HCN (80 kcal/mol [32]) than for its isomerization into **1** (73 kcal/mol [8]) and so it is not really surprising that its CA and NR mass spectra are so similar. However, for $1^{\bullet+}$ a more disconcerting possibility is that the neutral diaminocarbene formed by the (vertical) electron transfer has sufficient internal energy (> 50 kcal/mol [8]) to isomerize to the more stable formamidine molecule **2**.

Analysis of mass selected *survivor* ions by collision induced dissociation avoids the above mentioned interferences in NR spectra and this new technique is therefore uniquely suited to distinguish between these two possibilities. The resulting NR/CA mass spectrum reflects the behaviour of the **non**-decomposing neutrals: if these species do not isomerize and if the primary ion beam was "pure", then the NR/CA spectrum should be very close to the CA mass spectrum.

[#2] The CA, but not the NR, mass spectrum of $2^{\bullet+}$ contains a relatively intense m/z 29 peak (likely $H_2N\text{-}C\text{-}H^{\bullet+}$ formed by direct loss of NH), ratio m/z 29/ m/z 28 = 0.26. In 10 keV [O_2] CA mass spectra m/z 29 becomes even more intense (ratio = 0.40). When He is used as collision gas the CA and the NR mass spectra show the same low m/z 28 /29 ratio (0.06). This peculiar behaviour of O_2 as a collision gas parallels similar observations made for $HN{=}C(H)\text{-}OH^{\bullet+}$ [16c] but for which there is, at present, no explanation.

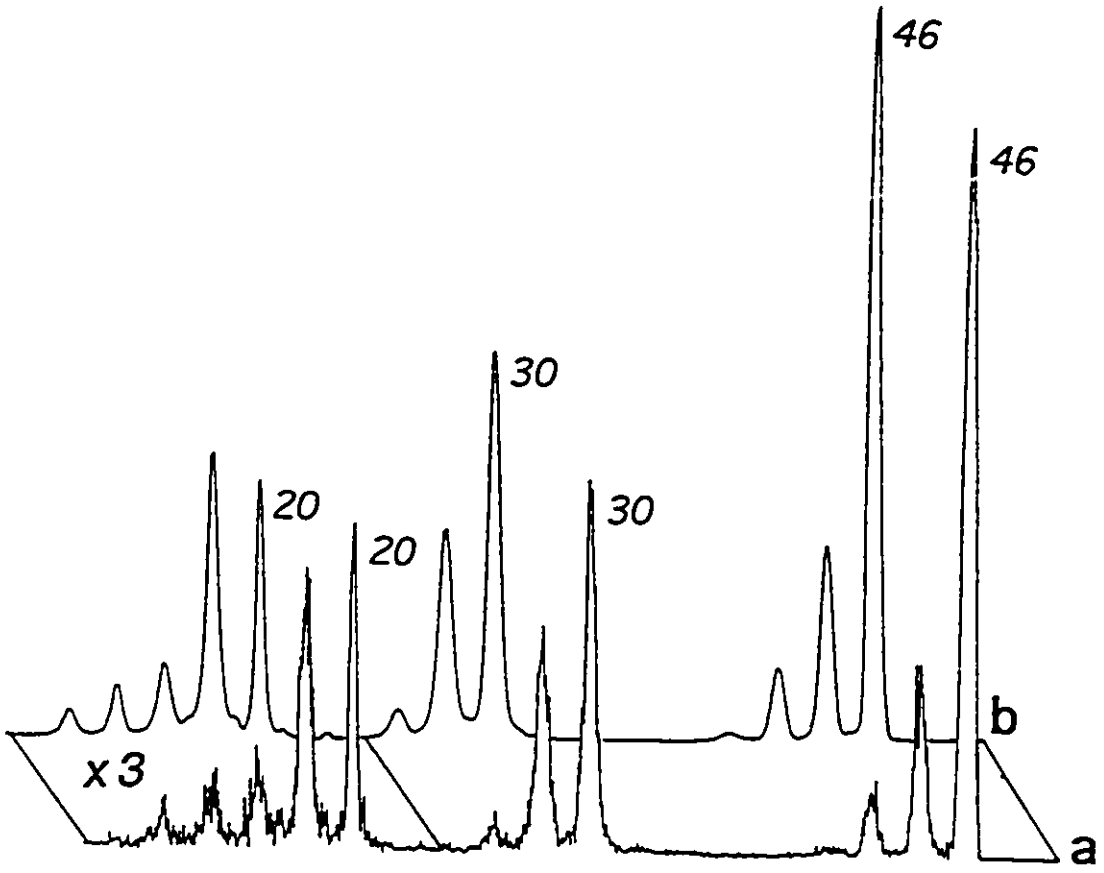

Fig. 8.2 Collisional Activation (CA) mass spectra of m/z 48 $D_2N\text{-}C\text{-}ND_2^{\bullet+}$ ions [3 ffr, He] generated from the *survivor* ions in the [NDMA/O_2] NR spectrum, item **a**, and from source generated ions, item **b**. The m/z 12-20 region in both spectra has been amplified by 3x.

Such spectra were obtained for both $\mathbf{1}^{\bullet+}$ and its deuterium labelled isotopomer $D_2N\text{-}C\text{-}ND_2^{\bullet+}$, $\mathbf{1a}^{\bullet+}$ and Fig. 8.2 compares the NR/CA mass spectrum of $\mathbf{1a}^{\bullet+}$ (Fig. 8.2a) with that of the source generated ions (Fig. 8.2b) [#3]. It is evident that the two spectra are virtually superimposable and thus the neutral carbene must have retained its structural integrity in the processes $\mathbf{1}^{\bullet+} \rightarrow \mathbf{1} \rightarrow \mathbf{1}^{\bullet+}$. Moreover, since the combined neutralization/collisional ionization efficiency of isomeric species will only be the same by coincidence, the original ion beam must have consisted of only one isomeric form, i.e. the source generated $CH_4N_2^{\bullet+}$ ions from aminoguanidine indeed have exclusively structure $\mathbf{1}^{\bullet+}$.

Conclusion

Dissociative electron impact ionization of aminoguanidine, $H\text{-}N{=}C(NH_2)\text{-}NH\text{-}NH_2$ cleanly produces diaminocarbene radical cations $H_2N\text{-}C\text{-}NH_2^{\bullet+}$. Their reduction by single electron transfer in Neutralization-Reionization (NR) mass spectrometric experiments yields the prototype nucleophilic carbene $H_2N\text{-}\ddot{C}\text{-}NH_2$ as a stable species in the gas phase, distinct from its isomer formamidine, $H_2N\text{-}C(H){=}NH$. Deuterium labelling and multiple collision experiments confirm the identities of the ions and neutrals. The experimental findings are in excellent agreement with the results of ab initio calculations. Computations using GAUSSIAN-2 (G2) theory lead to $\Delta H_f^0\,(H_2N\text{-}\ddot{C}\text{-}NH_2) =$ 39.4 kcal/mol and $\Delta H_f^0\,(H_2N\text{-}C\text{-}NH_2^{\bullet+}) = 221$ kcal/mol.

[#3] Note that the CA mass spectrum in Fig. 8.2 is not directly comparable to that of Fig.8.1 because the collision gases used and the resolution of the two spectra are not the same.

8.2) Dihydroxycarbene HO-C̈-OH: Its formation in the gas phase by electron transfer to its radical cation*

introduction

Ever since the parent carbene, methylene, $:CH_2$, was proposed as a product in the photochemical and thermochemical decomposition of diazomethane, carbenes have been the subject of intense study [2]. Today, methylene is a well understood molecule, it being in the ground state a triplet (diradical) with bent geometry [33].

Recently, much theoretical and experimental work has focussed on understanding the properties of substituted methylenes [33,34]. Of particular interest are methylenes substituted with electronegative groups [5c] such as OCH_3 and OH, where π-donation stabilizes the singlet state relative to the triplet state [6]; indeed, in contrast to the parent methylene many oxacarbenes are calculated to be nucleophilic singlets [5c], but with bent geometries nevertheless. A case in point is the parent dioxacarbene, dihydroxycarbene, HO-C̈-OH, which contains two strong resonance donors ($\sigma_R^+(OH)$ = -1.24 [35]) and for which calculations indicate a singlet ground state with an OCO angle of 106° [36-39]. The singlet-triplet gap is large, ΔE_{S-T} = ~ 56 kcal/mol [36,37] , and similar to that recently calculated for diaminocarbene [8]. Singlet dihydroxycarbene's most stable conformer is calculated [39] to be 41 kcal/mol higher in energy than its isomer, HC(=O)OH, formic acid. However, the formic acid → dihydroxycarbene 1,2-hydrogen shift isomerization is associated with a barrier of ~79 kcal/mol [38]. In addition, significant energy barriers have been computed for the carbene's decarboxylation and decarbonylation, ~30 and ~37 kcal/mol respectively [36], and thus theory predicts that HO-C̈-OH ought to be kinetically stable.

* P.C. Burgers, G.A. McGibbon and J.K. Terlouw, *Chem. Phys. Letters 224 (1994) 539-543.*

A variety of dioxacarbenes (for example, the "archetypal" nucleophile dimethoxycarbene) have been generated in the condensed phase by photolysis and thermolysis of judiciously chosen precursors [11,40]. An alternative method to generate thermodynamically unstable, but kinetically stable, species in the gas phase is by Neutralization-Reionization mass spectrometry (NRMS) [17,18]. This technique provides an appealing alternative when precursors for condensed-phase experiments are not readily available; thus, simple carbenes such as H-$\tilde{C}$-OH [13], F-$\tilde{C}$-OH [14], H_3C-$\tilde{C}$-OH [15], H_2N-$\tilde{C}$-NH_2 [41], HO-$\tilde{C}$-NH_2 [16,17] and HO-$\tilde{C}$-N(H)CH_3 [17] have been generated by NRMS.

However, as far as we are aware, the prototype dioxacarbene HO-$\tilde{C}$-OH has not yet been experimentally observed, although it has been postulated as an intermediate in the unimolecular decarboxylation of oxalic acid [42] and in the electrochemical oxidation of formaldehyde on Pt surfaces [43]. Its generation by electron transfer to the corresponding cation in an NR experiment seemed to be feasible for the following reasons. The cation has been generated by decarboxylation of ionized oxalic acid [44] and is thus experimentally accessible; like other ionized oxacarbenes (and in sharp contrast to the neutral species, see above) HO-C-OH$^{\bullet+}$ is thermodynamically a remarkably stable species [44-47] with a measured heat of formation ΔH_f = 175 kcal/mol [44], close to that of its "normal" isomer, ionized formic acid, ΔH_f = 170 kcal/mol [30]. In addition, substantial energy barriers prevent the ion [45] (and the singlet neutral) from isomerizing, so that a pure ion beam, a prerequisite for many NR experiments, can in principle be generated.

In this section the first-time generation and identification of dihydroxycarbene by means of Neutralization-Reionization mass spectrometry is discussed.

Results and Discussion

As mentioned above, HO-C-OH$^{\bullet+}$ can be generated by loss of CO_2 from ionized oxalic acid, but unfortunately a non-negligible amount (~10%) of ionized formic acid is co-produced [44]. Since the combined neutralization-reionization efficiencies in an NR experiment of isomeric ions may differ considerably, it is important to obtain pure ion fluxes. Recently, we discovered a better pathway to pure HO-C-OH$^{\bullet+}$: from dihydroxy-fumaric acid which upon ionization "breaks in half" and then undergoes decarbonylation via a reaction, whose mechanism will be discussed in detail elsewhere [48]:

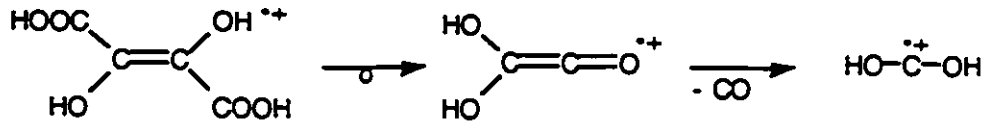

m/z 148 — Dihydroxyfumaric acid

m/z 74 — Dihydroxyketene

m/z 46 — Dihydroxycarbene

The m/z 148, 74 and 46 ions dominate the 70 eV electron impact mass spectrum and high resolution mass measurements showed that m/z 46 indeed has the composition CH_2O_2. The CA mass spectrum of these ions was similar to that published previously [44] and the structure characteristic part (m/z 12 - 18) is shown in Figure 8.3b, together with that of its isomer HC(=O)OH$^{\bullet+}$, Figure 8.3a. As discussed previously [20], the peak at m/z 13, CH^+, in Figure 8.3a could be interpreted in terms of the structure HC(=O)OH$^{\bullet+}$ (losses of OH$^\bullet$ and O$^\bullet$) while the peak at m/z 12 may result from H$^\bullet$ loss from CH^+ and conversely the near absence of m/z 13 in Figure 8.3b could be taken as showing that the produced ion is HO-C-OH$^{\bullet+}$ which does not contain a C-H unit. The $H_2O^{\bullet+}$ peak at m/z 18 results from low energy decarbonylation reactions; the mechanisms of this rearrangement have been unravelled by ab initio molecular orbital calculations [49].

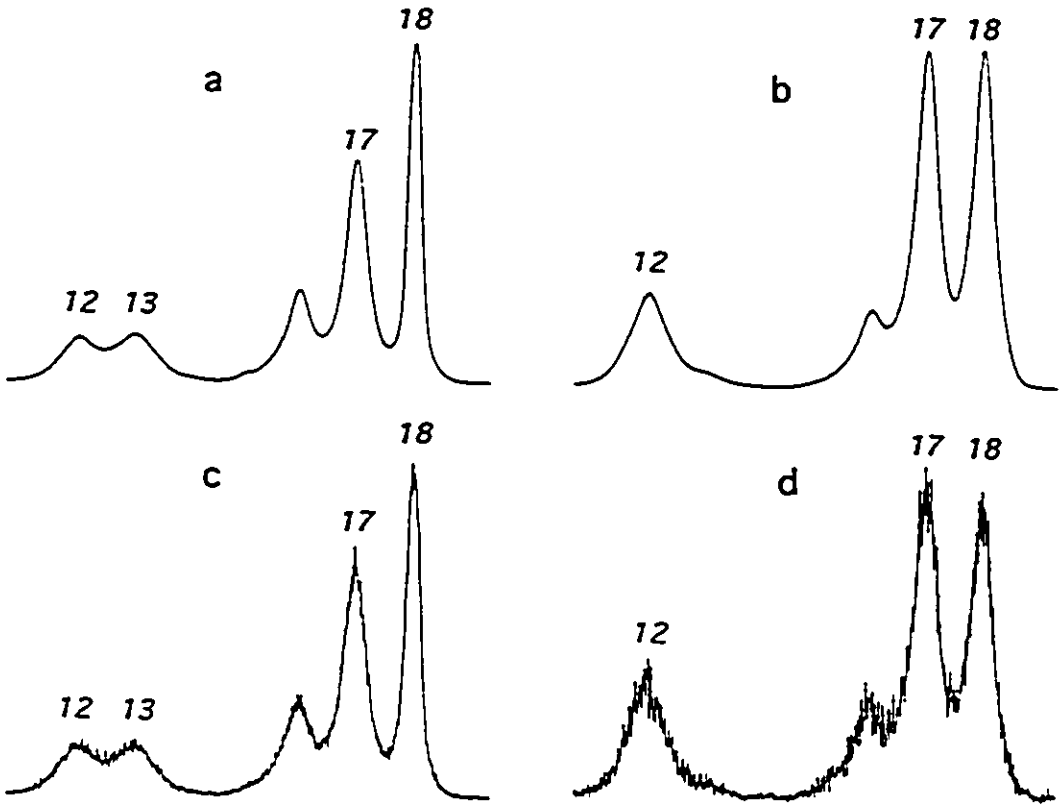

Fig. 8.3 Partial CA mass spectra [3FFR, He] of source generated ions $HC(=O)OH^{\bullet+}$ and $HO\text{-}C\text{-}OH^{\bullet+}$, items **a** and **b**, and of the *survivor* ions $HC(=O)OH^{\bullet+}$ and $HO\text{-}C\text{-}OH^{\bullet+}$ from the [NDMA/O_2] NR spectra, items **c** and **d**.

Definitive evidence for the proposed structures (and also for the purity of the respective ion beams) comes from the following double collision experiment. Both isomers, upon collisional activation, abundantly form m/z 29, $[H,C,O]^+$ [44]. Now both HCO^+ and COH^+ are stable species [50] with COH^+ lying 34 kcal/mol above HCO^+ [51]. If it could be shown that simple cleavage in $HO\text{-}C\text{-}OH^{\bullet+}$ produced the less stable isomer COH^+ only, then this would lend great support to the proposed structure and it would also attest to the purity of the ion beam. To characterize the $[H,C,O]^+$ product ion, m/z 46 was selectively transmitted through B and induced to decompose in the 2FFR by collision with O_2. The resulting m/z 29 was then selectively transmitted through E_1 and its CA mass spectrum was obtained in the 3FFR and compared with reference HCO^+/COH^+ CA mass spectra [52,53]. The spectra from these experiments (not shown) clearly indicate that $HO\text{-}C\text{-}OH^{\bullet+}$ predominantly forms COH^+, whereas $HC(=O)OH^{\bullet+}$ largely generates HCO^+. This constitutes good evidence for the structure $HO\text{-}C\text{-}OH^{\bullet+}$ and moreover, it indicates that the $HO\text{-}C\text{-}OH^{\bullet+}$ ion beam is virtually free from the isomeric form. Thus, the spectra in Figures 8.3a and 8.3b do indeed reflect the respective $CH_2O_2^{\bullet+}$ ion connectivities.

Next, the NR mass spectra of both isomers were recorded, see Figure 8.4. It can be seen that each isomer produces an intense survivor signal at m/z 46. Also, as evidenced by the increased intensity of m/z 28 in the NR spectra compared to the CA spectra, upon neutralization a considerable amount of CO is produced, probably from unstable excited neutral precursors as was also the case for $H_2N\text{-}C\text{-}OH^{\bullet+}$ [16,17]. These CO neutrals, upon reionization, produce C^+ and O^+ which obscure the structure diagnostic m/z 12 - 18 region of the NR mass spectrum that is of weak intensity, see Figure 8.4. To eliminate this interference, the *survivor* ions, i.e. the non-decomposing reionized neutrals, were selectively transmitted through E_1 and their CA mass spectrum was obtained in the 3FFR. The structure diagnostic region of the resulting NR/CA mass spectra of $HO\text{-}C\text{-}OH^{\bullet+}$ and $HC(=O)OH^{\bullet+}$ are shown in Figures 8.3d and 8.3c, respectively. It can be seen that the respective NR/CA mass spectra are superimposable on the respective CA mass spectra.

This reinforces the above conclusion that the original ion fluxes were essentially isomerically pure and, more importantly, it constitutes the first clear-cut experimental observation of dihydroxycarbene as a stable molecule in the gas phase, consistent with the predictions from ab initio calculations [36-39].

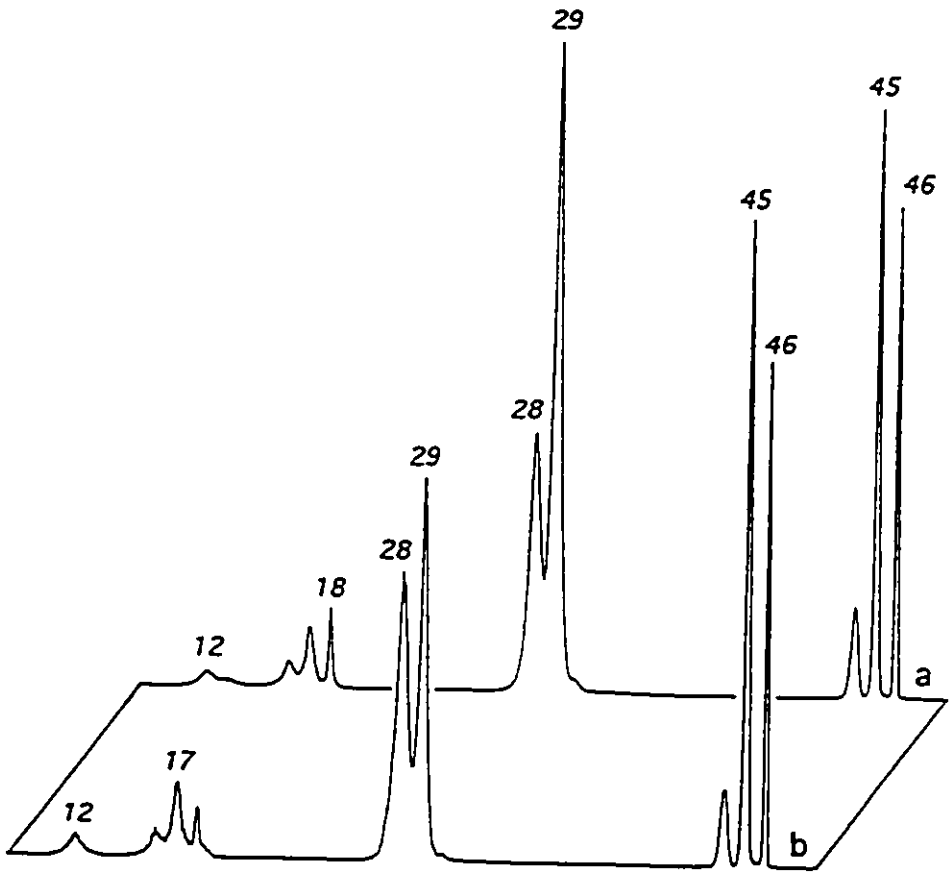

Fig. 8.4 [NDMA/O_2] NR mass spectra of $HC(=O)OH^{\bullet+}$ (item a) and $HO\text{-}C\text{-}OH^{\bullet+}$ (item b). In the corresponding CA mass spectra [2FFR, O_2] the m/z 28/29 ratios are 5.7 and 2.5.

Unfortunately, the above experiments do not unequivocally decide which state of the carbene (singlet and/or triplet) has been accessed. From the theoretical results quoted in the introduction of this section, and the experimental ΔH_f [HC(=O)OH] , -90.6 kcal/mol [30], the ΔH_f of singlet HO-$\bar{C}$-OH is assessed as -50 kcal/mol, while for the triplet state ΔH_f is 6 kcal/mol. Combining this with the experimental ΔH_f [HO-C-OH$^{\bullet+}$], 175 kcal/mol [44], ionization energies (IE) of ~7.3 and ~9.8 eV are obtained for the triplet and singlet states of the carbene. The first three vertical IE's of the neutralization agent, NDMA, are 7.5, 9.0 and 9.8 eV respectively [54]. Therefore, a close-to-resonant vertical electron tranfer from NDMA to HO-C-OH$^{\bullet+}$ is in principle available for the generation of either state. It is therefore entirely possible that both states are accomodated in our experiments. On the other hand, unfavourable Franck-Condon factors may militate against the formation of the triplet since, unlike the singlet, it has a non-planar geometry [6,36-39] that differs greatly from that of the planar ion [45].

With cyclopropane (CP) as the neutralization agent, only electron transfer leading to the singlet state is close-to-resonant (first IE_V (CP) = ~ 10.5 eV [30]). Nevertheless, the CP and NDMA NR mass spectra show little difference in appearance or neutralization efficiency. In addition, a careful comparison (under conditions of moderate energy resolution) of the position of the survivor ion signal on the energy scale [55] and the magnitude of the kinetic energy releases in the formation of the fragment ions, did not reveal clear differences between the two neutralization agents either. Use of atomic targets with IE's close to or below that of the triplet, in conjunction with as yet unavailable computational information on the *triplet's* dissociation chemistry, may shed more light on this matter.

Finally, one other experiment deserves brief comment. It concerns the NR/CA mass spectrum of the confirmed interstellar [56] species COH$^+$, the structure characteristic product of HO-C-OH$^{\bullet+}$. The ion COH$^+$ can be made in good yield from ionized squaric acid [53]. When it is neutralized and the *survivor* ion is analyzed by collisional activation a

NR/CA mass spectrum is obtained which is superimposable on that of its isomer HCO^+. There are two explanations for this: (i) CCH^+ after its formation, immediately rearranges to HCO^+ and (ii) the primary ion beam contains a small amount of HCO^+, and after the generation of HCO^+ and COH^+, the latter immediately dissociates to $CO + H^+$, leaving only HCO^+ to be reionized. In any case, the above experiments indicate that COH^+ is a transient species only.

Conclusion

Dihydroxycarbene, HO-$\ddot{C}$-OH, has been generated and identified in the gas phase by electron capture of the corresponding radical cations in Neutralization-Reionization experiments. The precursor ions were made by dissociative ionization of dihydroxy-fumaric acid and their structure was established on the basis of collision experiments. The experimental results are consistent with previously published ab initio calculations.

Note added after submission: Another NRMS study of HO-$\ddot{C}$-OH (using oxamic acid as a precursor) has subsequently appeared in the literature [57].

References

1. R.A. Moss, Acc. Chem. Res. 22 (1989) 15.
2. (a) W. Kirmse, Carbene Chemistry, 2nd Ed., Academic Press: New York (1971); (b) Carbenes, Vols. I /II, M. Jones, Jr. and R.A. Moss (eds.), Wiley: New York (1973/1975).
3. K. Kassam, D. Pole, M. El-Saidi, T. Tadey and J.Warkentin, J. Am. Chem. Soc. 114 (1992) 8751.
4. D.A. Dixon and A.J. Arduengo III, J. Chem. Phys. 95 (1991) 4180.
5. (a) J. Farras, S. Olivella, A. Sole and J. Vilarrasa, J. Comput. Chem. 7 (1986) 428; (b) M. Moreno, J.M. Lluch, A. Oliva and J. Bertran, Chem. Phys. 100 (1985) 33; (c) P.H. Mueller, N.G. Rondan, K.N. Houk, J.F. Harrison, D. Hooper, B.H. Willen and J.F. Liebman, J. Am. Chem. Soc. 103 (1981) 5049; (d) W.W. Schoeller and N. Aktekin, J. Chem. Soc. Chem. Commun. (1980) 124;

6. D. Feller, W.T. Borden, and E.R. Davidson, Chem. Phys. Letters 71 (1980) 22.

7. (a) A.J. Arduengo III, R.L. Harlow and M. Kline, J. Am. Chem. Soc. 113 (1991) 361; (b) A.J. Arduengo III, H.V. Rasika Dias, R.L. Harlow and M. Kline, J. Am. Chem. Soc. 114 (1992) 5530.

8. C. Heinemann and W. Thiel, Chem. Phys. Letters 217 (1994) 11;

9. (a) H. Wanzlich, Angew. Chem. Int. Ed. Engl. 1 (1962) 75; (b) H. Schönherr and H. Wanzlick, Chem. Ber. 103 (1970) 1037.

10. R.A. Moss, D.P. Cox and H. Tomioka, Tetrahedron Lett. 25 (1984) 1023 and references therein.

11. (a) X.M. Du, H. Fan, J.L. Goodman, M.A. Kesselmayer, K. Krogh-Jespersen, J.A. LaVilla, R.A. Moss, S. Shen, R.S. Sheridan, J. Am. Chem. Soc. 112 (1990) 1920; (b) R.A. Moss, M. Wlostowski, S. Shen, K. Krogh-Jespersen and A. Matro, *ibid* 110 (1988) 4443.

12. T. Wong, J. Warkentin and J.K. Terlouw, Int. J. Mass Spectrom. Ion Processes 115 (1992) 33.

13. (a) R. Feng, C. Wesdemiotis and F.W. McLafferty, J. Am. Chem. Soc. 109 (1987) 6521; (b) W.J. Bouma, P.C. Burgers, J.L. Holmes and L. Radom, J. Am. Chem. Soc. 108 (1986) 1767.

14. D. Sülzle, T. Drewello, B.L.M. van Baar, H. Schwarz, J. Am. Chem. Soc. 110 (1988) 8330.

15. C. Wesdemiotis and F.W. McLafferty, J. Am. Chem. Soc. 109 (1987) 4760.

16. (a) G. Schaftenaar, R. Postma, P.J.A. Ruttink, P.C. Burgers, G.A. McGibbon and J.K. Terlouw, Int. J. Mass Spectrom. Ion Processes 100 (1990) 521; (b) C.E.C.A. Hop, H. Chen, P.J.A. Ruttink and J.L. Holmes, Org. Mass Spectrom. 26 (1991) 697; (c) G.A. McGibbon, J.K. Terlouw and P.C. Burgers, Int. J. Mass Spectrom. Ion Processes (1994) in press.

17. J.K. Terlouw, Adv. Mass Spectrom. 11 (1989) 984.

18. (a) C. Wesdemiotis and F.W. McLafferty, Chem. Rev. 87 (1987) 485; (b) J.K. Terlouw and H. Schwarz, H. Angew. Chem. Int. Ed. Engl. 26 (1987) 805; (c) H. Schwarz, Pure Appl. Chem. 61 (1989) 685; (d) J.L. Holmes, Mass Spectrom. Rev. 8 (1989) 513; (e) F.W. McLafferty, Science 247 (1990) 925; (f) F.W. McLafferty, F.W. Int. J. Mass Spectrom. Ion Processes 118/119 (1992) 221.

19. H.F. van Garderen, P.J.A. Ruttink, P.C. Burgers, G.A. McGibbon and J.K. Terlouw, Int J. Mass Spectrom. Ion Processes 121 (1992) 159

20. S. Villeneuve, P.C. Burgers, Org. Mass Spectrom. 21 (1986) 733.

21. (a) M.-Y. Zhang and F.W. McLafferty, J. Am. Soc. Mass Spectrom. 3 (1992) 108; (b) T. Wong, J.K. Terlouw, T. Weiske and H. Schwarz, Int. J. Mass Spectrom. Ion Processes 113 (1992) R23.

22. M.J. Frisch, G.W. Trucks, M. Head-Gordon, P.M. Gill, M.W. Wong, J.B. Foresman, B.G. Johnson, H.B. Schlegel, M.A. Robb, E.S. Replogle, R. Gomberts, J.L. Andres, K. Raghavachari, J.S. Binkley, C. Gonzalez, R.L. Martin, D.J. Fox D.J. DeFrees, J. Baker, J.J.P. Steward and J. Pople, GAUSSIAN 92, Gaussian, Pittsburgh, PA (1992)

23. L.A. Curtiss, G.W. Trucks, K. Raghavachari and J.A. Pople, J. Chem. Phys. 93 (1990) 2537;

24. L.A. Curtiss, K. Raghavachari, G.W. Trucks and J.A. Pople, J. Chem. Phys. 94 (1991) 7221.

25. W.H. Graham, J. Am. Chem. Soc. 87 (1965) 4396.

26. R.A. Moss, in Chemistry of Diazirines, Vol. I, M.T.H. Liu (ed.), CRC Press: Boca Raton (1986).

27. J.H. Beynon, J.A. Hopkinson and A.E. Williams, Org. Mass Spectrom. 1 (1968) 169.

28. J. Barker, M. Jones and M. Kilner, Org. Mass Spectrom. 20 (1985) 619.

29. J.L. Holmes and J.K. Terlouw , Org. Mass Spectrom. 15 (1980) 383.

30. S.G. Lias, J.E. Bartmess, J.F. Liebman, J.L. Holmes, R.D. Levin, W.G. Mallard, J. Phys. Chem. Ref Data 17 (1988) Supplement 1.

31. P.C. Burgers, J.K. Terlouw, T. Weiske and H. Schwarz, Chem. Phys. Letters 132 (1986) 144.

32. J. Andrés, J. Krechl, M. Carda and E. Silla, Int. J. Quantum Chem. 40 (1991) 127.

33. For a review see I. Shavitt, Tetrahedron 41 (1985) 1531.

34. D.A. Modarelli, S. Morgan and M.S. Platz, J. Am. Chem. Soc. 114 (1992) 7034.

35. O. Exner, in Advances in Linear Free Energy Relationships, N.B. Chapman and J. Shorter (eds.), Plenum Press: New York (1972) p.37

36. R.L. Reddington, C.W. Bock and B. Aboab, J. Mol. Structure 224 (1990) 89.

37. M. Räsänen, T. Raska, H. Kunttu and J. Murto J. Mol. Struct. (Theochem) 208 (1990) 79.

38. J.D. Goddard, Y. Yamaguchi and H.F. Schaefer III, J. Chem. Phys. 96 (1992) 1158;

39 J.S. Francisco, J. Chem. Phys. 96 (1992) 1167.

40. K. Kassam, D.L. Pole, M. El-Saidi and J.Warkentin, J. Am. Chem. Soc. 116 (1994) 1161;

41. G.A. McGibbon, C.A. Kingsmill and J.K. Terlouw, Chem. Phys. Letters 222 (1994) 129.

42. C.W. Bock and R.L. Reddington, J. Chem. Phys. 85 (1986) 5391.

43. M.D. Spasojevic, R.R. Adzic and A.R. Despic, J. Electroanal. Chem. 109 (1980) 261.

44. P.C. Burgers, A.A. Mommers and J.L. Holmes, J. Am. Chem. Soc. 105 (1983) 5976.

45. E. Uggerud, W. Koch and H. Schwarz, Int J. Mass Spectrom. Ion Processes 73 (1986) 187.

46. W.J. Bouma, J.K. McLeod and L. Radom, Int J. Mass Spectrom. Ion Processes 33 (1980) 87.

47. P.C. Burgers, J.L. Holmes and J.K. Terlouw, J. Chem. Soc, Chem. Commun. (1984) 642.

48. J. Hrusak, G.A. McGibbon, H. Schwarz and J.K. Terlouw, in preparation.

49. P.J.A. Ruttink and P.C. Burgers, Int J. Mass Spectrom. Ion Processes 113 (1992) 23.

50. (a) A.J. Illies, M.F. Jarrold and M.T. Bowers, J. Chem. Phys. 77 (1982) 5847; (b) A.J. Illies, M.F. Jarrold and M.T. Bowers, J. Am. Chem. Soc. 105 (1983) 2562; (c) P.C. Burgers and J.L. Holmes, Chem. Phys. Letters 97 (1983) 236.

51. W.J. Bouma, P.C. Burgers, J.L. Holmes and L.Radom, J. Am. Chem. Soc. 108 (1986) 1767.

52. P.C. Burgers, J.L. Holmes and A.A. Mommers, J. Am. Chem. Soc. 107 (1985) 1099;

53. J.K. Terlouw, P.C. Burgers, B.L.M. van Baar, T. Weiske and H. Schwarz, Chimia 40 (1986) 357.

54. A.D. Baker, D.P. May and D.W. Turner, J. Chem. Soc. [B] 22 (1968).

55. J. Bordas-Nagy, J.L. Holmes and C.E.C.A. Hop, Int J. Mass Spectrom. Ion Processes 94 (1989) 189.

56. R.C. Woods, J. Mol. Struct. 97 (1983) 195.

57. F.A. Wiedmann, J. Cai and C. Wesdemiotis, 8 (1994) 804.

CHAPTER 9

The imidic acids H-N=C(H)-OH and CH_3-N=C(H)-OH and their tautomeric carbenes H_2N-$\ddot{C}$-OH and CH_3-N(H)-$\ddot{C}$-OH: Stable species in the gas-phase formed by one-electron reduction of their cations.

Introduction

In this chapter it is shown how a combination of collision induced dissociation (CID), Neutralization–Reionization (NR) and MS/MS/MS experiments on D and ^{15}N labelled isotopomers made it possible to assign structures to the prototype imidic acid, formimidic acid, H-N=C(H)-OH, **2** and aminohydroxycarbene, **3**, both isomeric with formamide, **1**. These species were generated in the gas-phase by one-electron reduction of the corresponding radical cations. Reduction of these ions in Neutralization-Reionization (NR) experiments produced intense "survivor" signals. While **1**, **2** and **3** were all found to be stable among the vibrationally excited molecules we find evidence for the simplest amide-iminol tautomerism, i.e. **1** ↔ **2**. The experimental findings on ions and neutrals **1-3** concur with previously published ab initio MO studies which were supplemented by our own results.

Using the same experimental methodology, the existence of the imidic acid CH_3-N=C(H)-OH and the carbene CH_3-N(H)-$\ddot{C}$-OH, the methyl homologues of **2** and **3**, was also established.

This work appears in a publication of the same name:

G.A. McGibbon, P.C. Burgers and J.K. Terlouw,

Int. J. Mass Spectrom. Ion Processes 136 (1994) 191- 208.

Proton exchange in amides, peptides and proteins is of fundamental importance in biochemistry and has been extensively studied [1]. The reaction is both acid- and base-catalyzed. The classical mechanism, shown in eq. 1, for the acid catalyzed exchange involves protonation on nitrogen.

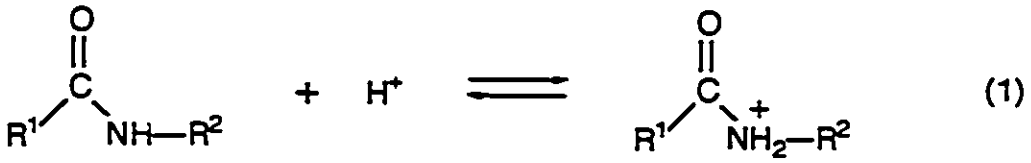

(1)

However, it has long been widely accepted that the more basic site of an amide is the oxygen atom, not the nitrogen atom; this has very recently been confirmed by NMR relaxation rate experiments [2]. Indeed, 20 years ago Perrin [3] argued that the earlier experimental evidence for the above mechanism is also consistent with an alternative pathway, eq. 2, that proceeds via the more facile protonation at oxygen, followed by deprotonation to yield the imidic acid tautomer.

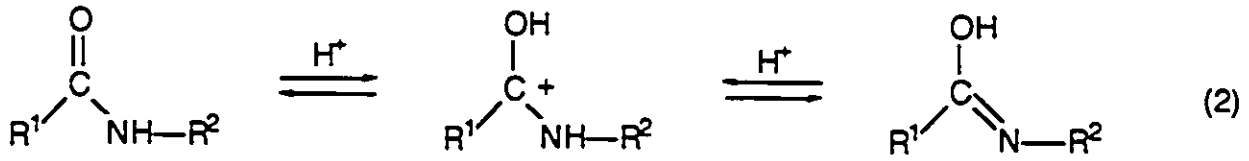

(2)

amide **imidic acid**

Experiments aimed at distinguishing the mechanisms have recently been lucidly reviewed [1] and it appears that, depending upon the substituents R^1 and R^2, either or both mechanism(s) may apply: for electron-donating groups proton exchanges follow eq. 1, while in the case of electron-withdrawing substituents they take place via the imidic acid mechanism, with intermediate cases where both mechanisms operate.

Although an amide could be an equilibrium of amide and iminol forms [4] (indeed

X-ray studies of amino acids and dipeptides indicate a short C-N (1.23Å) bond), free simple imidic acids have so far eluded direct observation. This is in marked contrast to enols, which have been generated and identified in the gas-phase by pyrolysis mass spectrometry [5] and by neutralization-reionization mass spectrometry (NRMS) [6]. The direct observation of simple imidic acids as stable (as opposed to transient) species would bolster greatly the imidic acid mechanism where there is evidence to support it.

The prototype imidic acid, formimidic acid, H-N=C(H)OH, **2**, and its relationship with its tautomer formamide, **1**, has been the subject of several *ab initio* molecular orbital calculations [7]. The imidic acid **2** is found to be an equilibrium structure (with the *Z* form being the more stable conformer) lying, according to the most sophisticated calculations [7i,j] c. 13 kcal/mol above **1**, whose experimental heat of formation is - 44 kcal/mol [8a]. Using experimental data from analogues, it was estimated [7g] that **2** lies 11 ± 4 kcal/mol above **1**, in good agreement with the computational results. Note that the heat of formation of **2** has also been estimated by additivity considerations (ΔH_f = -39 kcal/mol) [8b]. Calculations [7i] further predict that the isomerization barrier **1** → **2** is relatively high (49 kcal/mol above **1**). The imidic acid **2** has another tautomer, aminohydroxycarbene, H_2N-C̈-OH, **3**. The carbene has been calculated [9] to lie 39 kcal/mol above **1** with substantial isomerization barriers to **1** and **2** : TS **1** → **3** = 77 kcal/mol [9] whereas TS **2** → **3** = 86 kcal/mol (this work) coincides with the dissociation limit for $HCO^{\bullet} + NH_2$. It was further found that large barriers prevent the dissociation of **2** and **3** into the more stable products NH_3 + CO.

Calculations on the ions [9] do indicate that $\mathbf{1}^{\bullet+}$, $\mathbf{2}^{\bullet+}$ and $\mathbf{3}^{\bullet+}$ also lie in deep potential wells. The qualitative relationship among the ionic and neutral species as derived from theory and experiment is illustrated in Fig. 9.1. The sizable barriers that exist towards **intra**molecular isomerization of the neutral and ionic species make **2** an excellent target for generation by a one-electron reduction of its corresponding cation $\mathbf{2}^{\bullet+}$ in a NR experiment, provided that the ion can be generated in a pure form.

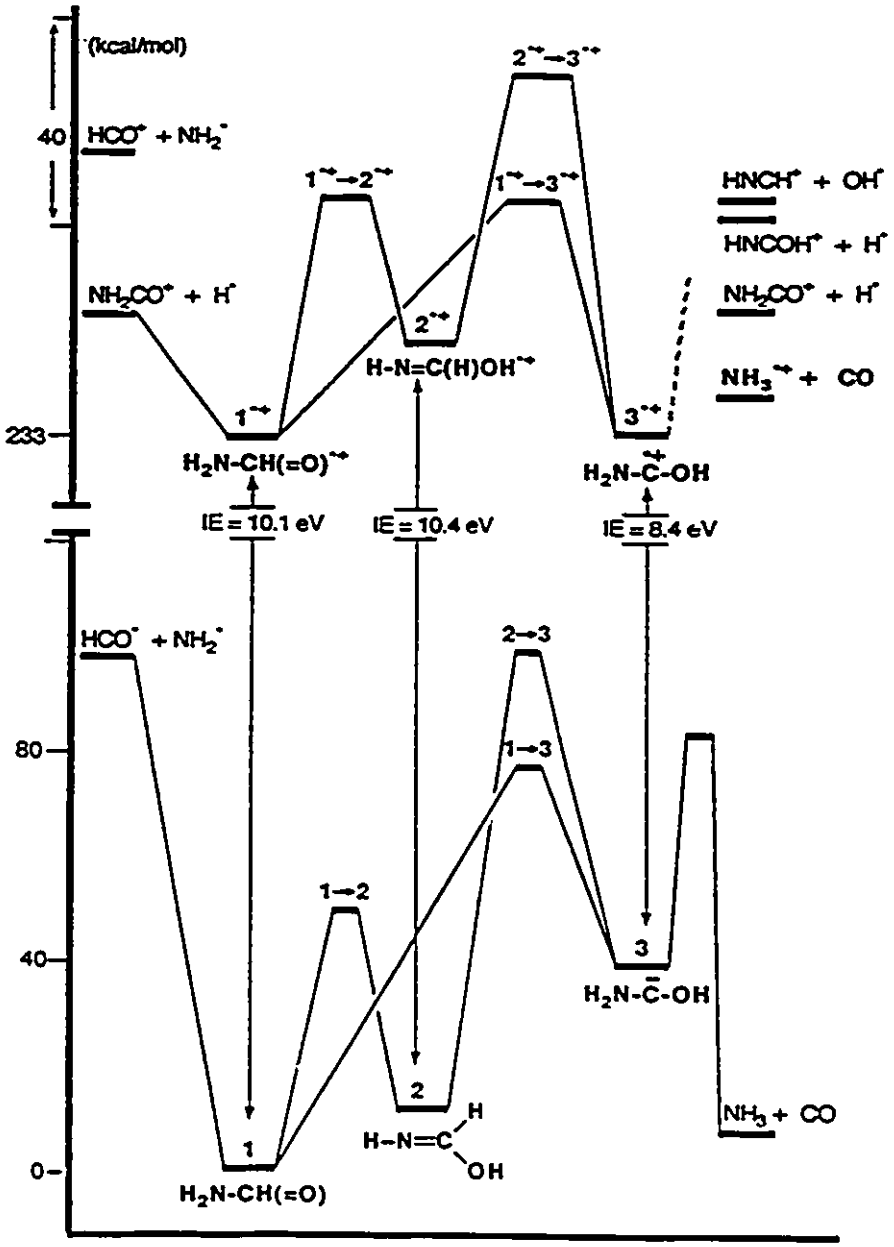

Fig. 9.1 Calculated energy diagram for formamide (1), formimidic acid (2) and aminohydroxycarbene (3) and their radical cations $1^{\cdot+}$ - $3^{\cdot+}$. Energies in kcal/mol are relative to ΔH_f (exp.) 1 (- 44 kcal/mol [8a]). The ordering of the levels for the ions was taken from the MR-CI (Pople) ab initio calculations in ref. 9, those for the neutral species are from ab initio calculations reported in ref. 7, 9 and this work. The energies of the ions and neutrals are connected via the adiabatic IE of 1, 10.1 eV [8a]; the levels for the dissociation products all refer to experimental values taken from ref. 8a.

Interestingly, the oxidized form of the carbene is predicted to be almost as stable as ionized formamide; this parallels observations made for H-C-OH$^{\bullet+}$ [10]. Thus ion **3**$^{\bullet+}$ may be readily accessible by dissociative ionization of suitable precursors and indeed in two recent NRMS studies the carbene **3** has been proposed to be generated [9,10d]. These studies further give ΔH_f (**3**$^{\bullet+}$) as 190 kcal/mol, i.e. equivalent to ΔH_f (**1**$^{\bullet+}$) [8a].

In contrast, the generation and identification of the iminol ion **2**$^{\bullet+}$ is less straightforward. Among the isomeric ions, **2**$^{\bullet+}$ has the highest heat of formation (cf. ionized enols which are generally more stable than their keto forms [5]) and this may make it difficult to generate ion beams containing purely iminol ions. In fact, our earlier attempt to make the methyl carbamate tautomer, H-N=C(OCH_3)-OH [11] was unsuccessful for this reason.

Moreover, the energy requirements for the structure diagnostic probe reactions in the CID spectra are unfavourable: apart from the non structure specific H$^{\bullet}$ loss, all other direct bond cleavage reactions yield products whose enthalpies lie near or above the calculated (inter)conversion barriers **2**$^{\bullet+}$ ↔ **1**$^{\bullet+}$ ↔ **3**$^{\bullet+}$. Thus, in CID experiments, definitive structure assignments may be compromised by **post**-collisional isomerization of the ions. Nevertheless, some of these probe reactions may actually be structure characteristic if it can be established that they specifically generate product ions of different structures, for instance, if loss of $^{\bullet}NH_2$ from **1**$^{\bullet+}$ and **3**$^{\bullet+}$ produces HCO^{+} and HOC^{+} respectively and loss of $^{\bullet}$OH from **2**$^{\bullet+}$ and **3**$^{\bullet+}$ gives rise to the isomers HNCH^{+} and H_2NC^{+} respectively. Collision experiments with the product ions observed in the CID spectra of the isomeric ions - double collision (CID/CID) experiments [12] - may provide an answer to this question. Such MS/MS/MS type experiments can also provide an answer to the question : has the reionized neutral ("survivor" ion) in a Neutralization-Reionization experiment retained its original structure ? Provided there is a sufficient flux of reionized neutrals these can be (mass) selected and subjected to CID. The resulting CID/NR spectrum [6d-g] may be used to decide whether differences between the NR

and CID spectra of a given ion are due to reionized decomposition products of the neutral and other interferences or (partial) isomerization of the neutralized precursor ion. Conversely, identical CID and CID/NR spectra attest to the isomeric purity of the primary ion beam since the combined neutralization / collisional ionization efficiency of isomeric species will only be similar by coincidence.

In the present paper we report the first-time generation and identification of formimidic acid by NRMS in conjunction with (multi) collision experiments on D and ^{15}N labelled isotopomers. In addition, earlier proposals [9,10d] that the carbene **3** is also a viable species in the gas-phase could be substantiated experimentally. *Ab initio* molecular orbital calculations confirm that **3** is a stable species with high barriers to isomerization and dissociation. Neutrals **2** are also in a deep potential well but those of higher energy exhibit the prototype amide-iminol tautomerization **1** ↔ **2** on the microsecond timescale. Similar experiments, see experimental for details [13-17], enabled the generation and identification of the methyl homologues of **2** and **3**, CH_3-N=C(H)-OH, **2a**, and CH_3-N(H)-$\ddot{C}$-OH, **3a**.

Theoretical section

To complete the energy diagram shown in Fig. 9.1 standard LCAO-MO-SCF (UHF) calculations were performed to evaluate the transition states **2**→**3** and **3** → NH_3 + CO using the Gaussian 90 series of programs [18]. The geometries, harmonic frequencies and zero-point vibrational energies (ZPVE's) were calculated with the 4-31G basis set [19]. The force constant matrices for the stationary points were checked to have the correct number of eigenvalues. Single-point calculations performed with the 6-31G* basis set [20] and Møller-Plesset correlation terminated at the MP3 level [21]. The resulting data were corrected for the scaled (0.9) contribution of ZPVE's (UHF/4-31G) [22]. The optimized energies and geometries of **1**, **2** and **3** and TS **1**→**2** were found to be in good agreement with previous calculations [6], and the computational details for

TS 2→3, 86 kcal/mol, and TS 3 → NH_3 + CO, 80 kcal/mol, will be presented elsewhere [23].

Results and Discussion

Formimidic acid, H-N=C(H)OH, and Aminohydroxycarbene

Although ionized enols are readily accessible via the ubiquitous McLafferty rearrangement the same is not necessarily true for iminols [11]. However, the base peak in the electron ionization mass spectrum of Gyromitrin [15b] (the poison of *Gyromitra esculenta*) $CH_3CH{=}N{-}N(CH_3)CHO$, is m/z 59, rationalized as loss of CH_3CN in a McLafferty type rearrangement. As will be shown below, there is good evidence that the product ion is the iminol $CH_3{-}N{=}C(H)OH^{\bullet+}$ and we therefore examined the homologue acetaldehyde, N-formylhydrazone, **I**, as a precursor for $H{-}N{=}C(H)OH^{\bullet+}$, eq. 3.

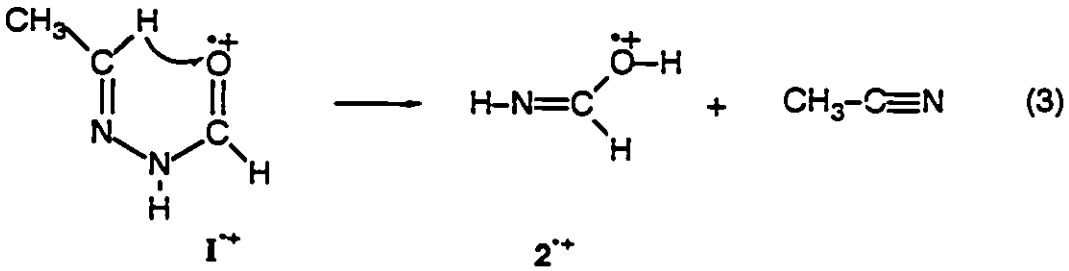

$I^{\bullet+}$ $2^{\bullet+}$

At high mass resolution, the spectrum of carefully purified **I** contains a single peak at m/z 45 (15 % of the base peak at m/z 42) having the elemental composition $[C,H_3,N,O]$, and as will be shown below these ions have structure $2^{\bullet+}$.

Another possible route to ion $2^{\bullet+}$ involves the loss of HNCO from 1,2-diformylhydrazine, **II**, eq. 4 :

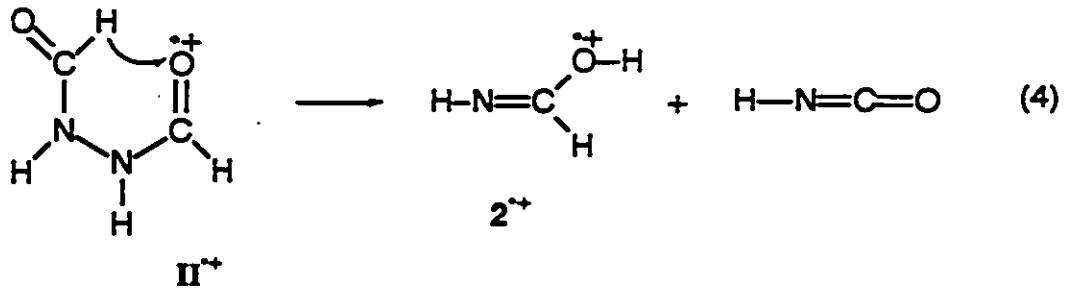

$II^{\bullet+}$ $2^{\bullet+}$ (4)

but it appears from an analysis of the CID spectra that **II** yields a mixture of $2^{\bullet+}$ and $1^{\bullet+}$; the latter ion could be produced by a 1,3-H shift from carbon to nitrogen.

In previous work [9,10d], ion $3^{\bullet+}$ was generated by the loss of CH_2=O from ionized methyl carbamate, $H_2NCOOCH_3^{\bullet+}$. Since it was desirable to analyse the specifically labelled ions $D_2{}^{15}N\text{-}C\text{-}OD^{\bullet+}$ (see below), we have also investigated the m/z 45 ions from oxamide, **III**. In the mass spectrum of **III**, m/z 45, $[C,H_3,N,O]^+$, is 60% of base peak, m/z 44. Its CID mass spectrum is indistinguishable from that of m/z 45 derived from methyl carbamate.

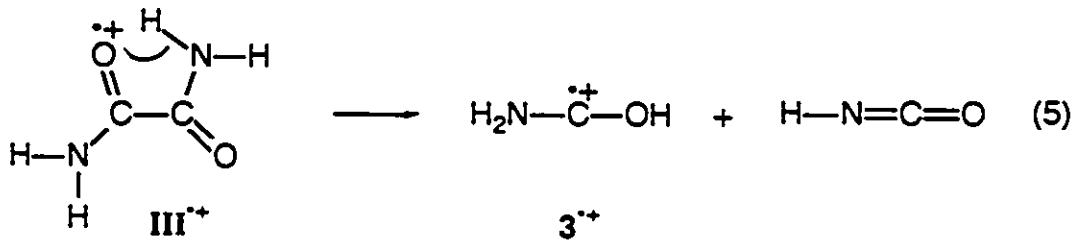

$III^{\bullet+}$ $3^{\bullet+}$ (5)

The MI spectra of $1^{\bullet+}$ and of putative ions $2^{\bullet+}$ and $3^{\bullet+}$ are shown in Table 9.1. (Note that our kinetic energy release ($T_{0.5}$) value for $H^{\bullet}$ loss from $3^{\bullet+}$ (70 meV) is much larger than that reported by Hop et al. (10 meV [9]). Our larger value was reproducible over many months and, as discussed below, is perfectly compatible with a carbene-type structure). Although unequivocal structure assignment is not possible from these spectra, both the intensity distributions and the $T_{0.5}$ values indicate that $2^{\bullet+}$ and $3^{\bullet+}$ are distinct from $1^{\bullet+}$: metastable ions $2^{\bullet+}$ and $3^{\bullet+}$ undergo decarbonylation in addition to

loss of H$^{\bullet}$. The $T_{0.5}$ values for loss of H$^{\bullet}$ are much larger for **2**$^{\bullet+}$ and **3**$^{\bullet+}$ than for **1**$^{\bullet+}$: the most stable $[M - H^{\bullet}]^+$ product ion is $H_2N\text{-}C{=}O^+$, ΔH_f = 167 kcal/mol [8a], with $HN{=}C\text{-}OH^+$ lying 19 kcal/mol higher in energy [24]; their characteristically different CID mass spectra have been recently published [25]. The CID spectra of the metastably generated $[M - H^{\bullet}]^+$ ions from **1**$^{\bullet+}$, **2**$^{\bullet+}$ and **3**$^{\bullet+}$ were obtained and they show that all isomers form $H_2N\text{-}C{=}O^+$ only. Ions **1**$^{\bullet+}$ and **3**$^{\bullet+}$ can produce $H_2N\text{-}C{=}O^+$ directly, whereas **2**$^{\bullet+}$ must rearrange; that for **3**$^{\bullet+}$ a large $T_{0.5}$ value is observed for direct cleavage is not in disagreement with its proposed structure: it is known from experiment [26a] and theory [26b] that O-H cleavages invariably involve significant reverse terms, whereas C-H cleavages usually do not [26c].

To probe the structure of the stable $[C,H_3,N,O]^{\bullet+}$ ions their CID mass spectra were recorded, see Table 9.2. Although there is no unique peak for any structure (but see below) the differences in intensities may be rationalized in terms of the putative structures. Thus, the more abundant loss of OH$^{\bullet}$ (yielding m/z 28) for **2**$^{\bullet+}$ and **3**$^{\bullet+}$ may be interpreted in terms of simple cleavage processes to produce $HNCH^+$ and H_2NC^+ respectively, both of which are stable products [27]. Also, since H_2NC^+ is much less stable (by 40 kcal/mol [28]) than $HNCH^+$, the former is more likely to dissociate further by loss of H$^{\bullet}$ yielding the more stable $[H,C,N]^{\bullet+}$ isomer $HNC^{\bullet+}$ and indeed for **3**$^{\bullet+}$ an intense peak is observed at m/z 27. Similarly, the lower intensities of NH_2^+, m/z 16 and m/z 29 for **2**$^{\bullet+}$ could be taken as showing that ion **2**$^{\bullet+}$ does not contain NH_2, HCO or HOC groups. Furthermore, the relatively intense peak for **2**$^{\bullet+}$ at m/z 30 (loss of NH) [#1] may originate from direct bond cleavage in $H\text{-}N{=}C(H)\text{-}OH^{\bullet+}$.

However, all of the above is purely circumstantial evidence. Unequivocal assignment to the proposed structures would come from actual structure determinations of the product ions; for example if it can be shown that $H_2N\text{-}C\text{-}OH^{\bullet+}$, upon collisional activation, produces HOC^+ [29a] and H_2NC^+ [27], as opposed to the more stable isomers

TABLE 9.1 Metastable ion (MI) spectra[a] of the $[CH_3NO]^{\bullet+}$ ions $\mathbf{1}^{\bullet+}$ - $\mathbf{3}^{\bullet+}$

Putative structure		m/z 44 (H$^\bullet$ loss)		m/z 17 (CO loss)	
		I (%)[b]	$T_{0.5}$ (meV)[c]	I (%)	$T_{0.5}$ (meV)
H_2N-C(H)=O$^{\bullet+}$	($\mathbf{1}^{\bullet+}$)	100	25	<2	9 [d]
H-N=C(H)-OH$^{\bullet+}$	($\mathbf{2}^{\bullet+}$)	100	90	35	45
H_2N-C-OH$^{\bullet+}$	($\mathbf{3}^{\bullet+}$)	50	70	100	40

a 2FFR, 8 keV ions; [b] Intensities relative to base peak = 100 %;
[c] Kinetic energy release values derived from the half height width of the metastable peak, corrected for the width of the main beam ;
[d] This weak peak may be of collision induced origin.

TABLE 9.2 Collision induced dissociation (CID) spectra[a] of the $[CH_3NO]^{\bullet+}$ ions $\mathbf{1}^{\bullet+}$ - $\mathbf{3}^{\bullet+}$

	m/z of daughter ion[b]										
Putative structure	15	16	17	26	27	28	29	30	42	43	44
H_2N-C(H)=O$^{\bullet+}$ ($\mathbf{1}^{\bullet+}$)	6	64	(190)	7	18	40	100	10	15	50	(330)
H-N=C(H)-OH$^{\bullet+}$ ($\mathbf{2}^{\bullet+}$)	4	28	(47)	7	30	100	55	20	10	40	(170)
H_2N-C-OH$^{\bullet+}$ ($\mathbf{3}^{\bullet+}$)	6	55	(55)	12	60	92	100	10	20	90	(400)

[a] 2FFR, 8 keV ions, collision gas O_2 ; [b] Intensities (±5%) relative to base peak = 100 %;
[c] Values in parentheses refer to low energy processes. By consensus [33], their intensities are not included in the normalization.

[8a] HCO^+ [29] and $HNCH^+$, then this greatly supports the proposed structure, $3^{\bullet+}$. Table 9.3 lists all potential reaction products, for the structure characteristic region m/z 27 - m/z 30, together with their combined enthalpies. Four structures are possible for m/z 29 : HCO^+, HOC^+, $H\text{-}C\text{-}NH_2^{\bullet+}$ [27a] and $H_2C{=}NH^{\bullet+}$ [27a] whereas m/z 28 could be $CO^{\bullet+}$, $HNCH^+$ and/or H_2NC^+. Table 9.3 further shows that loss of $^{\bullet}OH$ from $2^{\bullet+}$ requires only 27 kcal/mol and so its CID mass spectrum is expected to be dominated by m/z 28, $HNCH^+$.

To characterize the product ions in CID/CID experiments, m/z 45 is selectively transmitted by B and induced to decompose in the 2FFR by collision to e.g. m/z 28. The latter ion is then selected by E_1 and its CID mass spectrum is obtained in the 3FFR. The resulting CID mass spectra of m/z 28 for isomers $1^{\bullet+}$, $2^{\bullet+}$ and $3^{\bullet+}$ are shown in Fig. 9.2. Comparison with reference spectra [27b] shows that $2^{\bullet+}$ produces $HNCH^+$, as anticipated above. Similar experiments on the relatively intense peak at m/z 30 from $2^{\bullet+}$ established it to be $H\text{-}C\text{-}OH^{\bullet+}$ [10a,b]. These findings, together with the overall CID mass spectrum discussed above, provide good evidence for the structure $H\text{-}N{=}C(H)\text{-}OH^{\bullet+}$.

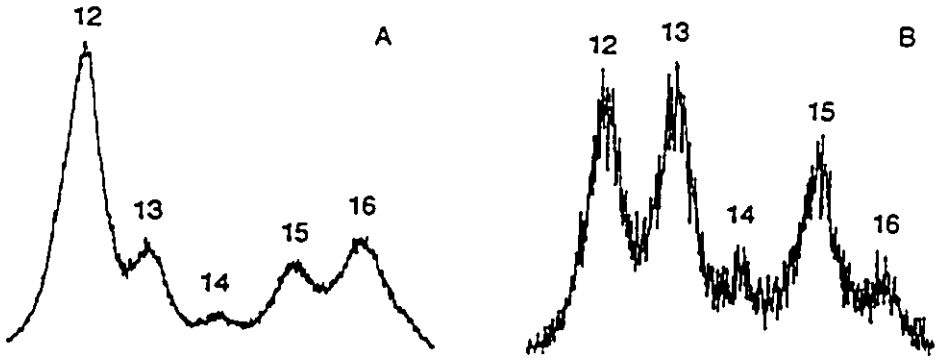

Fig. 9.2 Partial (He, 3FFR) CID mass spectra of m/z 28 generated from collisionally activated (O_2,2FFR) ions $H_2N\text{-}CH(=O)^{\bullet+}$ or $H_2N\text{-}C\text{-}OH^{\bullet+}$ (item A) and $H\text{-}N{=}C(H)OH^{\bullet+}$ ions (item B).

The closely similar CID/CID spectra of $\mathbf{1}^{\bullet+}$ and $\mathbf{3}^{\bullet+}$ (Fig. 9.2A) do not permit the assignment of structures to the $[H_2,C,N]^+$ ions. This is because a considerable amount of $CO^{\bullet+}$ is also present, as exemplified by the intense peaks at m/z 12 and m/z 16. Analysis of the relative collision efficiencies of $CO^{\bullet+}$ and $HNCH^+/H_2NC^+$ reveals that Fig. 9.2A represents a 1 : 1 mixture of $CO^{\bullet+}$ and $[C,H_2,N]^+$ [#2]. This interference problem was overcome by examining the isotopomers, $D_2{}^{15}N\text{-}CD(=O)^{\bullet+}$ and $D_2{}^{15}N\text{-}C\text{-}OD^{\bullet+}$, of $\mathbf{1}^{\bullet+}$ and $\mathbf{3}^{\bullet+}$ which produce fragment ions of unique elemental composition : m/z 27 $[^{15}NC]^+$, m/z 28 $[CO]^{\bullet+}$, m/z 29 $[D,C,^{15}N]^{\bullet+}$, m/z 30 $[D,C,O]^+$, m/z 31 $[D_2,C,^{15}N]^+$, m/z 32 $[D_2,C,O]^{\bullet+}$, and m/z 33 $[D_3,C,^{15}N]^+$. The partial CID mass spectra of $D_2{}^{15}N\text{-}CD(=O)^{\bullet+}$ and $D_2{}^{15}N\text{-}C\text{-}OD^{\bullet+}$ are given in Fig. 9.3A and 9.3C : considering that formation of $D^{15}NC^+$, DOC^+ and $D_2{}^{15}NC^+$ from $D_2{}^{15}N\text{-}C\text{-}OD^{\bullet+}$ have similar energy requirements (see Table 9.3) it is gratifying to observe that in Fig. 9.3C the peaks m/z 29, m/z 30 and m/z 31 are of similar intensity whereas the spectrum of $D_2{}^{15}N\text{-}CD(=O)^{\bullet+}$ is dominated by DCO^+. The CID spectra of the m/z 30 and 31 ions in these spectra (CID/CID) are shown in Fig. 9.4. Comparison with reference spectra confirms that $D_2{}^{15}N\text{-}C\text{-}OD^{\bullet+}$ forms largely DOC^+ and $D_2{}^{15}NC^+$, whereas $D_2{}^{15}N\text{-}CD(=O)^{\bullet+}$ generates largely DCO^+ and $D^{15}NCD^+$. Both precursor ions produce $D^{15}NC^{\bullet+}$, m/z 29 and $D\text{-}C\text{-}OD^{\bullet+}$, m/z 32. Thus $\mathbf{3}^{\bullet+}$ produces predominantly HOC^+ and H_2NC^+, instead of the more stable isomers HCO^+ and $HNCH^+$, which attests to the structure $H_2N\text{-}C\text{-}OH^{\bullet+}$.

Furthermore, it can be concluded that, after activation ions $\mathbf{1}^{\bullet+}$ and $\mathbf{3}^{\bullet+}$ do not interconvert to an appreciable extent. Since $\mathbf{2}^{\bullet+}$ generates $HNCH^+$, see above, ions $\mathbf{2}^{\bullet+}$ and $\mathbf{3}^{\bullet+}$ do not interconvert either [#3].

The collision induced formation of $HNCH^+$ from $\mathbf{1}^{\bullet+}$ is best rationalized by a **post**-collisional isomerization into $\mathbf{2}^{\bullet+}$ via a 1,3-hydrogen shift, followed by loss of $^{\bullet}OH$. This process may also explain the (weak) m/z 30 peak $(H\text{-}C\text{-}OH^{\bullet+})$ in the spectrum of $\mathbf{1}^{\bullet+}$. If $\mathbf{1}^{\bullet+}$ can isomerize to $\mathbf{2}^{\bullet+}$ then, see Fig. 9.1, $\mathbf{2}^{\bullet+}$ ought to isomerize to $\mathbf{1}^{\bullet+}$. Indeed, CID/CID experiments (spectra not given) show that the $[H,C,O]^+$ ions formed from $\mathbf{2}^{\bullet+}$ are

mostly (~75%) HCO^+, indicative of isomerization into $1^{\bullet+}$. The CID mass spectrum of the labelled ion $H\text{-}N{=}C(H)\text{-}OD^{\bullet+}$ shows an intensity distribution of m/z 27 : 28 : 29 : 30 : 31 = 26 : 100 : 40 : 17 : 20, which compares very well with the unlabelled spectrum (see Table 9.2) if m/z 29 and m/z 30 are summed, i.e. m/z 29 is HCO^+ (75%) and m/z 30 is DOC^+ (25%). Hence, post-collisional isomerization, i.e. $H\text{-}N{=}C(H)\text{-}OD^{\bullet+} \rightarrow HDN\text{-}CH(=O)^{\bullet+}$, is the most logical explanation for the significant formyl peak (m/z 29) in the spectrum of $2^{\bullet+}$ [#3].

Thus ions $1^{\bullet+}$, $2^{\bullet+}$ and $3^{\bullet+}$ are distinct stable species which, below the dissociation threshold of lowest energy requirement, do not rearrange to an appreciable extent, in good agreement with the results of the *ab initio* calculations. Rearrangements that are seen in collision experiments are due to **post**-collisional isomerizations of energized ions.

TABLE 9.3. Combined enthalpies[a] for dissociation products formed from $[CH_3NO]^{\bullet+}$ ions $1^{\bullet+}$-$3^{\bullet+}$

m/z	Products			$\Sigma\Delta H_f$	E_{act} (ion)[b]
30	$H_2C{=}O^{\bullet+}$	+	NH	315	
	$H\text{-}C\text{-}OH^{\bullet+}$	+	NH	320	
29	HCO^+	+	$^{\bullet}NH_2$	242	52 ($1^{\bullet+}$)
	HOC^+	+	$^{\bullet}NH_2$	275	85 ($3^{\bullet+}$)
	$H_2C{=}NH^{\bullet+}$	+	O	320	
	$H\text{-}C\text{-}NH_2^{\bullet+}$	+	O	318, 306[c]	
28	$CO^{\bullet+}$	+	NH_3	286	
	$HCNH^+$	+	$^{\bullet}OH$	235	27 ($2^{\bullet+}$)
	H_2NC^+	+	$^{\bullet}OH$	274	84 ($3^{\bullet+}$)
27	$HNC^{\bullet+}$	+	H_2O	278	
	$HCN^{\bullet+}$	+	H_2O	288	

[a] Values in kcal/mol, taken from ref. 8a ; [b] Activation energy, E_{act}, for direct bond cleavage from the ion in parentheses : using ΔH_f ($H_2N\text{-}C(H){=}O^{\bullet+}$) ($1^{\bullet+}$) = 190 kcal/mol [8a], ΔH_f ($H\text{-}N{=}C(H)\text{-}OH^{\bullet+}$ ($2^{\bullet+}$)) = 208 kcal/mol (from data in Fig. 9.1) and ΔH_f ($H_2N\text{-}C\text{-}OH^{\bullet+}$) ($3^{\bullet+}$) = 190 kcal/mol [9] ; [c] Ref. 34.

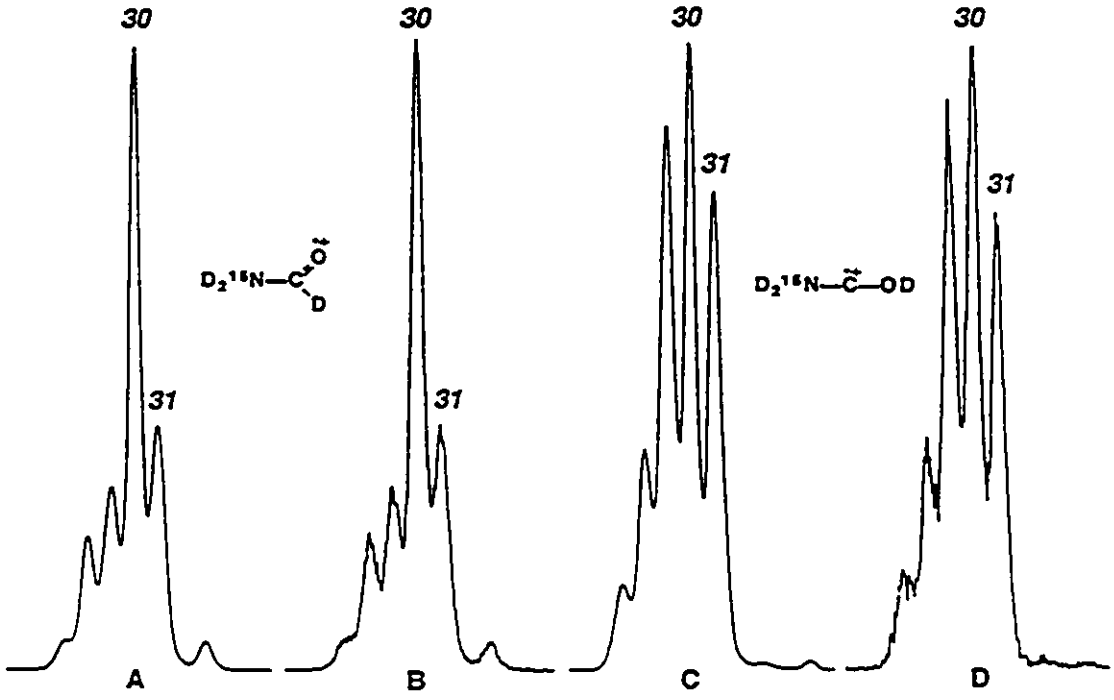

Fig. 9.3 Partial (He, 3FFR) CID mass spectra of source generated ions $D_2{}^{15}N\text{-}CD(=C)^{\bullet+}$ (item A) and $D_2{}^{15}N\text{-}C\text{-}OD^{\bullet+}$ (item C) and the (He, 3FFR) CID mass spectra of their NR "survivor" ions, (items B and D) respectively.

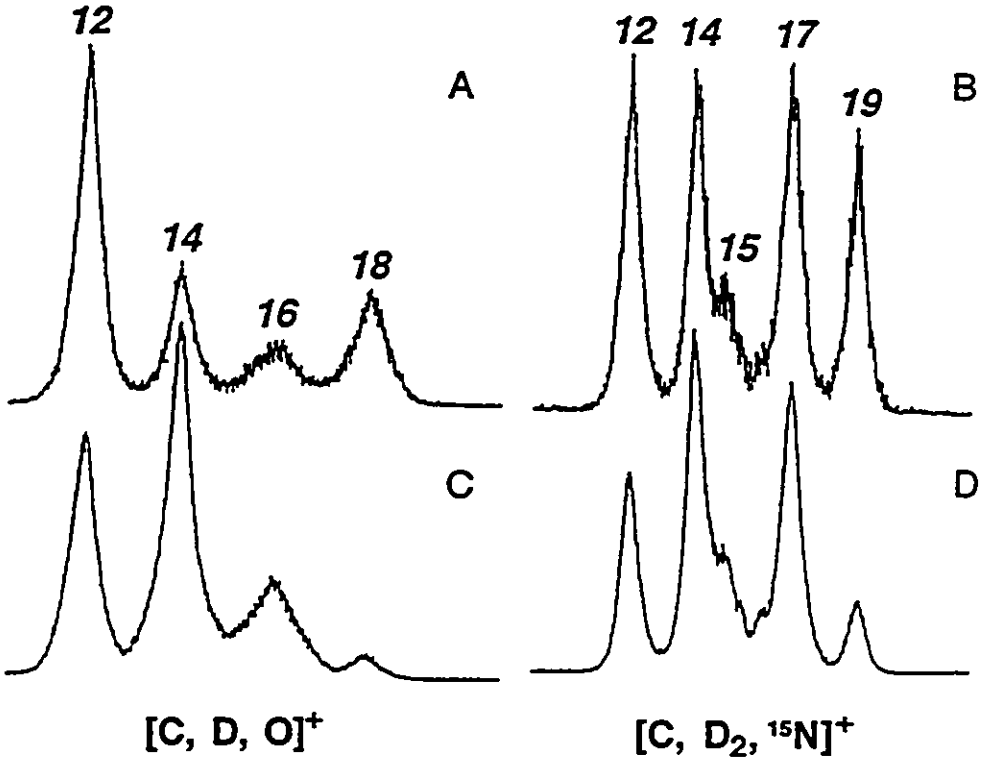

Fig. 9.4 Partial (He, 3FFR) CID mass spectra of m/z 30 and m/z 31 generated from collisionally activated (O_2, 2FFR) ions $D_2{}^{15}N\text{-}C\text{-}OD^{\bullet+}$, items A and B respectively, and ions $D_2{}^{15}N\text{-}CD(=O)^{\bullet+}$, items C and D respectively.

Neutralization-Reionization (NR) experiments

The NR mass spectra of **1**$^{\bullet+}$, **2**$^{\bullet+}$ and **3**$^{\bullet+}$ using N,N-dimethylaniline (NDMA) as the neutralizing reagent are shown in Fig. 9.5. In all [NDMA/O_2] NR spectra the "survivor" ion is the base peak. However, a comparison with the [O_2] CID spectra in Table 9.2, shows that the structure characteristic regions of the CID and NR spectra are clearly different : for **1**$^{\bullet+}$ and **3**$^{\bullet+}$ m/z 28 is relatively more intense in the NR spectrum compared to the CID spectrum whereas for **2**$^{\bullet+}$ m/z 29 is more intense. Therefore, a mere comparison between the NR and CID spectra does not permit a firm structure assignment to the neutral species generated. Neutralization- (collisional) reionization efficiencies of isobaric and even isomeric species can easily differ by a factor of 100 [6e,g], and it is therefore essential to carefully establish the purity of the primary ion beam in terms of undesired species of the same m/z value as described in the preceding section. However, even when the primary ions are pure, "interference" peaks may be present in NR spectra which make comparison with CID spectra difficult. These signals may arise from a variety of sources i.e., from neutrals formed from metastable ions (in our case CO, see Table 1), from collisionally activated ions or from excited neutralized precursors.

From additional NR experiments with ions **3**$^{\bullet+}$ it appeared that the m/z 28 peak became even more intense when either cyclopropane (CP) or Xe was used for neutralization : with NDMA m/z 28/ m/z 29 is 1.4 (see Fig. 9.5), for CP it becomes 2.3 (Fig. 9.5C, inset) and with Xe , in agreement with earlier work [9], it further rises to c. 4. That the increased contribution to m/z 28 is $CO^{\bullet+}$, not $HNCH^+$, was already likely from our earlier work on the isotopomer $H_2N\text{-}C\text{-}OD^{\bullet+}$ [10d], and it is further confirmed by the NR spectrum of $D_2{}^{15}N\text{-}C\text{-}OD^{\bullet+}$ (not shown). Hop et al. [9] attributed the enhanced $CO^{\bullet+}$ signal to a certain degree of fragmentation of excited neutrals **3** to CO and NH_3, (see Fig. 9.1) [#4]. Indeed, we observed that when the neutralization gas was replaced by He only m/z 28 remained, as expected, but its intensity was now lower by a factor of 3 than in the NR spectra. This shows that the increase of m/z 28 in the NR spectrum compared to the CID

spectrum is largely due to CO generated from excited neutralized precursors but, as discussed below, it is not necessary to trace these sources. The same conclusion holds true for ions $1^{\bullet+}$.

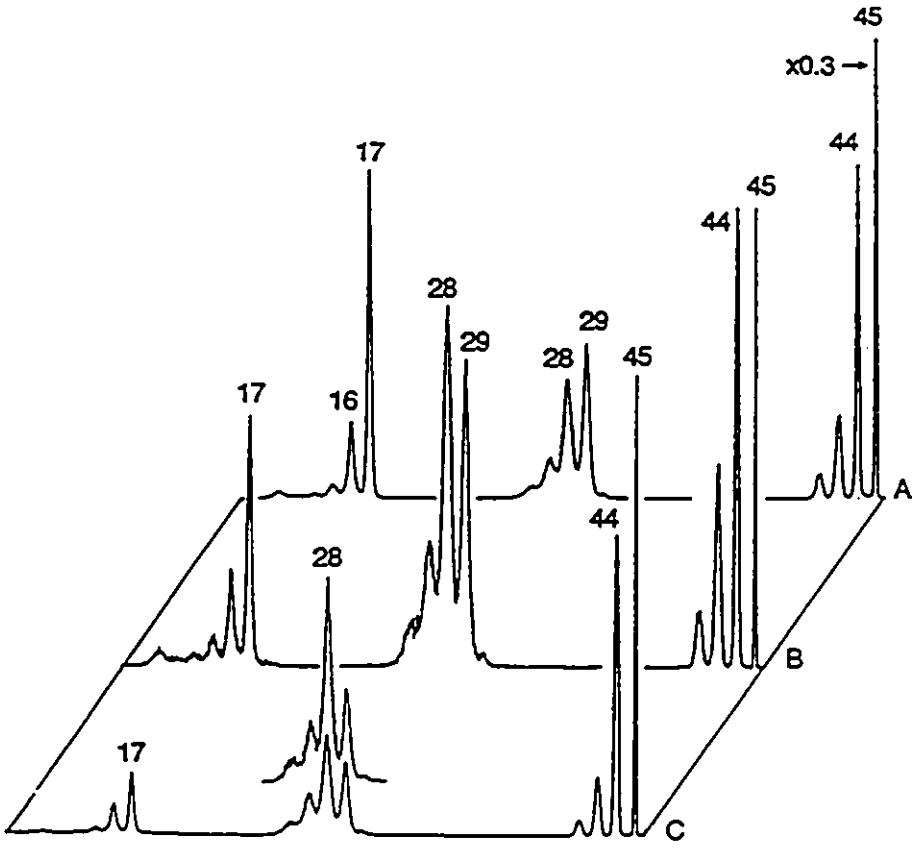

Fig. 9.5 (NDMA/O_2, 2FFR) NR mass spectra of H_2N-CH(=O)$^{\bullet+}$, $1^{\bullet+}$, (item A), H-N=C(H)OH$^{\bullet+}$, $2^{\bullet+}$, (item B) and H_2N-C-OH$^{\bullet+}$, $3^{\bullet+}$ (item C); inset item C: neutralization with cyclopropane. Product ion yields were $\Sigma[I^+]/[M^{\bullet+}]$ = 0.0010, 0.0002 and 0.0004 for $1^{\bullet+}$, $2^{\bullet+}$ and $3^{\bullet+}$ respectively.

Thus, although neutralization with NDMA causes less dissociation of the neutral than neutralization with CP or Xe, the reaction is nevertheless observed. This raises a disturbing possibility: if neutralization can lead to dissociation of the neutral then it could also lead to isomerization of the neutral precursor.

Fortunately, a powerful tool is available to probe this question: the MS/MS/MS type technique "CID spectrometry of NR "survivor" ions" avoids the above mentioned interferences in NR spectra. The technique involves selectively transmitting the "survivor" ion in the 2FFR NR spectrum through E_1 to the 3FFR where its CID mass spectrum is obtained. The CID/NR mass spectrum reflects the behaviour of the non-decomposing neutrals: if these species do not isomerize and if the primary ion beam is pure, then (barring internal energy effects, see below) the CID/NR spectrum should be very close to the CID mass spectrum. Applying this technique to the isotopomers of **1**, **2** and **3** may provide the clearest information about the extent of isomerization, if any, of the non-dissociating neutrals **1** - **3**.

In Fig. 9.6 are given, for $\mathbf{1}^{\bullet+}$, $\mathbf{2}^{\bullet+}$ and $\mathbf{3}^{\bullet+}$ the CID and CID/NR spectra in the structure diagnostic region whereas Fig. 9.3 shows a comparison of the CID and CID/NR spectra of the labelled ions $D_2{}^{15}N\text{-}CD(=O)^{\bullet+}$ and $D_2{}^{15}N\text{-}C\text{-}OD^{\bullet+}$. For $\mathbf{1}^{\bullet+}$ and $\mathbf{3}^{\bullet+}$ m/z 28 is more intense in the NR (see Fig. 9.5) than in the CID spectrum, due to dissociation of excited neutrals, see above. These neutrals do not interfere in the CID/NR spectrum and indeed the CID/NR spectra of $\mathbf{1}^{\bullet+}$ and $\mathbf{3}^{\bullet+}$ are gratifyingly close to their respective CID mass spectra. This result is already good evidence that neutral aminohydroxycarbene, **3**, is a stable species. This conclusion is reinforced by the spectra of the labelled species presented in Fig. 9.3 which clearly show that the reaction sequence $\mathbf{3}^{\bullet+} \rightarrow \mathbf{3} \rightarrow \mathbf{3}^{\bullet+}$ (and also $\mathbf{1}^{\bullet+} \rightarrow \mathbf{1} \rightarrow \mathbf{1}^{\bullet+}$), in agreement with the ab initio calculations, does not involve any appreciable rearrangement. This substantiates the earlier proposals [9,10d] for experimental observation of this species by NRMS.

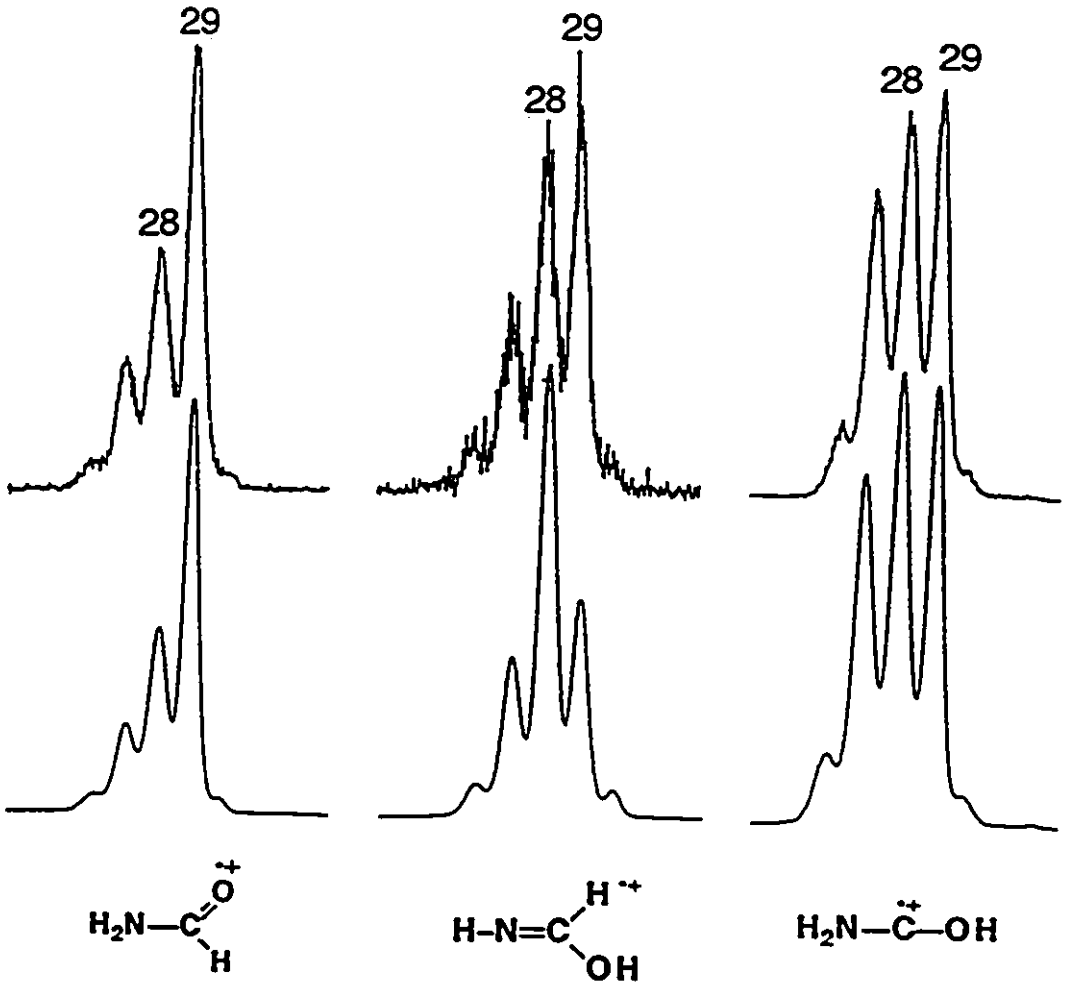

Fig. 9.6 Partial (He, 3FFR) CID mass spectra of NR "survivor" ions (top spectra) and (He, 3FFR) CID mass spectra of source generated ions (bottom spectra) of $H_2N\text{-}CH(=O)^{\bullet+}$, $1^{\bullet+}$, $H\text{-}N=C(H)OH^{\bullet+}$, $2^{\bullet+}$, and $H_2N\text{-}C\text{-}OH^{\bullet+}$, $3^{\bullet+}$.

However, a different situation pertains for **2**. This is seen by comparing the m/z 28 : m/z 29 ratio which for $\mathbf{2}^{\bullet+}$ continuously *decreases* in going from CID to NR to CID/NR , see Fig. 9.5 and 9.6. Now it is entirely possible that, as was the case for **1** and **3**, along neutralization of **2**, CO molecules are co-generated but then the resulting increase of m/z 28 in NR (Fig. 9.5) must be out-grown by an even larger relative increase in m/z 29. The (further) decrease of the m/z 28 : m/z 29 ratio in CID/NR can be rationalized in terms of elimination of the interfering CO molecules as was done for **1** and **3**. Hence, in going from CID to NR m/z 28 increases but m/z 29 grows even more: in going from NR to CID/NR m/z 29 stops increasing and m/z 28 decreases. These observations can most simply be explained in terms of the tautomerization **2** → **1** taking place among the neutrals, which upon reionization becomes frozen [#5]. Note that the reverse reaction explains the (slightly) higher intensity of m/z 28 in the CID/NR spectrum of $\mathbf{1}^{\bullet+}$, compared to its CID spectrum (see Fig. 6). Thus, although tautomerism is observed among the high energy molecules **2**, the low energy neutrals retain their structural integrity; hence *formimidic acid is a stable molecule* as predicted by *ab initio* calculations.

The above interpretation appears reasonable but, at least in principle, there is an alternative. Note, see Fig. 9.6, that the CID/NR spectrum of $\mathbf{2}^{\bullet+}$ is not drastically different from that of $\mathbf{3}^{\bullet+}$. One could therefore argue that the CID/NR spectrum of $\mathbf{2}^{\bullet+}$ actually represents the formation of **3** and that the observed intensity differences in the respective CID/NR spectra are due to differences in internal energies. It has already been established that the primary ion beam of $\mathbf{2}^{\bullet+}$ is free of ions $\mathbf{3}^{\bullet+}$ and so if structure **3** is formed it must have been generated from the *neutral* **2** , via a 1,2-hydrogen shift. This is unlikely since the calculations predict the barrier **2** → **3** to be much higher (by 50 kcal/mol) than that for **2** → **1** and so isomerization into **1** rather than **3** is expected. More importantly, we have good *experimental* evidence that neutral **2** does not rearrange into **3**. The labelled neutral H-N=C(H)-OD, if it isomerizes into **3**, would generate H_2N-C-OD

which upon reionization should specifically form DOC^+, m/z 30 and not m/z 29, HCO^+. This is not observed: upon reionization the labelled species almost specifically forms m/z 29, HCO^+. Moreover, ion $2^{\bullet+}$ exclusively eliminates the O-H hydrogen atom (see preceding section) and so the labelled neutral H-N=C(D)-OH, if it isomerizes to **3**, would generate HDN-C-OH, which, upon reionization, should specifically lose $H^\bullet$. The above labelled formimidic acid was not available but we did observe that the isotopomers H-N=C(H)-OD and D-N=C(H)-OH, upon reionization, both specifically lose $H^\bullet$. Hence, H-N=C(H)-OH, upon reionization, loses the C-H hydrogen atom only and so formimidic acid does not rearrange to aminohydroxycarbene. The possibility that **2** isomerizes into **3** via **1**, i.e. H-N=C(H)-OD → HDN-C(H)=O → HDN-$\ddot{C}$-OH , can also be ruled out : $2^{\bullet+}$ forms HCO^+ not HOC^+ and moreover, there is no direct evidence to suggest that **1** isomerizes into **3**.

Finally, we have good evidence that differences in internal energy have little, if any, effect on the intensity distributions in the CID/NR spectra of $3^{\bullet+}$. When cyclopropane (CP) was used as neutralizing agent for the reduction of $3^{\bullet+}$ and its isotopomer $D_2{}^{15}N$-C-OD, significantly more free CO was formed from excited neutrals [#6] (see inset Fig. 9.5), i.e., the neutrals generated by reduction with CP have a significantly higher energy content. It is therefore likely that the non-decomposing neutrals generated by neutralization with CP also have a larger internal energy content. However, the CID/NR mass spectra using NDMA (Figs. 9.3C and 9.6) and CP (not shown) are superimposable and so differences in internal energy have no effect on the intensities. This parallels the general observation of the small dependence on internal energy of the appearance of keV CID spectra.

N-methylformimidic acid, CH_3-N=C(H)OH, and N-methylaminohydroxycarbene

As mentioned above, the loss of CH_3CN from ionized Gyromitrin has been rationalized [15b] in terms of a McLafferty type rearrangement leading to CH_3-N=C(H)$OH^{\bullet+}$, eq. 6:

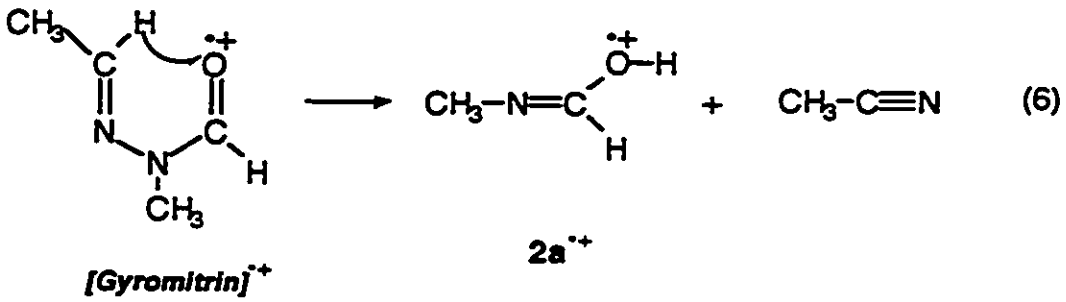

(6)

Ion **2a**$^{\bullet+}$ is tautomeric with ionized N-methyl formamide, CH_3-N(H)-C(H)=O$^{\bullet+}$, **1a**$^{\bullet+}$, which can be made by direct ionization of **1a**, and with the ionized carbene, CH_3-N(H)-C-OH$^{\bullet+}$, **3a**$^{\bullet+}$; the latter has been generated by loss of CH_2=O from CH_3-N(H)-C(=O)O$CH_3^{\bullet+}$ [25]. Unfortunately the isobaric species CH_3-O-C=O$^{\bullet+}$ is also produced [25] and to avoid interferences we have, analogous to the formation of **3**$^{\bullet+}$, generated **3a**$^{\bullet+}$ from N,N'-dimethyloxamide, eq. 7:

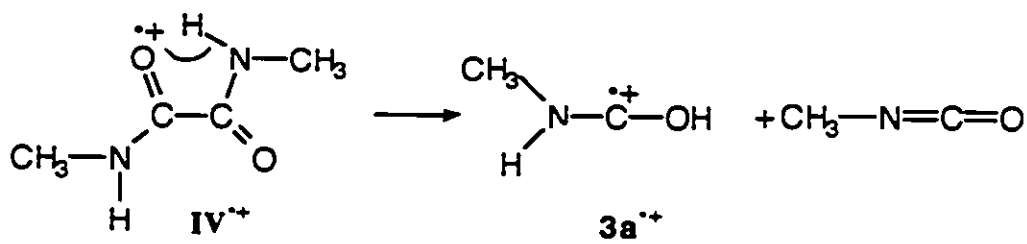

(7)

In the electron ionization mass spectrum of **IV**, m/z 59 is 50% of base peak, m/z 58.

There is a fourth isomer with a CNCO backbone, one which has no counterpart in the smaller $CH_3NO^{\bullet+}$ system, the distonic ion $^{\bullet}CH_2$-N(H)-C^{+}(H)-OH, **1d**$^{\bullet+}$. This ion may be generated by loss of C_3H_6 from ionized N-isobutyl formamide or CH_2=O from ionized formylaminoethanol.

The MI spectra of putative ions **2a**$^{\bullet+}$, **3a**$^{\bullet+}$, **1d**$^{\bullet+}$ of **1a**$^{\bullet+}$ are shown in Table 9.4.

TABLE 9.4. Metastable ion spectra of the $[C_2, H_5, N, O]^{\bullet+}$ ions[a,b]

Putative structure		m/z of daughter ions[c,d] 58	44		42		41		30	
$CH_3N(H)\text{-}C(H)\text{=}O^{\bullet+}$	($1a^{\bullet+}$)	60	-	(-)	-	(-)	10	(49)	100	(53)
$^{\bullet}CH_2\text{-}N(H)\text{-}C^{+}(H)\text{-}OH$	($1d^{\bullet+}$)	55	-	(-)	4	(30)	7	(42)	100	(66)
$CH_3\text{-}N\text{=}C(H)\text{-}OH^{\bullet+}$	($2a^{\bullet+}$)	100	-	(-)	2	(<150)[e]	12	(350)	75	(85)
$CH_3N(H)\text{-}C\text{-}OH^{\bullet+}$	($3a^{\bullet+}$)	55	35	(53)	-	(-)	5	(49)	100	(72)

[a] 2FFR, 8 keV ions; [b] Intensities relative to base peak = 100 %;
[c] Kinetic energy release values ($T_{0.5}$ in meV) derived from the half height width of the metastable peak, corrected for the width of the main beam; [d] Small peaks at m/z 31, 29 and 28 are omitted; [e] Difficult to measure because of broad overlapping peak at m/z 41.

TABLE 9.5. Combined enthalpies[a] for dissociation products of $[C_2, H_5, N, O]^{\bullet+}$ ions

m/z	Products			$\Sigma\Delta H_f$ (kcal/mol)
58	$CH_3NH\text{-}C\text{=}O^{+}$	+	$H^{\bullet}$	202
44	$H\text{-}N\text{=}C\text{-}OH^{+}$	+	$CH_3^{\bullet}$	220[b]
42	$CH_3NCH^{\bullet+}$	+	$OH^{\bullet}$	214
41	$CH_3NC^{\bullet+}$	+	H_2O	243
	$H_2C\text{=}N\text{=}CH^{\bullet+}$	+	H_2O	173[c]
30	$H_2C\text{=}NH_2^{+}$	+	$HCO^{\bullet}$	189

[a] Values in kcal/mol, taken from ref 8a ;
[b] Value for $H\text{-}N\text{=}C\text{-}OH^{+}$ from ref. 31 using $\Delta H_f[H_2N\text{-}C\text{=}O^{+}]$ = 167 kcal/mol [8a];
[c] $\Delta H_f[H_2C\text{=}N\text{=}CH^{\bullet+}]$ from ref. 35 using $\Delta H_f[H\text{-}C\equiv C\text{-}NH_2^{\bullet+}]$ = 251 kcal/mol [36].

It can be seen that isomer **3a**$^{\bullet+}$ is unique in that it loses a $CH_3^{\bullet}$ group [25]. This reaction has been shown to produce H-N=C-OH$^+$ via direct bond cleavage [25] and thus it is a highly structure characteristic feature of **3a**$^{\bullet+}$. In fact, **3a**$^{\bullet+}$ is the only isomer that can shed $CH_3^{\bullet}$ directly to produce a stable $[C,H_2,N,O]^+$ product ion; the formyl nitrenium ion H-N-C(H)=O$^+$, which could conceivably be generated from **1a**$^{\bullet+}$, has been shown to be a high energy transient species only [30], whereas its ring closed form lies 89 kcal/mol above H-N=C-OH$^+$ [31]. The ion $^+$N=C(H)-OH, which could have resulted from **2a**$^{\bullet+}$, is completely unknown.

All the $[C_2, H_5, N, O]^{\bullet+}$ ions abundantly lose HCO$^{\bullet}$ with varying $T_{0.5}$ values. This reaction is a rearrangement process even for the ions **1a**$^{\bullet+}$ as the daughter ions were shown to be $CH_2NH_2^+$ [32], the only known $[C,H_4,N]^+$ isomer. Ions **2a**$^{\bullet+}$ appear to be unique in that they lose H_2O with a large $T_{0.5}$ value. The combined enthalpies for the dissociation products formed from the metastable $[C_2, H_5, N, O]^{\bullet+}$ ions are shown in Table 9.5. For ion **1a**$^{\bullet+}$ the reverse term for loss of H$^{\bullet}$ is expected to be small [26c] and so the barrier for formation of $CH_2NH_2^+$ (possibly via a 1,2-hydrogen shift) cannot be much larger than 13 kcal/mol. Interestingly, loss of H_2O competes with H$^{\bullet}$ loss and so the m/z 41 daughter ions are most likely CH_2=N=CH$^{\bullet+}$ and not $CH_3NC^{\bullet+}$, see Table 9.5. Loss of the hydroxyl hydrogen from isomer **3a**$^{\bullet+}$ is expected to have a large reverse barrier [26b,c] (typically c. 1 eV) and so $CH_3^{\bullet}$ loss (for which the reverse barrier may well be small) can compete with H$^{\bullet}$ loss. Note that ions **2a**$^{\bullet+}$ can lose H_2O via a 1,4-hydrogen shift to produce CH_2=N=CH$^{\bullet+}$; the large $T_{0.5}$ value attests to the stability of this ion. Also, because of the small $T_{0.5}$ values ions **1a**$^{\bullet+}$ and **1d**$^{\bullet+}$ must shed H_2O via a different mechanism, e.g. via a 1,3-hydrogen shift in **1d**$^{\bullet+}$.

To assign structures to the stable $[C_2, H_5, N, O]^{\bullet+}$ ions their CID spectra were recorded, (see Fig. 9.7, items A, C, and E). Again isomer **3a**$^{\bullet+}$ is unique in that its CID mass spectrum is dominated by loss of $CH_3^{\bullet}$, which from MS/MS/MS experiments, see above, was indeed shown to be H-N=C-OH$^+$. By contrast, isomer **2a**$^{\bullet+}$ abundantly loses

•OH by a simple cleavage process to produce the stable ion CH_3NCH^+. Not only does this constitute convincing evidence for the proposed structures, it also indicates that these ions do not interconvert. Isomers **1a**•+ and **1d**•+ do not undergo these reactions; rather they decay via the abundant metastable loss of HCO•. The CID mass spectra of **1a**•+ (Fig. 9.7E) and putative **1d**•+ (not shown) are very similar, although **1d**•+ has a more intense peak at m/z 14, $CH_2^{\bullet+}$. Distonic ions of this type can be difficult to identify by CID [11]; however, although these ions may interconvert, they do not isomerize to either **2a**•+ or **3a**•+. The CID spectra of Fig. 9.7 (items A and C) therefore correspond to ions **3a**•+ and **2a**•+ respectively, whereas Fig. 9.7E corresponds to **1a**•+ or a mixture of and **1a**•+ and **1d**•+.

The NR mass spectra of **3a**•+, **2a**•+ and **1a**•+/**1d**•+ are shown in Fig. 9.8. Isomer **3a**•+ clearly produces the intense structure characteristic signal at m/z 44 indicating that the carbene is a stable species. Isomer **1a**•+ produces the most intense "survivor" signal whereas in the NR spectrum of putative **1d**•+ the "survivor" signal is much weaker. This in itself may indicate that most of the *ions* do indeed have the distonic structure. Note also that the "survivor" ion for **2a**•+ is equally weak. The NR efficiency of ions **2a**•+, measured as the intensity of the m/z 59 output flux relative to the m/z 59 input flux, is about 17 % of that of **1a**•+. In addition, it appears that the intensities in the structure diagnostic region of the NR spectrum of **2a**•+ are much weaker than in the CID spectrum or that the peaks at m/z 28-30 are more intense. Thus, it may well be that in the neutralization step excited species are generated which immediately dissociate by direct cleavage to, for instance, H-C-OH•+ which upon reionization yields m/z 30 and products therefrom. Thus it cannot immediately be concluded from these experiments that the "survivor" has the structure CH_3-N=C(H)OH; the presence of 17% of **1a**•+ in the primary ion beam could equally well account for the survivor signal.

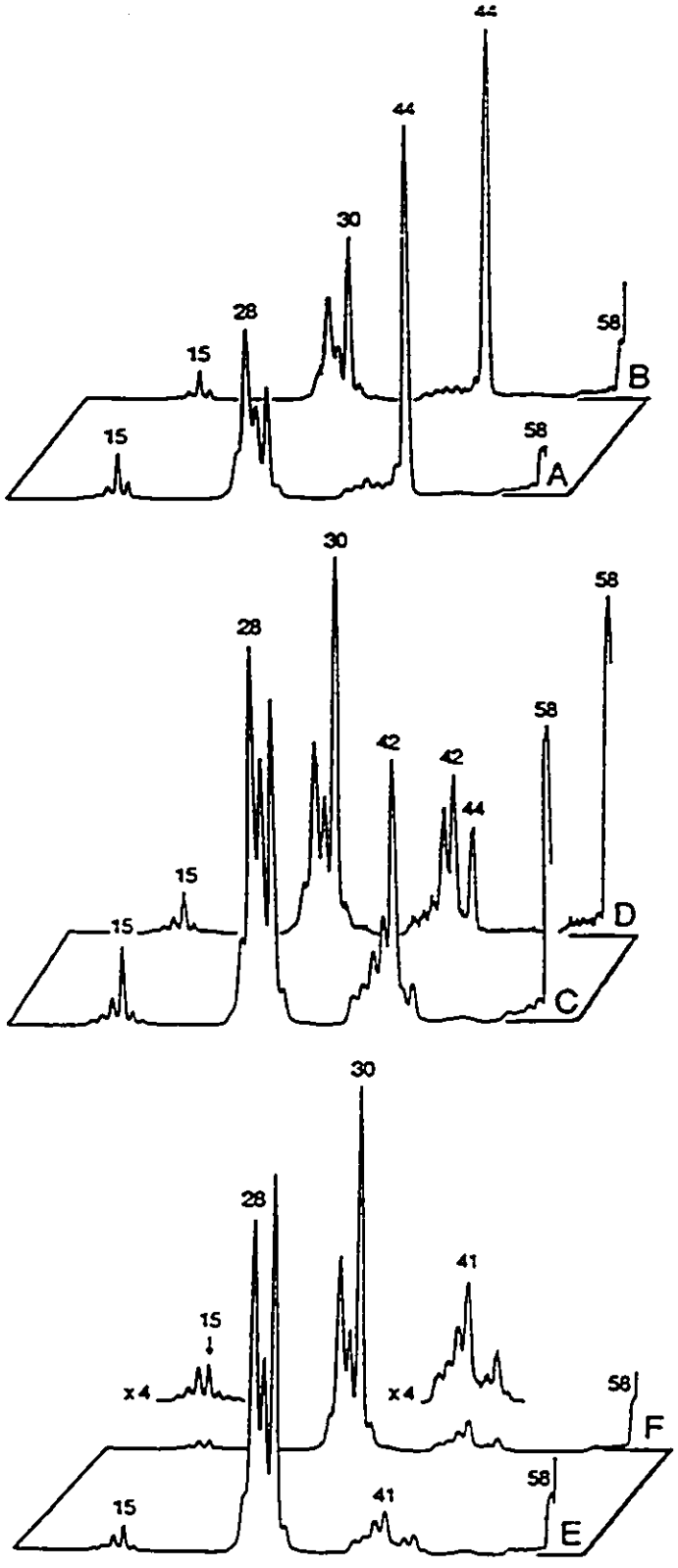

Fig. 9.7 (He, 3FFR) CID mass spectra of source generated ions $CH_3N(H)$-C-$OH^{\bullet+}$, $\mathbf{3a}^{\bullet+}$, (item A) CH_3-N=C(H)$OH^{\bullet+}$, $\mathbf{2a}^{\bullet+}$, (item C) and $CH_3N(H)$-CH(=O)$^{\bullet+}$, $\mathbf{1a}^{\bullet+}$, (item E) and (He, 3FFR) CID mass spectra of NR "survivor" ions, items B, D and F respectively.

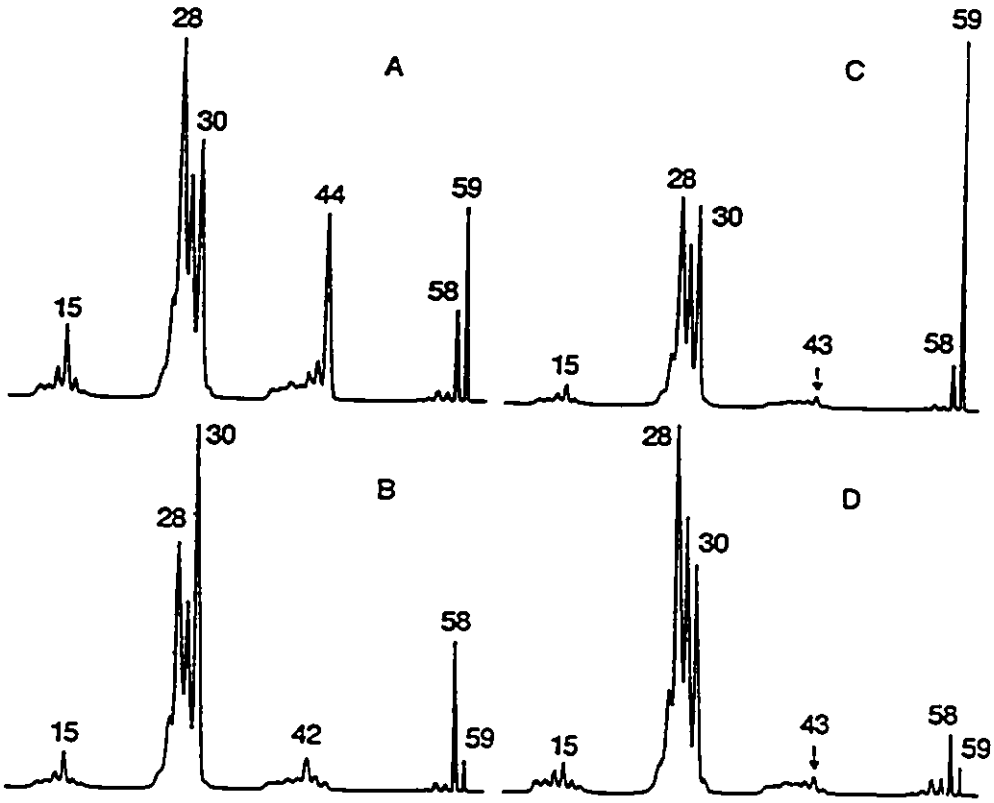

Fig. 9.8 (NDMA/O_2, 2FFR) NR mass spectra of $CH_3N(H)$-C-$OH^{\bullet+}$, **3a**$^{\bullet+}$, (item A) CH_3-N=C(H)$OH^{\bullet+}$, **2a**$^{\bullet+}$, (item B) $CH_3N(H)$-CH(=O)$^{\bullet+}$, **1a**$^{\bullet+}$ (item C) and [CH_2-N(H)-C(H)OH]$^{\bullet+}$, **1d**$^{\bullet+}$, (item D).

To determine the structure of the "survivor" ions their CID/NR spectra were recorded. They are shown in Fig. 9.7 (items B, D and F). The CID/NR spectrum of **3a**$^{\bullet+}$ (Fig. 9.7B) is close to its CID spectrum (Fig. 9.7A) and this indeed shows that the carbene is a stable species in the gas phase. For the iminol **2a**, the structure characteristic peak at m/z 42 persists in the CID/NR spectrum, compare Figs. 9.7C, 9.7D and 9.8B. No other isomer gives rise to this peak to any significant extent and thus it can be concluded that N-methylformimidic acid is also a stable molecule in the gas phase. However, a small fraction of the neutralized CH_3-N=C(H)OH$^{\bullet+}$ ions undergoes isomerization into CH_3-N(H)-$\ddot{C}$-OH, **3a** and CH_3-N(H)-C(H)=O, **1a**, as witnessed by the enhanced intensity of the m/z 44 and m/z 41 peaks in the CID/NR spectrum.

Endnotes

[#1] The m/z 30 H-C-OH$^{\bullet+}$ ion has a much higher relative abundance in O_2 CID spectra than in He CID spectra, particularly at high translational energies (at 10 keV the ratio m/z 30/29 is 0.5). The (as yet unexplained) effect is even more pronounced for the $CH_3^{\bullet}$ loss in the CID spectra of the $C_2H_5O^+$ isomer CH_3CHOH^+.

[#2] It might appear from Fig. 9.2a that m/z 28 is dominated by CO$^{\bullet+}$ with minor contributions from $[H_2,C,N]^+$, but surprisingly in Fig. 9.3c m/z 28, CO$^{\bullet+}$, is less intense than m/z 31, $[D_2,C,^{15}N]^+$. However, the collision efficiency (at c. 6 keV) to produce C^+ from CO is 2.7 ± 0.4 times higher than the formation of C^+ from $D_2{}^{15}NC^+$, even though the former process is more energy demanding (by 16 kcal/mol) [8a]. In this experiment $D_2{}^{15}$N-C-OD$^{\bullet+}$ was mass selected and induced to decompose in the 2FFR. Next the input-fluxes (IF) to the 3FFR of CO$^{\bullet+}$ (IF 28) and $D_2{}^{15}NC^+$ (IF 31) and the output-fluxes (OF) of C^+ for each species (OF 28 and OF 31 respectively) were measured; (OF 28)(IF 31) / (OF 31)(IF 28) is taken as the above relative efficiency.

[#3] A minor fraction of $3^{\bullet+}$ may isomerize into $2^{\bullet+}$ followed by loss of NH to produce m/z 30, $H\text{-}C\text{-}OH^{\bullet+}$ and the minor formation of DOC^{+} may be indicative of some isomerization of $2^{\bullet+}$ into $3^{\bullet+}$.

[#4] Methyl carbamate, not oxamide, was used as the precursor molecule in these experiments. This does not affect the conclusions since both precursor molecules generate isomerically pure beams of $3^{\bullet+}$.

[#5] It has been suggested that the CID/NR mass spectrum of 2 could be argued to correspond wholly to 1 and that the observed large intensity differences between CID/NR of 2 and CID of 1 result from internal energy effects. However, we feel that the experiments described below effectively rule out this possibility.

[#6] The endothermic redox reactions of $3^{\bullet+}$ with CP and also with Xe [9] generate considerably more excited neutrals 3 than the (formally) exothermic electron transfer with NDMA. (IE_V's [8a,c] : (Xe) = 12.1 eV; (CP) = 10.5 eV ; (NDMA) = 7.5 eV; (3) = 8.4 eV, see Fig. 9.1). This might be due to the larger number of vibrational degrees of freedom of NDMA compared with CP and Xe and thus NDMA may be a more effective energy sink.

References

(1) C.I. Perrin, Acc. Chem. Res., 22 (1989) 286 (and references cited therein).

(2) A. Bagno, C. Comuzzi and G. J. Scorrano, Chem. Soc. Perkin Trans 2, (1993) 283.

(3) C.L. Perrin, J. Am. Chem. Soc., 96 (1974) 5628.

(4) R. Roger and D.G. Neilson, Chem. Rev., 61 (1961) 179.

(5) F. Turecek, in Z. Rappoport (Ed.), The Chemistry of Enols, Wiley: Chichester, 1990, pp. 95-146.

(6) Reviews : (a) J.K. Terlouw and H. Schwarz, Angew. Chem., 99 (1987) 829; Angew. Chem. Int. Ed. Engl.,26 (1987) 805; (b) C. Wesdemiotis and F.W. McLafferty, Chem. Rev., 87 (1987) 485; (c) H. Schwarz, Pure Appl. Chem., 61 (1989) 685; (d) J.K. Terlouw, Adv. Mass Spectrom., 11 (1989) 984;

(e) J.L. Holmes, Mass Spectrom. Rev., 8 (1989) 513; (f) F.W. McLafferty, Science, 247 (1990) 925; (g) F.W. McLafferty, Int. J. Mass Spectrom. Ion Processes, 118/119 (1992) 221.

(7) (a) L. Radom, W.J. Hehre and J.A. Pople, J. Am. Chem. Soc., 93, (1971) 2299; (b) R.A. Whiteside, J.S. Binkley, R. Krishnan, D.J. DeFrees, H.B. Schlegel and J.A. Pople, "Carnegie-Mellon Quantum Chemistry Archive"; Carnegie-Mellon University: Pittsburgh, PA, (1980); (c) M.A. Robb and I.G. Csizmadia, J. Chem. Phys., 50 (1969) 1819; (d) J. Teyssere, J. Arriau, A. Dargelos, J. Elguero and A.R. Katritzky, Bull. Soc. Chim. Belg., 85 (1976) 39; (e) H. Lumbroso and G.C. Pappalardo, J. Mol. Struct., 43 (1978) 97; (f) A. Greenberg and R. Winkler, J. Mol. Struct., 63 (1980) 131; (g) H.B. Schlegel, P. Gund and E.M. Fluder, J. Am. Chem. Soc., 104 (1982) 5347; (h) R.A. Poirier, D. Majlessi and T.J. Zielinski, J. Comput. Chem. , 7 (1986) 464; (i) X.-C. Wang, J. Nichols, M. Feyereisen, M. Gutowski, J. Boatz, A.D.J. Haymet and J. J. Simons, Phys. Chem., 95 (1991) 10419; (j) M.W. Wong, K.B. Wiberg and M.J. Frisch, J. Am. Chem. Soc., 114 (1992) 1645; (k) P. Longevialle, G. Bouchoux and Y. Hoppilliard, Org. Mass Spectrom. 24 (1989) 919; (l) P. Longevialle, G. Bouchoux and Y. Hoppilliard, Org. Mass Spectrom. 25 (1980) 527.

(8) (a) S.G. Lias, J.E. Bartmess, J.F. Liebman, J.L. Holmes, R.D. Levin and W.G. Mallard, J. Phys. Chem. Ref. Data, 17 (suppl. 1) (1988); (b) R. Shaw, in S. Patai (Ed.), The chemistry of amidines and imidates, John Wiley & Sons: Toronto (1975), Ch. 11, pp. 547-565; (c) A.D. Baker, D.P. May and D.W. Turner, J. Chem. Soc. [B] 22 (1968).

(9) C.E.C.A. Hop, H. Chen, P.J.A. Ruttink and J.L. Holmes, Org. Mass Spectrom., 26 (1991) 679.

(10) (a) P.C. Burgers, A.A. Mommers and J.L. Holmes, J. Am. Chem. Soc., 105 (1983) 5976; (b) R. Feng, C. Wesdemiotis and F.W. McLafferty J. Am. Chem. Soc., 109 (1987) 6521; (c) D.J. DeFrees, A.D. McLean and E. Herbst, Astrophys. J., 279 (1984) 322; (d) G. Schaftenaar, R. Postma, P.J.A. Ruttink, P.C. Burgers, G.A. McGibbon and J.K. Terlouw, Int. J. Mass Spectrom. Ion Proc., 100 (1990) 521.

(11) G.A McGibbon, C.A. Kingsmill, J.K. Terlouw and P.C. Burgers, Org. Mass Spectrom., 27 (1992) 126.

(12) S. Villeneuve and P.C. Burgers, Org. Mass Spectrom., 21 (1986) 733.

(13) H.F. van Garderen, P.J.A. Ruttink, P.C. Burgers, G.A. McGibbon and J.K. Terlouw, Int. J. Mass Spectrom. Ion Processes, 121 (1992) 159.

(14) For the use of organic neutralization agents whose ionization energy is close to that of the recombination energy of the target ion see: (a) T. Wong, J.K. Terlouw, T. Weiske and H. Schwarz, Int. J. Mass Spectrom. Ion Processes, 113 (1992) R23; (b) M-Y. Zhang and F.W. McLafferty, J. Am. Soc. Mass Spectrom., 3 (1992) 108.

(15) (a) P.H. List and P. Luft, Archiv Pharmazie,301 (1968) 294; (b) H. Pyysalo and E. Honkanen, Acta Chem. Scand., B30 (1976) 792.

(16) I.K. Phelps and C.D. Deming, Amer. Journ. Science, 24 (1907) 173.

(17) N.V. Sidgewick, The Organic Chemistry of Nitrogen, Oxford University Press: Oxford, (1937).

(18) M.J. Frisch, M. Head-Gordon, G.W. Trucks, J.B. Foresman, H.B. Schlegel, K. Raghavachari, M.A. Robb, J.S. Binkley, C. Gonzales, D.J. DeFrees, D.J. Fox, R.A. Whiteside, R. Seeger, C.F.Melius, J. Baker, L. Martin, L.R. Kahn, J.J.P. Stewart, S. Topiol and J.A. Pople, Gaussian 90. Gaussian, Pittsburgh, PA (1990).

(19) W.J. Hehre and R. Ditchfield, Pople, J.A. J. Chem. Phys., 56 (1972) 2257.

(20) P.C. Harihan and J.A. Pople, Theor. Chim. Acta, 28 (1973) 213.

(21) (a) C. Møller and M.S. Plesset, Phys. Rev., 46 (1934) 618; (b) J.A. Pople, R. Seeger and R. Krishnan, Int J. Quantum Chem., Quantum Chem. Symp., 11 (1977) 149.

(22) J.A. Pople, H.B. Schlegel, R. Krishnan, D.J. DeFrees, J.S. Binkley, M.J. Frisch, R.A. Whiteside, R.F. Hout and W.J. Hehre, Int J. Quantum Chem., Quantum Chem. Symp., 15 (1981) 269.

(23) P.C. Burgers, P.J.A. Ruttink and J.K. Terlouw, in preparation.

(24) C.E.C.A Hop, J.L. Holmes, P.J.A. Ruttink, G. Schaftenaar and J.K. Terlouw, Chem. Phys. Lett.,156 (1989) 251.

(25) G.A. McGibbon, J.K. Terlouw and P.C. Burgers, Rapid Commun. Mass Spectrom.. 7 (1993) 138.

(26) (a) P.C. Burgers, J.L. Holmes and J.K. Terlouw, J. Chem. Soc. Chem. Commun., (1984) 642; (b) W.J. Bouma, P.C. Burgers, J.L. Holmes and L. Radom, J. Am. Chem. Soc., 108 (1986) 1767; (c) At the MRCI (Pople)/DZP level of theory, the loss of H$^{\bullet}$ from $3^{\bullet+}$ has a reverse barrier of 17.3 kcal/mol; this reaction and the mechanisms for the spontaneous decarbonylation of ions $2^{\bullet+}$ and $3^{\bullet+}$ will be discussed in detail elsewhere: see ref 23.

(27) (a) P.C. Burgers, J.L. Holmes and J.K. Terlouw, J. Am. Chem. Soc., 106 (1984) 2762; (b) P.C. Burgers, J.K. Terlouw, T. Weiske and H. Schwarz, Chem. Phys. Lett., 132 (1986) 69.

(28) T.K. Ha and M.T. Nguyen, Chem. Phys. Lett., 97 (1983) 503.

(29) (a) P.C. Burgers and J.L. Holmes, Chem. Phys. Lett., 97 (1983) 236; (b) A.J. Illies, M.F. Jarrold and M.T. Bowers, J. Chem. Phys., 77 (1982) 5847; (c) A.J. Illies, M.F. Jarrold and M.T. Bowers, J. Am. Chem. Soc., 105 (1983) 2562.

(30) J.P. Kiplinger, A.T. Maynard and M.M. Bursey, Org. Mass Spectrom., 22 (1987) 534.

(31) S. Green, J. Phys. Chem., 85 (1981) 1676.

(32) A.G. Loudon and K.S. Webb, Org. Mass Spectrom., 12 (1977) 283.

(33) J.L. Holmes, Org. Mass Spectrom., 20 (1985) 169.

(34) M.J. Frisch, K. Raghavachari, J.A. Pople, W.J. Bourna and L. Radom, Chem. Phys., 75 (1983) 323.

(35) B. van Baar, W. Koch, C. Lebrilla, J.K. Terlouw, T. Weiske and H. Schwarz, Angew. Chem. 98 (1986) 834.

(36) J.M. Buschek, J.L. Holmes and F.P. Lossing, Org. Mass Spectrom., 21 (1986) 729.

EXPERIMENTAL

The Mass Spectrometer

All the Metastable Ion (MI), Collisional Activation (CA), Collision-Induced Dissociative Ionization (CIDI), Neutralization-Reionization (NR) and multiple collision mass spectra (see INTRODUCTION), except those of methyl carbamate (Chapter 2), were recorded on the McMaster University VG Analytical ZAB-R mass spectrometer of $B(\perp Q)E_1E_2$ geometry (B = magnet, Q = quadrupole and E = electric sector) using an accelerating voltage of 8 or 10 keV. This three sector BEE-type instrument is based on the standard, non-extended geometry of the ZAB-2f [1]. Its source and focus housing - each with 160/700 Diffstak pumping - is that of the standard ZAB-2E/SE instruments. There are four inlet systems for sample introduction to the ion source. They are: (1) the septum inlet, for volatiles; (2) an all quartz direct insertion probe, for less volatile materials; (3) a direct insertion probe, for solids and; (4) an all glass heated inlet sytem (AGHIS) which doubles as a very low vapour pressure (VLVP) pyrolysis inlet. Located in the first field free region (1FFR), there is a collision gas chamber (cell 1). An Autospec magnet (B) precedes the 2FFR housing which has the form of a rectangular box [79 x 23 x 23 cm] with an easily removable top lid and side panels. Using four valves, the box may be quickly isolated from its two 160/700 Diffstaks and the other sectors. This allows rapid access to the three collision gas cells and the lens assemblies which are mounted on its "optical bench" type of internal base. Inside the box are three collision gas chambers: cell 2 which has dimensions [30(l) x 3(w) x 14(h) mm], cell 3 of dimensions [20(l) x 1(w) x 10(h) mm] and cell 4 which measures [20(l) x 1(w) x 10(h) mm]. The cells are located at distances of 270, 44 and 10 mm respectively from the focal point of the intermediate slit located next to the glass window situated on top of the box. Following the second sector (E_1), there is a box type collector housing which contains the 3FFR

collision gas chamber (cell 5) located in front of a small Autospec ESA (E_2). A fifth 160/700 Diffstak is used to pump this region. Cells 2 and 3 are both equipped with a deflector electrode and inlet systems for permanent gases and organic vapours. Mounted on one side of Cell 3 – perpendicular to the flight path of the fast moving ion beam – is a Quadrupole mass analyser which can be used to obtain spectra of ionized target molecules [2]. Cell 4 has a *y* focus/deflection lens assembly attached to the back. Cell 3 and 4 are both electrically insulated.

Typically, cell 2 was used for the neutralization experiments with N,N-dimethyl-aniline, (main beam transmission, T = 70%) whereas Cell 3 was used for neutralization with Xenon, cyclopropane and trimethylamine (T = 70%). For the use of organic organic neutralization agents with ionization energies close to that of the target ion see ref. 3. Cell 4 contained O_2 (T = 70-80%) when used for CA experiments and the reionization of neutral species in NR experiments. The total indicated analyzer pressure in CA experiments was usually 2-3 x 10^{-6} Torr whereas for NR experiments it was generally ~2 x 10^{-5} Torr. While O_2 was also used for collision experiments in the 3FFR, helium (T = 70%) was most commonly used for this purpose in cell 5.

MS/MS/MS "double collision" mass spectra were generally obtained with O_2 in the 2FFR and He (T=70%) in the 3FFR. CA mass spectra of the NR *survivor* ions (NR/CA mass spectra) were recorded in the 3FFR using He or O_2 as collision gases with neutralization (cell 2 or 3) and reionization (cell 4) taking place in the 2FFR.

The spectra were recorded with a PC based (80386, 33 MHz) data system using ZABCAT software (versions 1 to 5.1) developed by Mommers Technologies Inc. (Ottawa, Canada). The MS/MS/MS spectra represent the accumulation of 20 scans (30 seconds per scan).

The mass spectra relevant to the studies in Chapter 2 were obtained using the ZAB-2E (McMaster University) and the ZAB-2F (University of Utrecht, The Netherlands) two sector, BE, mass spectrometers. These mass spectra were recorded directly (1

scan) using a Kipp and Zonen plotter (The Netherlands).

Unless otherwise stated, all the various mass spectra obtained using the ZAB-type instruments were obtained under the following conditions: ionizing electron energy, 70eV; emission current, 50-500 μA; accelerating voltage, 8 keV; and source temperature, 150°C. Samples were generally introduced at indicated source pressures of 10^{-5} to 10^{-6} Torr.

The IE and AE values (Chapter 2) were obtained using monochromatic electrons on the instrument of Dr. F.P. Lossing (University of Ottawa) [4]. The AE values for metastable peaks (Chapter 5) were obtained by the comparative method of Burgers and Holmes [5] using the KRATOS MS 902S instrument which is also located at the University of Ottawa.

Neutralization-reionization (NR) mass spectrometry

For neutralization-reionization mass spectra obtained with the ZAB-R, ions M^+ produced at 70 eV electron energy and accelerated to 8 keV, are selectively transmitted by B to the 2FFR where, in the first collision chamber (cell 2 or 3), charge-exchange neutralization occurs with the target molecule e.g. N,N-dimethylaniline (NDMA):

$$M^+(8\ keV) + NDMA \rightarrow M^{\bullet}(8\ keV) + NDMA^{\bullet +}$$

The unreacted ions are deflected away and the remaining fast neutrals $M^{\bullet}$ are reionized with O_2 in the second collision cell i.e., $M^{\bullet}(8\ keV) + O_2 \rightarrow M^+(8\ keV) + O_2 + e^-$. Scanning E_1 yields the spectrum of the reionized neutrals M^+, the *survivor* ions, and their (structurally characteristic, see Introduction) charged dissociation products.

To obtain mass spectra of the reionized neutrals free from interferences (the so-called NR/CA or NR/CID mass spectra, see chapters 8 and 9), the fast moving *survivor* ions resulting from the NR experiment are selectively transmitted by E_1 to the 3FFR, whereupon, as they pass the through the collision chamber (cell 5) located therein, they undergo collisions with He. The resulting ionic dissociation products are

mass-analyzed by scanning E_2.

Chemicals

The chemicals for all experiments were obtained from Aldrich (Milwaukee, USA), unless otherwise indicated. Their purity was checked by mass spectrometry and NMR spectroscopy and they were purified when necessary.

Isotopically labelled samples of methyl carbamate were synthesized on a microscale from the appropriately labelled alcohols (CD_3OH, CD_2HOH, $CH_3{}^{18}OH$ and $^{13}CH_3OH$, isotopic purity > 95%, Merck Sharp & Dohme) and urea using zinc acetate as a catalyst [6]. Heating of the starting materials at ~110°C for 24h in sealed thick-walled quartz tubes (i.d. 3mm, length 10 cm) led to white crystals of the carbamate (after the slight excess quantity of methanol was evaporated), which could be introduced via the all quartz probe. For the synthesis of the doubly labelled ester $H_2N\text{-}C(=O)\text{-}^{18}O\text{-}^{13}CH_3$ a methanol sample was used (Amersham, UK) containing $^{13}CH_3{}^{18}OH$ (10 %), $^{13}CH_3{}^{16}OH$ (80 %) and $^{12}CH_3{}^{16}OH$ (10 %).

N-methoxycarbonylhydrazone, $CH_3C(H)=NN(H)COOCH_3$, was prepared in 90 % yield from methylhydrazinocarboxylate, $H_2NN(H)COOCH_3$, and acetaldehyde in ether which contained crushed molecular sieves (4Å, 8-12 mesh, Davison) and the minimum amount of methanol needed to dissolve the starting material. The white hydrazone precipitate was isolated and recrystallized by ether trituration from methanol.

N-Methyl-O-methyl carbamate, $CH_3N(H)COOCH_3$, a colorless oil (introduced via AGHIS), and its isotopically labelled variants were synthesized on a microscale from CH_3NCO and the appropriately labelled alcohols (CD_3OH, CD_2HOH, $CH_3{}^{18}OH$ and $^{13}CH_3OH$ (isotopic purity > 95%) Merck Sharp & Dohme, and a methanol sample containing $^{13}CH_3{}^{18}OH$ (10%), $^{13}CH_3{}^{16}OH$ (80%) and $^{12}CH_3{}^{16}OH$ (10%): Amersham, UK) [7], except for $CD_3N(H)COOCH_3$, which was prepared from $CD_3NH_2.HCl$ and methylchloroformate, $Cl\text{-}COOCH_3$, analogously to the procedure for methyl urethane [8].

For the experiments of Chapter 5, the deuterium labelled samples were obtained by exchange reactions with CH_3OD (for methylcarbazate and hydrazinoethanol) or D_2O (for 1,2-dimethylhydrazine). During the labelling of the pure hydrazine significant quantities of $(CH_3)_2ND$ and $CH_3N{=}N{-}N{=}NCH_3$ were co-generated.

N–(n-propyl)acetamide, its D-labeled analogues and *N*–methyl-iodoacetamide were synthesized using standard acylation procedures [9].

Two of the three C_2NO precursors of Chapter 7, methylcyanoformate (introduced via AGHIS from -78°C bath) and pyruvonitrile were commercially available. The third, dichloroglyoxime, $HON{=}C(Cl){-}C(Cl){=}NOH$, was obtained in 30% yield, by chlorination of (mono)chloroglyoxime [10]. The monochloro compound was prepared, in 40% yield (50 mmol scale), from Na_2CO_3, hydroxylamine and chloral hydrate [10]. Dichloroglyoxime (introduced via direct insertion probe, source temp. 250°C) should be handled with caution since it decomposes, thermally and under basic conditions, to produce the explosive cyanogen di-N-oxide, $O{\leftarrow}N{-}C{\equiv}C{-}N{\rightarrow}O$.

For the experiments described in chapter 8, dihydroxyfumaric acid (source temp. 100°C) and formic acid were commercially available. Research grade formamidine hydrochloride and the aminoguanidine hydrochloride and bicarbonate salts were used directly. Dissolution of the latter in D_2O acidified with H_2SO_4 yielded, after reprecipitation with Na_2CO_3, the deuterium labelled isotopomer.

Acetaldehyde, N-formylhydrazone was synthesized in the same way as the toxin gyromitrin [11]. A sufficiently pure sample for our studies (aliphatic hydrazones are notoriously difficult to purify) was obtained after pumping the reaction mixture at a rotary pump for 12 hours followed by exposure to high vacuum (10^{-7} Torr) for 24 h. The residual colourless oil was characterized by high resolution mass spectrometry (principal peaks : m/z 86 [$M^{\bullet+}$] (10 %), 71 (8 %), 58 (12 %), 57 (15 %), 45 (15 %), 44 (7 %), 43 (47 %), 42 (100 %)) ; ^1H NMR δ 8.23 (s, 1H), δ 7.33 (q, 1H, J = 4 Hz), δ 1.70 (d, 6H, J = 4 Hz) and FT-IR (KBr) ν cm^{-1} 3177 (m), 3036 (m), 2905 (m), 1675 (s), 1636 (s),

1548 (m), 1[illegible]5 (m), 1352 (w), 1216 (m), 1142 (m), 1014 (m), 890 (m), 700 (s), 739 (s), 662 (s). The compound is air sensitive, turning a bright yellow colour when exposed to air even when kept refrigerated. The isotopomer CH_3-CH=N-N(D)-CH=O was obtained by exchange with CH_3OD (99.5% atom D) while CH_3-CD=N-N(H)-CH=O was synthesized using CH_3-CD=O. The hydrazone samples were introduced via the quartz liquid probe kept at room temperature giving an indicated source pressure of 2×10^{-7} Torr. Formamide-D_3,^{15}N was obtained by exchanging, with CH_3OD, $H_2{}^{15}N$-C(D)=O which was prepared [12] using $^{15}NH_4Cl$, D_2O (MSD isotopes) and DCO_2H. The volatiles were evaporated by pumping briefly on a rotary pump. Oxamide-D_4,$^{15}N_2$ was synthesized [13] using $^{15}NH_4Cl$ and D_2O and diethyloxalate. The solid product was washed with D_2O and CH_3OD and dried under vacuum.

References

1. R.P. Morgan, J.H. Beynon, R.H. Bateman and B.N. Green, Int. J. Mass Spectrom. Ion Processes 28 (1978) 171.
2. T. Wong, J.K. Terlouw, T. Weiske and H. Schwarz, Int. J. Mass Spectrom. Ion Processes 113 (1992) R23.
3. M.-Y. Zhang and F.W. McLafferty, J. Am. Soc. Mass Spectrom 3 (1992) 108.
4. F.P. Lossing and J.C. Traeger, Int. J. Mass Spectrom. Ion Phys. 19 (1976) 9.
5. P.C. Burgers and J.L. Holmes, Org. Mass Spectrom. 17 (1982) 123.
6. A.M. Paquin, Z. Naturforschg. 1 (1946) 518.
7. (a) S.R. Sandler and W. Karo, Organic Functional Group Preparations, Academic Press: New York (1971) Chapter 10 and 11.
8. W.W. Hartman and M.R. Brethen, Organic Synthesis, 2 (1945) 278
9. J. March, Advanced Organic Chemistry: reactions, mechanisms and structure (4th Ed.), Wiley-Interscience: New York (1992) p. 417.
10. (a) J. Houben and H. Kaufman, Chem. Ber. 46 (1913) 2821; for Cl_2 see: (b) Smith's Inorganic

Chemistry, 2nd ed., J. Kendall (Ed.), D. Appleton-Century Co.: New York (1960) p. 239.

11. (a) P.H. List and P. Luft, Arch. Pharmazie 301 (1968) 294; (b) H. Pyysalo and E. Honkanen, Acta Chem. Scand. B30 (1976) 792.

12. I.K. Phelps and C.D. Deming, Amer. Journ. Science 24 (1907) 173

13. N.V. Sidgewick, The Organic Chemistry of Nitrogen, Oxford University Press: Oxford (1937).

SUMMARY

This thesis details the experimental study of some organic cations and neutrals in the gas phase by mass spectrometry. Attention is focussed on some fascinating types of ion and neutral structures, especially hydrogen-bridged radical cations and some elusive imidic acids and carbenes.

Beginning with a brief preamble, chapter one concisely introduces tandem mass spectrometric techniques and some empirical and computational approaches used to investigate structures, reaction mechanisms and thermochemistry of ions and neutrals in the gas phase. These methods are illustrated by appropriate examples from the gas phase chemistry of ionized dimethylsulfoxide. The information which can be obtained from Metastable Ion (MI), Collisional Activation or Collision-Induced Dissociation (CA or CID), Neutralization-Reionization (NR) and Collision-Induced Dissociative Ionization (CIDI) mass spectrometry, Appearance Energy (AE) measurements and from estimated or calculated thermochemical data is discussed. A preliminary description of hydrogen-bridged (radical) cations, ion-molecule complexes and distonic ions and some of their experimental characteristics is given along with some examples.

Chapter 2 discusses the unimolecular chemistry of the methyl carbamate radical cation, $H_2NCOOCH_3^{+\bullet}$ which was studied by MI, CA and NR mass spectrometry, AE measurements and *ab initio* molecular orbital calculations. The calculations predict at least seven species, including hydrogen-bridged radical cations and the important distonic ion $H_2N\text{-}^{+}C(OH)OCH_2^{\bullet}$, to be among the stable isomers of ionized methyl carbamate. The most stable isomer turns out to be $[H_2N\text{-}CH{=}O\cdots H\cdots O{=}C\text{-}H]^{+\bullet}$ while the ion $[H_2N\text{-}C{=}O\cdots H\cdots O{=}CH_2]^{+\bullet}$ is a key intermediate in the spontaneous unimolecular dissociations of $H_2NCOOCH_3^{+\bullet}$ to $H_2N\text{-}CH\text{-}OH^{+}$ + $HCO^{\bullet}$ (the components of the most stable isomer) and $[CH_2{=}O\cdots H\cdots NH_2]^{+\bullet}$ + CO. The products were characterized experimentally

but only with the aid of high level *ab initio* calculations could the dissociation mechanisms of $H_2NCOOCH_3^{+\bullet}$ be elucidated. Minimum energy requirement reaction paths for the multistep isomerizations were located computationally. They predict that the complex $[H_2C{=}O{\cdots}H{\cdots}NH_2C{=}O]^{+\bullet}$, which can be viewed as formaldehyde and a CO molecule interacting with $NH_3^{+\bullet}$, lies in a shallow well only, and it sheds C=O to produce $[CH_2{=}O{\cdots}H{\cdots}NH_2]^{+\bullet}$, as observed experimentally.

Chapter 3 further discusses the unimolecular chemistry of $H_2NCOOCH_3^{+\bullet}$. The difficulties faced in ion structure assignment are clearly illustrated in the attempts to generate the iminol ion $H\text{-}N{=}C(OH)\text{-}OCH_3^{+\bullet}$ by loss of CH_3CN from the molecular ion of $CH_3CH{=}N\text{-}NHCOOCH_3$. The stability of the iminol ion and the hydrogen-bridged species $[H_2C{=}O{\cdots}H{\cdots}N(H)COH]^{+\bullet}$ were evaluated computationally, as were the barriers for their formation from $H_2NCOOCH_3^{+\bullet}$ or from the distonic ion $H_2N\text{-}^{+}C(OH)OCH_2^{\bullet}$ via rearrangements.

By integration of results obtained from many experiments and from *ab initio* calculations, the product ion was assigned the distonic ion structure, a challenging task since it shows virtually identical dissociation characteristics to $H_2NCOOCH_3^{+\bullet}$. For the distonic ion, new transformations involving $[H_2C{=}O{\cdots}H{\cdots}N(H)COH]^{+\bullet}$ were determined. They explain the previously puzzling observation that $H_2NCOOCD_3^{+\bullet}$ forms both $CD_2OD^{\bullet}$ and $CD_2OH^{\bullet}$ in CA and NR experiments and they indicate that although the distonic ion is exceedingly difficult to characterize it is the key intermediate for all the observed dissociations of methyl carbamate radical cations.

Chapter 4 discusses a study of the unimolecular dissociations of N-methyl-O-methyl carbamate radical cations $CH_3N(H)COOCH_3^{+\bullet}$ in which a combination mass spectrometry based techniques (MI, CA, NR and MS/MS/MS) and D, ^{13}C and ^{18}O labelling experiments were used to characterize product ion structures and reaction mechanisms. The first section focusses on the surprising loss of a methyl radical from $CH_3N(H)COOCH_3^{+\bullet}$. The experimental evidence leads to a mechanistic proposal which

involves equilibration of $CH_3N(H)COOCH_3^{+\bullet}$ with two distonic isomers $CH_3N(H)\text{-}^{+}C(OH)OCH_2^{\bullet}$ and $CH_2=^{+}N(H)\text{-}^{\bullet}C(OH)OCH_3$, the latter serving as the immediate precursor for $^{\bullet}CH_3$ elimination. The product ion was identified as the N-carboxyiminium ion $CH_2=N(H)\text{-}COOH^+$ a putatively destabilized iminium ion. The heats of formation of the molecular ion and the product ion were estimated by additivity methods. The second section discusses how the O-protonated species, the elusive isoformylaminylium ion, $HNCOH^+$ was generated by successive degradation of ionized N-methyl-O-methylcarbamate in an MS/MS/MS type experiment: $CH_3NHC(=O)OCH_3^{\bullet+} \rightarrow CH_3NHCOH^{\bullet+} \rightarrow HNCOH^+$. This ion is not easy to make any other way since the aminoformylium ion, $H_2N\text{-}C{\equiv}O^+$ is thermodynamically the most stable $[H_2,C,N,O]$ isomer. The $HNCOH^+$ ion is identified from its characteristic CA mass spectrum. A comparison of the CA mass spectra of the ^2H labelled isotopomers $DNCOH^+$ and $HNCOD^+$ with that of the isomeric ion $HDNCO^+$ indicates that collisionally excited $HNCOH^+$ ions may isomerize into $H_2N\text{-}C{\equiv}O^+$.

Chapter 5 gives a discussion of the $CH_5N_2^+$ system which was investigated by high level ab initio computations and MI, CA and NR mass spectrometric experiments. AE measurements and theory were used to re-evaluate the heats of formation of: CH_3NHNH^+, $CH_3NNH_2^+$ and $CH_2=NH\text{-}NH_2^+$. Theoretical methods were also used to calculate their 1,2- and 1,3-hydrogen shift interconversion energy barriers and to evaluate the stabilities of two other isomers, namely, the ring-closed form of $CH_2=NH\text{-}NH_2^+$, and the hydrogen bridged entity $CH_2=N{:}\underline{H}{:}NH_2^+$; the former isomer is remarkably stable while the latter turned out not to correspond to a minimum on the potential energy surface. NR experiments indicated that the neutral $CH_2=NH\text{-}NH_2^{\bullet}$ is a stable species but that the fate of the majority of neutralized $CH_2=NH\text{-}NH_2^+$ ions was to dissociate into $CH_2=NH$ and $NH_2^{\bullet}$. This finding was rationalized in light of the different geometries predicted for ion and neutral $CH_2=NH\text{-}NH_2^{\bullet}$ by CASSCF Multireference CI type calculations. Mechanisms are proposed for the metastable dissociation reactions of $CH_5N_2^+$ ions to $HCNH^+ + NH_3$ and to $HC{\equiv}N + NH_4^+$, the latter rationalized in terms of a dissociating $[HC{\equiv}N\cdots NH_4]^+$ ion-dipole

complex. It should be noted however, that a lower energy pathway for this reaction has subsequently been located. This demonstrates that ultimately keen chemical intuition is crucial in the search for the lowest energy reaction pathway and that computations are not a panacea for gas phase ion chemistry problems.

Chapter 6 relates how the prototype amidoalkylating reagent, the N-acetylmethyl-iminium ion $CH_3C(=O)\text{-}N(H)=CH_2^+$ was generated and studied in the gas phase. Metastable ions $CH_3C(=O)\text{-}N(H)=CH_2^+$ dissociate by deacetylation to $CH_2NH_2^+$ with an exceedingly small translational energy release. A remarkable "all-or-nothing" deuterium isotope effect is associated with this process: the deuterium labelled isotopomer $CD_3C(=O)\text{-}N(H)=CH_2^+$ producing $CHDC=O + CH_2ND_2^+$ rather than $CD_2C=O + CH_2NHD^+$. By integration of results obtained from mass spectrometry based experiments (MI, CA and D-labelling) and from *ab initio* molecular orbital calculations, a mechanism for deacetylation could be derived. A hydrogen-bridged complex $[O=C=CH_2\cdots H\cdots N(H)=CH_2]^+$, which equilibrates with $CH_3C(=O)\text{-}N(H)=CH_2^+$ prior to its endothermic dissociation, is proposed to explain the H/D exchanges. The isotope effect is interpreted in terms of differences in the zero-point vibrational energies of the possible sets of products. Emphasis is placed on the observation of large isotope effects and exceedingly small translational energy releases as indications of the intermediacy of ion-molecule complexes. The isomeric $C_3H_6NO^+$ ions $[H_2C=C=O\cdots H\cdots N(H)=CH_2]^+$, $CH_2\text{-}O\text{-}C\text{-}N(H)\text{-}CH_3^+$, $CH_2=C(OH)\text{-}N(H)\text{-}CH_2^+$, $H_2N\text{-}CH_2\text{-}CH_2\text{-}C=O^+$, $CH_3C(OH)=N=CH_2^+$ and protonated 2-azetidinone, which were briefly examined and characterized, are also discussed.

The second part of the thesis focusses on the generation and identification of elusive radicals and molecules by neutralization-reionization mass spectrometry.

Chapter 8 discusses how CA experiments were used for characterizing isomeric $[C_2NO]$ cations, namely, $NCCO^+$, $CNCO^+$ and $CCNO^+$. NR and CIDI experiments revealed the existence of $NCCO^\bullet$, $CNCO^\bullet$ and $CCNO^\bullet$ as stable radicals in the diluted gas-phase. *Ab initio* MO calculations using the 6-31G* basis set and electron correlation show that

NCCO ions and neutrals are more stable than their CNCO counterparts, by 7.4 and 15.8 kcal/mol respectively. These calculations were not amenable to the determination of relative energies for ions and neutrals 3.

Chapter 8 gives a discussion of the generation and identification of diamino- and dihydroxycarbene. Dissociative electron impact ionization of aminoguanidine, H-N=C(NH_2)-NH-NH_2 cleanly produces diaminocarbene radical cations H_2N-C-$NH_2$$^{\bullet+}$ whereas, dihydroxycarbene radical cations HO-C-OH$^{\bullet+}$ were made by dissociative ionization of dihydroxyfumaric acid. Their structures were established on the basis of collision experiments. Reduction of the respective carbene radical cations by single electron transfer in NR mass spectrometric experiments yielded the prototype nucleophilic carbenes H_2N-$\bar{C}$-NH_2 and HO-$\bar{C}$-OH as stable species in the gas-phase, distinct from their isomers formamidine, H-N=C(H)NH_2 and formic acid, O=C(H)OH. Deuterium labelling and multiple collision experiments, in particular CID mass spectra of the NR "survivor" ions, confirm the identities of the ions and neutrals. The experimental results are consistent with previously published ab initio calculations.

Chapter 9 discusses how a combination of CID, NR and MS/MS/MS experiments on D and ^{15}N labelled isotopomers made it possible to assign structures to the prototype imidic acid, formimidic acid, H-N=C(H)-OH, and aminohydroxycarbene, H_2N-$\bar{C}$-OH, both isomeric with formamide. From a detailed analysis of CID mass spectra, especially MS/MS/MS data from D and ^{15}N labelled isotopomers, it was possible to establish that appropriate dissociative ionizations produced pure beams of the ionic precursors H-N=C(H)-OH$^{\bullet+}$ and H_2N-C-OH$^{\bullet+}$ and that direct ionization of formamide yielded H_2N-CHO$^{\bullet+}$. One-electron reduction of these radical cations in NR experiments produced intense "survivor" signals. By combining information contained in CID mass spectra of the "survivor"ions with that from labelling experiments, the existence of formimidic acid and aminohydroxycarbene as stable molecules in the gas phase was established. Among the vibrationally excited molecules we find evidence for the simplest amide-iminol

tautomerism, i.e. **1** ↔ **2**. The experimental findings on the ions and neutrals concur with previously published ab initio computational studies which were supplemented by our own results. Using the same experimental methodology, the existence of the imidic acid CH_3-N=C(H)-OH and the carbene CH_3-N(H)-$\bar{C}$-OH was also established.